

UNIVERSITÉ DE LIÈGE
Faculté des Sciences Appliquées



Global analysis and synthesis of oscillations: a dissipativity approach

Année académique
2004-2005

Thèse présentée par
Guy-Bart STAN
en vue de l'obtention du titre de
Docteur en Sciences Appliquées

MEMBERS OF THE JURY

EXTERNAL MEMBERS

DIRK AEYELS, Professor at the University of Gent

Address : University of Gent, Systems Research Group, Technologiepark - Zwijnaarde 9, 9052 Zwijnaarde, Belgium

CARLOS CANUDAS-DE-WIT, "Directeur de Recherche" at the CNRS

Address : Laboratoire d'Automatique de Grenoble, 38 402 ST. Martin d'Hères, France

JORGE GONCALVES, Professor at the University of Cambridge, U.K.

Address : University of Cambridge, Department of Engineering, Control Group, Trumpington Street, CB2 1PZ Cambridge , United Kingdom

HENK NIJMEIJER, Professor at the Eindhoven University of Technology

Address : Eindhoven University of Technology, Mechanical Engineering, Materials Technology, PO BOX 513, WH 0.144, 5600 MB Eindhoven, The Netherlands

INTERNAL MEMBERS

JACQUES DESTINÉ, Professor at the University of Liège (president)

RODOLPHE SEPULCHRE, Professor at the University of Liège (promotor)

LOUIS WEHENKEL, Professor at the University of Liège

Address : University of Liège, Faculty of Applied Sciences, Departement of Electrical Engineering and Computer Sciences, Montefiore Institute, Grande Traverse 10, Sart-Tilman, 4000 Liège, Belgium

*To the memory of my mother
To my father*

Acknowledgements

I am very glad to have the opportunity, by these few words, to express my gratitude to many people who have contributed to this work in different ways.

First of all, I would like to express my deepest gratitude and respect to Professor Rodolphe Sepulchre for his abundance of ideas, his incredible intuition, and his professionalism during these four years of research. I thank him for introducing me with enthusiasm to his field of research, for his confidence in me, and his enthusiastic encouragements even in the moments when I doubted. The most impressive and typical thing about him is his ability to 'feel' the results and the mathematics. I have learned a lot working with him during these years, and the experience and knowledge he shared with me are invaluable.

I thank all my colleagues at the University of Liège for creating this special, friendly and comfortable atmosphere that allows hard work to be done in a pleasant environment. In particular, I would like to thank Maxime Dechesne, Manuel Gérard, Fabian Lapierre, Axel Legay, Christophe Germy, Sébastien Jodogne, Jens Jordan, Renaud Ronsse, and Lara Vigneron. Special thanks to Pierre-Antoine Absil for helpful discussions and valuable comments at various stages of this work. My warmest thanks to Damien Ernst for his true friendship, his encouragements and his sharp advices.

I would like to thank Professor Carlos Canudas-de-Wit for inviting me to spend two months at the Laboratoire d'Automatique de Grenoble and for making this stay an enjoyable and instructive experience. I also would like to thank all the members of his research group at LAG for their kind hospitality, and especially, Denis Jacquet, Alessandro Zin, and Emmanuel Witrant.

I thank all Professors from the thesis jury for accepting to read and evaluate this thesis, and for their interest in my work.

I am very grateful to the FNRS (Fonds National de la Recherche Scientifique) for providing the financial support for my Ph.D.

Finally, I would like to address my personal thanks to those closest to me. In particular, I thank my parents for teaching me the value of education, for their unquestioned love, stimulating encouragements, and invaluable support. They have been, are, and certainly will be an extraordinary example and a constant source of inspiration for me. Last, but far from least, I express my thanks and deepest affection to Cristina who helped me disconnect from my equations and return to reality when I most needed it. Her affection, advices and encouragements mean a lot to me.

Guy-Bart STAN
Liège, Belgium
January 2005

Abstract

This thesis is devoted to the global (as opposed to local) analysis, and synthesis of stable limit cycle oscillations in dynamical systems described by differential equations. Dynamical systems that exhibit stable limit cycle oscillations are called oscillators. The main contribution is the development of a theory for oscillators seen as open systems, that is, as systems that can be interconnected to other systems through their inputs and outputs. The results are obtained by considering an input-output characterization of oscillators based on dissipativity theory. The use of a dissipativity characterization opens the way to limit cycle global convergence analysis and synthesis in high dimensional and interconnected models of oscillators.

In the first part of the thesis, we define a class of dynamical systems exhibiting globally attractive limit cycle oscillations, and study the fundamental mechanisms responsible for these oscillations. We name elements of this class “passive oscillators”. Passive oscillators consist in the feedback interconnection of a passive system with a static nonlinearity which is “locally active” and “globally dissipative”. For this nonlinearity, the slope at the origin is treated as a bifurcation parameter. For values of the parameter in the vicinity of a critical bifurcation value, we give sufficient conditions for the existence, unicity, and globally attractivity of a limit cycle oscillation. Central to these results is the characterization of passive oscillators by a specific dissipation inequality. This dissipation inequality provides an external characterization of oscillators which allows a rigorous global stability analysis of limit cycles in high dimensional systems.

In the second part of the thesis, we show the usefulness of the dissipativity characterization for the global analysis of networks of interconnected passive oscillators. In particular, we give sufficient conditions that allow straightforward extensions of the results obtained for an isolated passive oscillator to networks of passive oscillators. These extensions rely on a multivariable version of the dissipation inequality used to characterize the network. We also introduce an incremental version of this dissipation inequality and show its usefulness for proving existence, and global stability of synchronic oscillations in networks of identical passive oscillators.

Finally, we show the usefulness of the considered approach for the synthesis of oscillations. We show that a natural oscillation mechanism is induced when a passive system is put in feedback with a specific proportional-integral controller for which the sign of the proportional part is locally reversed. The main advantage of this controller is that it relies on existing energy-based stabilization theory for equilibrium points: once a stabilizing, passive output has been designed for the system, it is used to close the loop with the controller in order to generate limit cycle oscillations in the closed loop system.

Contents

1	Introduction	1
1.1	Thesis main contributions and related publications	1
1.1.1	Global stability analysis of an isolated oscillator	2
1.1.2	Global stability analysis of interconnections of oscillators	4
1.1.3	Global synchronization analysis of interconnections of identical oscillators	4
1.1.4	Synthesis of oscillations in stable systems	4
1.2	Bibliographical state of the art	5
1.2.1	Analysis of oscillations	5
1.2.2	Analysis of oscillations in networks	6
1.2.3	Analysis of synchronization in networks	7
1.2.4	Synthesis of oscillations	7
1.3	Organization of the thesis	8
2	Preliminaries	9
2.1	Passivity	9
2.1.1	General passivity definition	9
2.1.1.1	Class of systems	10
2.1.1.2	Basic concepts	11
2.1.2	Passivity of memoryless nonlinearities	12
2.1.3	Loop transformations	13
2.1.4	Passivity versus LYAPUNOV stability	14
2.1.4.1	LYAPUNOV stability	14
2.1.4.2	Passivity and LYAPUNOV stability	16
2.1.5	Interconnections of passive systems	17
2.1.6	Characterization of input-affine passive systems	20
2.1.7	Structural properties of input-affine passive systems	21
2.1.7.1	Relative degree	21
2.1.7.2	Weakly minimum phasesness	22
2.2	Absolute stability	22
2.3	Semi-global practical asymptotic stability	23
2.4	Limit cycles and nonlinear oscillations	24
2.4.1	Stability of periodic solutions	25
2.5	Center manifold theory and bifurcations	26
2.5.1	The center manifold theorem	27
2.6	The HOPF bifurcation theorem	29

2.7	The KRONECKER product	33
3	Global results for one oscillator	35
3.1	The VAN DER POL oscillator	35
3.1.1	VAN DER POL dynamics - Global results	36
3.1.2	The VAN DER POL model as a LURE feedback system	37
3.2	The FITZHUGH-NAGUMO oscillator	39
3.2.1	FITZHUGH-NAGUMO dynamics - Global results	40
3.2.2	The FITZHUGH-NAGUMO model as a LURE feedback system plus a feedback adaptation loop	42
3.3	First result of this thesis - Passive oscillator definition	44
3.3.1	Class of systems studied	45
3.3.2	Global boundedness results for Σ linear	47
3.3.3	Bifurcations in absolutely stable LURE feedback systems	49
3.3.4	Passive oscillator definition	54
3.4	Relaxation of the assumptions of Theorem 3.7 - Use of multipliers	54
3.5	Examples and simulation results	59
3.5.1	Forcing the HOPF bifurcation	60
3.5.1.1	Simulation results	61
3.5.1.2	Graphical interpretation of the multiplier effect	62
3.5.2	Not forcing the HOPF bifurcation - pitchfork bifurcation	65
3.5.2.1	Simulation results	65
3.5.3	Not forcing the HOPF bifurcation - HOPF bifurcation	67
3.6	Numerical analysis of PLS - GAS of the limit cycle for a particular value of the bifurcation parameter	67
3.6.1	Problem definition	68
3.6.2	Existence of limit cycles	69
3.6.3	Quadratic stability of impact maps	70
3.6.4	Bounds on switching times	72
3.6.4.1	Lower bounds on the switching times	73
3.6.4.2	Upper bound on t_1	73
3.6.4.3	Upper bounds on t_{2a} and t_{2b}	73
3.6.5	Simulation results	74
3.7	Summary	76
4	Global results for interconnected oscillators	79
4.1	Networks of passive oscillators	79
4.2	Second result of this thesis - Networks of passive oscillators	82
4.2.1	Global boundedness result for Υ linear and linear coupling	82
4.2.2	Bifurcations in networks of passive oscillators	84
4.2.2.1	Dimension of the center manifold for a network of identical passive oscillators with linear symmetric coupling	85
4.2.2.2	Relaxation oscillations in networks of passive oscillators	86
4.2.3	Relaxation of the assumptions of Theorem 4.5 - Use of multipliers	87
4.3	Illustrative examples	89

4.3.1	Case 1: $N = 2$	89
4.3.2	Case 2: $N = 3$	90
4.3.3	Case 3: $N > 3$	90
4.4	Third result of this thesis - Incremental passivity and synchronization	93
4.4.1	Incremental passivity	94
4.4.2	Synchronization	94
4.5	Examples and simulation results	98
4.6	Summary	100
5	Synthesis of stable oscillations	103
5.1	A proportional-integral mechanism to generate oscillations in a stabilizable system	103
5.2	Synthesis of stable oscillations in mechanical systems	107
5.3	Fully actuated, two degrees of freedom mechanical systems	107
5.3.1	Transforming a linear PCH system into a passive system that satisfies the assumptions of Theorem 4.5	108
5.3.2	Implementing specific dissipation by feedback	109
5.4	Direct application to underactuated, mechanical systems	110
5.4.1	Typical example of underactuated mechanical system: the inverted pendulum on a cart	111
5.4.2	Around the stable position of the pendulum	111
5.4.2.1	Design of a stabilizing output	112
5.4.2.2	Stabilization of the system	112
5.4.2.3	Creation of a limit cycle oscillation	113
5.4.2.4	Simulation results	113
5.4.3	Around the unstable position of the pendulum	113
5.4.3.1	Design of a stabilizing output	114
5.4.3.2	Stabilization of the system	115
5.4.3.3	Creation of a limit cycle oscillation	115
5.4.3.4	Simulation results	116
5.4.4	Balancing control of RABBIT	117
5.5	Summary	118
6	Conclusion and future work	119
6.1	Summary	119
6.2	Future work	120
A	Complement to Chapter 4	121
A.1	Real positive definite matrices	121
A.2	Synchronization topologies	122
A.3	Invariance of the kernel dynamics	123
A.4	Implication of observability for linear systems	124
B	Degenerate bifurcation in linear, conservative and detectable systems	125
B.1	Poles/zeros map of linear conservative systems	125
B.2	Degenerate bifurcation	127

CONTENTS

C Application of MEES results to our class of systems	129
C.1 The frequency domain HOPF bifurcation theorem	129
C.2 Application of Theorem C.1 to our class of systems	132
Bibliography	135

List of Figures

1.1	Block diagram of the LURE nonlinear system studied in this thesis.	2
2.1	Input-output representation of (2.1)-(2.2).	10
2.2	(a) and (b) are examples of passive nonlinearities; (c) is an example of a non-passive nonlinearity.	13
2.3	Loop transformation with dynamic multipliers.	13
2.4	(a) Feedback interconnection of H_1 and H_2 . (b) Parallel interconnection of H_1 and H_2	18
2.5	LURE feedback interconnection.	22
2.6	A linear LC circuit for the harmonic oscillator.	25
2.7	As μ increases, a sink changes to a source, expelling or absorbing a limit cycle. Line (a): supercritical bifurcation; Line (b): subcritical bifurcation.	30
2.8	Figures 2.7 (a) and (b) in (x_1, x_2, μ) space. Dashed lines are repellers and solid lines are attractors.	31
3.1	The VAN DER POL “tetrode multivibrator” circuit.	37
3.2	Block diagram corresponding to the LURE SISO nonlinear system interpretation of the VAN DER POL equation.	38
3.3	Block diagram representation of the VAN DER POL state model (3.6).	39
3.4	Nullclines for the original FITZHUGH-NAGUMO model (3.7) when $I_a = 0$. As the parameters b and γ vary there can be (a) one stable equilibrium point or, (b) three equilibrium points, one unstable, namely, S_1 , and two stable, namely, $(0, 0)$ and S_2	40
3.5	Nullclines for the original FITZHUGH-NAGUMO model (3.7) with different applied currents I_a . Cases (a), where $I_a < I_1$, and (c), where $I_a > I_2$, have linearly stable steady states, while in (b), where $I_1 < I_a < I_2$, the steady state can be unstable and limit cycle periodic solutions are possible. With the configuration (d), the steady states S_1 , S_3 are stable whereas S_2 is unstable. In the configuration (d), a perturbation from either S_1 or S_3 can effect a switch to the other.	41
3.6	Block diagram representation of the FITZHUGH-NAGUMO state model (3.12).	43
3.7	The hysteresis associated to a bistable system.	44
3.8	Equivalent representations of the LURE SISO nonlinear system.	45
3.9	Example of ARCAK [AT02]. (a) The initial condition belongs to the basin of attraction of the equilibrium point $(x_1, x_2, x_3) = (0, 0, -1)$; (b) The initial condition belongs to the basin of attraction of the limit cycle.	49

3.10	Converting the global bistability scenario into a relaxation oscillator with a slow adaptation mechanism ($\tau \gg (k - k^*)^{-1}$). The case $\Sigma = \frac{1}{s}$ corresponds to the FITZHUGH-NAGUMO oscillator.	53
3.11	Equivalent feedback loop with multipliers.	55
3.12	Mechanical example.	60
3.13	Forcing the HOPF bifurcation with an integrator in the feedback loop. The case $H(s) = \frac{1}{s}$ corresponds to the VAN DER POL oscillator.	60
3.14	(a) State-space for $k = 0.9$. (b) State-space for $k = 1.1$. (c) State-space for $k = 2$. (d) State-space for $k = 10$	62
3.15	(a) State-space for $k = 0.77$. (b) State-space for $k = 1$	63
3.16	(a) NYQUIST plot of $G(j\omega)$. (b) NYQUIST plot of $G_k(j\omega)$ for $k = k_{passive}^* - 0.1, k_{passive}^*, k_{passive}^* + 0.1$	63
3.17	Effect of the ZAMES-FALB multipliers. Column (a) Without multiplier. Column (b) With multiplier.	64
3.18	(a) State-space for $k = 0.9$ without adaptation feedback loop. (b) State-space for $k = 1.1$ without adaptation feedback loop.	65
3.19	(a) State-space for $k = 2$, without adaptation feedback loop. (b) Projection of the state space on the two dimensional space of the state variables of H for $k = 2$, with adaptation feedback loop.	66
3.20	Output of the relaxation oscillator.	66
3.21	Replacing the nonlinear function $\phi_k(\cdot)$ by a piecewise linear function $f_{pls}(\cdot)$	69
3.22	Limit cycle with four switches per period (first half period in plain line and second half period in dashed line).	70
3.23	Impact maps of the PLS; (a) impact map 1 and impact map 2a, (b) impact map 1 and impact map 2b.	71
3.24	Simulation results for the PLS defined by the parameters values $\alpha = 1, k = 1.2, p = 5$ and $\tau = 20$. Column (a): state-space. Column (b): time evolution of the state variables.	75
3.25	Time evolution of the minimum eigenvalues of $P_1(t_1)$ and $P_{2b}(t_{2b})$ for the PLS defined by the parameters values $\alpha = 1, k = 1.2, p = 5$ and $\tau = 20$	75
3.26	Simulation results for the PLS defined by the parameters values $\alpha = 1, k = 1.8, p = 5$ and $\tau = 2$. Column (a): state-space. Column (b): time evolution of the state variables.	76
3.27	Time evolution of the minimum eigenvalues of $P_1(t_1)$ and $P_{2b}(t_{2b})$ for the PLS defined by the parameters values $\alpha = 1, k = 1.8, p = 5$ and $\tau = 2$	77
4.1	MIMO representation of a network of passive oscillators. $\Phi_k(Y) = (\phi_k(y_1), \dots, \phi_k(y_N))^T$ is a multivariable repeated nonlinearity. The repeated nonlinear element is $\phi_k(y) = -ky + \phi(y)$ where $\phi(\cdot)$ is a static nonlinear function that satisfies the assumptions of Section 3.3.1. $F(Y)$ characterizes the coupling. Ξ denotes the feedback interconnection of Υ and $F(Y)$	80
4.2	Two equivalent representations of the LURE MIMO nonlinear system studied in this chapter. $\Phi_k(Y) = (\phi_k(y_1), \dots, \phi_k(y_N))^T$ is a multivariable repeated nonlinearity. The repeated nonlinear element is $\phi_k(y) = -ky + \phi(y)$ where $\phi(\cdot)$ is a static nonlinear function that satisfies the assumptions of Section 3.3.1.	81
4.3	Converting the global bistability scenario into a relaxation oscillator with a slow adaptation mechanism ($\tau \gg (k - k_{network}^*)^{-1}$).	86

4.4	Simulation results for a network of 2 identical oscillators of type (4.12)-(4.14). The circles represent the oscillators. Column (a) corresponds to Γ_1 and column (b) corresponds to Γ_2 . The parameters values are $\omega_n = 1$, $\zeta = 1.25$, $\tau = 2$, $k = 0.3$. The critical bifurcation value for an isolated oscillator is $k^* = 1$ and the corresponding bifurcation value for the network is $k_{network}^* = 0$. The trajectories generated in the state space of each oscillator are represented on the second row. A different color is used for each oscillator (red for the trajectory of oscillator 1 and blue for the trajectory of oscillator 2). The third row represents the time evolution of the outputs of the oscillators.	91
4.5	Network of 3 oscillators in chain structure.	92
4.6	Simulation results for a network of 3 identical oscillators of type (4.12)-(4.14) coupled according to Figure 4.5. The parameters values are $\omega_n = 1$, $\zeta = 1.25$, $\tau = 2$, $k = 2.1$. The critical bifurcation value for an isolated oscillator is $k^* = 1$ and the corresponding bifurcation value for the network is $k_{network}^* = 2$	92
4.7	Simulation results for a network of 5 identical oscillators of type (4.12)-(4.14) coupled through S_5 symmetry. The parameters values are $\omega_n = 1$, $\zeta = 1.25$, $\tau = 2$, $k = 2$, and $K = 1$. The critical bifurcation value for an isolated oscillator is $k^* = 1$ and the corresponding bifurcation value for the network is $k_{network}^* = 1$	93
4.8	Time evolution of the outputs in a network of 5 oscillators coupled through Z_5 symmetry.	98
4.9	Superposition of the state spaces of the 5 passive oscillators coupled through Z_5 symmetry.	99
4.10	Synchronizing bidirectional open chain structure.	100
4.11	Simulation results for networks of five identical passive oscillators. (a) Open chain, (b) Z_5 symmetry, (c) D_5 symmetry, (d) S_5 symmetry. The parameters values are $\omega_n = 1$, $\zeta = 1.25$, $\tau = 2$, $k = 2$. The critical bifurcation value for an isolated oscillator is $k^* = 1$ and the corresponding bifurcation value for the network is $k_{network}^* = 1$. The coupling strength value is $K = 3$. The same initial conditions have been used for the different network topologies.	100
5.1	Synthesis of oscillations by nonlinear PI control of a stable system.	105
5.2	The cart-pendulum system	112
5.3	Poles/zeros configuration for the cart pendulum system after feedback transformation into a stabilizable and conservative system.	113
5.4	Cart-pendulum system: creation of oscillations around the stable position of the pendulum. Column (a) $k = -1$, Column (b) $k = 1$, Column (c) $k = 2$. The first line represents the projection of the state space on the pendulum state variables plane. The second line represents the projection on the cart state variables plane. The third line represents the temporal evolution of the state variables.	114
5.5	Cart-pendulum system: creation of oscillations around the unstable position of the pendulum. Column (a) $k = -1$, Column (b) $k = 0.1$, Column (c) $k = 1$. The first line represents the projection of the state space on the pendulum state variables plane. The second line represents the projection on the cart state variables plane. The third line represents the temporal evolution of the state variables.	116
5.6	The bipedal robot RABBIT	117
5.7	Modelization of RABBIT as a three-link inverted pendulum.	117
B.1	Root locus. (a) Ξ_{a_k} , (b) Ξ_{b_k} , (c) Ξ_{c_k} . Legend: \times represent a pole, \circ represents a zero. The solid curves represents the root locus.	127

LIST OF FIGURES

C.1 Theorem C.1 in the case when $p = 2$. The characteristic loci are only shown for positive ω . The L_1 locus is the heavy straight line emanating from -1 : if the system was stable before bifurcation, and the λ_1 locus moves outwards to engulf -1 after bifurcation, the bifurcation is supercritical and the limit cycle is stable. 131

C.2 Characteristic locus of $-kG(j\omega)$ for passive oscillators. The characteristic locus (i.e. the NYQUIST plot) is only shown for positive ω 133

Frequently used notations

x^T	The transposition of the vector x
\dot{x}	The first time derivative of the vector x
\ddot{x}	The second time derivative of the vector x
$ x $	The euclidean norm of the vector x or the absolute value of the scalar x
$\ x\ _\infty$	The infinite norm of the vector x
I_N	The $N \times N$ Identity matrix
$\mathbf{1}$	The vector $(1, \dots, 1)^T$
$\text{diag}(\lambda_1, \dots, \lambda_N)$	Diagonal matrix with the elements $\lambda_1, \dots, \lambda_N$ along the diagonal
\otimes	KRONECKER product
\succ	Slightly greater than
$\ker(\Gamma)$	The kernel (or null-space) of the matrix Γ
$\text{range}(\Gamma)$	The range of the matrix Γ
$\text{rank}(\Gamma)$	The rank of the matrix Γ
A^\perp	The orthogonal complement of the set A
$\mathcal{O}(y ^p)$	Order of magnitude notation
\mathcal{C}^k	Continuously differentiable up to order k , $1 \leq k \leq \infty$
\mathbb{R}	Set of real numbers
$\mathbb{R}_{>0}$	Set of positive real numbers
\mathbb{C}	Set of complex numbers
\mathbb{C}_+	Set of complex numbers with nonnegative real part
$A \setminus B$	Set notation for A minus B
$\Re\{s\}$	Real part of complex number s
$\Im\{s\}$	Imaginary part of complex number s
$L_f h(x) = \frac{\partial h}{\partial x} f(x)$	LIE derivative where $f : \mathbb{R}^n \rightarrow \mathbb{R}^n$ is a vector field and $h : \mathbb{R}^n \rightarrow \mathbb{R}$ is a scalar function

Acronyms and abbreviations

CLF	Control LYAPUNOV Function
GAS	Global Asymptotic Stability or Globally Asymptotically Stable
GES	Global Exponential Stability or Globally Exponentially Stable
GS	Global Stability or Globally Stable
IFP	Input Feedforward Passive
ISS	Input-to-State Stability or Input-to-State Stable
KYP	KALMAN-YAKUBOVICH-POPOV
LMI	Linear Matrix Inequality
LTI	Linear Time-Invariant
MIMO	Multi Input Multi Output
OFP	Output Feedback Passive
OFL	Output Feedback Lossless
PCH	Port-Controlled Hamiltonian
PCHD	Port-Controlled Hamiltonian with Dissipation
PLS	Piecewise Linear System
SGPAS	Semi-Global Practical Asymptotic Stability
SISO	Single Input Single Output
ZSD	Zero-State Detectable
ZSO	Zero-State Observable

Chapter 1

Introduction

This thesis is devoted to the *global analysis and synthesis* of stable limit cycle oscillations. Dynamical systems that exhibit stable limit cycle oscillations are called *oscillators*. They are ubiquitous in physical and biological systems (see [Gol96, Mos97, Str03] for numerous examples of oscillators). Detailed models of oscillators abound in the literature, most frequently in the form of a set of nonlinear differential equations whose solutions robustly converge to a limit cycle oscillation. Local stability analysis is possible by means of FLOQUET theory [Far94, BM94] but global stability analysis is usually restricted to second order models. For these models, global analysis is performed by using specific low dimensional tools (phase plane methods, POINCARÉ-BENDIXON theorem, etc.) which do not easily generalize to higher dimensions. The lack of analytical tools in higher dimensions generally forces high dimensional models of oscillators to be studied through numerical methods thereby giving no insight into the fundamental oscillation mechanisms involved. Moreover, when considering interconnection, the methods used for the analysis of an isolated oscillator do not generalize to the network. These considerations show the need for developing general analysis methods for oscillators. These methods should allow the analysis of oscillators independently from their dimension and provide an interconnection theory for oscillators.

From an *analysis* point of view, the aim of this thesis is to develop a global analysis method. We characterize a class of high-dimensional feedback systems exhibiting globally asymptotically stable limit cycle oscillations and study the mechanisms responsible for these oscillations. To this end, we consider an external characterization of oscillators which fits their description by physical state space models but, at the same time, has important implications for the stability and synchrony analysis of their interconnections. This external characterization of oscillators follows the fundamental characterization of *open systems* by a dissipation inequality, which opens the way for the development of an interconnection theory for oscillators.

From a *synthesis* point of view, the aim is to provide a simple feedback mechanism that allows for the generation of stable limit cycle oscillations in stable systems. In other words, we study the design of a simple controller that yields stable limit cycle oscillations in stable systems.

1.1 Thesis main contributions and related publications

The main contribution of this thesis is the analysis of oscillators by a dissipativity theory. In particular, we show the implications of this dissipativity theory for (i) the global stability analysis of an isolated oscillator, (ii) the global stability analysis of interconnections of oscillators, and (iii) the

global synchrony analysis of interconnections of N identical oscillators. Regarding the synthesis of oscillations, the main contribution concerns the design of a proportional-integral controller to generate oscillations in stabilizable systems.

To give the reader a flavor of the results, we introduce hereafter the main ideas that will be developed in details in the next chapters.

1.1.1 Global stability analysis of an isolated oscillator

This research started with the analysis of two low dimensional systems which are well-known for their global limit cycle oscillations: the celebrated VAN DER POL and FITZHUGH-NAGUMO models. Each of these systems is a reference model for nonlinear oscillations in physical and biological systems. On the one hand, the VAN DER POL model is a basic example of oscillator in the framework of electromechanical systems. On the other hand, the FITZHUGH-NAGUMO model, which is a simplification of the HODGKIN-HUXLEY model for voltage oscillations in the neuron cell membrane, is a basic example of oscillator in biology. Starting from these two models, we characterize a common feedback structure in which the forward block is filled with a linear system and the feedback block with a static nonlinearity. This feedback interconnection structure is represented in Figure 1.1. It is commonly referred to as a LURE feedback interconnection.

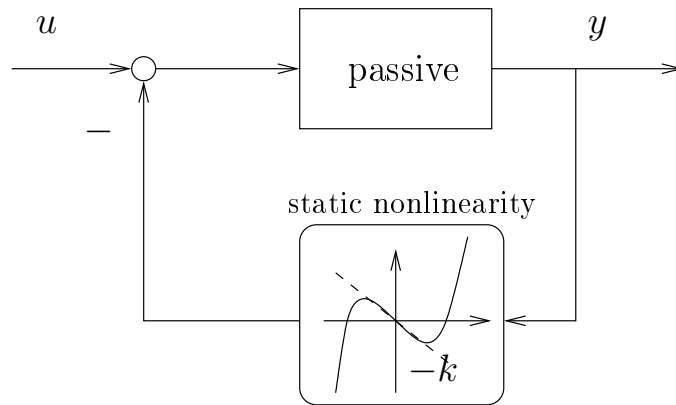


Figure 1.1: Block diagram of the LURE nonlinear system studied in this thesis.

The static nonlinearity in both models is characterized by a negative slope at the origin and a cubic behavior far from the origin, that is a nonlinear function of the form $-ky + y^3$. To understand the feedback mechanisms involved and, at the same time, obtain an interconnection theory for oscillators, we searched for an external characterization for both the dynamic and the static block. Passivity rapidly emerged as a natural external characterization. Passivity is a particular case of the general dissipativity theory introduced by WILLEMS [Wil72]. It provides a dimension-independent, interconnection theory for open systems described by state-space models. Open means that the system dynamics depend on external variables which describe the interaction with the environment. Passivity of an open system expresses that the rate of change of its internal energy is bounded by the rate at which the system can exchange energy with its environment through its external variables. The mathematical characterization of this physical property is the existence of a scalar, positive semidefinite function of the state $S(x)$, called the storage function, which is such that its time derivative satisfies the dissipation inequality $\dot{S} \leq uy$ where u and y represent the input and output of the system

respectively. For the feedback static nonlinearity, passivity amounts to satisfy a positivity condition: a static nonlinearity $\phi(\cdot)$ is passive if its graph belongs to the first and third quadrants, that is, if $y\phi(y) \geq 0$ for any y . Furthermore, if the nonlinearity $\phi(\cdot)$ is such that $\lim_{y \rightarrow \pm\infty} \frac{\phi(y)}{y} = \infty$, it is said to be stiffening. The common static nonlinearity of the VAN DER POL and FITZHUGH-NAGUMO oscillators has two terms: the first one y^3 is stiffening, passive and the second one $-ky$ is anti-passive or active. Since the feedback interconnection of two passive systems is passive, the active term necessarily plays a determinant role for the generation of limit cycle oscillations. We observed that, considering k as a parameter, a bifurcation occurs in both models at a certain critical value k^* . In the VAN DER POL model, a supercritical HOPF bifurcation occurs at $k = 0$: two complex conjugate eigenvalues cross the imaginary axis at $k = 0$, giving rise to a globally stable limit cycle surrounding the unique unstable equilibrium point $x = 0$ for $k > 0$. The supercritical HOPF bifurcation is directly responsible for the global oscillation. The corresponding feedback oscillation mechanism is an energy exchange between the storage variables of the forward passive system. This energy exchange is regulated by the static nonlinearity: when the internal energy of the system is too low, the active part of the nonlinearity forces its increase whereas the passive part forces its decrease when it is too high. In the FITZHUGH-NAGUMO model, the feedback oscillation mechanism can be seen as the addition of a slow feedback adaptation dynamic to a globally bistable system. This slow adaptation dynamic perpetually forces a switch from one equilibrium point to the other one, thereby transforming the globally bistable behavior into a global relaxation oscillation. The globally bistable system results from a supercritical pitchfork bifurcation occurring in a subpart of the FITZHUGH-NAGUMO dynamics. This subpart consists in a LURE feedback interconnection similar to the one sketched in Figure 1.1.

The passivity characterization of these two low dimensional oscillators raised the question if such global oscillation mechanisms still hold for a *high dimensional, nonlinear* system in the forward block and a more general static nonlinearity in the feedback block. The answer to this question constitutes the first main result presented in Chapter 3: under some technical assumptions, the LURE feedback interconnection of a passive system with a static nonlinearity possessing a parametrized active part ($-ky$) and a stiffening, passive part ($\phi(y)$) forces one of two bifurcation scenarii (Theorems 3.8 and 3.12). The first one corresponds to a supercritical HOPF bifurcation: two complex conjugate eigenvalues cross the imaginary axis at $k = k^*$, giving rise to a stable limit cycle surrounding the unique unstable equilibrium point $x = 0$ for $k \gtrsim k^*$ (the notation $k \gtrsim k^*$ is used to denote a value of the parameter k near the critical value k^* , i.e. $k \in (k^*, \bar{k}]$ for some $\bar{k} > k^*$). The second bifurcation scenario is a supercritical pitchfork bifurcation: the stable equilibrium $x = 0$ becomes a saddle point beyond the bifurcation value $k = k^*$ and two new stable equilibria appear for $k \gtrsim k^*$. This second bifurcation scenario can be transformed into a global oscillation by addition of a slow adaptation dynamic (Theorem 3.9). As meant by the notation $k \gtrsim k^*$, the results are local in the parameter space (they hold for values of the parameter in the vicinity of the critical bifurcation value) but they are global in the state-space, i.e. convergence to the stable limit cycle is proved for all initial conditions that do not belong to the stable manifold of the (unstable) equilibrium at the origin. Since passivity is the driving line and main assumption, we name the global oscillators corresponding to this first result *passive oscillators*. The results of Chapter 3 have been presented in [SS03], [SS04b] and in [SS05a].

1.1.2 Global stability analysis of interconnections of oscillators

A fundamental property of passivity is the analysis of interconnections. In the first part of Chapter 4 we show that the results obtained for an isolated passive oscillator extend to networks of passive oscillators when the static coupling between the oscillators satisfies a passivity (positivity) condition. To this end, we consider a MIMO representation of the network which is the multivariable analogue of the LURE feedback structure presented in Figure 1.1. As such, extension of the preceding results to a network of passive oscillators becomes straightforward (Theorems 4.5, 4.9, and 4.12). These results show that our approach not only provides results for isolated oscillators, but also for interconnections of oscillators. This is fundamental to the development of a system theory for oscillators and allows for the following analogy between passivity theory and passive oscillators theory: the building blocks of complex passive systems are their storage elements whereas the building blocks of complex oscillating networks are their passive oscillators.

1.1.3 Global synchronization analysis of interconnections of identical oscillators

After having determined the existence and stability of limit cycle oscillations in a network of interconnected passive oscillators, the important question of their relative oscillating behavior arises. Global synchronization among identical passive oscillators is studied in the second part of Chapter 4. In this part, we show that dissipativity not only provides an interconnection theory for oscillators but also, in its incremental form, a global synchronization theory. Synchronization refers to the tendency of interconnected oscillators to produce ensemble phenomena, that is, to phase lock as if an invisible conductor was orchestrating them. Synchronization is a convergence property for the *difference* between the solutions of different systems. Convergence properties for the difference between solutions of a closed system are characterized by notions of *incremental* stability. For open systems, the corresponding notion is *incremental passivity*. The main result (Theorem 4.15) concerns the implications of incremental passivity for the global stability of synchronic oscillations in networks of identical passive oscillators.

The results of Chapter 4 have been presented in [SS04a], [Sep04] and in [SS05b].

1.1.4 Synthesis of oscillations in stable systems

Our last contribution concerns the synthesis of oscillations in stabilizable systems. More specifically, we examine how to design a simple controller that yields stable limit cycle oscillations in a stabilizable system. To answer this question, we propose, in Chapter 5, a simple nonlinear proportional-integral feedback controller. The design of this controller is directly inspired from the analysis of the LURE feedback structure presented in the previous sections. Under some technical assumptions, it allows to generate oscillations in any stabilizable system. The main advantage of this controller is that it relies on stabilization theory for equilibrium points: once a stabilizing, passive output has been designed for the system, it is used to close the loop with the controller in order to generate limit cycle oscillations with large basins of attraction. The design of a stabilizing, passive output is a central topic in nonlinear control theory and many methods already exist to solve this problem (feedback passivation designs, controlled Hamiltonian and Lagrangian theory, energy shaping methods, etc.). Even in the case when the required technical assumptions are not satisfied, the proposed controller is expected to yield stable limit cycle oscillations thus providing a simple method to force oscillations by feedback. Application of this controller to benchmark underactuated mechanical systems such as the

cart-pendulum, the pendubot, the acrobot, or the balancing control of the bipedal robot RABBIT is part of ongoing research. In Chapter 5, we present simulation results obtained for the cart-pendulum. Real implementation of this controller for the balancing control of RABBIT is the subject of a current joint project in collaboration with the Laboratoire d'Automatique de Grenoble.

1.2 Bibliographical state of the art

1.2.1 Analysis of oscillations

The analysis of the fundamental mechanisms responsible for limit cycle oscillations in feedback systems is a longstanding problem. Earlier results in the literature have exploited the structure of LURE systems for the study of nonlinear oscillations. This structure was first investigated in the works of YAKUBOVICH [Yak73] and TOMBERG [TY89] which provided sufficient conditions for the *existence* of “auto-oscillations”. Auto-oscillation is there understood as [TY89] “stable, non-decaying oscillatory regimes that arise in nonlinear systems... it is not necessarily connected, as is sometimes done, with periodic movement”. The results presented in [Yak73, TY89] concern the existence of auto-oscillation but do not predict towards which auto-oscillatory regime the solution will converge nor its uniqueness. The mathematical concepts of auto-oscillation and self-oscillating system go back to the works of the A. A. ANDRONOV school [AVK66, AVK65]. This theory has been followed by many developments by the Russian school summarized in the survey book [LBS96] by LEONOV. In [LBS96], frequency conditions for the existence and local stability of limit cycle in high dimensional systems are presented. The main assumption of these frequency criteria is the LEVINSON dissipativity [Lev44, CL55] of the feedback system which implies that all the solutions are ultimately bounded. LEVINSON dissipativity may be proved with the help of the concept of *semi-passivity* introduced by POGROMSKY and NIJMEIJER in [Pog98, PGN99]. The presented existence conditions are based on high-dimensional generalizations of the annulus principle (i.e. the POINCARÉ-BENDIXON theorem) initiated in the work of SMITH [Smi79, Smi86]. The local stability conditions are mainly based on the geometrical construction and linear stability analysis of POINCARÉ maps. Unfortunately, no *periodicity*, *uniqueness* or *global convergence* result is provided. Furthermore, the physical interpretation of the underlying feedback mechanisms responsible for the oscillations is not discussed.

The analysis of feedback induced oscillations has also been investigated by MEES [MC79] where nonlinear feedback systems exhibiting supercritical HOPF bifurcations are considered. In [MC79], MEES presents a “frequency-domain” HOPF bifurcation theorem and graphical conditions corresponding to rigorous versions of the describing functions method (also known as the harmonic balance method) to conclude about local stability of limit cycles in feedback loops. If one is only interested in local stability properties of the limit cycle, then the results of MEES are well suited to draw conclusions for any particular feedback loop system consisting of a linear feedforward path and a nonlinear feedback path. For the particular case of HOPF induced bifurcation, a simple application of MEES results to our class of systems shows that, generically, a supercritical HOPF bifurcation arises (see Appendix C). Nevertheless, in [MC79], the fundamental properties of the feedforward and feedback path leading to global stability properties of the limit cycle are not discussed. Moreover, the extension of MEES results to several identical interconnected systems is not obvious and the procedure has to be restarted *ab initio* for the whole network.

Another way of analyzing limit cycle oscillations is to extend existing equilibrium point analysis

methods. In [HC94, CH95, CH97, CH98], HAUSER and CHUNG present an analysis framework for the computation of LYAPUNOV functions allowing to determine if a given limit cycle is *locally* exponentially stable. This framework is based on the definition of a local change of coordinates (θ, ρ) highlighting the $n - 1$ dimensional transverse dynamics of a periodic orbit. It allows to draw analogies from the equilibrium point stability analysis (transverse linearization instead of equilibrium point linearization, periodic LYAPUNOV equation instead of LYAPUNOV equation, \mathcal{L}_p stability and \mathcal{L}_2 gain of a periodic orbit). However, no condition allowing to conclude about existence, uniqueness or global stability of a limit cycle is given.

For the analysis of piecewise linear systems, GONCALVES [GMD01, GMD03] recently developed numerical tools to prove existence and *global* asymptotic stability of limit cycles. In his approach, GONCALVES reduces the problem of stability analysis of the limit cycle in piecewise linear systems to that of the (numerical) construction of a set of quadratic LYAPUNOV functions defined on the switching surfaces of the piecewise linear system. These LYAPUNOV functions are found by numerically solving a finite set of linear matrix inequalities. At the end of Chapter 3, we adapt the method of GONCALVES to the analysis of limit cycle oscillations in piecewise linear version of passive oscillators.

1.2.2 Analysis of oscillations in networks

Over the last decade, the analysis of networks of oscillators has been a very active research area in biology, chemistry, physics, control and applied mathematics (see [HI97, Mos97, NRA03, GS02, SS93, Kri97, Pog98, VG01, DM01, KE02, PSN02a, SW03, SWR04, RAN04] to cite just a few). The lack of an interconnection theory for oscillators generally forces an oversimplification of the models of each oscillator of the network. Two important networks models, extensively studied in the literature, are those of HOPFIELD [Hop82] and KURAMOTO [Kur84]. In HOPFIELD models, the dynamic of oscillator k in the network is described by a single scalar variable ρ_k which models an *average* activity of the oscillator (as a model for networks of neurons, this average activity is often thought of as the average firing rate of the neuron). HOPFIELD models abound in neuroscience and have been used to describe the dynamics of a number of computational tasks (see for instance [Wil99b] for several illustrations in vision). In these examples, the oscillatory behavior of the neuron is unimportant. The state ρ_k only models the storage capacity of the neuron. Storage models of oscillators neglect the phase variable of periodic solutions. As a consequence, they are inadequate for phase-locking or synchrony analysis. In contrast, in KURAMOTO phase models [Kur84, HI97], the dynamic of the oscillator k is described by a single scalar variable θ_k on the circle. These models neglect the radial variable of periodic solutions and thus disregard the dynamical behavior of the oscillator away from its limit cycle solution. They are inadequate for (global) orbital stability analysis. Several authors have studied how to reduce general models of oscillators to phase models in the limit of weak coupling, that is, when the coupling between the oscillators does not affect the convergence of each oscillator to a limit cycle solution. For more details about this reduction procedure and the stability analysis of interconnected phase models of oscillators, we refer the reader to the recent papers [BMH04, RA03] and references therein. In our approach, we do not make such simplifications. We characterize sufficient input-output properties that enable (global) limit cycle oscillations for an isolated oscillator. These input-output properties are then generalized to interconnections of oscillators, thereby providing sufficient conditions for (global) limit cycle oscillations in networks.

1.2.3 Analysis of synchronization in networks

The growing interest for synchronization in engineering applications is due to the robustness of collective phenomena, making an ensemble phenomenon insensitive to individual failures. The manifestations of synchronization are numerous both in nature and in engineered devices. The interested reader will find several compelling illustrations in [Str03] and [NRA03].

In [PN01, PSN02b, PSN02a], POGROMSKY and NIJMEIJER show that the existence of symmetry in the network implies the existence of linear invariant manifolds. This corresponds to so-called *partial synchronization*, or *clusterization*, a phenomenon occurring when some subsystems from the network operate in a synchronous manner. The authors present sufficient conditions guaranteeing global asymptotic stability of the partial synchronization manifolds. These conditions are based on the assumption that the systems in the network are *convergent*. In [LS98, WS], SLOTINE uses nonlinear *contraction* theory to derive results on global synchronization. Both convergence and contraction are incremental stability notions (see [Ang02, LS98, PPvdWN04]) that are defined specifically for closed systems. In these approaches, synchronization is thus not studied from an input-output perspective. In this thesis, we consider an input-output approach for the analysis of synchronization. Moreover, we put the emphasis on synchronization as a design principle, that is on the use of synchronization to achieve stable limit cycle oscillations in networks of identical systems. Most of the literature results on synchrony and phase-locking are based on the assumption that each isolated system of the network is characterized by a stable limit cycle. In our approach, we first prove that each isolated system is characterized by a globally stable limit cycle and then use synchronization to extend this property to a network of identical oscillators.

1.2.4 Synthesis of oscillations

The problem of synthesis of oscillations in control systems finds many applications. In the field of robotics, it plays an important role for the control of (underactuated) rhythmic tasks robot such as walking robots ([CAA⁺03, WGC02, TYS91]), juggling robots ([SA93, SA94, BKK94, ZRB99, LB01, GS04, RLS04]) or general dexterous robots (see e.g. [Wil99a]). Several paths to solve this problem have been investigated.

In [BM94, BM95a, BM95b, BMS96], BACCIOTTI and coworkers address the important problems of limit cycle generation by feedback and local stabilization of a preassigned limit cycle. For the limit cycle generation by feedback, they prove the existence of a polynomial feedback $u = u(x)$ for linear controllable systems ensuring the existence, uniqueness, and local asymptotic stability of a limit cycle. For the second problem, their results consist in the extension of the ARTSTEIN-SONTAG and JURDJEVIC-QUINN methods to guarantee stabilization of limit cycles under the assumption of the existence of a LYAPUNOV function for the limit cycle.

Another trend in the generation of stable limit cycle oscillation is due to ARACIL, GOMEZ-ESTERN and coworkers (see [GGEOA02, GAGE03, BAGGE04, GEBAG05]). Their method consists in two steps. First, a globally attractive oscillation is induced in a nominal second order subsystem by a particular controller. Then, the nominal stabilizing controller is extended to systems of arbitrary order via a method in the essence of backstepping.

The problem of forcing oscillations by feedback in *underactuated* mechanical systems is quite recent. In [BAGGE04], the method described in the preceding paragraph has been applied to generate locally stable oscillations in underactuated mechanical systems such as the ball and beam or the inverted pendulum on a cart. In [SC04], SHIRIAEV and CANUDAS-DE-WIT propose a constructive

method for generation and local orbital stabilization of pre-specified periodic solutions in underactuated mechanical systems with one degree of underactuation. Their results are based on a feedback structure that explicitly uses the general or full integral of the zero dynamics. Their method provides a control law that generates a limit cycle and makes it locally exponentially stable in the closed-loop system. This work was initiated by CANUDAS-DE-WIT in [CEU02] where a method to match a particular oscillatory exo-system, or a given closed curve was introduced.

Finally, the synthesis of oscillations can be seen as a particular case of the output regulation problem (see e.g. [Isi95, Chapter 8], [Pav04]). Output regulation methods deals with asymptotic tracking of prescribed reference signals. The class of reference signals consists of solutions of some external autonomous system called the *exosystem*. Reference signals generated by the exosystem are called *exosignals*. The output to regulate is called the *regulated output* (e.g. the tracking error in the tracking problem). The output available for measurement is called the *measured output*. The idea is to find a measured output feedback controller such that the closed loop system is internally stable and the regulated output tends to zero along solutions of the closed loop system. The internal stability requirement roughly means that all solutions of the closed loop system “forget” their initial conditions and converge to some limit solution which is determined only by the exosignal. To generate oscillations, the exosystem is designed to produce a specific oscillating exosignal. The use of output regulation methods to produce stable limit cycle oscillations is generally not easy because of the need to find specific output and controller that renders the closed loop system internally stable and at the same time allows to solve the regulation problem. Their advantage is that they allow to track a specific orbit in the state space.

1.3 Organization of the thesis

Chapter 2 contains mathematical preliminaries to the other chapters of the thesis. It recalls standard definitions about stability, passivity, absolute stability, bifurcations, and other concepts used in the thesis. Chapter 3 concerns the first main result of the thesis: global limit cycle oscillation analysis for *passive oscillators*. At the end of Chapter 3, we present an adaptation of the numerical method recently proposed in [GMD03] that allows the extension of our stability results in the parameter space. Chapter 4 contains the other two main results of the thesis: first, the extension of the results of Chapter 3 to networks of passive oscillators, and second, the study of global synchronic oscillations in networks of identical passive oscillators. Finally, in Chapter 5 we adopt a synthesis point of view for the generation of stable oscillations. Conclusion and future work are given in Chapter 6.

Chapter 2

Preliminaries

In this chapter, we recall some fundamental concepts and definitions that constitute the main mathematical prerequisites for the thesis. Most of the definitions are directly taken from popular reference books on differential equations and nonlinear systems. The interested reader is referred to these books for further details and comments. The proofs of the cited Lemmas and Theorems are not given since they can be found in the cited references.

2.1 Passivity

Passivity is a useful tool for the analysis of nonlinear systems, which relates nicely to LYAPUNOV stability. Very few system theory concepts can match passivity in its physical and intuitive appeal. This explains the longevity of the passivity concept from the time of its first appearance some 30 years ago (see [Wil72]), to its current use as a powerful tool for nonlinear feedback design (see [SJK97, vdS00]). The main passivity theorem states that the (negative) feedback interconnection of two passive systems is passive. Under additional zero-state detectability conditions, the feedback interconnection is also asymptotically stable. The passivity theorems and the small-gain theorem provide a conceptually important generalization of the fact that the feedback interconnection of two stable linear systems will be stable if the loop gain is less than one or the loop phase is less than 180 degrees. The connection between passivity and the phase of a transfer function comes from the frequency-domain characterization of positive real transfer functions. The phase of a positive real transfer function cannot exceed 90 degree. Hence, the loop phase cannot exceed 180 degrees. If one of the two transfer functions is strictly positive real, the loop phase will be strictly less than 180 degrees. Passivity results can be broadened with the help of loop transformations and multipliers which allow, in certain cases, to transform the feedback interconnection of two systems that may not be passive into an equivalent feedback interconnection of two passive systems.

2.1.1 General passivity definition

We begin by defining the concepts of storage function, supply rate, dissipativity, and passivity. Dissipativity theory, introduced by WILLEMS [Wil72], is an interconnection theory for open systems.

2.1.1.1 Class of systems

Although the dissipativity and passivity concepts apply to wider classes of systems, we restrict our attention to dynamical systems modeled by ordinary differential equations with an input vector u and an output vector y :

$$\dot{x} = f(x, u) \tag{2.1}$$

$$y = h(x, u) \tag{2.2}$$

We will be concerned with the case when the state $x(t)$, as a function of time, is uniquely determined by its initial value $x(0)$ and the input function $u(t)$. Throughout the thesis, we assume that $u : \mathbb{R}_{\geq 0} \rightarrow \mathbb{R}^p$ belongs to an input set U of functions which are bounded on all bounded subintervals of $\mathbb{R}_{\geq 0}$. In feedback designs u becomes a function of x , so the assumption $u \in U$ cannot be a priori verified. The satisfaction of this assumption for initial conditions in the region of interest will have to be a posteriori guaranteed by the design.

Another restriction is that the system (2.1)-(2.2) is “square”, that is, its input and output have the same dimension p . We also assume that $f : \mathbb{R}^n \times \mathbb{R}^p \rightarrow \mathbb{R}^n$ is continuous, and locally LIPSCHITZ¹, $h : \mathbb{R}^n \times \mathbb{R}^p \rightarrow \mathbb{R}^p$ is continuous. These assumptions imply that the system (2.1)-(2.2) has the local existence and uniqueness property of trajectories (see [Kha02] for definition of local existence and uniqueness of trajectories). Finally, an assumption made for convenience is that the system (2.1)-(2.2) has an equilibrium point at the origin, that is, $f(0, 0) = 0$, and $h(0, 0) = 0$.

We will find it helpful to visualize the system (2.1)-(2.2) as the input-output block diagram depicted in Figure 2.1. In such block diagram the dependence on the initial condition $x(0)$ will not be explicitly stressed, but must not be overlooked.

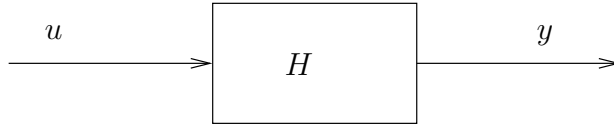


Figure 2.1: Input-output representation of (2.1)-(2.2).

The system description (2.1)-(2.2) includes as special cases the following three classes of systems:

- Nonlinear input-affine systems

$$\dot{x} = f(x) + g(x)u$$

$$y = h(x) + j(x)u$$

¹A function $f(x)$ is said to be *locally* LIPSCHITZ on a domain (open and connected set) $D \subset \mathbb{R}^n$ if each point of D has a neighborhood D_0 such that f satisfies the LIPSCHITZ condition

$$|f(a) - f(b)| \leq L|a - b| \tag{2.3}$$

for all points in D_0 with some LIPSCHITZ constant L_0 . We say that f is LIPSCHITZ on a set W if it satisfies the LIPSCHITZ condition (2.3) for all points in W , with the same LIPSCHITZ constant L . A locally LIPSCHITZ function on a domain D is not necessarily LIPSCHITZ on D , since the LIPSCHITZ condition may not hold uniformly (with the same constant L) for all points in D . However, a locally LIPSCHITZ function on a domain D is LIPSCHITZ on every compact (closed and bounded) subset of D . A function $f(x)$ is said to be *globally* LIPSCHITZ if it is LIPSCHITZ on \mathbb{R}^n . The LIPSCHITZ property of a function is stronger than continuity and weaker than continuous differentiability (see [Kha02]).

- Linear systems

$$\begin{aligned}\dot{x} &= Ax + Bu \\ y &= Cx + Du\end{aligned}$$

- Memoryless (or static) nonlinearity

$$y = \phi(t, u)$$

In the case of linear systems, we will let the system be represented by its transfer function $H(s) = C(sI - A)^{-1}B + D$ where $s = \sigma + j\omega$ is the complex variable.

2.1.1.2 Basic concepts

For an easy understanding of the concepts of dissipativity and passivity it is convenient to imagine a physical system with the property that its energy can be increased only through the supply from an external source. As an example, let us think of baking a potato in a microwave oven. As long as the potato is not allowed to burn, its energy can increase only as supplied by the oven. A similar observation can be made about an RLC-circuit connected to an external battery. The definitions given below are abstract generalization of such physical properties.

Definition 2.1 [SJK97] *Assume that associated with the system (2.1)-(2.2) is a function $w : \mathbb{R}^p \times \mathbb{R}^p \rightarrow \mathbb{R}$, called the supply rate, which is locally integrable for every $u \in U$, that is, it satisfies $\int_{t_0}^{t_1} |w(u(t), y(t))| dt < \infty$ for all $t_0 \leq t_1$. Let X be a connected subset of \mathbb{R}^n containing the origin. We say that the system is dissipative in X with the supply rate $w(u, y)$ if there exists a function $S(x)$, $S(0) = 0$, such that for all $x \in X$*

$$S(x) \geq 0 \quad \text{and} \quad S(x(T)) - S(x(0)) \leq \int_0^T w(u(t), y(t)) dt \quad (2.4)$$

for all $u \in U$ and all $T \geq 0$ such that $x(t) \in X$ for all $t \in [0, T]$. The function $S(x)$ is then called a storage function. If the dissipativity inequality (2.4) is satisfied with the equality sign, i.e. $S(x(T)) - S(x(0)) = \int_0^T w(u(t), y(t)) dt$, the system is said to be conservative or lossless.

In our RLC-circuit example, the storage function S is the energy, w is the input power, and $\int_0^T w(u(t), y(t)) dt$ is the energy supplied to the system from the external sources. The system is dissipative if the increase in its energy during the interval $(0, T)$ is not bigger than the energy supplied to the system during that interval.

Definition 2.2 [SJK97] *Passivity is dissipativity with the supply rate $w(u(t), y(t)) = u^T(t)y(t)$.*

If the storage function $S(x)$ is differentiable, the dissipation inequality (2.4) is equivalently written as

$$\dot{S}(x(t)) \leq w(u(t), y(t))$$

Again, the interpretation is that the rate of increase of energy is not bigger than the input power.

Throughout the thesis, we will assume that the storage function is differentiable. Under the assumption of a differentiable storage function $S(x)$, the following terminology is used:

Definition 2.3 [Kha02] *The dissipative system (2.1)-(2.2) with differentiable storage function $S(x)$ is said to be*

- input-feedforward passive if $\dot{S} \leq u^T y - u^T \nu(u)$ for some function $\nu(\cdot)$.
- input strictly passive if $\dot{S} \leq u^T y - u^T \nu(u)$ and $u^T \nu(u) > 0, \forall u \neq 0$.
- output-feedback passive if $\dot{S} \leq u^T y - y^T \rho(y)$ for some function $\rho(\cdot)$.
- output strictly passive if $\dot{S} \leq u^T y - y^T \rho(y)$ and $y^T \rho(y) > 0, \forall y \neq 0$.
- strictly passive if $\dot{S} \leq u^T y - \zeta(x)$ for some positive definite function $\zeta(\cdot)$.

In all cases, the inequality should hold for all (x, u) .

We also introduce the notion of *strong passivity* that will be used throughout the thesis.

Definition 2.4 (Strong passivity) *We say that the system (2.1)-(2.2) is strongly passive if it is passive and its storage function additionally satisfies the following assumptions:*

1. (smoothness) $S(x)$ is continuously differentiable (\mathcal{C}^1) in \mathbb{R}^n and twice continuously differentiable (\mathcal{C}^2) in a neighborhood of the origin.
2. (LYAPUNOV) $S(x)$ is positive definite, $S(x) > 0$, and radially unbounded, i.e. $S(x) \rightarrow \infty$ as $|x| \rightarrow \infty$.
3. (locally quadratic) The Hessian of $S(x)$ evaluated at zero $\left. \frac{\partial^2 S(x)}{\partial x^2} \right|_{x=0}$ is a symmetric positive definite matrix $P = P^T > 0$.

As it is well-known, these assumptions are always satisfied in the (detectable) linear case because linear passive systems have quadratic positive definite storage functions [Wil72]. In general, these assumptions are convenient to link the passivity of the system to the stability properties of the zero input system since $S(x)$ then serves as a (global) LYAPUNOV function.

Example 2.5 *An integrator is the simplest example of a dynamic passive system. Consider system*

$$\begin{aligned}\dot{x} &= u \\ y &= x\end{aligned}$$

This system is strongly passive with $S(x) = \frac{1}{2}x^2$ as a storage function.

2.1.2 Passivity of memoryless nonlinearities

We consider memoryless nonlinearities of the form $y = \phi(t, u)$, where $\phi : [0, \infty) \times \mathbb{R}^p \rightarrow \mathbb{R}^p$. Since their state space is void, Definitions 2.2 and 2.3 directly apply to the special case of (possibly time-varying) memoryless nonlinearities by considering that their storage function is identically zero ($S \equiv 0$). Passivity for a single input - single output (SISO) memoryless nonlinearity geometrically means that the $u - y$ curve must lie in the first and third quadrants, as shown in Figure 2.2 (a) and (b). When this condition is respected, we also say that the nonlinearity belongs to the sector

2.1. PASSIVITY

$[0, \infty]$, where zero and infinity are the slopes of the boundaries of the first-third quadrant region. The graphical representation is valid even when ϕ is time varying. In this case, the $u - y$ curve will be changing with time, but will always belong to the sector $[0, \infty]$. For a vector function, we can give a graphical representation in the special case when $\phi(t, u)$ is decoupled in the sense that $\phi_i(t, u)$ depends only on u_i . In this case, the graph of each component belongs to the sector $[0, \infty]$. In the general case, such graphical representation is not possible.

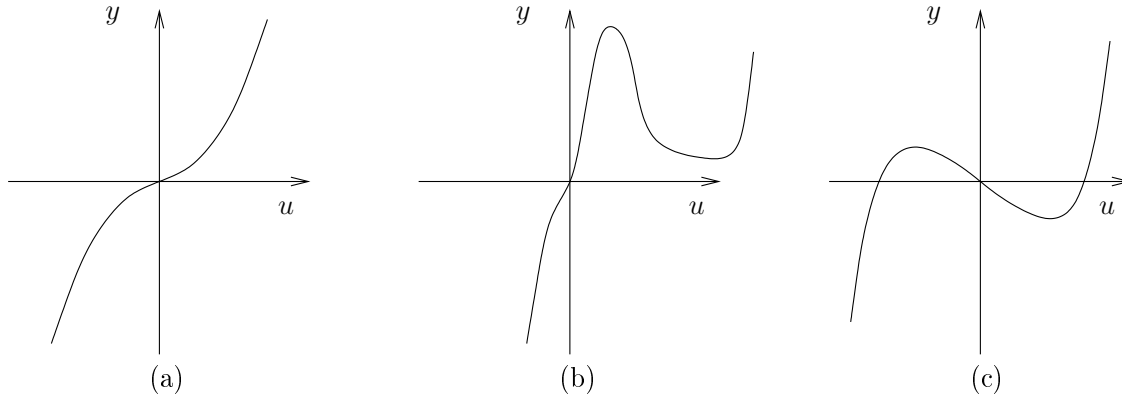


Figure 2.2: (a) and (b) are examples of passive nonlinearities; (c) is an example of a non-passive nonlinearity.

2.1.3 Loop transformations

In this section we present loop transformations which extend the utility of passivity theorems. Starting with a feedback interconnection in which one of the two feedback components is not passive or does not satisfy a condition that is needed in one of the passivity theorems, we may be able to reconfigure the feedback interconnection into an equivalent interconnection that has the desired properties. We illustrate the process for loop transformations with dynamic multipliers, as show in Figure 2.3.

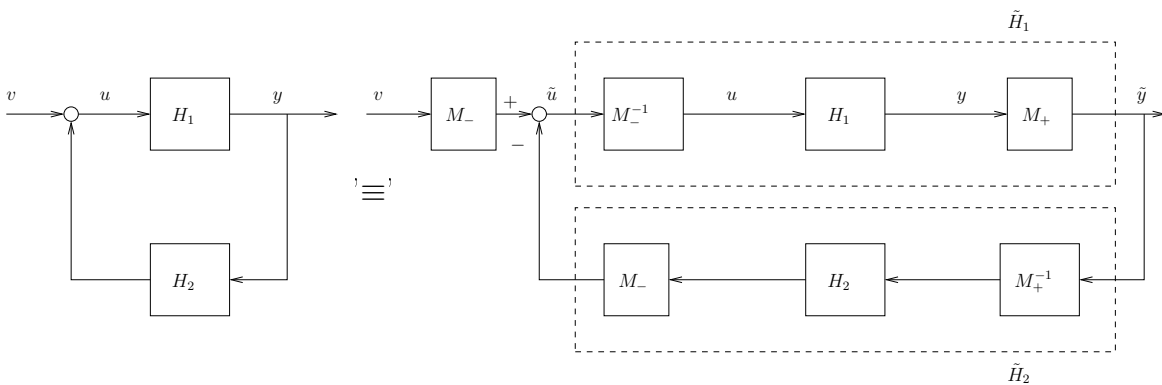


Figure 2.3: Loop transformation with dynamic multipliers.

Pre (resp. post) multiplying H_1 by a specific transfer function can be nullified by post (resp. pre)

multiplying H_2 by the inverse of this transfer function, provided that this inverse exists. This leads to an equivalent feedback system that is represented in its general form in Figure 2.3. The interest of such loop transformation is the ability to transform a feedback system that does not satisfy the conditions needed by one of the passivity theorem into an equivalent one that does it, thereby extending the utility of passivity theorems.

2.1.4 Passivity versus LYAPUNOV stability

In this section, we recall the important links that exist between passivity and LYAPUNOV stability. For the proofs of the different lemmas and theorems, the reader is referred to [Kha02]. We first recall the definitions of LYAPUNOV and asymptotic stability.

2.1.4.1 LYAPUNOV stability

LYAPUNOV stability and asymptotic stability are properties not of a dynamical system as a whole, but rather of its individual solutions.

Consider the time-invariant system

$$\dot{x} = f(x) \tag{2.5}$$

where $x \in \mathbb{R}^n$ and $f : \mathbb{R}^n \rightarrow \mathbb{R}^n$ is locally LIPSCHITZ continuous. The solution of (2.5) which starts from x_0 at time $t_0 \in \mathbb{R}$ is denoted as $x(t; x_0, t_0)$, so that $x(t_0; x_0, t_0) = x_0$. Because the solutions of (2.5) are invariant under translation of t_0 , that is, $x(t + T; x_0, t_0 + T) = x(t; x_0, t_0)$, the stability properties of $x(t; x_0, t_0)$ are *uniform*, that is they do not depend on t_0 . Without loss of generality, we assume $t_0 = 0$ and write $x(t; x_0)$ instead of $x(t; x_0, 0)$. LYAPUNOV stability is a continuity property of $x(t; x_0)$ with respect to x_0 . If the initial state x_0 is perturbed to \tilde{x}_0 , then, for stability, the perturbed solution $x(t; \tilde{x}_0)$ is required to stay close to $x(t; x_0)$ for all $t \geq 0$. In addition for asymptotic stability, the error $x(t; \tilde{x}_0) - x(t; x_0)$ is required to vanish as $t \rightarrow \infty$.

Definition 2.6 [SJK97] *The solution $x(t; x_0)$ of (2.5) is*

- bounded, *if there exists a constant $K(x_0)$ such that*

$$|x(t; x_0)| \leq K(x_0), \forall t \geq 0;$$

- stable, *if for each $\epsilon > 0$ there exists $\delta(\epsilon) > 0$ such that*

$$|\tilde{x}_0 - x_0| < \delta(\epsilon) \Rightarrow |x(t; \tilde{x}_0) - x(t; x_0)| < \epsilon, \forall t \geq 0; \tag{2.6}$$

- attractive, *if there exists an $r(x_0) > 0$ such that*

$$|\tilde{x}_0 - x_0| < r(x_0) \Rightarrow \lim_{t \rightarrow \infty} |x(t; \tilde{x}_0) - x(t; x_0)| = 0; \tag{2.7}$$

- asymptotically stable, *if it is stable and attractive;*
- unstable, *if it is not stable.*

2.1. PASSIVITY

Some solutions of a given system may be stable and some unstable. In particular, (2.5) may have stable and unstable *equilibria*, that is, constant solutions $x(t; x_e) \equiv x_e$ satisfying $f(x_e) = 0$. The above definitions of stability properties of an equilibrium x_e involve only initial states close to x_e , that is, they are *local*. If an equilibrium is attractive, then it has a *region of attraction*, i.e. a set Ω of initial states x_0 such that $x(t; x_0) \rightarrow x_e$ as $t \rightarrow \infty$ for all $x_0 \in \Omega$. In this thesis, our attention will be focused on *global* stability properties.

Definition 2.7 [SJK97] *An equilibrium point of (2.5) is*

- globally stable (GS) if it is stable and if all the solutions of (2.5) are bounded.
- globally asymptotically stable (GAS) if it is asymptotically stable and its region of attraction is \mathbb{R}^n .

Any equilibrium under investigation can be translated to the origin by redefining the state as $z = x - x_e$. For simplicity, we will assume that the translation has been performed, that is $f(0) = 0$, and thus the equilibrium under investigation is $z = 0$. When, for brevity, we say that “the system (2.5) is GS or GAS”, we mean that its equilibrium $z = 0$ is GS or GAS. While GAS of $z = 0$ prevents the existence of other equilibria, the reader should keep in mind that it is not so with GS.

The most often used method to establish stability of equilibrium points of nonlinear systems is the direct method of LYAPUNOV. The direct method of LYAPUNOV aims at determining the stability properties of $x(t; x_0)$ from the properties of $f(x)$ and its relationship with a positive definite function $V(x)$. Global results are obtained if this function is *radially unbounded*, i.e. $V(x) \rightarrow \infty$ as $|x| \rightarrow \infty$.

Theorem 2.8 (LYAPUNOV stability Theorem) [SJK97] *Let $x = 0$ be an equilibrium of (2.5) and suppose f is locally LIPSCHITZ continuous. Let $V : \mathbb{R}^n \rightarrow \mathbb{R}_{>0}$ be a C^1 positive definite and radially unbounded function $V(x)$ such that*

$$\dot{V} = \frac{\partial V}{\partial x}(x)f(x) \leq 0, \quad \forall x \in \mathbb{R}^n$$

Then $x = 0$ is GS and all solutions of (2.5) converge to the set E where $\dot{V}(x) \equiv 0$. If \dot{V} is negative definite, then $x = 0$ is GAS.

For a sharper characterization of convergence properties we employ the concept of *invariant sets*.

Definition 2.9 [SJK97] *A set M is called an invariant set of (2.5) if any solution $x(t)$ that belongs to M at some time t_1 belongs to M for all future and past time, i.e.*

$$x(t_1) \in M \Rightarrow x(t) \in M, \quad \forall t \in \mathbb{R}$$

Definition 2.10 [SJK97] *A set P is positively invariant if this is true for all future time only, i.e.*

$$x(t_1) \in P \Rightarrow x(t) \in P, \quad \forall t \geq t_1$$

An important result describing convergence to an invariant set is LA SALLE’s Invariance Principle.

Theorem 2.11 (LA SALLE’s Invariance Principle) [SJK97] *Let Ω be a positively invariant set of (2.5). Suppose that every solution starting in Ω converges to a set $E \subset \Omega$ and let M be the largest invariant set contained in E . Then, every bounded solution starting in Ω converges to M as $t \rightarrow \infty$.*

An application of the Invariance Principle is the following asymptotic stability condition.

Corollary 2.12 (Asymptotic stability) [SJK97] *Under the assumptions of Theorem 2.8, let $E = \{x \in \mathbb{R}^n \mid \dot{V}(x) = 0\}$. If no solution other than $x(t) \equiv 0$ can stay for all t in E , then the equilibrium $x = 0$ is GAS.*

While the LYAPUNOV stability theorem (Theorem 2.8) establishes that the solutions are bounded and converge to the set E where $\dot{V} \equiv 0$, Theorem 2.11 sharpens this result by establishing the convergence to a subset of E . Thanks to its invariance, this subset can be found by examining only those solutions which, having started in E , remain in E for all t .

In control systems, such invariance and convergence results are made possible by system’s observability properties. Typically, the convergence of the system output y to zero is established first, and then the next task is to investigate whether some (or all) of the states converge to zero. For this task we need to examine only the solutions satisfying $y(t) \equiv 0$. If it is known beforehand that $y(t) \equiv 0$ implies $x(t) \equiv 0$, then the asymptotic stability of $x = 0$ is established, as in Corollary 2.12.

2.1.4.2 Passivity and LYAPUNOV stability

The definitions of dissipativity and passivity do not require that the storage function $S(x)$ is positive definite. They are also satisfied if $S(x)$ is only positive *semidefinite*. As a consequence, in the presence of an unobservable unstable part of the system, they allow $x = 0$ to be unstable. For instance, the unstable system

$$\begin{aligned}\dot{x}_1 &= x_1 \\ \dot{x}_2 &= u \\ y &= x_2\end{aligned}$$

is passive with the storage function $S = \frac{1}{2}x_2^2$.

For passivity to imply LYAPUNOV stability, we must exclude such situations. In linear systems this is achieved with a detectability assumption, which requires that the unobservable part of the system is asymptotically stable. Zero-state detectability defines an analogous concept for nonlinear systems (see [SJK97] or [vdS00]).

Definition 2.13 [SJK97] *Consider the system (2.1)-(2.2) with zero input, that is $\dot{x} = f(x, 0)$ and $y = h(x, 0)$, and let $Z \subset \mathbb{R}^n$ be its largest positively invariant set contained in $\{x \in \mathbb{R}^n \mid y = h(x, 0) = 0\}$. We say that the zero input system is zero-state detectable (ZSD) if $x = 0$ is asymptotically stable conditionally to Z , that is if (2.6) and (2.7) hold for any $x_0 \in Z$. If $Z = \{0\}$, we say that the zero input system is zero-state observable (ZSO).*

For a linear system, the notions of detectability and zero-state detectability are equivalent.

Whenever we use the ZSD property to establish a *global* result, we assume that $x = 0$ is GAS conditionally to Z . One of the benefits from the ZSD property is that passivity and stability are connected even when the storage function $S(x)$ is only positive semidefinite.

Lemma 2.14 [SJK97] Consider the system (2.1)-(2.2). Suppose that this system is passive with a \mathcal{C}^1 storage function $S(x)$ and $h(x, u)$ is \mathcal{C}^1 in u for all x .

Then,

(1) the origin of $\dot{x} = f(x, 0)$ is stable if

- the storage function $S(x)$ is positive definite, or
- the system is ZSD.

(2) the origin of $\dot{x} = f(x, 0)$ is asymptotically stable if the system is

- strictly passive, or
- output strictly passive and ZSD.

(3) when there is no throughput, $y = h(x)$, then the feedback $u = -y$ achieves asymptotic stability of $x = 0$ if and only if the system is ZSD.

Furthermore, if the storage function is radially unbounded, the origin will be globally asymptotically stable.

2.1.5 Interconnections of passive systems

Consider the feedback interconnection of Figure 2.4 where each of the feedback components H_1 and H_2 is either a time-invariant dynamical system represented by the state model

$$\dot{x}_i = f_i(x_i, e_i) \tag{2.8}$$

$$y_i = h_i(x_i, e_i), \tag{2.9}$$

with $f_i(0, 0) = 0$ and $h_i(0, 0) = 0$, $i \in \{1, 2\}$, or a (possibly time-varying) memoryless function represented by

$$y_i = \phi_i(t, e_i), \tag{2.10}$$

$i \in \{1, 2\}$.

We are interested in using passivity properties of the feedback components H_1 and H_2 to analyse stability of the parallel and feedback interconnections. Assuming that both H_1 and H_2 are in the form (2.8)-(2.9), we first must make sure that the interconnection is also in the form (2.8)-(2.9). This is obviously true for the parallel interconnection. However the feedback interconnection may not be in the form (2.8)-(2.9) and may fail to have a well-defined solution. Let us consider the two possibilities (2.8)-(2.9) and (2.8)-(2.10) separately.

When both components H_1 and H_2 are dynamical systems, the closed-loop state model takes the form

$$\dot{x} = f(x, u) \tag{2.11}$$

$$y = h(x, u) \tag{2.12}$$

where $x = (x_1^T, x_2^T)^T$, $u = (u_1^T, u_2^T)^T$, and $y = (y_1^T, y_2^T)^T$. We assume that f is locally LIPSCHITZ, h is continuous, $f(0, 0) = 0$, and $h(0, 0) = 0$. It can be verified that the feedback interconnection will have a well-defined state model if the equations

$$e_1 = u_1 - h_2(x_2, e_2) \tag{2.13}$$

$$e_2 = u_2 + h_1(x_1, e_1) \tag{2.14}$$

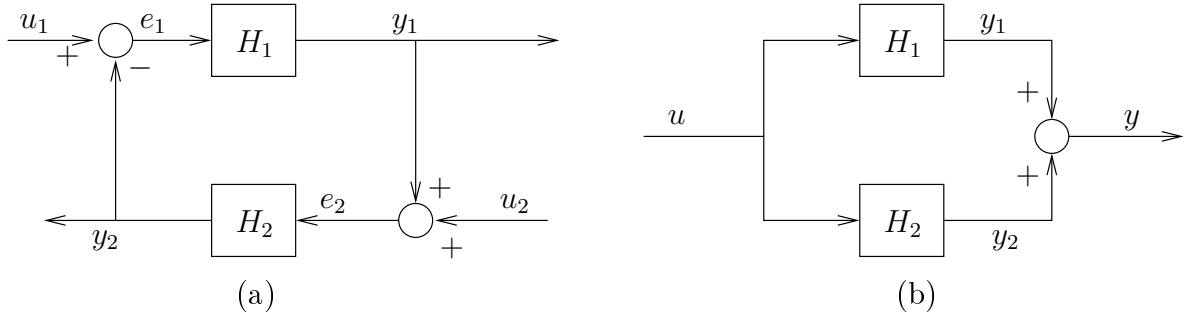


Figure 2.4: (a) Feedback interconnection of H_1 and H_2 . (b) Parallel interconnection of H_1 and H_2 .

have a unique solution (e_1, e_2) for every (x_1, x_2, u_1, u_2) . The properties $f(0, 0) = 0$ and $h(0, 0) = 0$ follow from $f_i(0, 0) = 0$ and $h_i(0, 0) = 0$. It is also easy to see that (2.13)-(2.14) will always have a unique solution if h_1 is independent of e_1 or h_2 is independent of e_2 . In this case, the functions f and h of the closed-loop state model inherit smoothness properties of the functions f_i and h_i of the feedback components. In particular, if f_i and h_i are locally LIPSCHITZ, so are f and h . For linear systems, requiring h_i to be independent of e_i is equivalent to requiring the transfer function of H_i to be strictly proper.

When one component, say H_1 , is a dynamical system, while the other one is a memoryless function, the closed-loop state model takes the form

$$\dot{x} = f(t, x, u) \quad (2.15)$$

$$y = h(t, x, u) \quad (2.16)$$

where $x = x_1$, $u = (u_1^T, u_2^T)^T$, and $y = (y_1^T, y_2^T)^T$. We assume that f is piecewise-continuous in t and locally LIPSCHITZ in (x, u) , h is piecewise continuous in t and continuous in (x, u) , $f(t, 0, 0) = 0$, and $h(t, 0, 0) = 0$. The feedback interconnection will have a well-defined state model if the equations

$$\begin{aligned} e_1 &= u_1 - \phi_2(t, e_2) \\ e_2 &= u_2 + h_1(x_1, e_1) \end{aligned}$$

have a unique solution (e_1, e_2) for every (x_1, t, u_1, u_2) . This will be always the case when h_1 is independent of e_1 . The case when both components are memoryless functions is less important and follows directly as a special case when the state x does not exist. In this case, the feedback interconnection is represented by $y = h(t, u)$. Theorem 2.15 constitutes the main property for parallel and feedback interconnections of passive systems.

Theorem 2.15 [Kha02] *The feedback and parallel interconnection of passive systems is passive.*

The proof is straightforward by taking as storage function for the interconnection system the sum of the storage functions of each system and taking into account the interconnection rules.

Using Theorem 2.15 and the results on stability properties of passive systems, we can arrive at some straightforward conclusions on stability of the feedback interconnection. We are interested in studying stability and asymptotic stability of the origin of the feedback closed-loop system when $u = 0$. Stability of the origin follows trivially from Theorem 2.15 and the first part of Lemma 2.14.

Therefore, we focus our attention on studying asymptotic stability. The next theorem is an immediate consequence of Theorem 2.15 and Lemma 2.14.

Theorem 2.16 [Kha02] *Consider the feedback interconnection of two time-invariant dynamical systems of the form (2.8)-(2.9). The origin of the closed-loop system (2.11) (when $u = 0$) is asymptotically stable if*

- *both feedback components are strictly passive, or*
- *both feedback components are output strictly passive and ZSD, or*
- *one component is strictly passive and the other one is output strictly passive and ZSD.*

Furthermore, if the storage function for each component is radially unbounded, the origin is globally asymptotically stable.

The proof uses a simple idea, namely, that the sum of the storage functions for the feedback components is a LYAPUNOV function for the feedback interconnection. In fact, this is too restrictive since to show that $\dot{S} = \dot{S}_1 + \dot{S}_2 \leq 0$, we insist that both $\dot{S}_1 \leq 0$ and $\dot{S}_2 \leq 0$. Clearly, this is not necessary. One term, say \dot{S}_1 , could be positive over some region as long as $\dot{S} \leq 0$ over the same region. This is a manifestation of the idea that shortage of passivity of one component can be compensated for by the excess of passivity of the other component.

When the feedback interconnection has a dynamical system as one component and a memoryless function as the other component, we can perform LYAPUNOV analysis by using the storage function of the dynamical system as a LYAPUNOV function. It is important, however, to distinguish between the time-invariant and the time-varying memoryless functions, for in the latter case the closed-loop system will be nonautonomous and we cannot apply LA SALLE invariance principle. We treat these two cases separately in the next two theorems.

Theorem 2.17 [Kha02] *Consider the feedback interconnection of a strictly passive, time-invariant, dynamical system of the form (2.8)-(2.9) with a passive (possibly time-varying) memoryless function of the form (2.10). Then, the origin of the closed-loop system (2.15) (when $u = 0$) is uniformly asymptotically stable. Furthermore, if the storage function for the dynamical system is radially unbounded, the origin will be globally uniformly asymptotically stable.*

Theorem 2.18 [Kha02] *Consider the feedback interconnection of a time-invariant dynamical system H_1 of the form (2.8)-(2.9) with a time-invariant memoryless function H_2 of the form (2.10). Suppose that H_1 is ZSD and has a positive definite storage function, which satisfies*

$$\dot{S}_1 \leq e_1^T y_1 - y_1^T \rho_1(y_1)$$

and that H_2 satisfies

$$e_2^T \nu_2(e_2) \leq e_2^T y_2$$

Then, the origin of the closed-loop system (2.15) (when $u = 0$) is asymptotically stable if

$$v^T (\rho_1(v) + \nu_2(v)) > 0, \quad \forall v \neq 0$$

Furthermore, if V_1 is radially unbounded, the origin will be globally asymptotically stable.

Theorem 2.18 is once again a manifestation of the idea that shortage of passivity in one component can be compensated for by excess of passivity in the other component.

2.1.6 Characterization of input-affine passive systems

Consider the input-affine system

$$\dot{x} = f(x) + g(x)u \quad (2.17)$$

$$y = h(x) \quad (2.18)$$

The passivity condition amounts to $\dot{S} = \frac{\partial S(x)}{\partial x}(f(x) + g(x)u) \leq u^T h(x)$, $\forall x \in \mathbb{R}^n$, $\forall u \in \mathbb{R}^p$, or equivalently (set first $u = 0$, and then use linearity in u) to the HILL-MOYLAN passivity conditions [HM76]

$$L_f S(x) \leq 0 \quad (2.19)$$

$$L_g S(x) = h^T(x) \quad (2.20)$$

where we have used the notation $L_f S(x) = \frac{\partial S(x)}{\partial x} f(x)$. If the system is linear

$$\dot{x} = Ax + Bu$$

$$y = Cx$$

then there exists a quadratic storage function $S(x) = x^T P x$, with $P = P^T \geq 0$, and the HILL-MOYLAN passivity conditions become algebraic

$$PA + A^T P \leq 0 \quad (2.21)$$

$$B^T P = C \quad (2.22)$$

The equivalence of the conditions (2.21)-(2.22) with the frequency-domain characterization of passivity was established by the celebrated KALMAN-YAKUBOVICH-POPOV lemma. Before the statement of the KYP lemma, we introduce the definition of a positive real transfer function.

Definition 2.19 [Kha02] *A $p \times p$ proper rational transfer function matrix $G(s)$ is called positive real if*

- *poles of all elements of $G(s)$ are in $\Re\{s\} \leq 0$,*
- *for all real ω for which $j\omega$ is not a pole of any element of $G(s)$, the matrix $G(j\omega) + G^T(-j\omega)$ is positive semidefinite, and*
- *any pure imaginary pole $j\omega$ of any element of $G(s)$ is a simple pole and the residue $\lim_{s \rightarrow j\omega} (s - j\omega)G(s)$ is positive semidefinite Hermitian.*

The transfer function $G(s)$ is called strictly positive real if $G(s - \epsilon)$ is positive real for some $\epsilon > 0$.

When $p = 1$, the second condition of Definition 2.19 reduces to $\Re\{G(j\omega)\} \geq 0$, $\forall \omega \in \mathbb{R}$, which holds when the NYQUIST plot of $G(j\omega)$ lies in the closed right-half complex plane. This is a condition that can be satisfied only if the relative degree of the transfer function is zero or one.

Lemma 2.20, presented hereafter, states the KALMAN-YAKUBOVICH-POPOV (KYP) lemma in the particular case when (A, B, C) is a minimal realization. Extensions of the KYP lemma to non-minimal realizations can be found in [IT87, TI88].

Lemma 2.20 (KALMAN-YAKUBOVICH-POPOV lemma) [Kha02] *Let $G(s) = C(sI - A)^{-1}B + D$ be a $p \times p$ transfer function matrix, where (A, B) is controllable and (A, C) is observable. Then, $G(s)$ is strictly positive real if and only if there exists $P = P^T > 0$, L , and W , and a positive constant ϵ such that*

$$\begin{aligned} PA + A^T P &= -L^T L - \epsilon P \\ PB &= C^T - L^T W \\ W^T W &= D + D^T \end{aligned}$$

For linear, throughput-free ($D = 0$), passive systems, possessing a minimal realization, the link with the HILL-MOYLAN conditions (2.21)-(2.22) is obvious. In the general case when $D \neq 0$, this link is expressed in Lemma 2.21.

Lemma 2.21 [Kha02] *The linear time-invariant minimal realization*

$$\begin{aligned} \dot{x} &= Ax + Bu \\ y &= Cx + Du \end{aligned}$$

with $G(s) = C(sI - A)^{-1}B + D$ is

- passive if $G(s)$ is positive real,
- strictly passive if $G(s)$ is strictly positive real.

2.1.7 Structural properties of input-affine passive systems

In this section, we consider two structural properties of input-affine passive systems. By structural we mean that they are invariant under feedback transformations of the form $u = \alpha(x) + \beta(x)v$. These two structural properties are the relative degree of input-affine passive systems and their weakly minimum phaseness.

2.1.7.1 Relative degree

The relative degree of a system is an integer that quantifies the number of times that the output must be differentiated w.r.t. time for the input to appear explicitly. The statement “the system has relative degree r ” means that the input appears explicitly for the first time in the r^{th} time derivative of the output. For SISO linear systems, the relative degree is the difference between the number of poles and zeros in the transfer function.

Consider the (MIMO) nonlinear input-affine system (2.17)-(2.18). This system has relative degree one at $x = 0$ if the matrix $L_g h(0)$ is invertible.

Lemma 2.22 [SJK97] *If the system (2.17)-(2.18) is passive with a C^2 storage function $S(x)$ then it has relative degree one at $x = 0$.*

For a proof the reader is referred to [SJK97].

2.1.7.2 Weakly minimum phaseness

The remaining dynamics when we impose the constraint $y(t) = h(x) \equiv 0$ is called the zero dynamics. If the zero dynamics is asymptotically stable, the initial system is said to be *minimum phase*. If the zero dynamics is only LYAPUNOV stable with a C^2 positive definite LYAPUNOV function, then the system is said to be *weakly minimum phase*.

Lemma 2.23 [SJK97] *If the system (2.17)-(2.18) is passive with a C^2 positive definite storage function $S(x)$ then it is weakly minimum phase.*

For a proof the reader is referred to [SJK97].

2.2 Absolute stability

Consider the feedback interconnection of Figure 2.5 where $G(s)$ represents a linear system and $\phi(\cdot)$ a memoryless nonlinearity. We assume that the external input $v = 0$. The unforced system is said to be *absolutely stable* if it has a globally (uniformly) asymptotically stable equilibrium point at the origin for all nonlinearities in a given sector. The problem was originally formulated by LURE and is sometimes called LURE's problem. The LURE problem has a very concrete motivation since it represents a basic feedback loop in automatic control. This (hard) problem motivated central developments of system theory. It has led to the emergence of several stability criteria which make use of the input-output properties of the linear block $G(s)$, and characterize classes of nonlinearities which ensure stability.

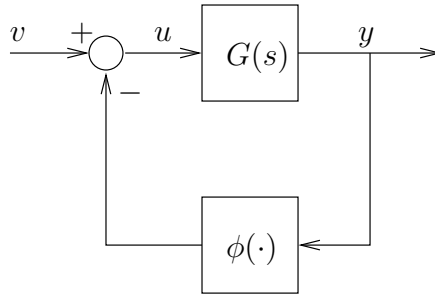


Figure 2.5: LURE feedback interconnection.

Passivity is useful for solving the LURE problem. A LYAPUNOV function can be chosen by using the passivity tools of the previous sections. In particular, if the closed-loop system can be represented as a feedback interconnection of two passive systems, then the sum of the two storage functions can be used as a LYAPUNOV function candidate for the closed-loop system. The use of loop transformations allows to cover various sectors and LYAPUNOV function candidates, leading to the circle [San64a, San64b] and POPOV [Pop62, Pop73] criteria which give frequency-domain sufficient conditions for absolute stability in the form of strict positive realness of certain transfer functions. In the single input - single output (SISO) case, both criteria can be applied graphically rendering them very easy to use in practice. Nowadays, numerical methods based on Integral Quadratic Constraints theory (IQC) are used to prove absolute stability of LURE feedback systems (see [MR97]).

2.3 Semi-global practical asymptotic stability

In this section, we present the notion of semi-global practical asymptotic stability for systems depending on a small parameter. This section is inspired by the results of MOREAU, summarized in [MA00]. The results of MOREAU show that if the reference system $\dot{x} = g(x)$ is globally asymptotically stable then, starting from an arbitrarily large set of initial conditions, the trajectories of the parameterized system $\dot{x} = f^\epsilon(x)$ converge to an arbitrarily small residual set around the origin when $\epsilon > 0$ is taken sufficiently small, under the assumption that trajectories of the parametrized system converge (uniformly on compact time intervals) to trajectories of the reference system. We restrict the presented results to the case of time-invariant dynamics. Nevertheless, the results presented in [MA00] hold for the general case of time-varying dynamics.

Consider two systems:

- a system that depends on a (small) parameter $\epsilon \in (0, \epsilon_0]$ ($\epsilon_0 \in (0, \infty)$)

$$\dot{x} = f^\epsilon(x) \tag{2.23}$$

- and a system

$$\dot{x} = g(x) \tag{2.24}$$

We assume that $f^\epsilon : \mathbb{R}^n \rightarrow \mathbb{R}^n$ and $g : \mathbb{R}^n \rightarrow \mathbb{R}^n$ are continuous and locally LIPSCHITZ. We do not assume forward completeness of the solutions, i.e. we do not exclude finite escape times. We denote by $x_{f^\epsilon}(t; x_0)$ (resp. $x_g(t; x_0)$) the solution of (2.23) (resp. the solution of (2.24)) that starts from x_0 at $t = 0$.

The main result of MOREAU relies on the assumption that trajectories of (2.23) converge to those of (2.24) in the following sense:

Convergence of trajectories² [MA00]: For every $T \in (0, \infty)$ and compact set $K \subset \mathbb{R}^n$ satisfying $\{(t; x_0) \in \mathbb{R} \times \mathbb{R}^n \mid t \in [0, T], x_0 \in K\} \subset \text{Dom}(x_g)$, for every $d \in (0, \infty)$, there exists $\epsilon^* \in (0, \epsilon_0]$ such that for all $x_0 \in K$ and for all $\epsilon \in (0, \epsilon^*)$

$$\begin{cases} x_{f^\epsilon}(t; x_0) \text{ exists} \\ |x_{f^\epsilon}(t; x_0) - x_g(t; x_0)| < d \end{cases} \quad \forall t \in [0, T] \tag{2.25}$$

In other words, it is required that trajectories of (2.23) converge on compact time intervals to trajectories of (2.24) as $\epsilon \rightarrow 0$, and furthermore we assume that this convergence occurs for all x_0 belonging to compact sets. It is important to notice that the assumed convergence is not stated in terms of vector fields, but in terms of trajectories; it is not assumed that f^ϵ converges point-wise to g as $\epsilon \rightarrow 0$.

Under the assumption of convergence of trajectories, GAS for (2.24) implies semi-global practical asymptotic stability for (2.23). We first recall the definition of semi-global practical asymptotic stability given by MOREAU [MA00].

Definition 2.24 [MA00] *Consider system (2.23). Assume that the assumptions on f^ϵ are satisfied. We call the origin of this system semi-globally practically asymptotically stable (SGPAS) if the following three conditions are satisfied:*

²In this definition $\text{Dom}(x_g)$ denotes the domain of definition of the function $(t; x_0) \rightarrow x_g(t; x_0)$ that defines the flow of the vector field g .

1. For every $c_2 \in (0, \infty)$, there exists $c_1 \in (0, \infty)$ and $\hat{\epsilon} \in (0, \epsilon_0]$ such that for all $x_0 \in \mathbb{R}^n$ with $|x_0| < c_1$ and for all $\epsilon \in (0, \hat{\epsilon})$

$$\begin{cases} x_{f^\epsilon}(t; x_0) \text{ exists} \\ |x_{f^\epsilon}(t; x_0)| < c_2 \end{cases} \quad \forall t \in (0, \infty]$$

2. For every $c_1 \in (0, \infty)$, there exists $c_2 \in (0, \infty)$ and $\hat{\epsilon} \in (0, \epsilon_0]$ such that for all $x_0 \in \mathbb{R}^n$ with $|x_0| < c_1$ and for all $\epsilon \in (0, \hat{\epsilon})$

$$\begin{cases} x_{f^\epsilon}(t; x_0) \text{ exists} \\ |x_{f^\epsilon}(t; x_0)| < c_2 \end{cases} \quad \forall t \in (0, \infty]$$

3. For every $c_1, c_2 \in (0, \infty)$, there exists $T \in (0, \infty)$ and $\hat{\epsilon} \in (0, \epsilon_0]$ such that for all $x_0 \in \mathbb{R}^n$ with $|x_0| < c_1$ and for all $\epsilon \in (0, \hat{\epsilon})$

$$\begin{cases} x_{f^\epsilon}(t; x_0) \text{ exists} & \forall t \in (0, \infty], \\ |x_{f^\epsilon}(t; x_0)| < c_2, & \forall t \in (T, \infty] \end{cases}$$

The notion of SGPAS may be interpreted as follows. Condition 1 of Definition 2.24 defines a practical version of stability of the origin. Condition 2 defines a practical version of boundedness. Condition 3 defines a practical version of global attractivity: all trajectories starting in an arbitrarily large ball centered at the origin end up in an arbitrarily small ball centered at the origin for appropriate – depending on the radii of the considered balls – values of the parameter ϵ . Notice that the origin is not required to be an equilibrium point in Definition 2.24, nor that the solution be forward complete.

Consider systems (2.23) and (2.24) introduced above satisfying the convergence of trajectories assumption. Assume that the origin is a GAS equilibrium of (2.24). It is well known that this does not imply that the origin is a GAS equilibrium point of (2.23) even if ϵ is small. It seems however reasonable to expect that (2.23) inherits some weaker notion of stability: the SGPAS. The following theorem asserts that this weaker stability property is indeed inherited by (2.23) if the origin is a GAS equilibrium of (2.24).

Theorem 2.25 (SGPAS theorem) [MA00] *Given systems (2.23) and (2.24) satisfying the convergence of trajectories assumption. If the origin is a GAS equilibrium point of (2.24), the origin of (2.23) is SGPAS.*

For a proof, the reader is referred to [MA00].

In Chapter 3, the SGPAS theorem will be very useful for the proving that the global stability of the equilibrium point at criticality is transmitted to the bifurcated solution for values of the parameter 'slightly larger' than the critical value.

2.4 Limit cycles and nonlinear oscillations

Oscillation is one of the most important phenomena that occur in dynamical systems. A system oscillates when it has a nontrivial periodic solution

$$x(t + T) = x(t), \quad \forall t \geq 0$$

for some $T > 0$. The word “nontrivial” is used to exclude constant solutions corresponding to equilibrium points. The image of a periodic solution in the state space is a closed trajectory, which is usually called a *periodic orbit* or a *closed orbit*. The simplest example of nontrivial periodic solution is given by the solutions of a second-order linear system with eigenvalues $\pm j\beta$. It is usually referred to as the *harmonic oscillator*. If we think of the harmonic oscillator as a model for a linear *LC* electrical circuit (see Figure 2.6), then we can see that the physical mechanism leading to these oscillations is a periodic exchange (without dissipation) of the energy stored in the capacitor’s electric field with the energy stored in the inductor’s magnetic field.

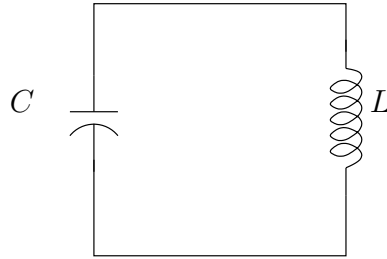


Figure 2.6: A linear LC circuit for the harmonic oscillator.

There are, however, two fundamental problems with this linear oscillator. The first problem is one of robustness. Infinitesimally small perturbations (linear or nonlinear) of the linear vector field will destroy the oscillation, i.e. the linear oscillator is not structurally stable. The second problem is that the amplitude of the oscillations is dependent on the initial conditions. These two fundamental problems can be eliminated in nonlinear oscillators. The VAN DER POL oscillator that we will consider in more details in Chapter 3 is the simplest example of such nonlinear oscillators. In the case of the harmonic oscillator, there is a continuum of closed orbits around the equilibrium point, while in the VAN DER POL oscillator, there is only one isolated periodic orbit. Such isolated periodic orbit is called a *limit cycle*. Isolated means that neighbouring trajectories are not closed; they spiral either toward or away from the limit cycle. Stable limit cycles are very important scientifically – they model systems that exhibit self-sustained oscillations. In other words, these systems oscillate even in the absence of external periodic forcing. Of the many examples that could be given, we mention only a few: the beating of a heart, the periodic firing of a pacemaker neuron, daily rhythms in human body temperature and hormone secretion, and chemical reactions that oscillate spontaneously. In each case, there is a limit oscillation of some preferred period, waveform, and amplitude. If the system is perturbed slightly, it always returns to the limit cycle. This leads us to the definition of stability of periodic solutions.

2.4.1 Stability of periodic solutions

Consider the autonomous system

$$\dot{x} = f(x) \tag{2.26}$$

where $f : D \rightarrow \mathbb{R}^n$ is continuously differentiable and $D \subseteq \mathbb{R}^n$ is a domain included into \mathbb{R}^n . Let $M \subseteq D$ be a closed invariant set of (2.26). Define an ϵ -neighborhood of M by

$$U_\epsilon = \{x \in \mathbb{R}^n \mid \text{dist}(x, M) < \epsilon\}$$

where $\text{dist}(x, M)$ is the minimum distance from x to a point in M , i.e.

$$\text{dist}(x, M) = \inf_{y \in M} |x - y|$$

Definition 2.26 [Kha02] *The closed invariant set M of (2.26) is*

- *stable if, for each $\epsilon > 0$, there is $\delta > 0$ such that*

$$x(0) \in U_\delta \Rightarrow x(t) \in U_\epsilon, \quad \forall t \geq 0$$

- *asymptotically stable if it is stable and δ can be chosen such that*

$$x(0) \in U_\delta \Rightarrow \lim_{t \rightarrow \infty} \text{dist}(x(t), M) = 0$$

In particular, we will apply these concepts to the specific case when the invariant set M is the closed orbit associated with a periodic solution. Let $u(t)$ be a nontrivial periodic solution of the autonomous system (2.26) with period T , and let γ be the closed orbit defined by

$$\gamma = \{x \in \mathbb{R}^n \mid x = u(t), 0 \leq t \leq T\}$$

The closed orbit γ is the image of $u(t)$ in the state space. It is an invariant set whose stability properties are characterized by Definition 2.26. Having defined the stability properties of closed orbits, we can now define the stability properties of periodic solutions.

Definition 2.27 [Kha02] *A nontrivial periodic solution $u(t)$ of (2.26) is*

- *orbitally stable if the closed orbit γ generated by $u(t)$ is stable.*
- *asymptotically orbitally stable if the closed orbit γ generated by $u(t)$ is asymptotically stable.*

2.5 Center manifold theory and bifurcations

The local asymptotic stability of an equilibrium point of a nonlinear system can be determined through the stability analysis of the linearized system if this equilibrium point is hyperbolic (HARTMAN-GROBMAN Theorem [Wig90, Theorem 2.2.6]). When the equilibrium point is not hyperbolic (i.e. the Jacobian matrix of the system linearized around this equilibrium point possesses at least one eigenvalue on the imaginary axis), the stability analysis of the equilibrium point depends on the nonlinear terms neglected through the linearization process.

For systems depending on a parameter μ , the topological character of equilibria can change at a critical value of the parameter, e.g. perhaps two branches of equilibria cross or a branch loses or gains stability. Such a state and parameter is called a *bifurcation point* of the parametrized vector field. A local *bifurcation* takes place at a parameter value where the system loses structural stability with respect to parameter variations, i.e. the phase portrait around the equilibrium point at the critical parameter value is not locally topologically conjugate³ to the phase portrait around the equilibrium

³If the local linearizations at two equilibria have no poles on the imaginary axis, the same number of strictly stable and the same number of strictly unstable poles then the local phase portraits are topologically conjugate.

at nearby parameter values. Therefore a local bifurcation is mathematically characterized by one or more eigenvalues of the linearized system crossing the imaginary axis.

A standard approach to analyzing the behavior of parametrized ordinary differential equations around a bifurcation point is to treat the parameter as an additional state variable with dynamic $\dot{\mu} = 0$ and to compute the center manifold of the extended dynamics through the bifurcation point and the dynamics restricted to this manifold (see [Wig90]). The *center manifold* is an invariant manifold of the differential equation which is tangent at the bifurcation point to the eigenspace of the neutrally stable eigenvalues. In practice, one does not compute the center manifold and its dynamics exactly. In most cases of interest, an approximation of degree two or three suffices. If the other eigenvalues are in the open left-half plane, then this part of the dynamics is locally asymptotically stable and therefore can be neglected in a local stability analysis around the bifurcation point.

2.5.1 The center manifold theorem

Consider the autonomous system

$$\dot{x} = f(x) \tag{2.27}$$

where $f : D \rightarrow \mathbb{R}^n$ is twice continuously differentiable and $D \subseteq \mathbb{R}^n$ is a domain that contains the origin $x = 0$. Suppose that the origin is a non-hyperbolic equilibrium point of (2.27). The center manifold theorem states that the stability properties of the origin can be determined by analyzing a lower order nonlinear system.

Equation (2.27) can be represented as

$$\dot{x} = Ax + (f(x) - Ax) = Ax + \tilde{f}(x), \tag{2.28}$$

where $A = \left. \frac{\partial f}{\partial x} \right|_{x=0}$ and $\tilde{f}(x) = f(x) - Ax$. $\tilde{f}(x)$ is twice continuously differentiable and $\tilde{f}(0) = 0$, $\left. \frac{\partial \tilde{f}}{\partial x} \right|_{x=0} = 0$. Since the origin $x = 0$ is assumed to be a non-hyperbolic equilibrium point of (2.27), let k be the number of eigenvalues with zero real parts and $m = n - k$ the number of eigenvalues with negative real parts. We can always find a similarity transformation matrix T that transforms A into a block diagonal matrix, i.e.

$$TAT^{-1} = \begin{pmatrix} A_1 & 0 \\ 0 & A_2 \end{pmatrix}$$

where all the eigenvalues of A_1 have zero real parts and all the eigenvalues of A_2 have negative real parts. Clearly, A_1 is $k \times k$ and A_2 is $m \times m$. The change of variables

$$\begin{pmatrix} y \\ z \end{pmatrix} = Tx, \quad y \in \mathbb{R}^k, \quad z \in \mathbb{R}^m$$

transforms (2.28) into the form

$$\begin{aligned} \dot{y} &= A_1 y + g_1(y, z) \\ \dot{z} &= A_2 z + g_2(y, z) \end{aligned} \tag{2.29}$$

where g_1 and g_2 inherit the properties of \tilde{f} . In particular, they are twice continuously differentiable and

$$g_i(0, 0) = 0, \quad \left. \frac{\partial g_i}{\partial y} \right|_{(y,z)=0} = 0, \quad \left. \frac{\partial g_i}{\partial z} \right|_{(y,z)=0} = 0 \tag{2.30}$$

for $i = 1, 2$. If $z = h(y)$ is an invariant manifold of (2.29) and h is smooth, then it is called a *center manifold* if

$$h(0) = 0, \quad \left. \frac{\partial h}{\partial y} \right|_{y=0} = 0.$$

Theorem 2.28 (Center manifold theorem) [Kha02] *If g_1 and g_2 are twice continuously differentiable and satisfy (2.30), all eigenvalues of A_1 have zero real parts, and all eigenvalues of A_2 have negative real parts, then there exists a constant $\delta > 0$ and a continuously differentiable function $h(y)$, defined for all $|y| < \delta$, such that $z = h(y)$ is a center manifold for (2.29).*

If the initial state of the system (2.29) lies in the center manifold, i.e. $z(0) = h(y(0))$, then the solution $(y(t), z(t))$ will lie in the manifold for all $t \geq 0$, i.e. $z(t) \equiv h(y(t))$. In this case, the motion of the system in the center manifold is described by the k -th order differential equation

$$\dot{y} = A_1 y + g_1(y, h(y)) \tag{2.31}$$

which we refer to as the *reduced system*. Even if $z(0) \neq h(y(0))$, it can be shown (see [Kha02]) that the stability properties of the origin are determined by the reduced system (2.31). This is summarized in the next theorem, known as the *reduction principle*.

Theorem 2.29 (Reduction principle) [Kha02] *Under the assumptions of Theorem 2.28, if the origin $y = 0$ of the reduced system (2.31) is asymptotically stable (respectively, unstable) then the origin of the full system (2.29) is also asymptotically stable (respectively, unstable).*

To use Theorem 2.29, we need to find the center manifold $z = h(y)$. The function h is a solution of the partial differential equation

$$\mathcal{N}(h(y)) = \frac{\partial h}{\partial y}(y) (A_1 y + g_1(y, h(y))) - A_2 h(y) - g_2(y, h(y)) = 0,$$

with boundary conditions

$$h(0) = 0, \quad \left. \frac{\partial h}{\partial y} \right|_{y=0} = 0.$$

This equation for h cannot be solved exactly in most cases (to do so would imply that a solution of the full system (2.29) has been found), but its solution can be approximated arbitrarily closely as a TAYLOR series in y . This result is summarized in Theorem 2.30.

Theorem 2.30 [Kha02] *If a continuously differentiable function $\phi(y)$ with $\phi(0) = 0$ and $\left. \frac{\partial \phi}{\partial y} \right|_{y=0} = 0$ can be found such that $\mathcal{N}(\phi(y)) = \mathcal{O}(|y|^p)$ for some $p > 1$, then for sufficiently small $|y|$,*

$$h(y) - \phi(y) = \mathcal{O}(|y|^p),$$

and the reduced system (2.31) can be represented as

$$\dot{y} = A_1 y + g_1(y, \phi(y)) + \mathcal{O}(|y|^{p+1}).$$

Remark 2.31 *In Theorem 2.30, the order of magnitude notation $f(|y|) = \mathcal{O}(|y|^p)$ is used as a shorthand notation for $|f(y)| \leq k|y|^p$ for sufficiently small $|y|$.*

2.6 The HOPF bifurcation theorem

In this section, we state (a version of) the HOPF bifurcation theorem and point out the important hypotheses required for the appearance of a limit cycle. Loosely, HOPF's theorem says that if an n -dimensional ordinary differential equation $\dot{x} = f(x, \mu)$ depends on a real parameter μ , and if on linearizing about an equilibrium point we find that pairs of complex conjugate eigenvalues of the linearized system cross the imaginary axis as μ varies through certain critical values, then for near-critical values of μ there exist limit cycles close to the equilibrium point. Just how near to criticality μ has to be is not determined, and indeed unless a certain rather complicated expression (we shall call it the curvature coefficient) is nonzero, the usual statement of the theorem does not guarantee existence at all. The sign of the curvature coefficient determines the stability of the limit cycle, and whether the limit cycle exists for subcritical ($\mu < \mu_0$) or supercritical ($\mu > \mu_0$) parameter values. (We shall adopt the convention that near $\mu = \mu_0$ the real parts of the eigenvalues increase as μ increases.)

HOPF first proved the theorem for analytic f by series expansion [Hop42]. The more recent geometrical approach presented in [MM76, HKW81] is less restrictive and more intuitive, though extremely heavy algebra is required in the detailed proof. In [Far94], another version of the HOPF bifurcation theorem based on the notion of h -asymptotic stability⁴ is given. This version of the HOPF bifurcation theorem is useful in order to avoid the computation of the curvature coefficient since h -asymptotic stability can be verified through the construction of an appropriate LYAPUNOV function. A graphical interpretation of the HOPF bifurcation theorem based on a rigorous version of the describing function method has been given by MEES in [Mee81]. The application of the graphical HOPF bifurcation theorem of MEES to the class of *passive oscillators* (defined in Chapter 3) is done in Appendix C.

The HOPF bifurcation theorem is an important tool for understanding systems described by ordinary differential equations because it is one of the few reliable methods for establishing the existence of limit cycles in high-dimensional systems. To use it effectively, one must be aware of both its advantages and its disadvantages. The principal advantage of the HOPF theorem in 'real-world' problems is its ability to handle high-dimensional systems; its principal disadvantage is the fact that the range of allowed values of μ is unknown, so one never knows if a given value of μ corresponds to the existence of a limit cycle. The HOPF theorem is thus 'local' in the sense that it only makes predictions for unspecified regions of parameter space and state space. These predictions may be valid over regions which are very big or very small, and the usual form of the theorem gives little help in determining their size. Nevertheless, we can reasonably expect the parameter region to be large as emphasized by MEES [MEE81]: "The HOPF theorem only makes predictions for an unspecified, probably small range of values of the bifurcation parameter. Nevertheless, experience tends to confirm that predictions often remain qualitatively correct even when the system is very far from bifurcation. This is not surprising if one imagines how the limit cycle grows out from equilibrium in the state space: even if the limit cycle bifurcates repeatedly, there will always be at least one limit cycle present (not necessarily stable). If it does not grow to infinite amplitude it can only disappear completely either by collapsing back into the equilibrium or by coalescing with another limit cycle having complementary stability properties: this other limit cycle would have to have been generated by an independent bifurcation process."

To introduce the HOPF bifurcation, consider a two-dimensional ordinary differential equation.

⁴A system is said to be h -asymptotically stable if its asymptotic stability is robust to perturbations of its vector field by term of order $h + 1$.

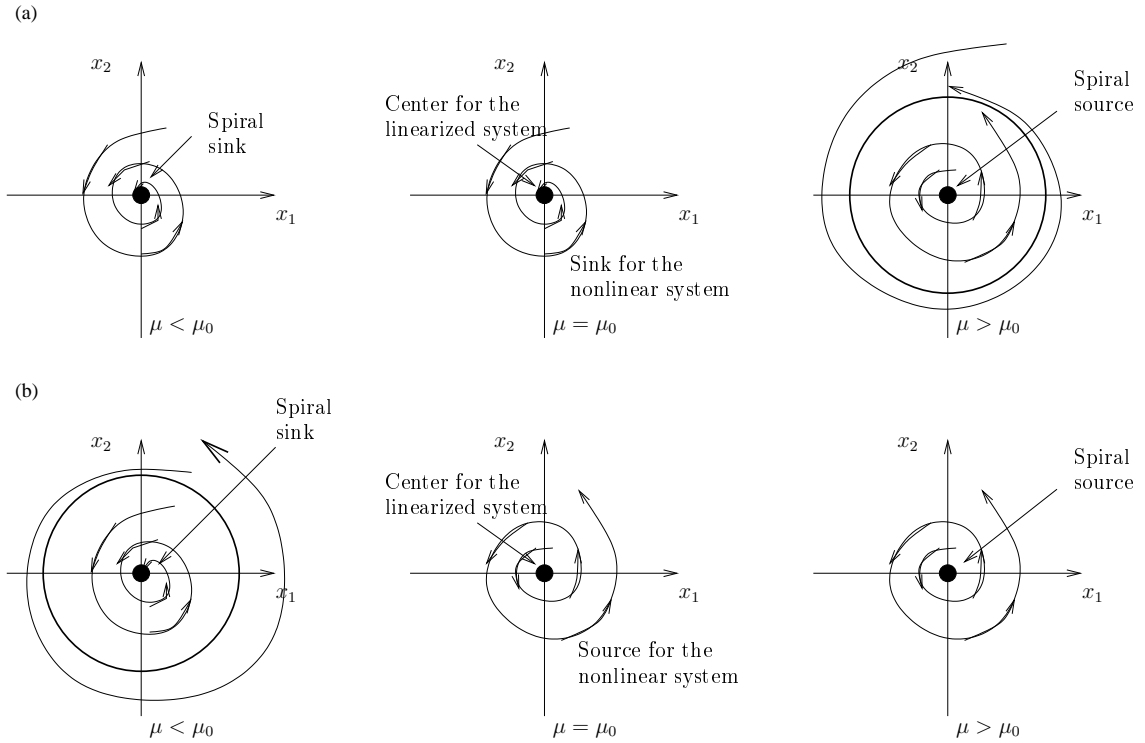


Figure 2.7: As μ increases, a sink changes to a source, expelling or absorbing a limit cycle. Line (a): supercritical bifurcation; Line (b): subcritical bifurcation.

Figure 2.7 shows how the phase portrait might alter as a parameter is varied, causing a spiral sink to become a spiral source. At a critical parameter value μ_0 , the equilibrium point is a center, i.e. the local linearization is equivalent to undamped simple harmonic motion of period $\frac{2\pi}{\omega}$, where $\pm j\omega$ are the eigenvalues of the Jacobian at criticality. When $\mu \neq \mu_0$, the system behaves as if it is linear very close to the equilibrium, but a little further out the effects of nonlinearity sometimes manifest themselves in the appearance of a limit cycle. In Figure 2.7 (a) the limit cycle grows outwards from the center as μ increases through μ_0 , and so the period is likely to be not far from $\frac{2\pi}{\omega}$. Figure 2.7 (b) shows another possibility in which the stability behavior of the equilibrium point (and therefore the behavior of the eigenvalues of the linearization) is indistinguishable from that of Figure 2.7 (a), but in which an unstable limit cycle collapses into the sink instead of a stable one growing out. Figure 2.8 represents what is happening in the (x_1, x_2, μ) space. Here the slices $\mu = \text{constant}$ are phase portraits. The “bowl” in each case represents a locus of limit cycles. In Figure 2.8 (a) corresponding to Figure 2.7 (a), an attracting limit cycle appears as μ reaches criticality, and grows as μ increases further, while in Figure 2.8 (b), corresponding to Figure 2.7 (b), a repelling limit cycle gets smaller as μ increases, disappearing as μ reaches criticality. In both cases, the equilibrium itself is attracting for $\mu < \mu_0$ and repelling for $\mu > \mu_0$. We can distinguish between the two cases by whether the bowl is the right way up or upside down, and in fact the curvature coefficient mentioned earlier is just a constant factor times the curvature coefficient of the bowl at the critical point. Note that if the curvature is non-vanishing the bowl is parabolic, so the radius of the limit cycle grows as $\sqrt{|\mu - \mu_0|}$ (i.e. much faster than $|\mu - \mu_0|$ at first). If the curvature vanishes, it is possible, though not certain, that the

2.6. THE HOPF BIFURCATION THEOREM

bowl is flat out to infinity, in which case the periodic orbits exist only at the critical parameter value. An example of this case is given by the linear system

$$\ddot{x} + \mu\dot{x} + x = 0$$

and an example where the curvature coefficient vanishes but the bowl is nevertheless not flat is given by

$$\ddot{x} + \mu\dot{x} + x = g(x, \dot{x})$$

where all partial derivatives of g at the origin vanish up to the 4th order, but there is a non-vanishing 5th partial derivative.

Global theorems do not transfer easily from 2 to n dimensions. The HOPF bifurcation theorem, however, is local and the transition is comparatively painless thanks to the invariant manifold theorem (see [Kha02]) which lets us take the eigenspace of the bifurcating eigenvalues as an approximation to a two dimensional manifold – the center manifold – that contains the limit cycle if there is one. The HOPF bifurcation theorem for two dimensions can thus be used to establish existence of a limit cycle in the center manifold, which of course implies existence in the whole space. The curvature coefficient has an extra contribution from the curvature of the center manifold relative to the eigenspace used to approximate it, and the limit cycle may, of course, attract some trajectories and repel others.

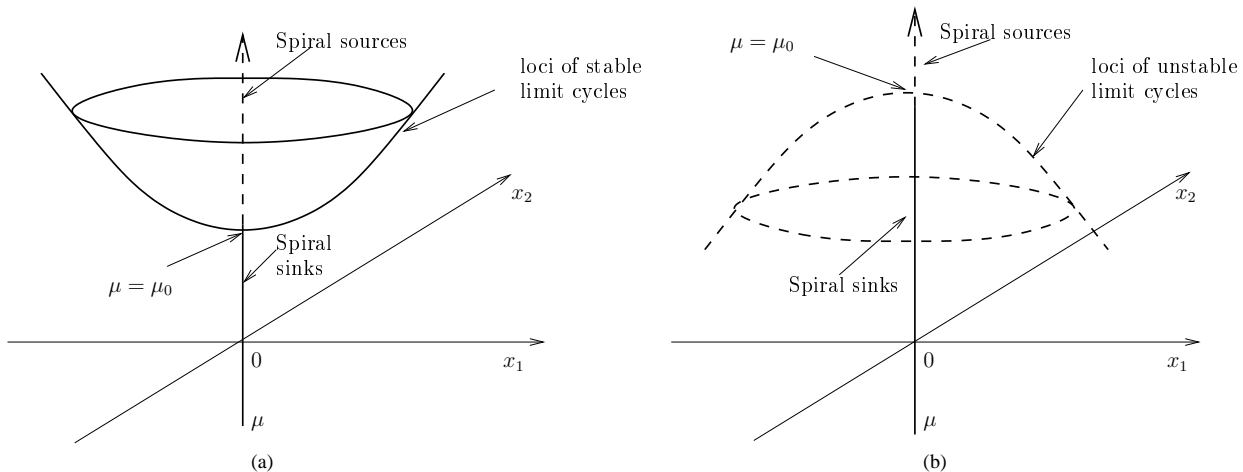


Figure 2.8: Figures 2.7 (a) and (b) in (x_1, x_2, μ) space. Dashed lines are repellers and solid lines are attractors.

We shall now state a theorem which, though not the most general statement of the HOPF bifurcation, is adequate for the majority of problems. A continuity condition is imposed to ensure that, in spite of possible losses of differentiability, the bowl is smooth enough so that its curvature can be calculated.

Theorem 2.32 (HOPF bifurcation theorem) [Mee81]

Let f^μ be a vector field on \mathbb{R}^n ($n \geq 2$), parametrized by $\mu \in \mathbb{R}$ and C^k ($k \geq 4$) jointly in $x \in \mathbb{R}^n$ and μ . Suppose $f^\mu(\hat{x}(\mu)) = 0$ for a locally unique point $\hat{x}(\mu)$ and write J^μ for the Jacobian $\frac{\partial f^\mu}{\partial x} |_{\hat{x}(\mu)}$. Suppose

(a) J^μ has a pair of complex conjugate eigenvalues $\lambda(\mu)$, $\bar{\lambda}(\mu)$ for which $\Re\{\lambda(\mu)\} = 0$ at $\mu = \mu_0$ and

$$\frac{d}{d\mu}\Re\{\lambda(\mu)\} > 0, \quad \Im\{\lambda(\mu)\} > 0$$

at $\mu = \mu_0$;

(b) Every eigenvalue $\nu(\mu)$ of J^μ except $\lambda(\mu)$ and $\bar{\lambda}(\mu)$ satisfies

$$\Re\{\nu(\mu_0)\} \neq 0;$$

(c) The curvature coefficient a given in (2.32) is nonzero.

Then there is a range either of positive or of negative values of $\Delta\mu \equiv \mu - \mu_0$ in which every value of μ corresponds to a unique limit cycle at a distance $\mathcal{O}(\sqrt{|\Delta\mu|})$ from $\hat{x}(\mu)$, and of period $\frac{2\pi}{\Im\{\lambda(\mu_0)\}} + \mathcal{O}(\Delta\mu)$. Furthermore,

(d) If $a < 0$ and $\Re\{\nu(\mu_0)\} < 0$, $\forall \nu$, the limit cycle is attracting, while if $a > 0$ and $\Re\{\nu(\mu_0)\} > 0$, the limit cycle is repelling.

The curvature coefficient a is given by (see [Mee81, eq. (6.1.4)])

$$\begin{aligned} a &= \Re\{\psi\}, \text{ where} \\ \psi &= u_p v_j v_k \bar{v}_l \left(f_{jkl}^p - 2f_{jm}^p J_{mq}^{-1} f_{kl}^q - f_{lm}^p (J - 2i\omega)_{mq}^{-1} f_{jk}^q \right) \end{aligned} \quad (2.32)$$

where $J = J^{\mu_0}$ and u^T and v are respectively left and right eigenvectors of J belonging to $\lambda(\mu_0)$, normalized so that $u^T v = 1$. Repeated subscripts imply summation from 1 to n and f_{jk}^p means $\frac{\partial f_p^\mu(x)}{\partial x_k \partial x_j}$ (where f_p^μ is the p^{th} component of f^μ) evaluated at $x = \hat{x}(\mu_0)$. For two-dimensional systems, it can be shown (see [Mee81, eq. (6.2.9)]) that the expression of the curvature coefficient is

$$\begin{aligned} a &= \frac{1}{16} (f_{111}^1 + f_{122}^1 + f_{112}^2 + f_{222}^2) \\ &\quad - \frac{1}{16\omega_0} (f_{12}^1 (f_{11}^1 + f_{22}^1) - f_{12}^2 (f_{11}^2 + f_{22}^2) - f_{11}^1 f_{11}^2 + f_{22}^1 f_{22}^2). \end{aligned} \quad (2.33)$$

where $\omega_0 = \omega(\mu_0) = \Im\{\lambda(\mu_0)\}$ and all derivatives are evaluated at $x = \hat{x}(\mu_0)$ and $\mu = \mu_0$.

The conditions (a) and (b) of the theorem are natural and are satisfied typically. If the equilibrium $\hat{x}(\mu)$ is linearly asymptotically stable for μ 's in an interval, i.e. all the eigenvalues of J^μ have negative real parts, then as μ is increased (or decreased) one may expect that at a certain value of μ either a negative eigenvalue crosses the imaginary axis or a pair of complex conjugate eigenvalues crosses into the right-hand half plane. It is "unlikely" and generically does not happen in a *one parameter* family of systems that two pairs of complex eigenvalues or a pair and a real eigenvalue cross simultaneously into the positive half of the complex plane resulting in the destabilization of the equilibrium point. (In the case the family depends on two or more parameters, such a situation may generically occur, giving rise to so-called "codimension two or higher bifurcations"; see e.g., LANGFORD [LAN79] and GOLUBITSKY-SCHAEFFER [GSS85]). Condition (a) insists that the eigenvalues cross the imaginary axis with nonzero speed, while condition (b) is stronger than necessary, but simplifies the uniqueness statement following (c). Unfortunately, condition (c) is not so easy to check because of the need

to find n^4 third partial derivatives and n^3 second partial derivatives when calculating a . This is unavoidable, since the whole point of the HOPF bifurcation is that it deals with the case when first derivatives do not determine behavior. If the curvature coefficient a is nonzero, its sign determines the local stability of the bifurcated limit cycle. The calculation of a quickly becomes tedious for high dimensional systems. In Chapter 3 we will show that for the class of feedback nonlinear system we consider, explicit computation of the curvature coefficient is unnecessary: the passivity properties of our systems imply that the limit cycle is attracting.

2.7 The KRONECKER product

The use of the KRONECKER product is very useful when considering interconnection of identical systems (see Chapter 4). In this section, we recall its definition and main properties. We refer the reader to [Gra81] for more details on the use and applications of the KRONECKER product.

For matrices A and B the notation $A \otimes B$ (the KRONECKER product of A and B) stands for the matrix composed of sub-matrices $A_{ij}B$, i.e.

$$A \otimes B = \begin{pmatrix} A_{11}B & A_{12}B & \cdots & A_{1n}B \\ A_{21}B & A_{22}B & \cdots & A_{2n}B \\ \vdots & \vdots & \ddots & \vdots \\ A_{m1}B & A_{m2}B & \cdots & A_{mn}B \end{pmatrix},$$

where A_{ij} , $i = 1, \dots, m$, $j = 1, \dots, n$, stands for the ij -th entry of the $m \times n$ matrix A .

The main properties of the KRONECKER product are summarized hereafter. In the following, we assume that A , B , C , and D are real valued matrices. Some identities only hold for appropriately dimensioned matrices.

- The KRONECKER product is a bi-linear operator. Given $\alpha \in \mathbb{R}$,

$$\begin{aligned} A \otimes (\alpha B) &= \alpha(A \otimes B) \\ (\alpha A) \otimes B &= \alpha(A \otimes B) \end{aligned}$$

- The KRONECKER product distributes over addition

$$\begin{aligned} (A + B) \otimes C &= (A \otimes C) + (B \otimes C) \\ A \otimes (B + C) &= (A \otimes B) + (A \otimes C) \end{aligned}$$

- The KRONECKER product is associative

$$(A \otimes B) \otimes C = A \otimes (B \otimes C)$$

- The KRONECKER product is not commutative

$$A \otimes B \neq B \otimes A$$

- Transpose distributes over the KRONECKER product

$$(A \otimes B)^T = A^T \otimes B^T$$

- When dimensions are appropriate, matrix multiplication satisfies

$$(A \otimes B)(C \otimes D) = AC \otimes BD$$

In particular, we have

1. $(A \otimes I_n)(I_m \otimes B) = (A \otimes B) = (I_m \otimes B)(A \otimes I_n)$ for $A \in \mathbb{R}^{m \times m}$ and $B \in \mathbb{R}^{n \times n}$,
2. $(A \otimes I_n)(I_m \otimes B) = (I_m \otimes B)A$ for $A \in \mathbb{R}^{m \times m}$ and $B \in \mathbb{R}^{n \times 1}$,
3. $(I_m \otimes C)(A \otimes I_n) = A(I_m \otimes C)$ for $A \in \mathbb{R}^{m \times m}$ and $C \in \mathbb{R}^{1 \times n}$.

- When A and B are square and full rank

$$(A \otimes B)^{-1} = (A^{-1} \otimes B^{-1})$$

- The determinant of KRONECKER product is

$$\det(A_{m \times m} \otimes B_{n \times n}) = \det(A)^n \det(B)^m$$

- The trace of KRONECKER product is

$$\text{trace}(A \otimes B) = \text{trace}(A) \text{trace}(B)$$

Chapter 3

Global results for one oscillator

Oscillators are dynamical systems that exhibit stable limit cycle oscillations. The emphasis in this chapter is on oscillators as *open* systems, that is, as systems that can be interconnected to other systems through their inputs and outputs. The aim is to show that dissipativity theory can be usefully applied to study the existence of limit cycle oscillations and their global stability properties and also to give simple explanations for the feedback mechanisms responsible for these oscillations. An obvious benefit of this dissipativity approach for the characterization of limit cycles is that it is not restricted to low-dimensional systems. A further benefit is that it is well-suited to the analysis of interconnections. The important topic of networks of oscillators will be treated in Chapter 4.

Starting from two of the most simple examples of nonlinear systems exhibiting globally attractive limit cycles oscillations, namely the VAN DER POL oscillator (Section 3.1) and the FITZHUGH-NAGUMO oscillator (Section 3.2), we present two different feedback oscillation mechanisms responsible for global limit cycle oscillations in (generalized) LURE feedback systems (Section 3.3). The limit cycle either results from a supercritical HOPF bifurcation or from the addition of a slow adaptation dynamic to a globally bistable system created through a supercritical pitchfork bifurcation. The first scenario provides a high-dimensional generalization of the VAN DER POL oscillator. Its energy interpretation fits the qualitative description of many physical oscillations, described as the lossless exchange of energy between two storage elements, regulated by a locally active but globally dissipative element. The second scenario provides a high-dimensional generalization of FITZHUGH-NAGUMO oscillators. Its energy interpretation fits the qualitative description of many oscillation mechanisms in biology, viewed as periodic switches between two quasi-stable steady-states. Since the central assumption for these results is *passivity*, we name the resulting global oscillators, *passive oscillators*. Central to the results of this chapter is the characterization of passive oscillators by the dissipation inequality

$$\dot{S} \leq (k - k^*) y^2 - y\phi(y) + uy. \quad (3.1)$$

Beyond the stability results, the dissipation inequality (3.1) provides an external characterization of oscillators which opens the way to a rigorous stability analysis of limit cycles in possibly high-dimensional systems and interconnections of such systems.

3.1 The VAN DER POL oscillator

In the early days of nonlinear dynamics, say from about 1920 to 1950, intensive research was done on nonlinear oscillations. One of the very first to propose a model for global limit cycle oscillations

was the Dutch electrical engineer BALTHAZAR VAN DER POL. VAN DER POL is nowadays considered as the pioneer engineer in the fields of radio and telecommunications. In an era when these topics were much less advanced than they are today, vacuum tubes were used to control the flow of electricity in the circuitry of transmitters and receivers. Contemporary with LORENZ, THOMPSON, and APPLETON, VAN DER POL experimented with oscillations in a vacuum tube triode circuit and concluded that all initial conditions converged to the same periodic orbit of finite amplitude. Since this behavior is different from the behavior of solutions of linear equations, VAN DER POL proposed a nonlinear differential equation, commonly referred to as the VAN DER POL equation, as a model for the behavior observed in the experiment. Since its introduction in the 1920's, the VAN DER POL equation has been a prototype for systems with self-excited limit cycle oscillations.

In this section, we will show that the VAN DER POL oscillator can be seen as a particular LURE feedback system and that the main feedback mechanism responsible for global oscillations in the VAN DER POL oscillator is the HOPF bifurcation.

3.1.1 VAN DER POL dynamics - Global results

Oscillations in physical systems generally result from a sustained energy exchange between two or several storage elements. In the VAN DER POL oscillator the two storage elements are a capacitor and an inductor, whereas the dissipation is regulated by means of a nonlinear static element. Figure 3.1 shows a sketch of the “tetrode multivibrator” circuit used in the earliest commercial radios and analyzed by VAN DER POL. The inductor and the capacitor are assumed to be linear, time invariant and passive, that is, $L > 0$ and $C > 0$. In VAN DER POL's day, the nonlinear static element was a vacuum tube; today it would be a semiconductor device implementing a twin-tunnel-diode circuit. This nonlinear element acts like an ordinary resistor for high currents, but like a negative resistor for low currents. Its current-voltage characteristic $i = \phi_R(v)$ resembles a cubic function with a negative slope at the origin, as represented on Figure 3.1. The function $\phi_R(\cdot)$ satisfies the conditions

$$\phi_R(0) = 0, \quad \phi'_R(0) = -R < 0, \quad \phi''_R(0) = 0, \quad \phi'''_R(0) > 0$$

and

$$\lim_{v \rightarrow +\infty} \phi_R(v) = +\infty, \quad \lim_{v \rightarrow -\infty} \phi_R(v) = -\infty,$$

where $\phi'_R(v)$ and $\phi''_R(v)$ are the first and second derivative of $\phi_R(v)$ with respect to v respectively. For the VAN DER POL equation,

$$\phi_R(v) = \frac{1}{3}v^3 - Rv \tag{3.2}$$

where R parameterizes the slope at the origin.

Using KIRCHHOFF's laws, the second order dynamics of the VAN DER POL circuit of Figure 3.1 are

$$LC \frac{d^2v}{dt^2} + L(v^2 - R) \frac{dv}{dt} + v = 0.$$

The foregoing equation can be written in a form that coincides with some well-known equations in nonlinear systems theory. To do that, let us change the time variable from t to $\tau = \frac{t}{\sqrt{LC}}$. Denoting the derivative of v with respect to τ by \dot{v} , we can rewrite the circuit equation as

$$\ddot{v} + \sqrt{\frac{L}{C}}(v^2 - R)\dot{v} + v = 0. \tag{3.3}$$

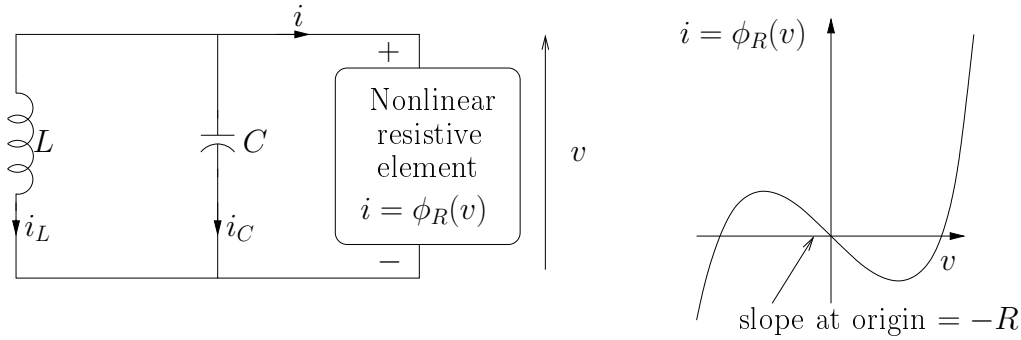


Figure 3.1: The VAN DER POL “tetrode multivibrator” circuit.

This last equation is known as the VAN DER POL equation and is a special case of LIÉNARD’s equation

$$\ddot{v} + f(v)\dot{v} + g(v) = 0, \quad (3.4)$$

where $f(v) = \sqrt{\frac{L}{C}}\phi'_R(v) = \sqrt{\frac{L}{C}}(v^2 - R)$ and $g(v) = v$. It can also be interpreted mechanically as the equation of motion for a unit mass subject to a nonlinear damping force $-f(v)\dot{v}$ and a nonlinear restoring force $-g(v)$. LIÉNARD systems are well known in the literature for their nonlinear oscillations properties. The following theorem states that LIÉNARD systems have a unique, stable limit cycle under appropriate hypotheses on $f(\cdot)$ and $g(\cdot)$. For a proof, see [JS87], [Gri90], or [Per91].

Theorem 3.1 (LIÉNARD’s Theorem) [Str00] *Suppose that $f(v)$ and $g(v)$ satisfy the following conditions:*

1. $f(v)$ and $g(v)$ are continuously differentiable for all $v \in \mathbb{R}$;
2. $g(-v) = -g(v)$ for all $v \in \mathbb{R}$;
3. $g(v) > 0$ for $v > 0$;
4. $f(-v) = f(v)$ for all v ;
5. The odd function $F(v) = \int_0^v f(u) du$ has exactly one positive zero at $v = a$, is negative for $0 < v < a$, is positive and nondecreasing for $v > a$, and $F(v) \rightarrow \infty$ as $v \rightarrow \infty$.

Then the system (3.4) has a unique, stable limit cycle surrounding the origin in the phase plane.

The assumptions on $g(v)$ mean that the restoring force acts like an ordinary spring, and tends to reduce any displacement, whereas the assumptions on $f(v)$ imply that the damping is negative at small $|v|$ and positive at large $|v|$. Since small oscillations are pumped up and large oscillations are damped down, it is not surprising that the system tends to settle into a self-sustained nonlinear oscillation at some intermediate amplitude.

3.1.2 The VAN DER POL model as a LURE feedback system

The VAN DER POL oscillator may be seen as a particular LURE feedback system that admits the block diagram representation of Figure 3.2, which is the feedback interconnection of a dynamical passive system with a static nonlinearity characterized by a negative slope at the origin.

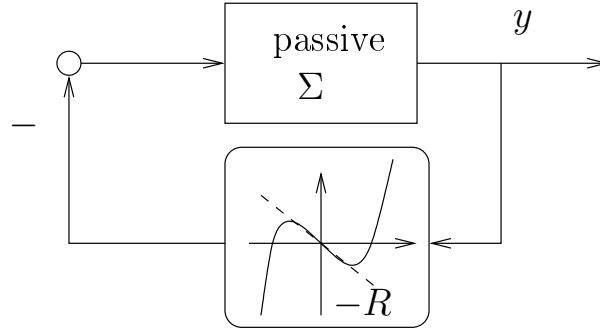


Figure 3.2: Block diagram corresponding to the LURE SISO nonlinear system interpretation of the VAN DER POL equation.

This is easily seen by choosing the state variables as the voltage across the capacitor and the current through the inductor. Denoting the state variables by $z_1 = i_L$ and $z_2 = v$, the state model is given by

$$\begin{aligned}\frac{dz_1}{dt} &= \frac{1}{L}z_2 \\ \frac{dz_2}{dt} &= -\frac{1}{C}\left(z_1 + \left(\frac{1}{3}z_2^3 - Rz_2\right)\right)\end{aligned}$$

Since the first model (3.3) has been written with respect to the time variable $\tau = \frac{t}{\sqrt{LC}}$, let us write this model with respect to τ . We obtain

$$\begin{aligned}\dot{z}_1 &= \sqrt{\frac{C}{L}}z_2 \\ \dot{z}_2 &= -\sqrt{\frac{L}{C}}\left(z_1 + \left(\frac{1}{3}z_2^3 - Rz_2\right)\right)\end{aligned}\tag{3.5}$$

Let us assume, without loss of generality, that $L = C = 1$. We then get the VAN DER POL state model

$$\begin{aligned}\dot{z}_1 &= z_2 \\ \dot{z}_2 &= -z_1 - \left(\frac{1}{3}z_2^3 - Rz_2\right)\end{aligned}\tag{3.6}$$

The state model (3.6) admits the block diagram representation depicted in Figure 3.3. Since an integrator is the most simple example of a passive dynamical system and the feedback interconnection of passive systems is passive (see Theorem 2.15), the block diagram representation given in Figure 3.3 clearly corresponds to the LURE feedback system of Figure 3.2. In Section 3.3, we will prove that the class of LURE feedback systems depicted in Figure 3.2 extends the fundamental properties of the VAN DER POL oscillator to high-dimensional systems, i.e. to feedback systems characterized by a unique limit cycle which is (almost) globally attractive.

The feedback mechanism responsible for global oscillations in the VAN DER POL model (3.6) is the HOPF bifurcation. This is easily seen by considering R as a parameter and performing a bifurcation analysis on the linearized system. The Jacobian matrix of the linearized system is

$$A = \begin{pmatrix} 0 & 1 \\ -1 & R \end{pmatrix}.$$

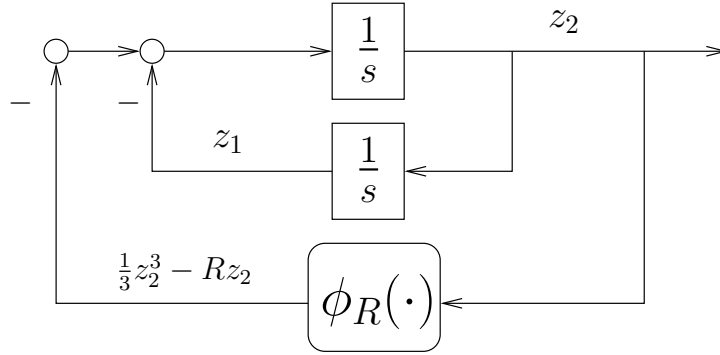


Figure 3.3: Block diagram representation of the VAN DER POL state model (3.6).

For negative values of R , the origin $(z_1, z_2) = (0, 0)$ is asymptotically stable whereas for positive values of R , the origin is unstable. For $R = 0$, the origin of the linearized system is marginally stable with two eigenvalues $(\pm i)$ on the imaginary axis. Moreover, as R is increased through 0, the corresponding eigenvalues cross the imaginary axis with nonzero speed. The assumptions of the HOPF bifurcation in Theorem 2.32 are thus satisfied. The type of HOPF bifurcation is determined by the sign of the curvature coefficient a given in (2.33), i.e.

$$a = \frac{1}{16} (f_{z_1 z_1 z_1}^1 + f_{z_1 z_2 z_2}^1 + f_{z_1 z_1 z_2}^2 + f_{z_2 z_2 z_2}^2) - \frac{1}{16} (f_{z_1 z_2}^1 (f_{z_1 z_1}^1 + f_{z_2 z_2}^1) - f_{z_1 z_2}^2 (f_{z_1 z_1}^2 + f_{z_2 z_2}^2) - f_{z_1 z_1}^1 f_{z_1 z_1}^2 + f_{z_2 z_2}^1 f_{z_2 z_2}^2),$$

where f^i denotes the i^{th} component of the vector field at the critical value $R = 0$, i.e. $\begin{pmatrix} f^1 \\ f^2 \end{pmatrix} = \begin{pmatrix} f^1(z_1, z_2, 0) \\ f^2(z_1, z_2, 0) \end{pmatrix} = \begin{pmatrix} z_2 \\ -z_1 - \frac{1}{3}z_2^3 \end{pmatrix}$ and all partial derivatives are evaluated at the bifurcation point, i.e. $(z_1, z_2, R) = (0, 0, 0)$. In the VAN DER POL model, we obtain $a = -\frac{1}{8} < 0$. Since a is negative, we deduce that the HOPF bifurcation is supercritical and gives rise to a locally stable limit cycle for $R > 0$. Furthermore, from the LIÉNARD Theorem 3.1, we know that this limit cycle is unique and globally asymptotically stable for $R > 0$. It can also be shown that the origin of the VAN DER POL state model (3.6) is globally asymptotically stable for $R \leq 0$ (see [Kha02]). In Section 3.3, we will see that the global asymptotic stability of the origin before the critical bifurcation value $R = 0$ (i.e. for $R \leq 0$) is an important condition for obtaining a globally attractive limit cycle for values of R greater than 0.

3.2 The FITZHUGH-NAGUMO oscillator

Oscillations in biological systems generally result from a relaxation oscillation characterized by rapid switches between two quasi steady states (see [Mur02]). Most of the time, this relaxation oscillation is the result of the feedback addition of a slow adaptation mechanism to a globally bistable system. In this section, we are interested in one of the most simple models for voltage oscillations in the neuron cell membrane, the FITZHUGH-NAGUMO model. We will show that, under certain assumptions, this model admits the LURE feedback representation of Figure 3.2, plus a feedback adaptation loop.

In the FITZHUGH-NAGUMO model, the LURE feedback system is globally bistable. The oscillation mechanism consists in the transformation of this globally bistable system into a relaxation oscillation through the addition of a slow adaptation dynamic.

3.2.1 FITZHUGH-NAGUMO dynamics - Global results

The simplest model that has been proposed for spike generation is the FITZHUGH-NAGUMO model. This model is a simplification of the HODGKIN-HUXLEY model for voltage oscillations in the neuron cell membrane [HH52].

In 1952, HODGKIN and HUXLEY [HH52] proposed a mathematical model to explain pulse generation by neurons. According to their analysis, the electrical pulses arise because the neuron cell membrane is preferentially permeable to various chemical ions with the permeabilities affected by the currents and ions present. The key elements in the system are potassium ions (K^+) and sodium ions (Na^+). The HODGKIN-HUXLEY equations are characterized by a threshold for generating limit cycles and thus provide a qualitative approximation to spike generation thresholds. Simplifications of the model of HODGKIN and HUXLEY lead to the well-known second order FITZHUGH-NAGUMO model which qualitatively preserves its important properties.

The FITZHUGH-NAGUMO dimensionless model is (see [Mur02])

$$\begin{aligned}\dot{v} &= f(v) - w + I_a \\ \dot{w} &= bv - \gamma w,\end{aligned}\tag{3.7}$$

where I_a models the external excitation current, $f(v) = -v(v-a)(v-1)$, $0 < a < 1$, and b and γ are positive constants. The corresponding nullclines are $w = \frac{b}{\gamma}v$ and $w = f(v) + I_a$.

With $I_a = 0$, the possible phase portraits, as illustrated in Figure 3.4, show that there can be no periodic solutions since we either have a unique, asymptotically stable equilibrium point or a bistable system, i.e. two stable equilibrium points with a saddle point in between.

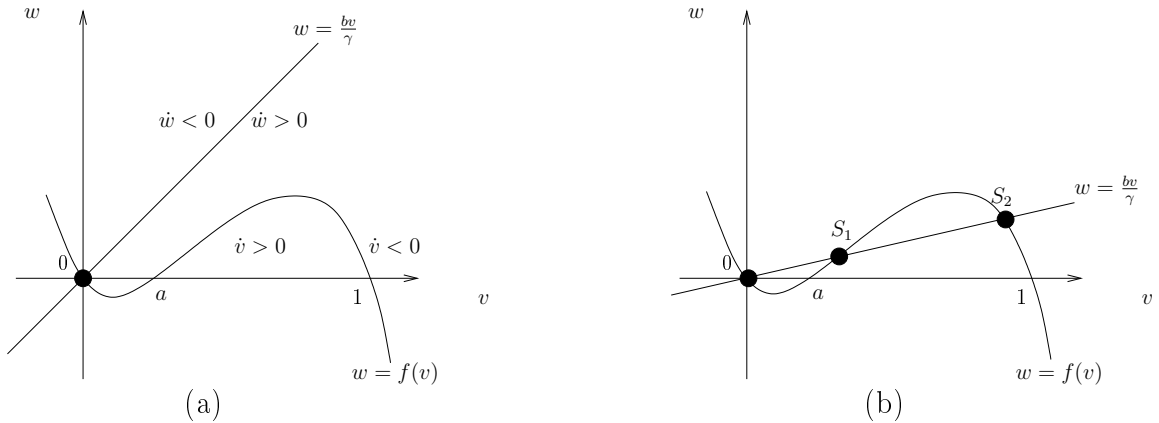


Figure 3.4: Nullclines for the original FITZHUGH-NAGUMO model (3.7) when $I_a = 0$. As the parameters b and γ vary there can be (a) one stable equilibrium point or, (b) three equilibrium points, one unstable, namely, S_1 , and two stable, namely, $(0, 0)$ and S_2 .

Suppose now that there is an applied current $I_a > 0$. The effect on the nullclines is simply to move the v nullcline, with $I_a = 0$, up the w -axis. The corresponding nullclines are illustrated in

3.2. THE FITZHUGH-NAGUMO OSCILLATOR

Figure 3.5 (a) to (d) for several $I_a > 0$. With parameter values such that the nullclines are as in Figure 3.4-(a), we can see that by varying only I_a there is a range of applied currents (I_1, I_2) where the steady state can be unstable and limit cycle oscillations possible, that is, a nullcline situation like that in Figure 3.5-(b). The algebra to determine the various parameter ranges for a, b, γ and I_a for each of these various possibilities to hold is straightforward [Mur02]. Finally, with the situation exhibited in Figure 3.5-(d) limit cycle solutions are not possible. On the other hand this form can exhibit equilibria switch properties.

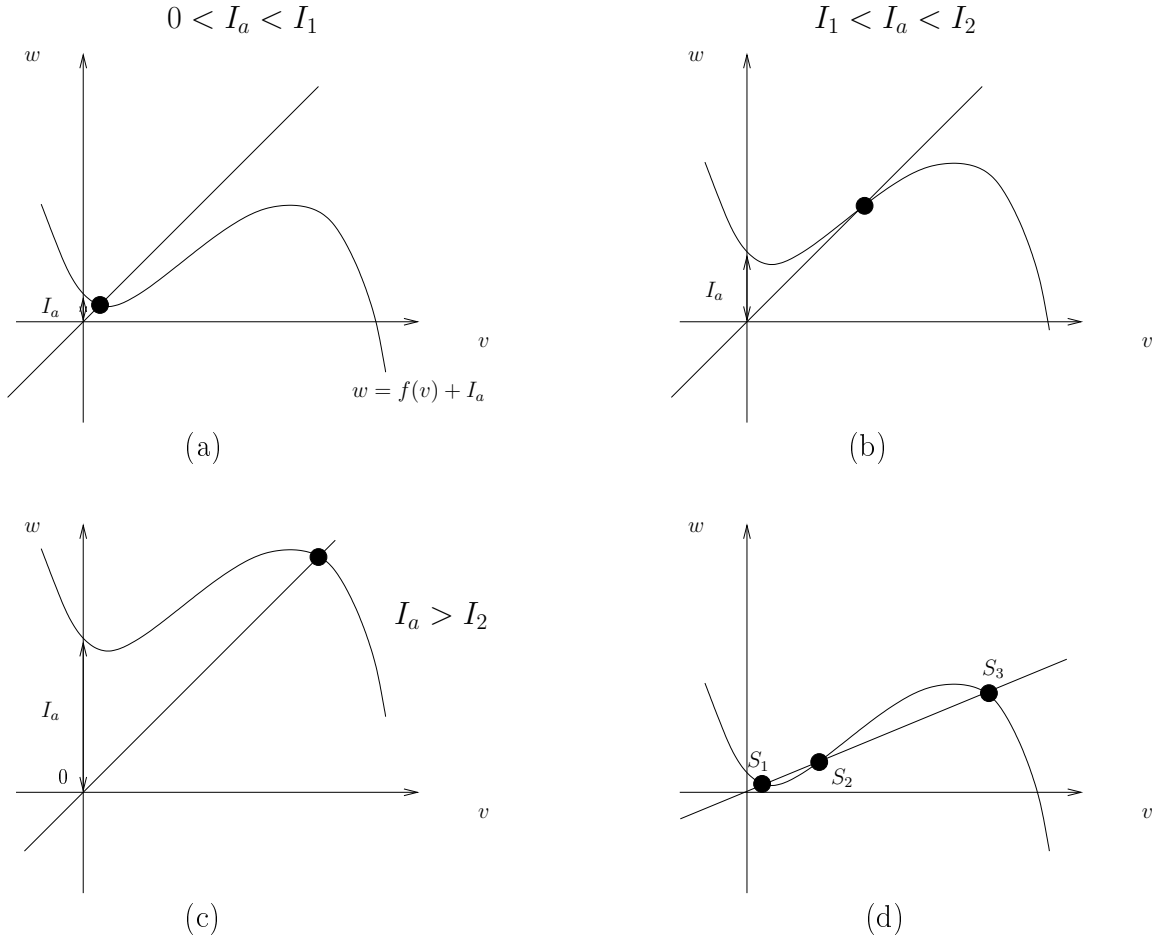


Figure 3.5: Nullclines for the original FITZHUGH-NAGUMO model (3.7) with different applied currents I_a . Cases (a), where $I_a < I_1$, and (c), where $I_a > I_2$, have linearly stable steady states, while in (b), where $I_1 < I_a < I_2$, the steady state can be unstable and limit cycle periodic solutions are possible. With the configuration (d), the steady states S_1, S_3 are stable whereas S_2 is unstable. In the configuration (d), a perturbation from either S_1 or S_3 can effect a switch to the other.

Since we are interested in the situation where a limit cycle oscillation occurs in the FITZHUGH-NAGUMO model (3.7), the positive constants a, b, γ , and I_a are chosen such that the system possesses a unique unstable equilibrium point as in Figure 3.5-(b). For nullclines to be as in Figure 3.5-(b), we must impose that the slope at the inflexion point ($v = \frac{a+1}{3}$) of the nullcline $w = f(v) + I_a$ is less than

$\frac{b}{\gamma}$ (the slope of the nullcline $w = \frac{b}{\gamma}v$). This leads to the condition

$$\frac{b}{\gamma} > \frac{1}{3}(a^2 - a + 1) \quad (3.8)$$

which guarantees uniqueness of the equilibrium point of the state model (3.7).

Suppose now that for a particular value \bar{I}_a of I_a , the equilibrium point is the inflexion point of the nullcline, i.e. $\bar{w} = f(\bar{v}) + \bar{I}_a = \frac{b}{\gamma}\bar{v}$ with $\bar{v} = \frac{a+1}{3}$. Then for the inflexion point to be unstable we must further impose the condition

$$\gamma < \frac{1}{3}(a^2 - a + 1). \quad (3.9)$$

It may be similarly showed that the equilibrium point is unstable in the range of values

$$\bar{V}_1 \leq \bar{v} \leq \bar{V}_2, \quad (3.10)$$

where $\bar{V}_1 = \frac{a+1}{3} - \frac{\sqrt{(a^2-a+1)-3\gamma}}{3}$ and $\bar{V}_2 = \frac{a+1}{3} + \frac{\sqrt{(a^2-a+1)-3\gamma}}{3}$ with $(a^2 - a + 1) - 3\gamma > 0$ from condition (3.9).

From condition (3.10) we may approximate the range of values for the excitation current I_a (leading to a situation similar to that described in Figure 3.5 (b)) by

$$I_1 \leq I_a \leq I_2, \quad (3.11)$$

where $I_1 = \frac{b}{\gamma}\bar{V}_1 - f(\bar{V}_1)$ and $I_2 = \frac{b}{\gamma}\bar{V}_2 - f(\bar{V}_2)$.

3.2.2 The FITZHUGH-NAGUMO model as a LURE feedback system plus a feedback adaptation loop

In this section we perform several changes of coordinates in order to obtain a state model of the FITZHUGH-NAGUMO equations (3.7) that admits the LURE feedback representation of Figure 3.2, plus a feedback adaptation loop.

In order to center the origin of the axes in Figure 3.5-(b) at the inflexion point of the function $f(v)$, we perform the following change of coordinates

$$\begin{aligned} z_1 &= w - f\left(\frac{a+1}{3}\right) - I_a \\ z_2 &= v - \frac{a+1}{3}, \end{aligned}$$

which leads to the equivalent model

$$\begin{aligned} \frac{1}{\gamma}\dot{z}_1 &= \frac{b}{\gamma}z_2 - z_1 + \left(\frac{b}{\gamma}\frac{a+1}{3} - f\left(\frac{a+1}{3}\right) - I_a\right) \\ \dot{z}_2 &= -z_1 - \left(z_2^3 - \frac{1}{3}(a^2 - a + 1)z_2\right). \end{aligned}$$

If we assume that $I_a = \frac{b}{\gamma}\frac{a+1}{3} - f\left(\frac{a+1}{3}\right)$ (which belongs to the current range (3.11)), the state model becomes

$$\begin{aligned} \tau\dot{z}_1 &= b\tau z_2 - z_1, \\ \dot{z}_2 &= -z_1 - \left(z_2^3 - \frac{1}{3}(a^2 - a + 1)z_2\right), \end{aligned} \quad (3.12)$$

3.2. THE FITZHUGH-NAGUMO OSCILLATOR

where $\tau = \frac{1}{\gamma}$, and admits the feedback representation of Figure 3.6 where $\phi_a(z_2) = z_2^3 - \frac{1}{3}(a^2 - a + 1)z_2$. In the model (3.12), the uniqueness of the equilibrium point is guaranteed by the condition $\frac{1}{3}(a^2 - a + 1) < b\tau$ and its instability by the condition $\frac{1}{3}(a^2 - a + 1) > \frac{1}{\tau}$. We clearly see that both conditions are simultaneously satisfied for τ large enough.

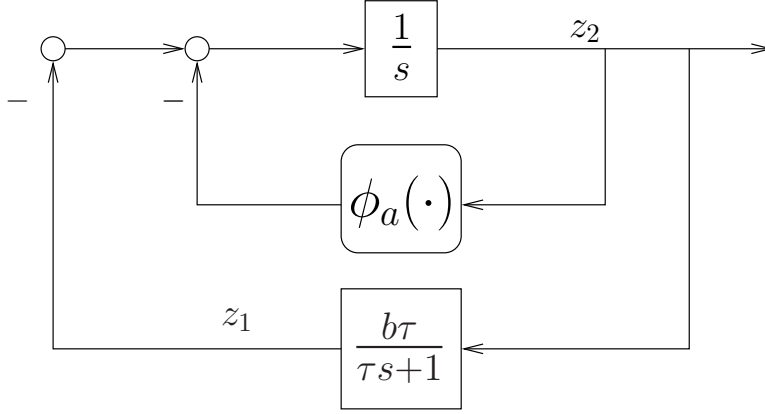


Figure 3.6: Block diagram representation of the FITZHUGH-NAGUMO state model (3.12).

We are now ready to interpret the oscillation mechanism of the FITZHUGH-NAGUMO oscillator. The inner-loop dynamic

$$\dot{z}_2 = k_a z_2 - z_2^3, \quad (3.13)$$

where we have posed $k_a = \frac{1}{3}(a^2 - a + 1) > 0$, constitutes a globally bistable system. The most natural way to obtain a bistable system from a scalar parameterized system is through a pitchfork bifurcation. The FITZHUGH-NAGUMO oscillator exploits this idea. Consider exclusively the inner loop dynamic (3.13) of the FITZHUGH-NAGUMO model parameterized by $k \in \mathbb{R}$, we obtain

$$\dot{z}_2 = k z_2 - z_2^3. \quad (3.14)$$

It is easy to see that this first order system undergoes a supercritical pitchfork bifurcation at $k = 0$ since for $k < 0$, the origin of (3.14) is globally asymptotically stable, whereas for $k > 0$, the origin is a saddle point and there exists two other asymptotically stable equilibrium points located at $\pm\sqrt{k}$. Considering only the inner loop dynamic (3.14), one thus obtains the phase portrait shown in Figure 3.7-(a) for $k = k_a > 0$.

The outer-loop in Figure 3.6 or equivalently the *adaptation* equation

$$\tau \dot{z}_1 = -z_1 + b\tau z_2 \quad (3.15)$$

converts the bistable behavior into a limit cycle in the phase plane (z_1, z_2) as shown in Figure 3.7-(b). The limit cycle is guaranteed to be globally asymptotically stable provided that the time constant τ is large enough, i.e. the adaptation is slow enough to let the "fast" dynamics converge to quasi steady state (this is easily seen by applying singular perturbation theory – see [Kha02]).

The *global bistability* of the inner loop combined with the *slow adaptation* of the outer loop thus provides a second feedback mechanism for global oscillations. The resulting *relaxation* oscillation is characterized by rapid switches between two quasi steady states.

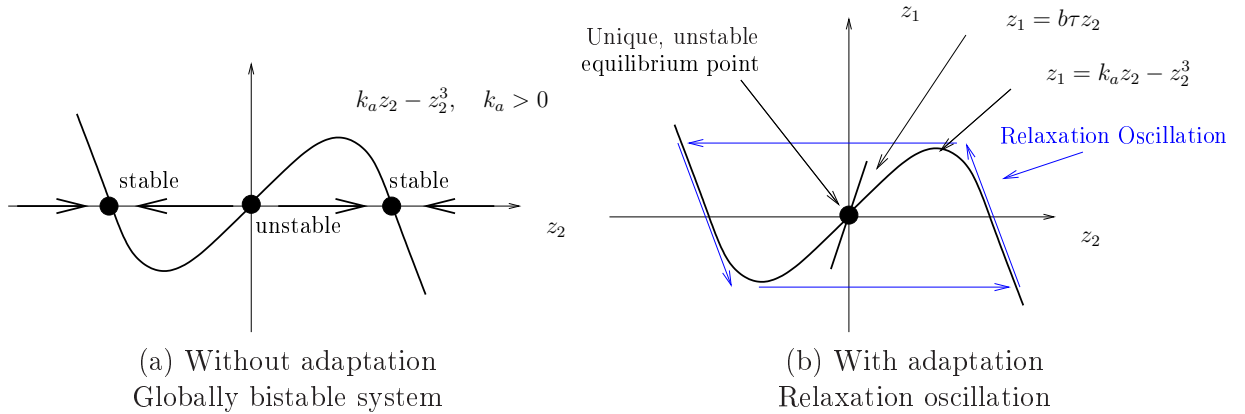


Figure 3.7: The hysteresis associated to a bistable system.

3.3 First result of this thesis - Passive oscillator definition

The aim of this section is to construct a class of high-dimensional systems that generalizes the *global* limit cycle oscillation mechanisms of the VAN DER POL and FITZHUGH-NAGUMO oscillators. In the VAN DER POL example (3.6), the feedback mechanism responsible for the generation of global limit cycle oscillation is the supercritical HOPF bifurcation that occurs at $R = 0$. In the FITZHUGH-NAGUMO example (3.12), the global oscillation feedback mechanism consists in the addition of a slow adaptation dynamic to a globally bistable system.

Both in the VAN DER POL and the FITZHUGH-NAGUMO models, the bifurcations occur in a structure that corresponds to the feedback interconnection of a conservative system with a static nonlinearity of the form $\phi_k(y) = -ky + y^3$, i.e. a nonlinearity $\phi(y) = y^3$ that satisfies the sector condition $y\phi(y) > 0, \forall y \in \mathbb{R}$ plus a parameterized slope at the origin $-ky$. In the VAN DER POL example (3.6), the conservative system consists in the feedback interconnection of two simple integrators whereas in the FITZHUGH-NAGUMO situation (3.12), the conservative system is a single integrator.

To generalize the VAN DER POL and FITZHUGH-NAGUMO global oscillation properties to higher-dimensional systems, the ideal situation would be to replace the integrator appearing in the forward path of Figures 3.3 and 3.6 directly by a general passive system. This is a sufficient condition for proving global boundedness of the solutions of the feedback system as we will see in Section 3.3.2. However, it is a too general assumption that cannot reasonably lead to global oscillations in the general case. In Section 3.3.3, we will prove that in order to obtain global stability properties through a supercritical bifurcation, it is essential that the system under consideration possesses a unique, globally asymptotically stable equilibrium point before the bifurcation. In other words, the system must be absolutely stable for values of the bifurcation parameter less or equal to the critical value. This will allow the global stability property of the equilibrium point to be transmitted to the bifurcated solution, at least in the vicinity of the critical bifurcation value. Replacing the forward integrator in Figures 3.3 and 3.6 by a passive system does not lead to a situation where this condition is satisfied generically. As we will see, for a general LURE system of the form represented in Figure 3.8, passivity of the parameterized system Σ_k is generically lost before its stability as the parameter k is increased (i.e. before the bifurcation), leading to a situation where the feedback system is not necessarily globally asymptotically stable before the bifurcation. Stronger assumptions are to be imposed to the forward system Σ_k if one is interested in global oscillations. These assumptions will be discussed in

Section 3.3.3.

3.3.1 Class of systems studied

Consider the LURE system shown in Figure 3.8 which represents the feedback interconnection of the nonlinear system Σ with a static nonlinearity $\phi_k(\cdot)$. Throughout this chapter, we make the following assumptions. We assume that the (SISO) system Σ is described by the state-space model

$$(\Sigma) \begin{cases} \dot{x} = f(x) + g(x)v, & x \in \mathbb{R}^n, \quad v \in \mathbb{R} \\ y = h(x), & y \in \mathbb{R} \end{cases} \quad (3.16)$$

where the vector fields f and g and the scalar function h are smooth¹. We assume that the origin $x = 0$ is an equilibrium point, i.e. $f(0) = 0$, and that $h(0) = 0$ and $g(0) \neq 0$. We also assume zero-state detectability of the pair (f, h) , i.e. that every solution $x(t)$ of $\dot{x} = f(x)$ that verifies $y(t) = h(x(t)) \equiv 0$ asymptotically converges to the zero solution $x = 0$ as $t \rightarrow \infty$.

The static nonlinearity $\phi_k(\cdot) : \mathbb{R} \rightarrow \mathbb{R}$ is described as

$$\phi_k(y) = -ky + \phi(y), \quad (3.17)$$

where $\phi(\cdot)$ is a smooth sector nonlinearity in the sector $(0, \infty)$, which satisfies $\phi'(0) = \phi''(0) = 0$, $\phi'''(0) = \kappa > 0$ and $\lim_{|s| \rightarrow \infty} \frac{\phi(s)}{s} = +\infty$ (“stiffening” nonlinearity). The parameter k regulates the level of “activation” near the equilibrium $x = 0$.

The feedback interconnection is defined by

$$v = -\phi_k(y) + u, \quad (3.18)$$

where $u \in \mathbb{R}$ represents the external input of the feedback nonlinear system. Since, in this chapter, we are interested in self-oscillating systems, the external input u is considered to be equal to zero. In Chapter 4 it will be used to interconnect several systems (oscillators) into a network.

We denote by $G(s)$ the transfer function of the linearization of Σ at $x = 0$ and by Σ_k the (positive) feedback interconnection of Σ with the feedback gain k . Similarly, we denote by $G_k(s) = \frac{G(s)}{1 - kG(s)}$ the transfer function of the linearization of Σ_k at $x = 0$. The feedback system is equally described as the feedback interconnection of Σ_k and the nonlinearity $\phi(\cdot)$ (see Figure 3.8).

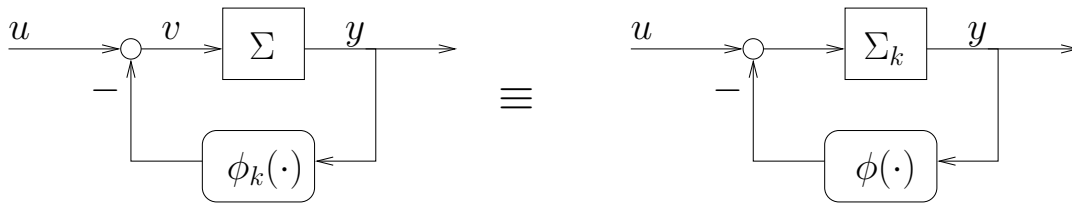


Figure 3.8: Equivalent representations of the LURE SISO nonlinear system.

We assume that the system Σ is *strongly passive* with storage function $S(x)$ (see Definition 2.4). For clarity, we recall here the three additional assumptions characterizing the storage function $S(x)$ of a strongly passive system.

¹By smooth, we mean continuously differentiable up to order k (\mathcal{C}^k) with k large enough to satisfy our needs (i.e. to fulfil the requirements of the theorems we are using, such as the theorem on existence and uniqueness of solutions, the theorem on continuous dependence of a solution on the initial condition (see [KhalilBook2, Sections 3.1 and 3.2]), the HOPF bifurcation theorem, etc.).

1. (smoothness) $S(x)$ is continuously differentiable (\mathcal{C}^1) in \mathbb{R}^n and twice continuously differentiable (\mathcal{C}^2) in a neighborhood of the origin.
2. (LYAPUNOV) $S(x)$ is positive definite, $S(x) > 0$, and radially unbounded, i.e. $S(x) \rightarrow \infty$ as $|x| \rightarrow \infty$.
3. (locally quadratic) The Hessian of $S(x)$ evaluated at zero $\left. \frac{\partial^2 S(x)}{\partial x^2} \right|_{x=0}$ is a symmetric positive definite matrix $P = P^T > 0$.

As it is well-known, these assumptions are always satisfied in the (detectable) linear case because linear passive systems have quadratic positive definite storage functions [Wil72]. In general, these assumptions are convenient to link the passivity of Σ to the stability properties of the zero input system since $S(x)$ then serves as a (global) LYAPUNOV function. The locally quadratic assumption further ensures that the linearization of Σ is passive, with the quadratic approximation of $S(x)$ as a storage function. It also implies that the system has a relative degree one², i.e. $\frac{\partial h}{\partial x}(x)g(x) > 0$ for all x in a (small) neighborhood of the origin $x = 0$, and that it is weakly minimum phase, i.e. its zero dynamics are LYAPUNOV stable [BIW91].

The first question if we are interested in global results concerns the global boundedness of the solutions of the feedback system (3.16),(3.17),(3.18) with $u \equiv 0$. To this end, we introduce an extra property for the feedback system in Figure 3.8. The feedback interconnection of Σ and $\phi_k(\cdot)$ is called *ultimately bounded*³ if all solutions enter in finite time a compact set $\Omega = \Omega(k)$. The main result of this chapter (see Section 3.3.3) states ultimate boundedness as an extra assumption to strong passivity and zero-state detectability of Σ . Following the argument of ARCAK and TEEL in [AT02], we observe that this extra assumption is always satisfied when the feedback interconnection of Σ with a stiffening, strictly passive nonlinearity is input-to-state stable. This is because the stiffening nonlinearity $\phi_k(\cdot)$ always admits the decomposition

$$\phi_k(y) = \psi(y) + \chi_k(y),$$

with $\psi(y)$ strictly passive and $\chi_k(y)$ uniformly bounded by a constant $C = C(k)$. If Σ is passive, the feedback interconnection of Σ and $\phi_k(\cdot)$ is thus equivalent to the feedback interconnection of Σ with $\psi(\cdot)$, which is strictly passive, forced by the bounded input $\chi_k(y)$. Ultimate boundedness is thus implied by input-to-state stability (see [Son89]) of the strictly passive interconnection of Σ and $\psi(\cdot)$, whereas strict passivity only implies a finite \mathcal{L}_2 gain when Σ is nonlinear. In the particular case of Σ linear, ARCAK and TEEL [AT02] have proved that weakly minimum phaseness and detectability of the linear system Σ necessarily implies ultimate boundedness of the feedback interconnection of Σ

²This can be easily seen from the second HILL-MOYLAN condition (2.20). Condition (2.20) implies

$$\frac{\partial}{\partial x} \left(g^T(x) \left(\frac{\partial S}{\partial x} \right)^T \right) g(x) = \frac{\partial h(x)}{\partial x} g(x)$$

By definition of the storage function $S(x)$, $\left. \frac{\partial S}{\partial x} \right|_{x=0} = 0$, and we obtain $g^T(0) \left. \frac{\partial^2 S}{\partial x^2} \right|_{x=0} g(0) = L_g h(x)|_{x=0}$. Since, by assumption, $\left. \frac{\partial^2 S}{\partial x^2} \right|_{x=0}$ is a symmetric, positive definite matrix, and $g(0) \neq 0$, this implies, $L_g h(x)|_{x=0} > 0$, which means that the system has relative degree one around the origin (see [SJK97, Appendix A.1]).

³In the literature, this property is often called *dissipativity* (or LEVINSON dissipativity) which should not be confused with the dissipativity notion in this document. In [Pog98, PGN99] this ultimate boundedness property is proved using the concept of *semi-passive* system.

with the stiffening, static nonlinearity $\phi_k(\cdot)$. For the seek of completeness, we summarize the results of ARCAK and TEEL for Σ linear in the following section. For proofs of the cited theorems, the interested reader is referred to the paper [AT02].

3.3.2 Global boundedness results for Σ linear

ARCAK and TEEL [AT02] have given sufficient conditions for input-to-state stability (ISS⁴) of the feedback interconnection of a linear, passive, and detectable block with a static nonlinear element. In the absolute stability framework, they prove ISS from the passivity of the linear block, by restricting the sector nonlinearity to grow unbounded as its argument tends to infinity. When this growth property is violated, examples show that the ISS property is lost. The ISS result of ARCAK and TEEL can be used to give a simple proof of boundedness for negative resistance oscillators, such as the VAN DER POL oscillator. Their main result is recalled in Theorem 3.2.

Theorem 3.2 (ARCAK's Theorem [AT02]) *Consider the system*

$$\dot{x} = Ax + B[-\phi(y) + d] \quad (3.19)$$

$$y = Cx \quad (3.20)$$

where $x \in \mathbb{R}^n$, $\phi(\cdot) : \mathbb{R}^m \rightarrow \mathbb{R}^m$, and (C, A) is detectable. If there exists a matrix $P = P^T \geq 0$ satisfying the HILL-MOYLAN conditions

$$A^T P + PA \leq 0, \quad (3.21)$$

$$C = B^T P, \quad (3.22)$$

a constant $\mu > 0$, and a class \mathcal{K}_∞ function $\phi_l(\cdot)$, such that

$$\|y\|_\infty \phi_l(\|y\|_\infty) \leq y^T \phi(y) \text{ for all } y \in \mathbb{R}^m, \quad (3.23)$$

$$\|\phi(y)\|_\infty \leq y^T \phi(y) \text{ when } \|y\|_\infty \geq \mu, \quad (3.24)$$

then the system is ISS with respect to d .

Remark 3.3 [AT02] *When (A, B, C) is a minimal realization, a straightforward modification of the KALMAN-YAKUBOVICH-POPOV lemma 2.20 for $P \geq 0$ shows that assumptions (3.21), (3.22) are equivalent to the positive realness of $H(s) = C(sI - A)^{-1}B$. For a more general result, in Theorem 3.2, ARCAK and TEEL allow non-minimal realizations and only restricts (C, A) to be detectable.*

Remark 3.4 [AT02] *For scalar nonlinearities $\phi(\cdot) : \mathbb{R} \rightarrow \mathbb{R}$ the condition (3.23) is equivalent to the sector property*

$$y\phi(y) > 0, \forall y \neq 0, \quad (3.25)$$

⁴A dynamical system of the form $\dot{x} = f(x, u)$, $y = h(x)$ is input-to-state stable (ISS) if there exist $\gamma \in \mathcal{K}, \beta \in \mathcal{KL}$ such that for all x_0, u and $t \geq 0$:

$$|x(t, x_0, u)| \leq \beta(|x_0|, t) + \gamma(\|u\|_\infty)$$

A function $\gamma : \mathbb{R}_{\geq 0} \rightarrow \mathbb{R}_{\geq 0}$ is of class \mathcal{K} if it is continuous, positive definite, and strictly increasing. It is of class \mathcal{K}_∞ if it is also unbounded.

A function $\beta : \mathbb{R}_{\geq 0} \times \mathbb{R}_{\geq 0} \rightarrow \mathbb{R}_{\geq 0}$ is of class \mathcal{KL} if, for each fixed $t \geq 0$, $\beta(\cdot, t)$ is of class \mathcal{K} and, for each fixed $s \geq 0$, $\beta(s, t)$ decreases to 0 as $t \rightarrow \infty$.

and the growth condition

$$|y| \rightarrow \infty \Rightarrow |\phi(y)| \rightarrow \infty. \quad (3.26)$$

For scalar nonlinearities, the condition (3.24) is redundant because (3.23) implies $y\phi(y) = |y||\phi(y)|$ and, thus, (3.24) holds with $\mu = 1$. For multivariable nonlinearities, (3.23) does not imply (3.24). A counterexample is

$$\phi(y) = y + |y|^3 Jy,$$

where J satisfies $J + J^T = 0$ and $J^T J = I$. In this example, $y^T \phi(y) = |y|^2$ and $|\phi(y)| = \sqrt{|y|^2 + |y|^8}$, which means that (3.23) is satisfied with $\phi_l(|y|) = |y|$, but (3.24) is violated.

The ISS result of Theorem 3.2 can be used to prove boundedness for negative resistance oscillators such as the VAN DER POL oscillator as well as for the larger class (3.19),(3.20), which includes higher order systems and bounded disturbances. This second result of ARCAK and TEEL is summarized in Theorem 3.5.

Theorem 3.5 [AT02] Consider the system (3.19),(3.20) where $x \in \mathbb{R}^n$, $\phi(\cdot) : \mathbb{R} \rightarrow \mathbb{R}$, (C, A) is detectable, and d is a bounded disturbance. If there exists a matrix $P = P^T \geq 0$ satisfying conditions (3.21) and (3.22), and if the nonlinearity $\phi(\cdot)$ satisfies $\phi(y) \rightarrow -\infty$ as $y \rightarrow -\infty$ and $\phi(y) \rightarrow \infty$ as $y \rightarrow \infty$, then all the trajectories are bounded.

This result can be further generalized: Theorem 3.5 can be used to establish boundedness of trajectories for a relative degree one, weakly minimum phase, linear block, in feedback with a *stiffening* nonlinearity, defined by the property

$$\lim_{|y| \rightarrow \infty} \frac{\phi(y)}{y} \rightarrow +\infty. \quad (3.27)$$

Using the ISIDORI normal form [Isi95] for relative degree one systems, this feedback interconnection is expressed as

$$\dot{z} = A_0 z + B_0 y \quad (3.28)$$

$$\dot{y} = -C_0 z - ay - \phi(y) + d, \quad (3.29)$$

where the z -subsystem represents the zero dynamics of the linear block. This third result of ARCAK and TEEL is summarized in Theorem 3.6.

Theorem 3.6 [AT02] Consider the system (3.28),(3.29), where d is a bounded disturbance, (C_0, A_0) is a detectable pair, and there exists a matrix $P_0 = P_0^T \geq 0$ such that

$$A_0^T P_0 + P_0 A_0 \leq 0, \quad P_0 B_0 = C_0^T \quad (3.30)$$

If the nonlinearity $\phi(\cdot) : \mathbb{R} \rightarrow \mathbb{R}$ satisfies the stiffening property (3.27), then the trajectories are bounded.

This last result is useful to prove boundedness for systems with imaginary axis zeros. To illustrate Theorem 3.6, we consider the following example:

Example 3.7 Consider the negative feedback interconnection of the linear system $H(s) = \frac{s^2+1}{s^3-s^2+2s-1}$ with the stiffening nonlinearity $\phi(y) = y^3$. To apply Theorem 3.6, we note that $H(s)$ is relative degree one, and rewrite the system as in (3.28)-(3.29) with $d = 0$ and

$$A_0 = \begin{pmatrix} 0 & 1 \\ -1 & 0 \end{pmatrix}, \quad B_0 = \begin{pmatrix} 0 \\ 1 \end{pmatrix}, \quad C_0 = (0 \ 1), \quad a = -1.$$

The origin is unstable from the Jacobian linearization. However, because (3.30) holds with $P_0 = I$, Theorem 3.6 ensures boundedness. Numerical simulations indicate that the trajectories converge to one of the two stable equilibria $(x_1, x_2, x_3) = \pm(0, 0, 1)$ (Figure 3.9-(a)), or to a limit cycle as shown (Figure 3.9-(b)).

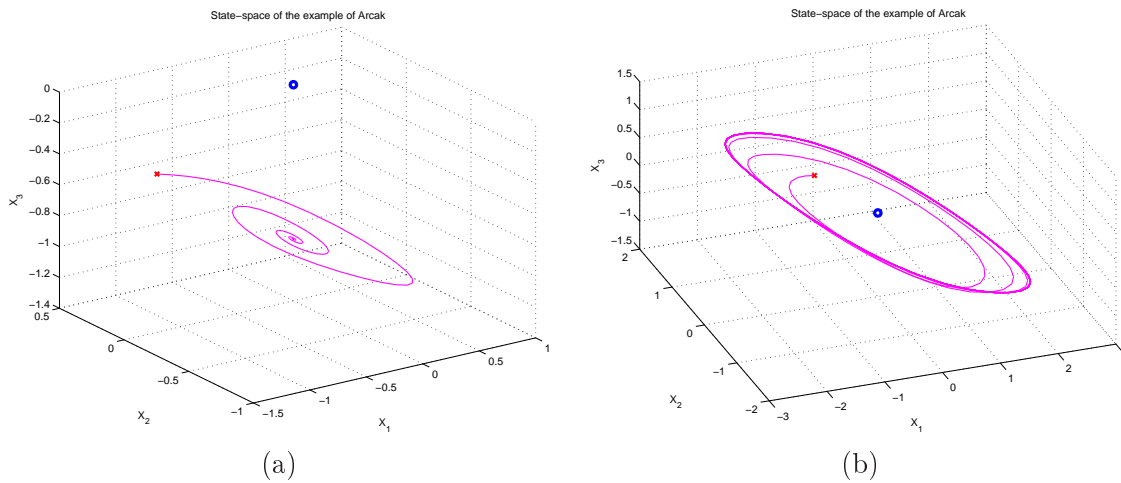


Figure 3.9: Example of ARCAK [AT02]. (a) The initial condition belongs to the basin of attraction of the equilibrium point $(x_1, x_2, x_3) = (0, 0, -1)$; (b) The initial condition belongs to the basin of attraction of the limit cycle.

As a consequence of the results of ARCAK and TEEL, we may conclude that for linear systems Σ , weakly minimum phaseness⁵ and detectability seem to be important sufficient conditions for ultimate boundedness of the LURE feedback interconnection represented in Figure 3.8. Nevertheless, as we have seen in example 3.7, these conditions are not sufficient to guarantee existence, uniqueness and global asymptotic stability of the limit cycle. In the next section, we give sufficient conditions for the existence, uniqueness and global asymptotic stability of a limit cycle in LURE feedback systems satisfying the representation given in Figure 3.8.

3.3.3 Bifurcations in absolutely stable LURE feedback systems

In this section, we present the main results of this chapter, i.e. Theorems 3.8, 3.9, and 3.12. These results concern the high dimensional extension of the feedback (global) oscillation mechanisms present in the VAN DER POL and FITZHUGH-NAGUMO models introduced in Sections 3.1 and 3.2. Theorem 3.8 presents the typical bifurcation scenarii that occur in LURE feedback systems satisfying

⁵We recall that weakly minimum phaseness is a structural property of input-affine passive systems (see Section 2.1.7).

the representation given in Figure 3.8, i.e. supercritical HOPF and supercritical pitchfork bifurcations. Theorem 3.12 extends the results presented in Theorem 3.8 by weakening its assumptions through the use of multipliers. Finally, Theorem 3.9 shows that the global bistability behavior that appears through the supercritical pitchfork bifurcation scenario can be transformed into a global relaxation oscillation by addition of a feedback adaptation loop to the LURE system.

The feedback system (3.16),(3.17),(3.18) with $u \equiv 0$ is *absolutely stable* when the equilibrium $x = 0$ is globally asymptotically stable (GAS) for any nonlinearity $\phi(\cdot)$ in the sector $(0, +\infty)$. Because the sector memoryless nonlinearity $\bar{v} = \phi(y)$ is strictly input passive, a sufficient condition for absolute stability is that Σ_k is strongly passive and zero-state detectable. This results from Theorem 2.18.

Assuming that Σ is strongly passive and zero-state detectable, the feedback system (3.16),(3.17),(3.18) with $u \equiv 0$ is absolutely stable for $k = 0$. As k increases, a root locus argument shows that the feedback system must lose stability at some critical value k^* ⁶. The following result characterizes the possible bifurcations under a passivity assumption for G_{k^*} . The notation $k \gtrsim k^*$ is used to denote a value of the parameter *near* the bifurcation, i.e. $k \in (k^*, \bar{k}]$ for some $\bar{k} > k^*$.

Theorem 3.8 *Consider the system shown in Figure 3.8 and characterized by (3.16),(3.17),(3.18) with $u \equiv 0$. Assume that Σ is strongly passive, that both Σ and its linearization are zero-state detectable and that the feedback interconnection of Σ and $\phi_k(\cdot)$ is ultimately bounded. Let $k^* \geq 0$ be the minimum value for which the transfer function $G_k(s)$ has a pole on the imaginary axis.*

If $G_{k^}(s)$ has a unique pole on the imaginary axis and if Σ_{k^*} is strongly passive, then the bifurcation is a supercritical pitchfork bifurcation; for $k \gtrsim k^*$ the system is globally bistable, that is, the equilibrium $x = 0$ is a saddle and its stable manifold $E_s(0)$ separates the state space in two open sets, each of which is the basin of attraction of a stable equilibrium.*

If $G_{k^}(s)$ has a unique pair of conjugated poles on the imaginary axis and if Σ_{k^*} is strongly passive, then the bifurcation is a supercritical HOPF bifurcation; for $k \gtrsim k^*$ the system has a stable limit cycle which is globally asymptotically stable in $\mathbb{R}^n \setminus E_s(0)$.*

Proof

The proof is divided into a local argument and a global argument. Both arguments rely on the dissipation inequality

$$\dot{S} \leq -y\phi(y) \tag{3.31}$$

at the bifurcation point, where $S(x)$ denotes a storage function for Σ_{k^*} . The local argument will show the existence of a supercritical HOPF (respectively, pitchfork) bifurcation at $\epsilon = k - k^* = 0$. This implies the existence of a constant $\bar{\epsilon}_1 > 0$ and a neighborhood U of $x = 0$ such that for each $\epsilon \in (0, \bar{\epsilon}_1]$, all solutions with initial condition in U either converge to the unstable equilibrium $x = 0$ or to a unique stable limit cycle of radius $\mathcal{O}(\sqrt{\epsilon})$ (respectively, one of two stable equilibria located at a distance $\mathcal{O}(\sqrt{\epsilon})$ of the origin). The global argument will show that there exists a constant $0 < \bar{\epsilon}_2 \leq \bar{\epsilon}_1$, such that for each $\epsilon \in (0, \bar{\epsilon}_2]$, all solutions enter the set U in finite time (which means

⁶For the *positive* feedback interconnection of $G(s)$ with the static gain k , the root locus is such that parts of the real axis located at the *left* of an even number of real singularities (poles or zeros) and at the right of the rightmost real singularity belong to the root locus. As the transfer function of a strongly passive system, $G(s)$ has a relative degree equal to one and all its poles and zeros belong to the closed left-half complex plane. As a consequence, one branch (at least) of the root locus must enter the right-half complex plane since the positive part of the real axis necessarily belongs to the root locus.

that the local argument eventually applies to each solution).

We first prove the global argument. Ultimate boundedness implies that for each $\epsilon \in (0, \bar{\epsilon}_3]$, all solutions enter in finite time an invariant compact set $\Omega = \Omega(\epsilon)$. Furthermore, the robustness of global asymptotic stability at $\epsilon = 0$ implies semi-global practical asymptotic stability of the solution $x = 0$ (see Theorem 2.25⁷), i.e. the existence of $\bar{\epsilon}_2 \leq \bar{\epsilon}_3$ such that, for each $\epsilon \in (0, \bar{\epsilon}_2]$, all solutions with initial condition in Ω enter in finite time the set U .

Next we turn to the local argument. At the bifurcation, i.e. for $k = k^*$, the system possesses a center manifold. In a neighborhood of the origin $x = 0$, the dissipation inequality (3.31) writes

$$\dot{S} \leq -\kappa y^4 + \mathcal{O}(y^5), \quad \kappa = \phi'''(0) > 0 \quad (3.32)$$

with $S(x)$ being locally quadratic positive definite. In particular, this last inequality holds valid on the center manifold as well. The restriction of $S(x)$ on the center manifold is thus a locally quadratic LYAPUNOV function that satisfies (3.32). Moreover, detectability of the linearization of Σ implies observability of the linearized center manifold dynamics⁸.

Case (1): If $G_{k^*}(s)$ has a unique pole on the imaginary axis, the center manifold is one-dimensional. For a one dimensional manifold, the assumption $h(0) = 0$ implies that the output of the system is $y = c\xi + \mathcal{O}(|\xi|^2)$ with $\xi \in \mathbb{R}$. Since the linearization of the center manifold dynamic is observable, c is nonzero. This implies that y qualifies for a local coordinate in the center manifold. In normal form, the center manifold dynamic thus writes [Wig90]

$$\dot{y} = a_3 y^3 + \mathcal{O}(y^4), \quad y \in \mathbb{R}. \quad (3.33)$$

The restriction of the storage function on the center manifold is a locally quadratic function of the form $S_{\text{center manifold}} = \frac{1}{2}P_1 y^2 + \mathcal{O}(y^3)$ (with $P_1 > 0$ from the strong passivity assumption of Σ_{k^*}) that satisfies the dissipation inequality

$$\dot{S}_{\text{center manifold}} = P_1 y \dot{y} \leq -\kappa y^4 + \mathcal{O}(y^5). \quad (3.34)$$

We thus obtain

$$a_3 P_1 y^4 + \mathcal{O}(y^5) \leq -\kappa y^4 + \mathcal{O}(y^5),$$

which in turn implies that $a_3 < 0$. As a consequence, the pitchfork bifurcation is supercritical pitchfork, that is, there exists one unstable equilibrium at $y = 0$ and two asymptotically stable equilibria $y = \pm \mathcal{O}(\sqrt{\epsilon})$ for small $\epsilon > 0$.

Case (2): If $G_{k^*}(s)$ has two conjugated poles at $s = \pm j\omega$, the center manifold is two-dimensional.

⁷With the notations of Theorem 2.25, f^ϵ corresponds to the vector field of Σ_k with $k \gtrsim k^*$ and g to the vector field of Σ_{k^*} . This implies that the convergence assumption is necessarily satisfied since f^ϵ converges point-wise to g as $\epsilon \rightarrow 0$.

⁸If a linear system is (zero-state) detectable then its unobservable modes are asymptotically stable. This can also be formulated as follows: If a linear system is (zero-state) detectable then its non asymptotically stable modes are observable.

The normal form of the center manifold dynamics is [Wig90]

$$\dot{\xi} = A_c \xi + |\xi|^2 \begin{pmatrix} a_3 \xi_1 - b_3 \xi_2 \\ b_3 \xi_1 + a_3 \xi_2 \end{pmatrix} + \mathcal{O}(|\xi|^4), \quad A_c = \begin{pmatrix} 0 & \omega \\ -\omega & 0 \end{pmatrix} \quad (3.35)$$

which, in polar coordinates, yields

$$\begin{cases} \dot{\rho} &= a_3 \rho^3 + \mathcal{O}(\rho^4) \\ \dot{\theta} &= \omega + \mathcal{O}(\rho^2) \end{cases} \quad (3.36)$$

The restriction of S on the center manifold is a locally quadratic LYAPUNOV function $S = \xi^T Q \xi + \mathcal{O}(|\xi|^3)$ which satisfies

$$\dot{S} = \xi^T (Q A_c + A_c^T Q) \xi + \mathcal{O}(|\xi|^3) \leq -\kappa y^4 + \mathcal{O}(y^5). \quad (3.37)$$

Up to a scaling factor, the only positive definite solution Q of $Q A_c + A_c^T Q \leq 0$ is $Q = \frac{1}{2}I$, which implies $S = \frac{1}{2}\rho^2 + \mathcal{O}(\rho^3)$. For initial conditions in the center manifold, the dissipation inequality (3.37) thus satisfies

$$\dot{S} = a_3 \rho^4 + \mathcal{O}(\rho^5) \leq -\kappa y^4 + \mathcal{O}(y^5).$$

Integration on both sides over an arbitrarily chosen time interval $T > 0$ yields

$$a_3 \int_0^T (\rho(t))^4 dt \leq -\kappa \int_0^T (y(t))^4 dt + \mathcal{O}(y^5)$$

which, from the observability of the linearized center manifold dynamics, forces $a_3 < 0$. This implies that the bifurcation is a supercritical HOPF bifurcation, that is, for small $\epsilon > 0$, all solutions in U either converge to the unstable equilibrium $x = 0$ or to a unique stable limit cycle of radius $\mathcal{O}(\sqrt{\epsilon})$. This concludes the proof. \blacksquare

The HOPF bifurcation scenario of Theorem 3.8 provides a high dimensional generalization of the global limit cycle oscillation mechanism satisfied by the VAN DER POL oscillator. It has the following energy interpretation: passivity at the bifurcation point allows for a lossless exchange of energy between at least two storage elements⁹. The static nonlinearity ϕ_k "regulates" the dissipation in the LURE feedback system, restoring energy when it is too low and dissipating it when it is too high.

On the other hand, the pitchfork bifurcation scenario provides a high dimensional generalization of the global bistability behavior occurring in the inner loop of Figure 3.6. The following result transforms this global bistability behavior into a feedback mechanism for global oscillations.

Theorem 3.9 *Under the assumptions of Theorem 3.8, suppose that the feedback interconnection of Σ and $\phi_k(\cdot)$ undergoes a supercritical pitchfork bifurcation at $k = k^*$ and that the feedback system shown in Figure 3.10 is ultimately bounded. Then there exists constants $\bar{\epsilon} > 0$, and $\tau > 0$ such that for all $k \in (k^*, k^* + \bar{\epsilon})$ and $\tau \gg (k - k^*)^{-1}$, the feedback system shown in Figure 3.10 is characterized by a globally asymptotically stable limit cycle in $\mathbb{R}^{n+1} \setminus E_s(0)$.*

⁹In the VAN DER POL oscillators these two elements are the two integrators appearing in Figure 3.3.

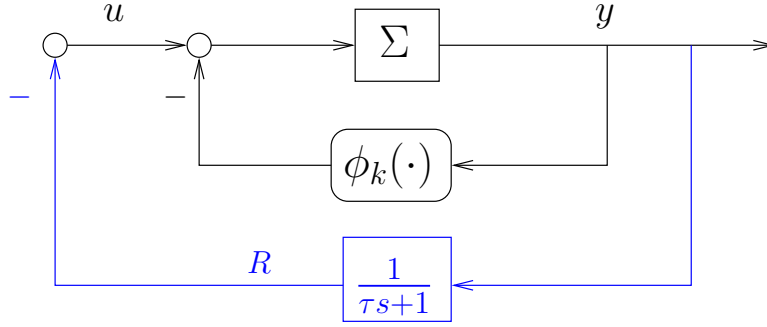


Figure 3.10: Converting the global bistability scenario into a relaxation oscillator with a slow adaptation mechanism ($\tau \gg (k - k^*)^{-1}$). The case $\Sigma = \frac{1}{s}$ corresponds to the FITZHUGH-NAGUMO oscillator.

Proof

The proof is similar to the proof of Theorem 3.8. Let $\epsilon = (k - k^*)$. Consider the system represented on Figure 3.10. By assumption, the feedback interconnection of Σ and $\phi_k(\cdot)$ possesses a one dimensional center manifold at $\epsilon = 0$. For $u \neq 0$, strong passivity of Σ implies that the center-unstable manifold dynamic writes¹⁰

$$\dot{y} = \epsilon y + a_3 y^3 + bu + \mathcal{O}(y^4), \quad a_3 < 0, \quad b > 0.$$

Thus, if we augment the one-dimensional center-unstable manifold of the original system (without adaptation) with the adaptation equation, we obtain

$$\begin{aligned} \dot{y} &= \epsilon y + a_3 y^3 - bR + \mathcal{O}(|(y, R)|^4), \quad a_3 < 0, \quad b > 0, \\ \dot{R} &= \delta(-R + y), \\ (\dot{\epsilon} &= 0, \\ \dot{\delta} &= 0), \end{aligned} \tag{3.38}$$

where treating $\delta = \tau^{-1}$ as a state variable makes the adaptation equation part of the center-unstable manifold locally defined around $(x, R, \epsilon, \delta) = (0, 0, 0, 0)$ (see [Wig90, Section 2.1b]). The equilibrium $(y, R) = (0, 0)$ of (3.38) is stable for $\epsilon < \delta > 0$ and unstable for $\epsilon > \delta > 0$. Standard arguments based on singular perturbation theory (see [Kha02, pp. 445-448]) prove that there exists a constant $\bar{\epsilon} > 0$ and a neighborhood U of the equilibrium $(y, R) = (0, 0)$ of (3.38) such that for any fixed $0 < \delta \ll \epsilon$, $\epsilon \in (0, \bar{\epsilon}]$, all solutions with initial condition in $U \setminus \{0\}$ converge to a unique limit cycle. Because of the time-scale separation, this limit cycle corresponds to a relaxation oscillation.

The global part of the proof is as in Theorem 3.8: for $\delta > 0$ and $\epsilon = 0$, the equilibrium $(x, R) = (0, 0)$ is globally asymptotically stable because the augmented storage $V = \delta S + \frac{1}{2}R^2$ satisfies the dissipation inequality $\dot{V} = \delta \dot{S} + \dot{R}R = -\delta y \phi(y) - \delta y R + \delta R(-R + y) \leq -\delta y \phi(y)$, which is analogous to (3.31). ■

¹⁰The strong passivity of Σ and the assumption $g(0) \neq 0$ imply that Σ has relative degree one at $x = 0$. This, in turn, implies that for x in a neighborhood of the origin, the input v of Σ directly enters the \dot{y} dynamics, i.e. $\dot{y} = \frac{\partial h}{\partial x} \dot{x} = L_f h(x) + L_g h(x)v$ with $L_g h(0) = \frac{\partial h}{\partial x} \Big|_{x=0} g(0) = b > 0$.

Remark 3.10 *If the forward system Σ is linear, strongly passive and detectable, then ultimate boundedness results from Theorem 3.6 since the adaptation dynamic is passive.*

Theorems 3.8 and 3.9 provide high dimensional extensions of the fundamental global oscillation mechanisms present in the VAN DER POL and FITZHUGH-NAGUMO models thus allowing for the definition of high dimensional, global nonlinear oscillators. Since the main property of the system Σ is its strong passivity, we name such oscillators *passive oscillators*. In the next section, we give the general definition of a passive oscillator.

3.3.4 Passive oscillator definition

We define a *passive oscillator* as a system that admits the feedback representation in Figure 3.8, is characterized by (3.16), (3.17), and (3.18), and satisfies the two following conditions:

1. the feedback system satisfies the dissipation inequality $\dot{S} \leq (k - k_{passive}^*) y^2 - y\phi(y) + uy$ where $S(x)$ represents the storage function of Σ and $k_{passive}^* \geq 0$ is the critical value of k above which the system Σ_k loses passivity;
2. when unforced ($u \equiv 0$), the feedback system possesses a global limit cycle, i.e. a stable limit cycle which attracts all solutions except those belonging to the stable manifold of the origin.

The first condition necessarily holds if we assume that the forward block Σ is strongly passive. In Theorems 3.8 and 3.9, we provided sufficient conditions for the second condition to be satisfied as well. The most restrictive assumption of Theorem 3.8 is the strong passivity assumption of Σ_{k^*} . It amounts to impose that, increasing k , Σ_k remains passive until it loses stability, i.e. to impose that $k_{passive}^* = k^*$. In the next section, we show that this assumption can be weakened through the use of multipliers.

The external characterization of our – possibly high-dimensional – passive oscillators by a dissipation inequality plays a role both in the supercritical character of the bifurcation and in the preservation of global convergence properties beyond the bifurcation value. In Chapter 4, we show that this external characterization also plays an important role in the study of oscillations in networks of interconnected passive oscillators.

3.4 Relaxation of the assumptions of Theorem 3.7 - Use of multipliers

The important property used in the proof of Theorem 3.8 is the absolute stability of the system at criticality (i.e. when $k = k^*$). As we have seen, this property is satisfied under the assumption that Σ_{k^*} is strongly passive. The assumption that Σ_{k^*} is strongly passive is rather restrictive. It requires that Σ_k loses stability and passivity for the same value of the parameter k . In general, this is not the case. As the parameter k increases, passivity of Σ_k is generally lost before stability. Special cases where passivity and stability are lost simultaneously include lossless systems, e.g. the simple integrator $\frac{1}{s}$ or general Output Feedback Lossless (OFL) systems, i.e. systems that can be rendered lossless by feedback. This quite restricts the applicability of Theorem 3.8. Fortunately, the assumptions of Theorem 3.8 can be relaxed with the help of multipliers (see [MR97] for a recent and

general treatment of multipliers). In this section, we will see how multipliers can be used to relax the Σ_{k^*} strong passivity assumption but still guarantee the absolute stability at $k = k^*$.

For the results of the present chapter, the main observation is that, when $H_1(s)$ and $H_2(s)$ are two transfer functions with both poles and zeros in the open left-half complex plane, then the feedback interconnection of Σ_k and ϕ in Figure 3.8 is equivalent to the feedback interconnection of $\tilde{\Sigma}_k = H_1 \Sigma_k H_2^{-1}$ and $\tilde{\phi} = H_2 \phi H_1^{-1}$ showed in Figure 3.11. If H_1 and H_2 are such that $\tilde{\phi}$ is strictly passive, then strong passivity of $\tilde{\Sigma}_k$ becomes sufficient for absolute stability, yielding relaxed conditions for the stability of the feedback system.

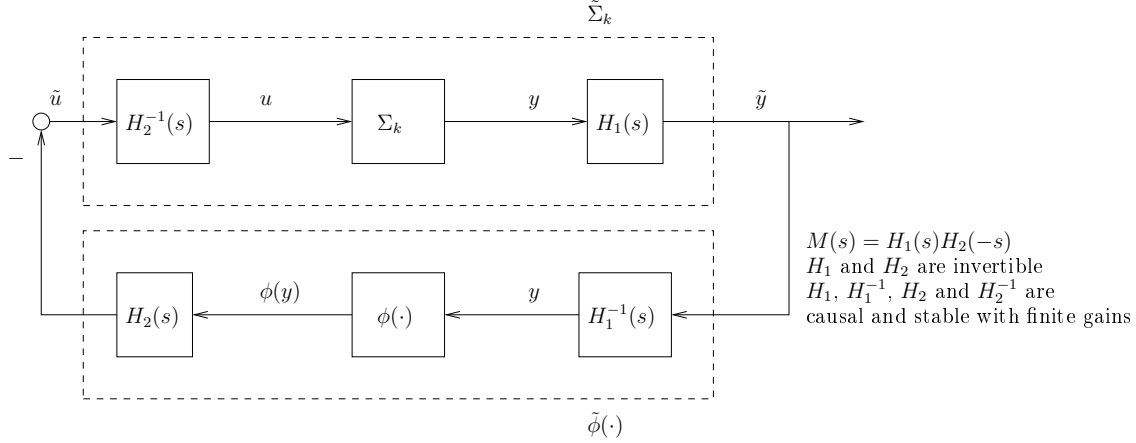


Figure 3.11: Equivalent feedback loop with multipliers.

For the sector nonlinearity ϕ , the simplest example of multiplier is the POPOV multiplier

$$M(s) = H_1(s) = 1 + \gamma s, \quad \gamma > 0.$$

Requiring strong passivity of the system $(1 + \gamma s)\Sigma_k$ for absolute stability of the feedback system (3.16),(3.17),(3.18) with $u \equiv 0$ is POPOV *criterion* [Kha02]. For *monotone increasing* static nonlinearities, a broad class of multipliers was introduced by ZAMES and FALB [ZF68] in the form

$$M(j\omega) = 1 - Z(j\omega) = 1 - \int_{-\infty}^{+\infty} z(t)e^{-j\omega t} dt, \quad \int_{-\infty}^{\infty} |z(t)| dt < 1. \quad (3.39)$$

The additional assumption $z(t) \geq 0$ is also needed unless $\phi(\cdot)$ is odd. ZAMES and FALB [ZF68] showed that multipliers of the form (3.39), which are not necessarily causal, can always be factored in the form

$$M(s) = H_1(s)H_2(-s)$$

with H_1 , H_2 , and their inverses being causal and stable and with the operator $\tilde{\phi} = H_2 \phi H_1^{-1}$ being strictly passive. As a consequence, strong passivity of $\tilde{\Sigma}_k$ is sufficient for absolute stability of the feedback system. Note that when Σ_k is a linear system, (strong) passivity of $\tilde{\Sigma}_k$ is equivalent to positive realness of the transfer function $G_k(s)H_1(s)H_2^{-1}(s)$ (see Lemma 2.21).

We summarize the following sufficient conditions for absolute stability of the feedback system in Figure 3.8.

Theorem 3.11 Consider the system shown in Figure 3.8 and characterized by (3.16), (3.17), (3.18) with $u \equiv 0$. Assume that Σ and its linearization are zero-state detectable and that all solutions of the feedback system are bounded. Then each of the following conditions is sufficient for global asymptotic stability of the equilibrium $x = 0$ of the feedback system.

- ϕ is in the sector $(0, \infty)$ and there exists $\gamma > 0$ such that $\tilde{\Sigma}_k = (1 + \gamma s)\Sigma_k$ is strongly passive;
- ϕ is monotone increasing in the sector $(0, \infty)$ and there exists $M(s) = H_1(s)H_2(-s)$ in the form (3.39), $z(t) \geq 0$, such that $\tilde{\Sigma}_k = H_1\Sigma_k H_2^{-1}$ is strongly passive;
- ϕ is odd, monotone increasing in the sector $(0, \infty)$ and there exists $M(s) = H_1(s)H_2(-s)$ in the form (3.39) such that $\tilde{\Sigma}_k = H_1\Sigma_k H_2^{-1}$ is strongly passive.

Proof

Let x be the state of $\tilde{\Sigma}_k$ and $\tilde{S}(x)$ be its the storage function. Strong passivity of $\tilde{\Sigma}_k$ implies

$$\dot{\tilde{S}} \leq \tilde{u}\tilde{y}, \quad (3.40)$$

where $\tilde{y} = H_1 y$ and \tilde{u} is the output of the operator $(-\tilde{\phi})$.

For the POPOV multiplier, this yields

$$\dot{\tilde{S}} \leq -\phi(y)(y + \gamma\dot{y}).$$

A LYAPUNOV function for the interconnection is given by $V = \tilde{S} + \gamma \int_0^y \phi(s) ds$, which satisfies

$$\dot{V} = \dot{\tilde{S}} + \gamma\phi(y)\dot{y} \leq -y\phi(y).$$

For ZAMES-FALB multipliers, the operator $(-\tilde{\phi})$ is of the form

$$(-\tilde{\phi}) \begin{cases} \dot{w}_1 = A_1 w_1 + B_1 \tilde{y}, & y = C_1 w_1 + D_1 \tilde{y} \\ \dot{w}_2 = A_2 w_2 + B_2 \phi(y), & \tilde{u} = -C_2 w_2 - D_2 \phi(y) \end{cases} \quad (3.41)$$

with (A_i, B_i, C_i, D_i) , $i = 1, 2$, being minimal realizations of the (stable) filters H_1^{-1} and H_2 , respectively. For a given $\tilde{y}(t)$, $t \geq 0$, we denote by $-\tilde{\phi}(\tilde{y}(t))$ the (unique) output $\tilde{u}(t)$ of (3.41) for the initial condition $w(0) = (w_1(0), w_2(0)) = (0, 0)$. Strict passivity of the operator $\tilde{\phi}$ is established in [ZF68]. It implies

$$\int_0^T \tilde{y}(t)\tilde{\phi}(\tilde{y}(t)) dt > 0$$

for all $T > 0$, which in turn implies that the integral monotonically increases as a function of T . For an arbitrary initial condition $w(0)$, the difference $\tilde{u}(t) + \tilde{\phi}(\tilde{y}(t))$ is exponentially decaying, and because $\tilde{y}(t)$ is bounded for all $t \geq 0$, we have

$$\int_0^\infty (\tilde{u}(t) + \tilde{\phi}(\tilde{y}(t))) \tilde{y}(t) dt \leq C(w(0)),$$

where the constant C continuously depends on the initial condition and satisfies $C(0) = 0$. Integrating the dissipation inequality (3.40), we obtain

$$\begin{aligned}
 \forall T \geq 0 : \quad -\tilde{S}(x(0)) &< \tilde{S}(x(T)) - \tilde{S}(x(0)) &\leq \int_0^T \tilde{u}(t)\tilde{y}(t) dt \\
 & &= \int_0^T (\tilde{u}(t) + \tilde{\phi}(\tilde{y}(t))) \tilde{y}(t) dt \\
 & &- \int_0^T \tilde{y}(t)\tilde{\phi}(\tilde{y}(t)) dt \\
 & &\leq C(w(0)) - \int_0^T \tilde{y}(t)\tilde{\phi}(\tilde{y}(t)) dt.
 \end{aligned}$$

This yields

$$\forall T \geq 0 : \quad \int_0^T \tilde{y}(t)\tilde{\phi}(\tilde{y}(t)) dt < \tilde{S}(x(0)) + C(w(0)).$$

Because the integral in the left hand side monotonically increases as a function of T , the finite upper bound in the right hand side forces asymptotic convergence of $\tilde{y}(t)$ to zero as $t \rightarrow \infty$. Convergence of the state follows from the zero-state detectability of $\tilde{\Sigma}_k$. Finally, LYAPUNOV stability of the origin follows from the continuous dependence of $\tilde{S}(x(0)) + C(w(0))$ on the initial condition and from the detectability of the linearized system. Global attractivity and LYAPUNOV stability of the origin imply that system resulting from the feedback interconnection of $\tilde{\Sigma}_k$ and $\tilde{\phi}$ is globally asymptotically stable. This concludes the proof. \blacksquare

Using Theorem 3.11, the assumptions of Theorem 3.8 can be weakened. Theorem 3.12 constitutes the multiplier version of Theorem 3.8.

Theorem 3.12 *The statements of Theorem 3.8 hold if the strong passivity assumption on Σ_{k^*} is replaced by one of the following conditions:*

- $\phi(\cdot)$ is in the sector $(0, \infty)$ and there exists $\gamma > 0$ such that $(1 + \gamma s)\Sigma_{k^*}$ is strongly passive;
- $\phi(\cdot)$ is monotone increasing in the sector $(0, \infty)$ and there exists $M(s) = H_1(s)H_2(-s)$ in the form (3.39), $z(t) \geq 0$, such that $\tilde{\Sigma}_{k^*} = H_1\Sigma_{k^*}H_2^{-1}$ is strongly passive;
- $\phi(\cdot)$ is odd, monotone increasing in the sector $(0, \infty)$ and there exists $M(s) = H_1(s)H_2(-s)$ in the form (3.39) such that $\tilde{\Sigma}_{k^*} = H_1\Sigma_{k^*}H_2^{-1}$ is strongly passive.

Proof

The global argument of the proof of Theorem 3.8 is unchanged because it relies on the absolute stability of the system when $\epsilon = k - k^* = 0$. Conditions of Theorem 3.11 still guarantee absolute stability when $\epsilon = 0$. For the local argument, in the case of POPOV multiplier, the dissipation inequality (3.31) is recovered with the new storage $\tilde{S} + \gamma \int_0^y \phi(s) ds$. In the case of ZAMES-FALB multipliers, we consider, as in the proof of Theorem 3.11, a C^1 and locally quadratic storage function

\tilde{S} for $\tilde{\Sigma}_{k^*}$, which satisfies the dissipation inequality

$$\dot{\tilde{S}} \leq \tilde{u}\tilde{y} \quad (3.42)$$

with $\tilde{y} = H_1 y$ and \tilde{u} the output of (3.41).

From the assumptions of ZAMES and FALB [ZF68], H_1 and H_2 are invertible and $H_1, H_1^{-1}, H_2,$ and H_2^{-1} are causal and bounded (i.e. have finite gains) operators. As a consequence, the filters $H_1, H_1^{-1}, H_2,$ and H_2^{-1} do not change the dimension of the center manifold. In normal form, the center manifold dynamics write [Wig90]

$$\dot{\xi} = A_c \xi + \mathcal{O}(|\xi|^3) \quad (3.43)$$

with $\xi \in \mathbb{R}$ and $A_c = 0$ when $G_{k^*}(s)$ has a unique pole at $s = 0$, and with (3.43) repeated from (3.35) when $G_{k^*}(s)$ has two conjugated poles at $s = \pm j\omega$.

In order to analyze the dissipation inequality (3.42) on the center manifold, we approximate the expression of \tilde{u} and \tilde{y} as functions of ξ up to suitable order. We note $\tilde{u} = \tilde{u}^{(3)}(\xi) + \mathcal{O}(|\xi|^4)$, $w_2 = h_2^{(3)}(\xi) + \mathcal{O}(|\xi|^4)$, $\tilde{y} = \tilde{c}\xi + \mathcal{O}(|\xi|^2)$, and $w_1 = h_1\xi + \mathcal{O}(|\xi|^2)$. By definition, we have

$$\tilde{u}^{(3)}(\xi) = -C_2 h_2^{(3)}(\xi) - D_2 \kappa (c\xi)^3, \quad c = C_1 h_1 + D_1 \tilde{c}.$$

The function $h_2^{(3)}$ is the solution of the partial differential equation that expresses the invariance of the center manifold up to terms $\mathcal{O}(|\xi|^4)$ (see [Car81]):

$$\left(-C_2 \frac{\partial h_2^{(3)}}{\partial \xi} - D_2 3\kappa (c\xi)^2 c \right) A_c \xi = -C_2 A_2 h_2^{(3)}(\xi) - C_2 B_2 \kappa (c\xi)^3 - D_2 3\kappa (c\xi)^2 c A_c \xi \quad (3.44)$$

with the boundary conditions $h_2^{(3)}(0) = 0$, $\left. \frac{\partial h_2^{(3)}}{\partial \xi} \right|_{\xi=0} = 0$. Because they satisfy the same partial differential equation (see [Isi95, Chapter 8]), the solution $\tilde{u}^{(3)}(\xi(t))$ coincides with the unique steady-state output of the operator $(-\tilde{\phi}^{(3)})$, which is the operator $(-\tilde{\phi})$ with $\phi(\cdot)$ replaced by its cubic approximation, to the (periodic) input $\tilde{y}^{(1)} = \tilde{c}e^{A_c t} \xi(0)$.

Case (1): When $\xi \in \mathbb{R}$, the constant input $\tilde{y}^{(1)} = \tilde{c}\xi$ gives rise to the constant output $\tilde{u}^{(3)}(\xi) = \beta\xi^3$. Strict positivity [ZF68] of the operator $\tilde{\phi}^{(3)}$ implies that $\tilde{c}\beta = -\gamma < 0$. The dissipation inequality thus becomes

$$\dot{\tilde{S}} \leq \tilde{u}^{(3)}(\xi)\tilde{y}^{(1)}(\xi) + \mathcal{O}(|\xi|^5) = -\gamma\xi^4 + \mathcal{O}(|\xi|^5),$$

which forces the existence of a supercritical pitchfork bifurcation, as in the proof of Theorem 3.8.

Case (2): When $\xi \in \mathbb{R}^2$, the periodic input $\tilde{y}^{(1)}(\xi(t)) = \tilde{c}e^{A_c t} \xi(0)$ gives rise to the periodic output $\tilde{u}^{(3)}(\xi(t))$. Strict positivity [ZF68] and homogeneity of the operator $\tilde{\phi}^{(3)}$ implies

$$\int_0^T \tilde{u}^{(3)}(\xi(t))\tilde{y}^{(1)}(\xi(t)) dt < -\gamma|\xi(0)|^4 + \mathcal{O}(|\xi(0)|^5), \quad T = \frac{2\pi}{\omega}.$$

Using the same argument as in the proof of Theorem 3.8, integration of (3.42) over one period yields for initial conditions in the center manifold

$$\tilde{S}(x(T)) - \tilde{S}(x(0)) = a_3 \int_0^T \rho^4(t) dt + \mathcal{O}\left((\rho(0))^5\right) < -\gamma(\rho(0))^4 + \mathcal{O}\left((\rho(0))^5\right).$$

This forces $a_3 < 0$ in the center manifold dynamics (3.36), which proves the existence of a supercritical HOPF bifurcation. This concludes the proof. \blacksquare

3.5 Examples and simulation results

We illustrate the main result of Section 3.4 with the second-order system

$$\ddot{\theta} + \omega_n^2 \theta + 2\zeta \omega_n \dot{\theta} = u, \quad \tau > 0, \quad \omega_n > 0. \quad (3.45)$$

The choice of the output $y = \tau \dot{\theta} + \omega_n^2 \theta$ results in the transfer function

$$H(s) = \frac{\tau s + \omega_n^2}{s^2 + 2\zeta \omega_n s + \omega_n^2}, \quad (3.46)$$

which is passive if

$$2\zeta \geq \frac{\omega_n}{\tau} > 0. \quad (3.47)$$

Such a transfer function is a model for the mechanical system represented in Figure 3.12. The mass m glides on the ground without friction. It is attached to a spring and a dashpot linked to each other through a gearing. Denoting by d the damping factor of the dashpot, by r the spring factor, by l_0 the natural length of the spring, and by α the gearing ratio, the dynamical equation of this mechanical system is

$$m\ddot{x} = -d(\dot{x} - \dot{v}) - r(x - u - l_0),$$

where u is the input of the system and $x - l_0$ its output. Since $v = \alpha u$, the corresponding transfer function of the system is

$$H(s) = \frac{d\alpha s + r}{ms^2 + ds + r} = \frac{\frac{d\alpha}{m}s + \frac{r}{m}}{s^2 + \frac{d}{m}s + \frac{r}{m}},$$

where the passivity condition (3.47) is satisfied if $d^2 \geq \frac{r}{\alpha} m > 0$.

In the next sections, we illustrate the results of Theorems 3.8, 3.9, and 3.12 on this simple mechanical example. To this end, we consider the LURE feedback system in Figure 3.8 where $\Sigma = H(s)$. $\phi(\cdot)$ is assumed to satisfy the assumptions of Section 3.3.1 and additionally to be odd (this is useful for the use of ZAMES-FALB multipliers) and monotone increasing (this will be useful for illustrations used in Chapter 4).

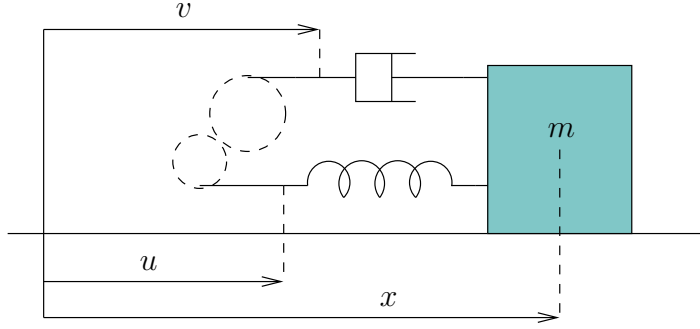
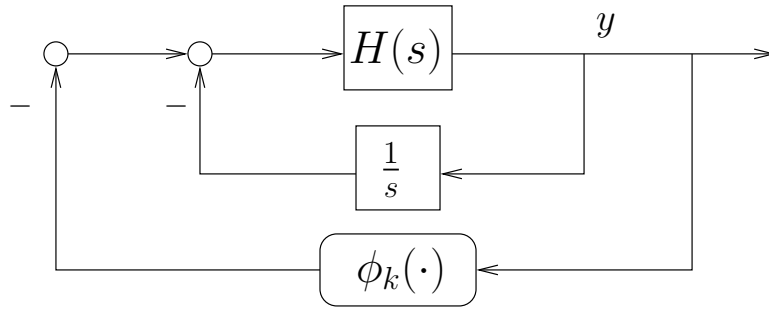


Figure 3.12: Mechanical example.


 Figure 3.13: Forcing the HOPF bifurcation with an integrator in the feedback loop. The case $H(s) = \frac{1}{s}$ corresponds to the VAN DER POL oscillator.

3.5.1 Forcing the HOPF bifurcation

As a first illustration, we force the HOPF bifurcation scenario by considering the feedback system shown in Figure 3.13. Rewriting the system in the LURE form of Figure 3.8, the HOPF bifurcation is forced because of the presence of a single zero at $s = 0$ in the transfer function $G(s) = \frac{sH(s)}{s+H(s)}$. As we have seen, in Section 3.3.3, the positive part of the real axis belongs to the root locus. The presence of a single zero at $s = 0$ then necessarily forces the HOPF bifurcation scenario.

The system is equivalently described by the feedback interconnection of $G_k(s) = \frac{sH(s)}{s+(1-k)sH(s)}$ with the static nonlinearity $\phi(\cdot)$. Here, the transfer function $G_k(s)$ is

$$G_k(s) = \frac{s(\tau s + \omega_n^2)}{s^3 + (2\zeta\omega_n - k\tau)s^2 + (\tau + \omega_n^2(1-k))s + \omega_n^2}.$$

A HOPF bifurcation arises at

$$k^* = \frac{\tau(\tau + \omega_n^2) + 2\zeta\omega_n^3 - \sqrt{\tau^4 + 2\omega_n^2\tau^3 + \omega_n^3(\omega_n - 4\zeta)\tau^2 + 4\omega_n^4\tau(1 - \zeta\omega_n) + 4\zeta^2\omega_n^6}}{2\omega_n^2\tau}, \quad (3.48)$$

with

$$G_{k^*}(s) = \frac{sH(s)}{s + (1 - k^*s)H(s)} = \frac{s(\tau s + \omega_n^2)}{(s + \alpha)(s^2 + \Omega^2)},$$

and

$$\alpha = 2\zeta\omega_n - k^*\tau, \quad \Omega = \sqrt{\tau + \omega_n^2(1 - k^*)}.$$

Furthermore, $G_k(j\omega)$ is passive (see Lemma 2.21) if $k \leq k_{passive}^*$, with

$$k_{passive}^* = \min \left(1, \left(2\zeta - \frac{\omega_n}{\tau} \right) \frac{\omega_n}{\tau} \right). \quad (3.49)$$

If $k_{passive}^* = k^*$, we may directly use Theorem 3.8 to conclude to the existence of a globally asymptotically stable limit cycle for $k \gtrsim k^*$.

If $k_{passive}^* < k^*$, we may still obtain the result with the help of Theorem 3.12. Indeed, when $k_{passive}^* < k^*$, and $0 < \alpha < 2\frac{\omega_n^2}{\tau}$ (which is equivalent to the condition $2\frac{\omega_n}{\tau}(\zeta - \frac{\omega_n}{\tau}) < k^* < 2\zeta\frac{\omega_n}{\tau}$), we may use a ZAMES-FALB multiplier to prove absolute stability at the critical bifurcation value $k = k^*$. This ZAMES-FALB multiplier is

$$M(s) = H_1(s) = 1 - Z(s), \quad Z(s) = \frac{\frac{\omega_n^2}{\tau} - \alpha}{s + \frac{\omega_n^2}{\tau}}, \quad \text{ROC} = \left\{ s \in \mathbb{C} \mid \Re\{s\} > -\frac{\omega_n^2}{\tau} \right\}, \quad (3.50)$$

which, at $k = k^*$, yields the passive transfer function

$$G_{k^*}(s)H_1(s) = \tau \frac{s}{s^2 + \Omega^2}.$$

By Theorem 3.12, for $\tau > 0$, $\omega_n > 0$, and $\zeta > 0$ satisfying (3.47), and k^* given in (3.48) satisfying $2\frac{\omega_n}{\tau}(\zeta - \frac{\omega_n}{\tau}) < k^* < 2\zeta\frac{\omega_n}{\tau}$, the feedback system in Figure 3.13 with $H(s)$ defined by (3.46), is absolutely stable for all $k \leq k^*$ and possesses a globally asymptotically stable limit cycle for $k \gtrsim k^*$.

3.5.1.1 Simulation results

Suppose we chose the parameters values as $\omega_n = 1$, $\tau = 2$ and $\zeta = 1.25$. We thus have $H(s) = \frac{2s+1}{s^2+2.5s+1}$. From these parameters values we can compute the critical value k^* of the bifurcation parameter and the quantity $k_{passive}^*$ defining the excess of passivity of H (see (3.48) and (3.49)). We obtain $k^* = 1$ and $k_{passive}^* = 1$. In this particular case, there is no need of a multiplier to prove the absolute stability at $k = k^*$ since the system loses passivity and stability simultaneously at $k = 1$. Direct application of Theorem 3.8 allows to conclude to the existence of a globally asymptotically stable limit cycle for $k \gtrsim k^*$.

For the simulations, we considered the feedback interconnection of $G(s) = \frac{sH(s)}{s+H(s)}$ with the nonlinearity $\phi_k(y) = y^3 - ky$. We simulated the system obtained with $H(s) = \frac{2s+1}{s^2+2.5s+1}$ for different values of k around the critical value $k^* = 1$ and for different initial conditions. Figure 3.14 illustrates the simulation results for an arbitrarily chosen initial condition. As can be seen, the origin of the feedback nonlinear system is GAS for $k \leq 1$ whereas a limit cycle appears for values of $k \gtrsim 1$. To test the range of values of k for which the result holds, we have simulated the system with many different values of $k > 1$. In all cases, we obtained an asymptotically stable limit cycle whose amplitude is proportional to the value of $k - k^*$ as predicted by the HOPF bifurcation theorem.

To illustrate a case where the multiplier (3.50) is needed to prove absolute stability at $k = k^*$, we considered the following parameters values: $\omega_n = 1$, $\tau = 2$ and $\zeta = 1$. We thus have $H(s) = \frac{2s+1}{s^2+2s+1}$. With these parameters values, we obtain $k_{passive}^* = 0.75$ and $k^* = 0.7753$. Since the condition

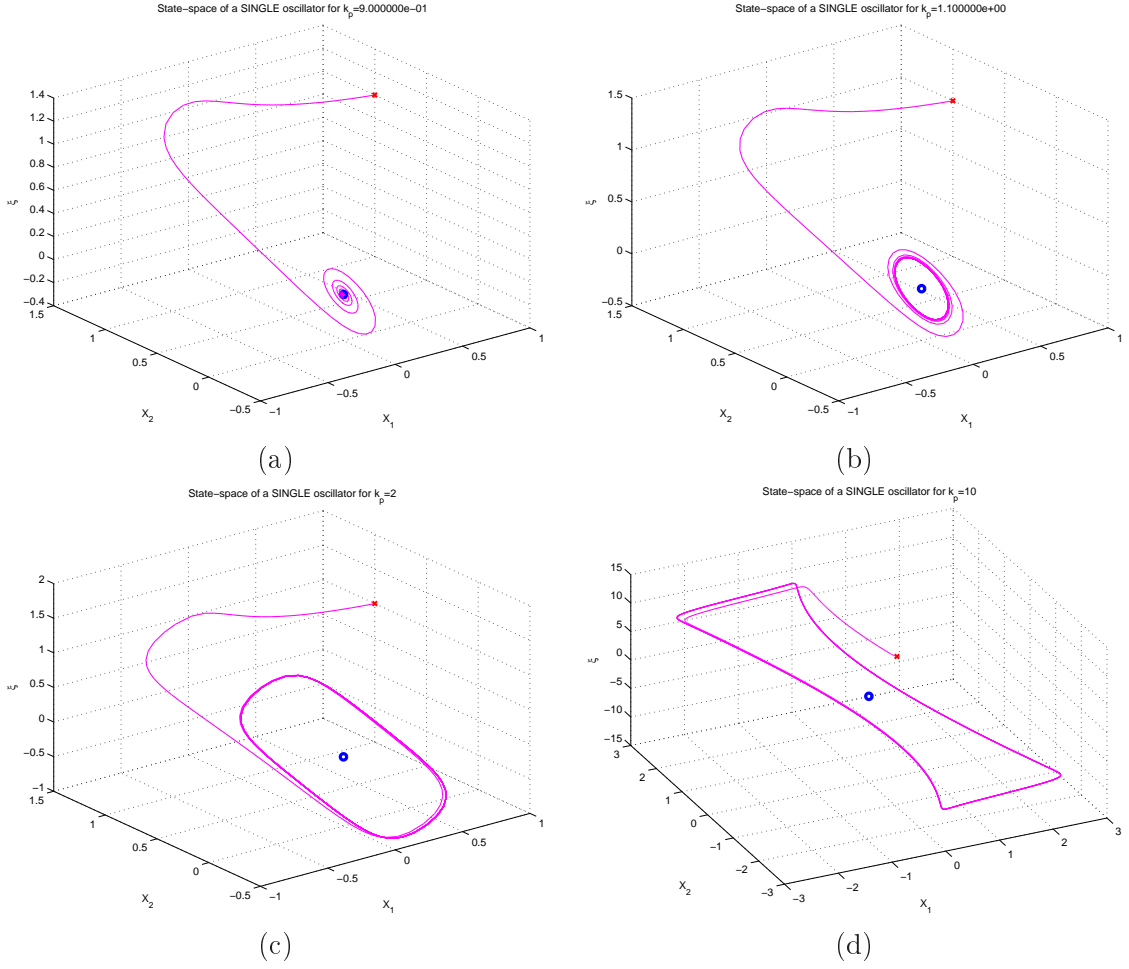


Figure 3.14: (a) State-space for $k = 0.9$. (b) State-space for $k = 1.1$. (c) State-space for $k = 2$. (d) State-space for $k = 10$

$2\frac{\omega_n}{\tau} \left(\zeta - \frac{\omega_n}{\tau}\right) < k^* < 2\zeta\frac{\omega_n}{\tau}$ is satisfied, we can use the ZAMES-FALB multiplier (3.50) to prove absolute stability at $k = k^*$.

For the simulations, we considered, once again, the feedback interconnection of $G(s) = \frac{sH(s)}{s+H(s)}$ with the nonlinearity $\phi_k(y) = y^3 - ky$. We simulated the system obtained with $H(s) = \frac{2s+1}{s^2+2s+1}$ for different values of k around the critical value $k^* = 0.7753$, and for different initial conditions. Figure 3.15 illustrates the simulation results for an arbitrarily chosen initial condition. As can be seen, the origin of the feedback nonlinear system is GAS for $k \leq k^*$ whereas a limit cycle appears for values of $k \gtrsim k^*$.

3.5.1.2 Graphical interpretation of the multiplier effect

In this section, we consider the example given in the previous section and show the effect of the multiplier on the NYQUIST and BODE plots of the transfer function $G_k(j\omega)$.

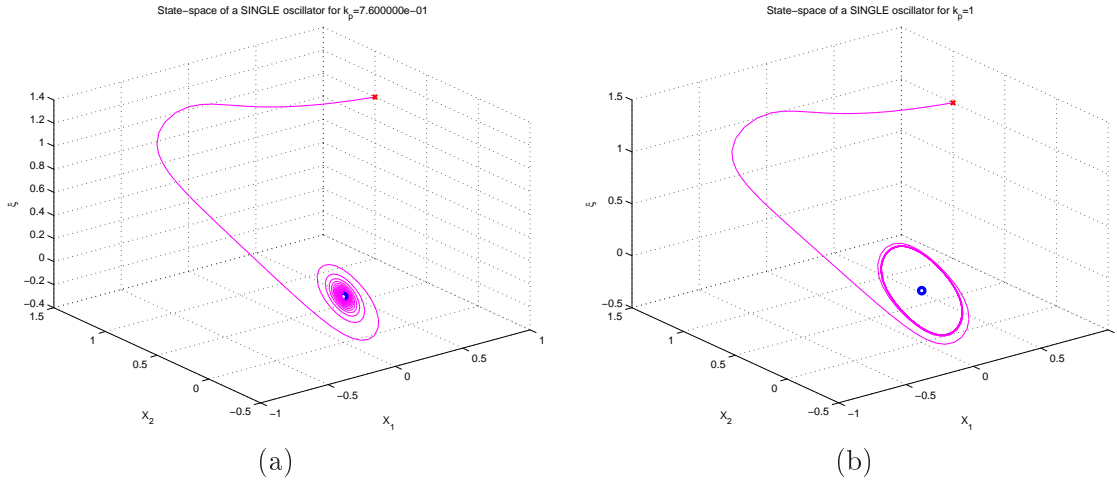


Figure 3.15: (a) State-space for $k = 0.77$. (b) State-space for $k = 1$.

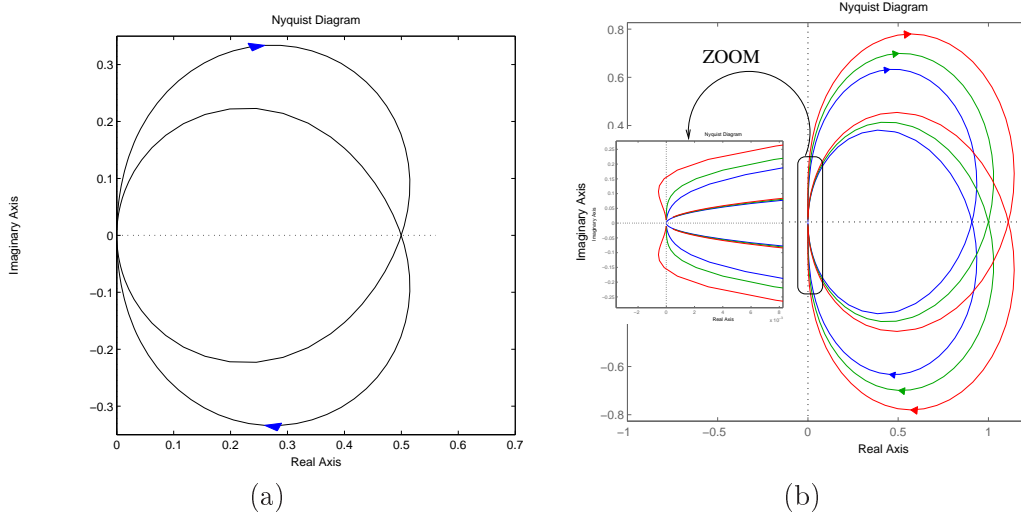


Figure 3.16: (a) NYQUIST plot of $G(j\omega)$. (b) NYQUIST plot of $G_k(j\omega)$ for $k = k_{passive}^* - 0.1$, $k_{passive}^*$, $k_{passive}^* + 0.1$.

As was the case in the multiplier illustrative example of the preceding section, consider the transfer function $G(s) = \frac{sH(s)}{s+H(s)}$ with $H(s) = \frac{2s+1}{s^2+2s+1}$. Figure 3.16 represents the NYQUIST plots of $G(j\omega)$ and $G_k(j\omega)$ ($G_k(j\omega)$ is the (positive) feedback interconnection of $G(j\omega)$ with the static gain k ; it corresponds to the the transfer function of the linearization of Σ_k and is used to perform the bifurcation analysis). Figure 3.16 represents the NYQUIST plots of $G(j\omega)$ and $G_k(j\omega)$. As can be seen on the NYQUIST plot of $G(j\omega)$, the point of loss of passivity (intersection of the disk margin¹¹ with the real axis, see [SJK97]) does not coincide with the point of loss of stability (intersection of

¹¹The disk margin is the smallest disk that entirely contains the NYQUIST plot of $G(j\omega)$. It corresponds to the open disk in the complex plane with its center on the real axis and its boundary intersecting the real axis at the points $(0, 0)$ and $(0, \frac{1}{k_{passive}^*})$.

the NYQUIST plot of $G(j\omega)$ with the real axis). As a result, when k is increased, the system loses passivity before losing stability. The effect of the ZAMES-FALB multipliers is to transform the initial feedback loop into an equivalent one (see Figure 3.11) where the forward path $\tilde{\Sigma}_k$ is strongly passive for $k \leq k^*$. This can be seen in Figure 3.17. In this figure, we see that, without multiplier, $G_k(j\omega)$ loses passivity at $k_{passive}^* = \min(1, (2\zeta - \frac{\omega_n}{\tau}) \frac{\omega_n}{\tau})$. This is trivially seen on the NYQUIST plot of $G_k(j\omega)$ where the positive realness condition $\Re(G_k(j\omega)) \geq 0, \forall \omega$ of Lemma 2.21 is not satisfied for $k > k_{passive}^*$, or on the BODE phase diagram where the passivity phase condition $\angle(G_k(j\omega)) \leq \frac{\pi}{2}$ is not satisfied for $k > k_{passive}^*$. On the contrary, the transfer function $G_k(j\omega)M(j\omega)$ satisfies these conditions for $k \leq k^*$ which equivalently means that $k_{passive}^* = k^*$ for the system with multiplier.

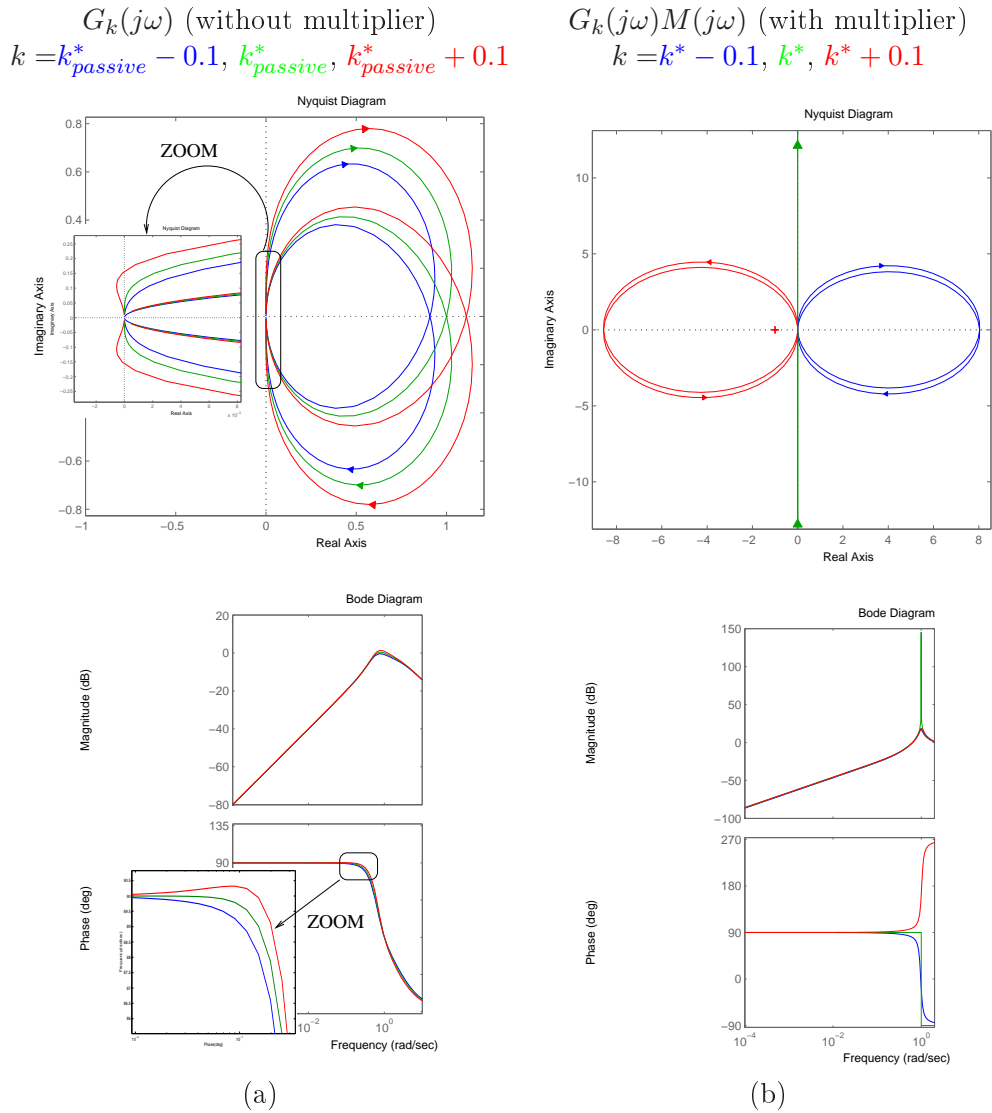


Figure 3.17: Effect of the ZAMES-FALB multipliers. Column (a) Without multiplier. Column (b) With multiplier.

3.5.2 Not forcing the HOPF bifurcation - pitchfork bifurcation

As a second illustration, we do not force the HOPF bifurcation with an additional integrator. We analyze bifurcations in the feedback interconnection of $H(s)$ with $\phi_k(\cdot)$. Different bifurcation scenarios are possible. To see this, consider the transfer function

$$H_k(s) = \frac{H(s)}{1 - kH(s)} = \frac{\tau s + \omega_n^2}{s^2 + (2\zeta\omega_n - k\tau)s + (1 - k)\omega_n^2}. \quad (3.51)$$

The bifurcation in the feedback loop differs according to the relative position of the poles and zero of $H(s)$. If $2\zeta\omega_n > \tau$, then a pitchfork bifurcation occurs at $k^* = 1$, and

$$H_{k^*}(s) = \frac{\tau s + \omega_n^2}{s(s + 2\zeta\omega_n - \tau)}.$$

The (POPOV) multiplier $M(s) = 1 + s(2\zeta\omega_n - \tau)^{-1}$ makes the transfer function $H_{k^*}(s)M(s) = \frac{\tau s + \omega_n^2}{(2\zeta\omega_n - \tau)s}$ passive for $k \leq k^*$. By Theorem 3.12, the feedback interconnection of $H_{k^*}(s)$ with $\phi(\cdot)$ is absolutely stable for $k \leq k^*$ and globally bistable for $k \gtrsim k^*$.

3.5.2.1 Simulation results

To illustrate the global bistability behavior, we have chosen the following parameters values: $\omega_n = 1$, $\tau = 2$ and $\zeta = 2.5$. With these parameters values, we are in the case where $2\zeta\omega_n > \tau$. We then considered the feedback interconnection of $H(s)$ with the nonlinearity $\phi_k(y) = y^3 - ky$. We simulated the feedback system for different values of k around the critical value $k^* = 1$. Figure 3.18 illustrates the simulation results. As can be seen, the origin of the feedback nonlinear system is GAS for $k \leq 1$ whereas it is globally bistable for $k \gtrsim 1$. To clearly see the two stable equilibria we performed the simulation twice with two opposed sign initial conditions.

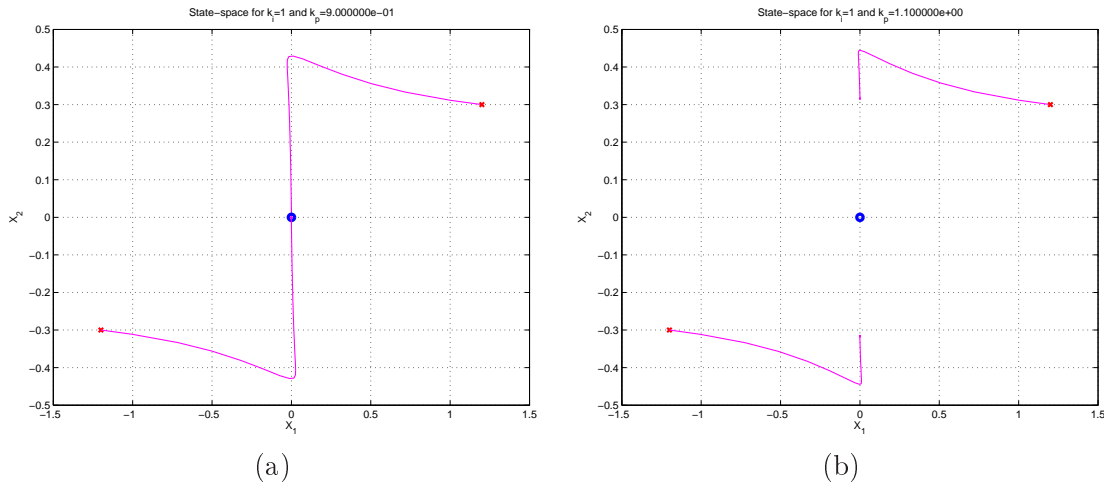


Figure 3.18: (a) State-space for $k = 0.9$ without adaptation feedback loop. (b) State-space for $k = 1.1$ without adaptation feedback loop.

To illustrate the results of Theorem 3.9, we then performed simulations of the feedback system when an additional adaptation loop is present as in Figure 3.10. The system resulting from the addition of the feedback adaptation loop is of order 3. The adaptation parameter is chosen as $\tau = 100(k - k^*)^{-1}$. The simulation results are shown in Figure 3.19 for $k = 2$. In Figure 3.19-(b), we show the projection of the state space on the two dimensional space of the state variables of H . The relaxation nature of the oscillation is clearly seen in Figure 3.20 which represents the output y of the system.

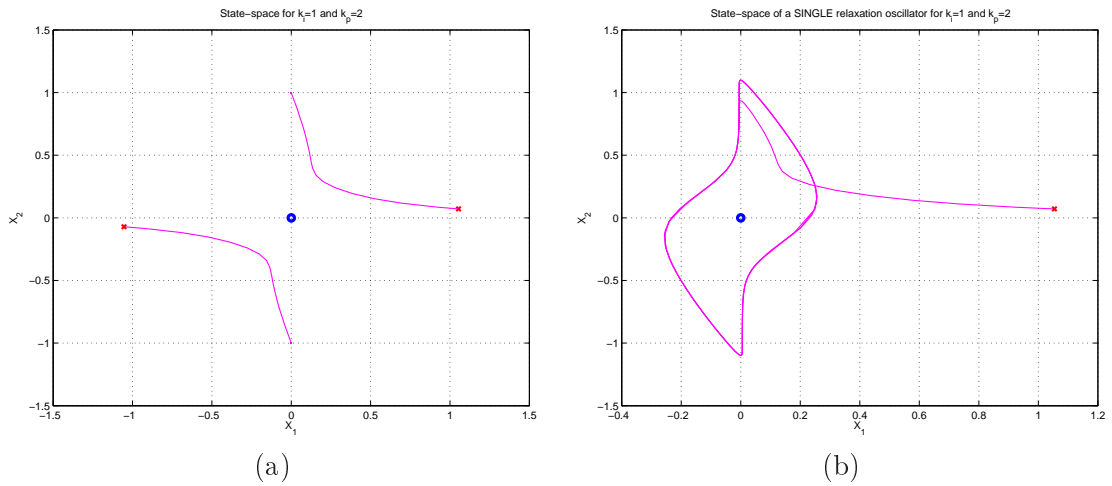


Figure 3.19: (a) State-space for $k = 2$, without adaptation feedback loop. (b) Projection of the state space on the two dimensional space of the state variables of H for $k = 2$, with adaptation feedback loop.

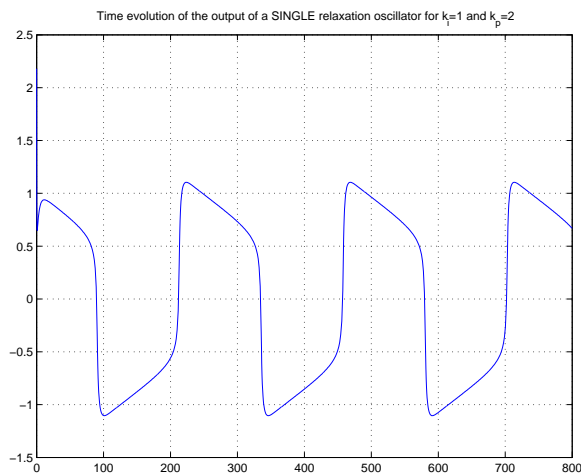


Figure 3.20: Output of the relaxation oscillator.

3.5.3 Not forcing the HOPF bifurcation - HOPF bifurcation

Consider, once again, the transfer function (3.51). If $2\zeta\omega_n < \tau$, then a HOPF bifurcation arises at $k^* = \frac{2\zeta\omega_n}{\tau}$, and

$$H_{k^*}(s) = \frac{\tau s + \omega_n^2}{s^2 + \left(1 - \frac{2\zeta\omega_n}{\tau}\right)\omega_n^2}.$$

No valid multiplier could be found to prove absolute stability of the feedback loop for $k \leq k^*$. The results of Theorem 3.12 do not apply in this situation and the stability properties of the limit cycle may depend on the particular nonlinearity $\phi(\cdot)$.

3.6 Numerical analysis of PLS - GAS of the limit cycle for a particular value of the bifurcation parameter

In Section 3.3.3, we defined a class of parameter-dependent nonlinear systems exhibiting an almost globally asymptotically stable limit cycle. The results were proved for values of the parameter in the vicinity of a bifurcation value. Unfortunately, Theorems 3.8 and 3.9 do not give any prediction about the range of parameter values in which the results hold. In order to be able to conclude about global asymptotic stability of the limit cycle for a particular value of the parameter, we consider an equivalent piecewise linear characterization of this class of systems and adapt numerical tools recently proposed in the literature (see [GMD03]).

In [GMD03], GONCALVES developed a constructive numerical method in order to analyse the behavior of *piecewise linear systems* (PLS). These systems are characterized by a finite number of affine linear dynamical models together with a set of rules for switching among these models. The methodology developed by GONCALVES consists in inferring global properties of PLS solely by studying their behavior at their corresponding switching surfaces. The method allows the global stability analysis of equilibrium points as well as that of limit cycles through the same concepts. The main idea is to analyze *impact maps*, i.e. maps from one switching surface to the next switching surface. These maps are proved globally stable by constructing quadratic LYAPUNOV functions on the switching surfaces. The notion of an impact map can be thought as a generalization of a POINCARÉ map. Proving that all the impact maps are globally contracting around some specific points is a sufficient condition for proving that the POINCARÉ map associated to the PLS is globally contracting. In this way global asymptotic stability of a limit cycle can be proved by checking global contraction of the impact maps around the specific switching points that this limit cycle has in common with the switching surfaces.

The key result of GONCALVES concerns a representation of impact maps that allows to use them to conclude about stability of PLS. Impact maps are known to be “unfriendly” maps in the sense that they are highly nonlinear, multivalued, and not continuous. Although analysis of nonlinear systems at switching surfaces has already been studied (e.g. POINCARÉ), with the exception of very simple systems, no one really knew how to use impact maps to analyse global properties of PLS. The reason why GONCALVES was able to use impact maps in the global analysis of certain classes of hybrid systems is based on the discovery that an impact map induced by an LTI (linear time-invariant) flow between two switching surfaces can be represented as a linear transformation analytically parametrized by a scalar function of the state. This parameter is simply the switching time associated with the impact map. This representation of impact maps allows the search for quadratic LYAPUNOV functions on switching surfaces to be done by simply solving a set of *linear matrix inequalities* (LMIs) using

efficient computational algorithms. Global asymptotic stability of limit cycles and equilibrium points of PLS can in this way be efficiently checked.

The algorithms developed by GONCALVES depend on the switching structure imposed by the particular PLS under consideration. These algorithms have to be adapted to each particular type of piecewise linear system. This amounts to adapt the definition of the switching surfaces, their position in the state space and the particular linear dynamics in each region.

In the next sections, we define a piecewise linear version of the passive oscillator. We then show how the method of GONCALVES may be adapted to numerically prove global asymptotic stability of the limit cycle for second order piecewise linear passive oscillators. Extension of this numerical method to high-order piecewise linear passive oscillator is part of ongoing research.

3.6.1 Problem definition

We start by defining a piecewise linear system (PLS) qualitatively equivalent to the class of passive oscillators. For this, we consider the PLS resulting from the feedback interconnection of a strongly passive, linear system with a piecewise linear approximation of the nonlinearity $\phi_k(\cdot)$ defined by (3.17). In other words, we consider the feedback interconnection of a linear system H whose dynamics are

$$H : \begin{cases} \dot{x} &= Ax + Bv, & x \in \mathbb{R}^n (n \geq 2), & v \in \mathbb{R} \\ y &= Cx, & & y \in \mathbb{R} \end{cases} \quad (3.52)$$

with a piecewise linear function $f_{pls}(y)$:

$$v = -f_{pls}(y) = \begin{cases} -p(y + m) - km & \text{for } y < -m \\ ky & \text{for } -m \leq y \leq m \\ -p(y - m) + km & \text{for } y > m \end{cases} \quad (3.53)$$

The system H is assumed to be strongly passive and detectable. The parameters of the piecewise linear function $f_{pls}(\cdot)$ satisfy $k > 0$, $m = \sqrt{\frac{k}{3}}$ and $p > 0$. The function $f_{pls}(\cdot)$ is a piecewise linear approximation of the cubic nonlinearity $\phi_k(y) = -ky + y^3$ that appears in the VAN DER POL and FITZHUGH-NAGUMO oscillators, as can be seen in Figure 3.21. This cubic nonlinearity is one of the most simple example of nonlinearity that satisfies the assumptions made in Theorems 3.8 and 3.9. The method presented here can be applied to any other kind of nonlinearity. For more complicated nonlinearities, the complexity of its piecewise approximation (i.e. the number of piecewise linear regions) increases and so does the complexity of the corresponding algorithm.

Since $f_{pls}(\cdot)$ is odd, the resulting system is *symmetric* in the sense that if $x(t)$ is a solution starting at x_0 then $-x(t)$ is another solution starting at $-x_0$. As we will see shortly, this symmetry property helps in reducing the complexity of the numerical algorithm.

The piecewise linear system resulting from the feedback interconnection of (3.52) and (3.53) consists of three regions, (R_1) , (R_2) , and (R_3) in the state space delimited by two switching surfaces, S_0 and S_1 . The linear dynamics in each region are respectively

1. (R_1) $y(t) < -m$
 $\dot{x} = (A - pBC)x - dB = A_1x - dB,$
2. (R_2) $-m \leq y(t) \leq m$
 $\dot{x} = (A + kBC)x = A_2x,$

3.6. NUMERICAL ANALYSIS OF PLS - GAS OF THE LIMIT CYCLE FOR A PARTICULAR VALUE OF THE BIFURCATION PARAMETER

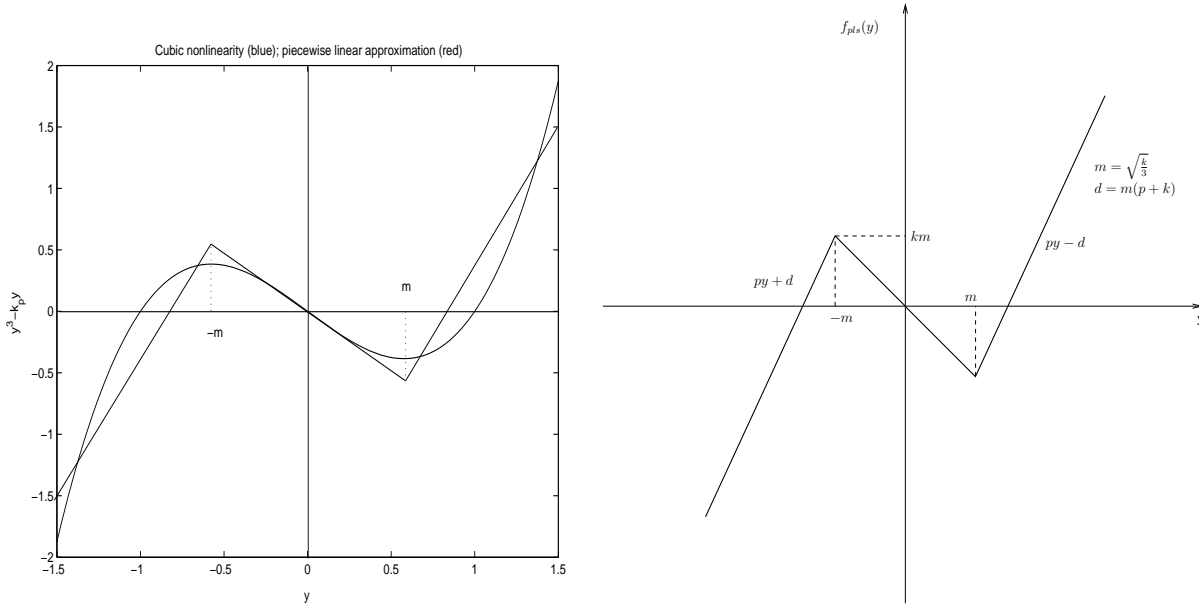


Figure 3.21: Replacing the nonlinear function $\phi_k(\cdot)$ by a piecewise linear function $f_{pls}(\cdot)$.

3. (R_3) $y(t) > m$
 $\dot{x} = (A - pBC)x + dB = A_1x + dB,$

where $d = m(k + p)$.

Throughout this section, we assume that A_2 has no real unstable eigenvalue. We also assume that $\frac{1}{k+p} > -CA_1^{-1}B$ in order to guarantee that the system (3.52),(3.53) has a unique equilibrium, located at $x = 0$.

Because the feedforward linear system H is assumed to be (strongly) passive and detectable, the matrix A_1 is HURWITZ for any positive value of p . Since the functions $\phi(\cdot)$ and $f_{pls}(\cdot)$ have the same linearization around the origin, the dynamics in the intermediate region (R_2) is the same as the dynamics of the nonlinear feedback system linearized around the origin. This implies that the matrix A_2 has at least 2 eigenvalues with positive real parts for $k > k^*$.

The switching surfaces of the PLS are defined by

$$\begin{aligned} S_0 &= \{x \in \mathbb{R}^n \mid Cx = -m\}, \\ S_1 &= \{x \in \mathbb{R}^n \mid Cx = m\} = -S_0. \end{aligned}$$

Our analysis, based on [GMD03], will be in terms of contraction properties of impact maps that solutions of the PLS define between switching surfaces. The key observation in [GMD03] is that these impact maps are linear maps parametrized by the switching time, which is a scalar function of the state.

3.6.2 Existence of limit cycles

We will only be interested in cycles of (3.52),(3.53) that are of the type illustrated in Figure 3.22: a (periodic) solution initialized at $-x_1^* \in S_0$ obeys the linear dynamics (R_1) and reaches a point

$x_0^* \in S_0$ after a finite switching time t_1^* ; it then obeys the linear dynamics (R_2) and reaches the point $x_1^* \in S_1$ after a finite switching time t_2^* . The values x_0^* , x_1^* , t_1^* and t_2^* that determine the periodic solution satisfy the algebraic equations (see [GMD03])

$$f_1(t_1^*, t_2^*) = Cx_0^*(t_1^*, t_2^*) + m = 0, \quad (3.54)$$

$$f_2(t_1^*, t_2^*) = Cx_1^*(t_1^*, t_2^*) - m = 0, \quad (3.55)$$

where

$$x_0^*(t_1^*, t_2^*) = \left(I + e^{A_1 t_1^*} e^{A_2 t_2^*} \right)^{-1} A_1^{-1} \left(I - e^{A_1 t_1^*} \right) dB,$$

$$x_1^*(t_1^*, t_2^*) = \left(I + e^{A_2 t_2^*} e^{A_1 t_1^*} \right)^{-1} e^{A_2 t_2^*} A_1^{-1} \left(I - e^{A_1 t_1^*} \right) dB.$$

These solutions simply characterize the switching points that the limit cycle of Figure 3.22 defines on the switching surfaces.

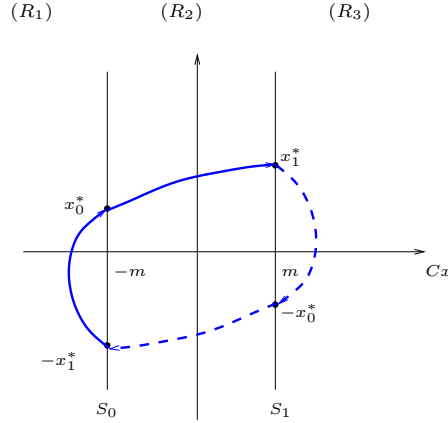


Figure 3.22: Limit cycle with four switches per period (first half period in plain line and second half period in dashed line).

The roots of (3.54),(3.55) determine periodic solutions of (3.52),(3.53). Simulations of the system (3.52),(3.53) provide a good initial guess for the numerical search of (t_1^*, t_2^*) solving (3.54),(3.55).

3.6.3 Quadratic stability of impact maps

As we have stated in the introduction of Section 3.6, stability of the limit cycle can be studied through quadratic stability of the impact maps of the system. Indeed, consider a subset S_0^+ of S_0 given by $S_0^+ = \{x \in S_0 : CA_2x \geq 0\}$. S_0^+ is the set of points in S_0 that can be reached by trajectories initialized in (R_1) . In a similar way, define $S_0^- \subset S_0$ as $S_0^- = \{x \in S_0 : CA_2x \leq 0\}$ and also $S_1^+ = -S_0^-$ and $S_1^- = -S_0^+$. From symmetry considerations, three impact maps only are of interest for the analysis. The first impact map (impact map 1) takes points from S_0^- and maps them in S_0^+ . The second impact map (impact map 2a) takes points from $S_0^+ \setminus \{x_0^*\}$ and maps them back to $S_0^- \setminus \{x_0^*\}$. Finally, the third impact map (impact map 2b) takes points from S_0^+ and maps them to S_1^+ . Let x_1 be a point in $S_0^- \setminus \{-x_1^*\}$. Since A_1 is HURWITZ and $\frac{1}{k+p} > -CA_1^{-1}B$, the trajectory $x_1(t)$ will necessarily switch after a finite switching time t_1 at $x_2 = x_1(t_1)$. Since A_2 is not HURWITZ and

3.6. NUMERICAL ANALYSIS OF PLS - GAS OF THE LIMIT CYCLE FOR A PARTICULAR VALUE OF THE BIFURCATION PARAMETER

has no real unstable eigenvalue, a trajectory starting at $x_2 \in S_0^+ \setminus \{x_0^*\}$ can either switch at some point in S_0 , or at some point in S_1 , or not switch at all if x_2 belongs to the stable manifold of the origin. Let $S_a \subset S_0^+ \setminus \{x_0^*\}$ (resp. $S_b \subset S_0^+$) be the set of points that switch in S_0 (resp. S_1). If $x_2 \in S_a$ (resp. $x_2 \in S_b$), the trajectory switches in finite time t_{2a} (resp. t_{2b}) at $x_{3a} = x_2(t_{2a}) \in S_0^- \setminus \{-x_1^*\}$ (resp. $x_{3b} = x_2(t_{2b}) \in S_1^+$). Then, it switches again at $x_{4a} = x_{3a}(t_{3a})$ (resp. $x_{4b} = x_{3b}(t_{3b})$), and so on (see Figure 3.23).

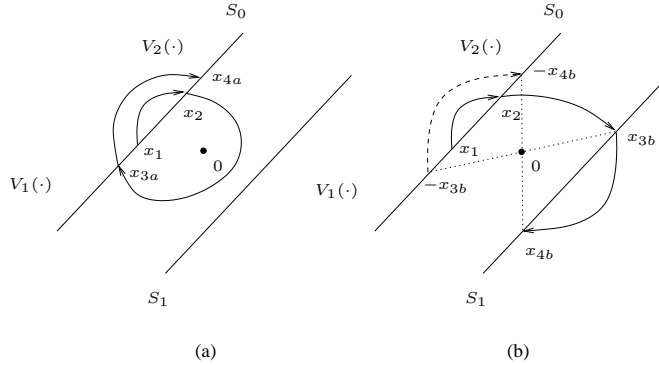


Figure 3.23: Impact maps of the PLS; (a) impact map 1 and impact map 2a, (b) impact map 1 and impact map 2b.

The symmetry of the system allows to perform the analysis on a half trajectory. This means that it is equivalent to consider the trajectory starting at x_2 or $-x_2$. To perform asymptotic stability of the limit cycle, the idea is to check if x_{3a} (resp. $-x_{3b}$) is closer to $-x_1^*$ than x_1 . If so for any point $x_1 \in S_0^- \setminus \{-x_1^*\}$, the limit cycle is globally asymptotically stable.

Since $x_1, x_2, x_{3a} \in S_0$ and $x_{3b} \in S_1$, we can write $x_1 = -x_1^* + \Delta_1$, $x_2 = x_0^* + \Delta_2$, $x_{3a} = -x_1^* + \Delta_{3a}$, and $x_{3b} = x_1^* + \Delta_{3b}$, where x_0^* and x_1^* have been found as numerical solutions of (3.54),(3.55) and $C\Delta_1 = C\Delta_2 = C\Delta_{3a} = C\Delta_{3b} = 0$. A *sufficient* condition for the POINCARÉ map to be contracting around x_0^* is

$$\begin{aligned} V_2(\Delta_2) &< V_1(\Delta_1) \text{ for all } \Delta_1 \in S_0^- \setminus \{-x_1^*\}, \\ V_1(\Delta_{3a}) &< V_2(\Delta_2) \text{ for all } \Delta_2 \in S_a \setminus \{x_0^*\}, \\ V_1(\Delta_{3b}) &< V_2(\Delta_2) \text{ for all } \Delta_2 \in S_b \setminus \{x_0^*\}, \end{aligned}$$

where $V_1(\cdot)$ and $V_2(\cdot)$ are quadratic LYAPUNOV functions defined on S_0^- and S_0^+ respectively (see Figure 3.23).

The key result of [GMD03] is that the impact maps induced by an LTI (linear time invariant) flow between two switching surfaces can be represented as a linear transformation analytically parametrized by a scalar function of the state. This parameter is simply the switching time associated with the impact map. We thus have $\Delta_2 = H_1(t_1)\Delta_1$, $\Delta_{3a} = H_{2a}(t_{2a})\Delta_2$, $\Delta_{3b} = H_{2b}(t_{2b})\Delta_2$, where (see [GMD03])

$$\begin{aligned}
 H_1(t_1) &= (-x_1^*(t_1) - x_0^*) w_1(t_1) + e^{A_1 t_1}, \\
 w_1(t_1) &= \frac{C e^{A_1 t_1}}{-m + C x_1^*(t_1)}, \\
 -x_1^*(t_1) &= -e^{A_1 t_1} x_1^* + A_1^{-1} (I - e^{A_1 t_1}) dB,
 \end{aligned}$$

$$\begin{aligned}
 H_2(t_{2a}) &= (x_0^*(t_{2a}) + x_1^*) w_{2a}(t_{2a}) + e^{A_2 t_{2a}}, \\
 w_{2a}(t_{2a}) &= \frac{C e^{A_2 t_{2a}}}{-m - C x_0^*(t_{2a})}, \\
 x_0^*(t_{2a}) &= e^{A_2 t_{2a}} x_0^*,
 \end{aligned}$$

$$\begin{aligned}
 H_2(t_{2b}) &= (x_0^*(t_{2b}) - x_1^*) w_{2b}(t_{2b}) + e^{A_2 t_{2b}}, \\
 w_{2b}(t_{2b}) &= \frac{C e^{A_2 t_{2b}}}{m - C x_0^*(t_{2b})}, \\
 x_0^*(t_{2b}) &= e^{A_2 t_{2b}} x_0^*.
 \end{aligned}$$

We then have to prove that

$$\begin{aligned}
 r_1(t_1) &\triangleq \Delta_1^T P_1(t_1) \Delta_1 & (3.56) \\
 &= V_1(\Delta_1) - V_2(H_1(t_1) \Delta_1) > 0,
 \end{aligned}$$

$$\begin{aligned}
 r_{2a}(t_{2a}) &\triangleq \Delta_2^T P_{2a}(t_{2a}) \Delta_2 & (3.57) \\
 &= V_2(\Delta_2) - V_1(H_{2a}(t_{2a}) \Delta_2) > 0,
 \end{aligned}$$

$$\begin{aligned}
 r_{2b}(t_{2b}) &\triangleq \Delta_2^T P_{2b}(t_{2b}) \Delta_2 & (3.58) \\
 &= V_2(\Delta_2) - V_1(H_{2b}(t_{2b}) \Delta_2) > 0
 \end{aligned}$$

for all expected switching times $t_1 \in \mathcal{T}_1$, $t_{2a} \in \mathcal{T}_{2a}$ and $t_{2b} \in \mathcal{T}_{2b}$ where \mathcal{T}_1 , \mathcal{T}_{2a} and \mathcal{T}_{2b} denote the set of all expected switching times corresponding respectively to all $\Delta_1 \in S_0^- \setminus \{-x_1^*\}$, $\Delta_2 \in S_a \setminus \{x_0^*\}$, and $\Delta_2 \in S_b \setminus \{x_0^*\}$. If the sets of expected switching times are bounded, then by discretizing the sets of expected switching times, inequalities (3.56), (3.57), and (3.58) define a finite set of LMIs in the unknowns $P_i(t_i) > 0$, $i = 1, 2a, 2b$.

3.6.4 Bounds on switching times

Computationally, it is impossible to check directly if the stability conditions (3.56), (3.57) and (3.58) are satisfied for all expected switching times. An alternative is to find some intervals such that if (3.56), (3.57) and (3.58) are satisfied in these intervals, then stability follows. In other words, we would like to find a lower and an upper bound for each switching time. We denote them respectively by t_{1min} , t_{1max} , t_{2amin} , t_{2amax} , t_{2bmin} , t_{2bmax} . We then only need to solve the LMIs $r_i(t) > 0 \forall t \in [t_{imin}, t_{imax}]$, where $i = 1, 2a, 2b$. This can be done by discretizing each $[t_{imin}, t_{imax}]$ interval,

and solving the corresponding LMIs at those discrete time instants. In order to do so, we must be able to guarantee that there exists a t_0 such that the difference between any two consecutive switching times of a trajectory $x(t)$ for $t > t_0$ is higher than t_{min} , but lower than t_{max} . Such bounds can be computed, for instance, when the linear dynamics in each region are HURWITZ and possess no equilibrium (see [GMD03] for details).

3.6.4.1 Lower bounds on the switching times

For the PLS (3.52),(3.53), the lower bounds are 0, i.e. $t_{1min} = t_{2amin} = t_{2bmin} = 0$.

3.6.4.2 Upper bound on t_1

To compute upper bounds, GONCALVES proposes a general method in [GMD03, Propositions B.1 and B.2]. The idea can be summarized by the following steps. First, the existence of a bounded invariant set where every trajectory will eventually enter is proved. Second, bounds on the expected switching times are found by computing bounds on switching times of trajectories inside that bounded invariant set. This method holds valid for PLS for which the feedback piecewise linear function is bounded such as for relay feedback systems and saturation systems. For these systems, it is possible to guarantee that there exists a \bar{t} such that the difference between any two consecutive switching times of a trajectory $x(t)$ for $t > \bar{t}$ is lower than t_{max} . Unfortunately, in our case $f_{pls}(\cdot)$ is not bounded and the method cannot be applied.

GONCALVES also presents a method for computing upper bounds on t_1 when a bounded invariant set cannot be guaranteed. In this case, the analysis must be done for all $t_i \geq 0$. The idea is the following: for large values of t_i , we compute the value of $r(\infty)$ and show that this value is nonnegative. We then show that for large enough t_{max} , $r(t) > 0$ for all $t \geq t_{max}$. To this end, we show that $\dot{r}(t) < 0$ for all $t \geq t_{max}$. If the matrix A_1 of the considered impact map is stable this is done according to the method described in [GMD03, Appendix A.3].

3.6.4.3 Upper bounds on t_{2a} and t_{2b}

The unstable equilibrium $x = 0$ of (3.52),(3.53) typically possesses a stable manifold when $n > 2$. In this case, the switching times are unbounded because of intersections between the stable eigenspace of A_2 and the switching surfaces S_0 and S_1 : any trajectory starting on a point belonging to these intersections will remain on the stable manifold until it asymptotically reaches the origin. As a consequence, the corresponding switching time will tend towards infinity. Intuitively, trajectories starting in a neighborhood of such an intersection point will be characterized by a switching time inversely proportional to the distance to this point. In other words, the closer we start from the intersection, the longer the switching time. A solution to apply the LMI numerical method of GONCALVES would be to geometrically characterize a neighborhood of the intersection points and to compute the upper bounds on the switching time associated to points which do not belong to this neighborhood. The method of GONCALVES can then be applied to study contraction of impact maps defined for any point which is not in the defined neighborhood. For points in the neighborhood, new contraction conditions expressed in the form of LMIs would have to be satisfied. This solution is still under research.

If we restrict our attention to the 2-dimensional case, then $x = 0$ has no stable manifold (A_2 is anti-stable). Moreover, in this case, by symmetry considerations, any trajectory belonging to S_0^+ will necessarily switch at a point belonging to S_1 . As a consequence, there are only two impact maps to

consider, i.e. impact map 1 and impact map 2b. The upper bound on t_1 is computed by considering the worst switching scenario for a point belonging to S_0^+ . This worst switching scenario occurs when $Cx = -m$ and $C\dot{x} = 0$. There exists only one point on S_0^+ corresponding to this situation. The upper bound is thus the switching time associated with this point.

3.6.5 Simulation results

To illustrate the numerical method presented in the previous sections, we present here the results obtained for two dimensional systems corresponding to Figure 3.10 where the transfer function describing the forward linear system is $\Sigma = G(s) = \frac{1}{s+\alpha}$ with $\alpha > 0$ and the adaptation parameter τ is such that $\tau \gg (k - k^*)^{-1}$. The critical bifurcation value of $G_k(s)$ is $k^* = k_{passive}^* = \alpha$ and the corresponding transfer function is $G_{k^*}(s) = \frac{1}{s}$. The condition $\tau \gg (k - k^*)^{-1}$ thus writes $\tau \gg (k - \alpha)^{-1}$. From Theorems 3.8 and 3.9, we expect the feedback system to be characterized by a globally asymptotically limit cycle for $k \gtrsim \alpha$ and $\tau \gg (k - \alpha)^{-1}$. Nevertheless, the range of values of k for which this behavior holds is not known. Replacing $\phi_k(y) = -ky + y^3$ by $f_{pls}(y)$ (see (3.53)) in Figure 3.10, and choosing values for p and k such that $p > 0$ and $k > k^*$, we may use the numerical analysis method presented in Section 3.6.3 to conclude about existence and global asymptotic stability of a limit cycle for any fixed value of k .

Before presenting the simulation results, we briefly describe the inputs and outputs of the algorithm. The inputs are the transfer function $G(s)$ together with the parameters α , $k > \alpha$, $p > 0$ and $\tau \gg (k - \alpha)^{-1}$. A graphic showing the minimum eigenvalues of each $P_i(t_i)$, $i = 1, 2b$ (see (3.56), and (3.58)) is generated. GAS of the limit cycle is then concluded if the minimum eigenvalues are positive on their respective set of expected switching times.

To illustrate the application of the numerical method, we considered the parameters values $\alpha = 1$ and $\tau = 20$. From these values, we compute $k^* = k_{passive}^* = 1$. We then have chosen the following values for k and p : $k = 1.2$ and $p = 5$. The corresponding values of m and d are $m = 0.63$ and $d = 3.92$. The simulation results showing the state space and the time evolution of the state variables for a particular initial condition are given on Figure 3.24. The numerical algorithm described previously is then applied to this particular PLS. The number of (t_1^*, t_2^*) solutions found by the algorithm for (3.54) and (3.55) is equal to one, i.e. $t_1^* = 8.4$ and $t_2^* = 8.88$. These values agree with those found by simulation of the dynamical system. The algorithm then solves the finite set of LMIs defined by the discretization of (3.56) and (3.58) on their expected switching times interval \mathcal{T}_1 and \mathcal{T}_{2b} and plots Figure 3.25. On this figure, we see that the minimum eigenvalue of each $P_i(t_i)$, $i = 1, 2b$ is positive on its respective set of expected switching times \mathcal{T}_1 and \mathcal{T}_{2b} . The set of expected switching times in this example are approximately $\mathcal{T}_1 = (0, 12)$ and $\mathcal{T}_{2b} = (0, 9.0414)$. The first upper bound $t_{1max} = 12$ was chosen arbitrarily. We then numerically checked that $r_1(t_1) > 0$ for all $t_1 \geq t_{1max}$ as explained in Section 3.6.4.2. The second upper bound was computed according to the worst switching scenario method: if $t_{2b} \geq 9.0414$, there is no point in S_0^+ with switching time equal to t_{2b} . Using conditions (3.56) and (3.58), we thus have shown that the system possesses a globally asymptotically stable limit cycle in $\mathbb{R}^2 \setminus \{0\}$.

Remark 3.13 *If we consider Figure 3.8 where the forward system Σ results from the feedback interconnection of $G(s) = \frac{1}{s+\alpha}$ with the transfer function $\frac{1}{\tau s+1}$, the bifurcation analysis is different. The transfer function corresponding to the feedback interconnection of $\frac{1}{s+\alpha}$ with $\frac{1}{\tau s+1}$ is $\Sigma = H(s) = \frac{\tau s+1}{\tau s^2+(1+\alpha\tau)s+(\alpha+1)}$. The system in Figure 3.8 is equivalently described as the (negative) feedback*

3.6. NUMERICAL ANALYSIS OF PLS - GAS OF THE LIMIT CYCLE FOR A PARTICULAR VALUE OF THE BIFURCATION PARAMETER

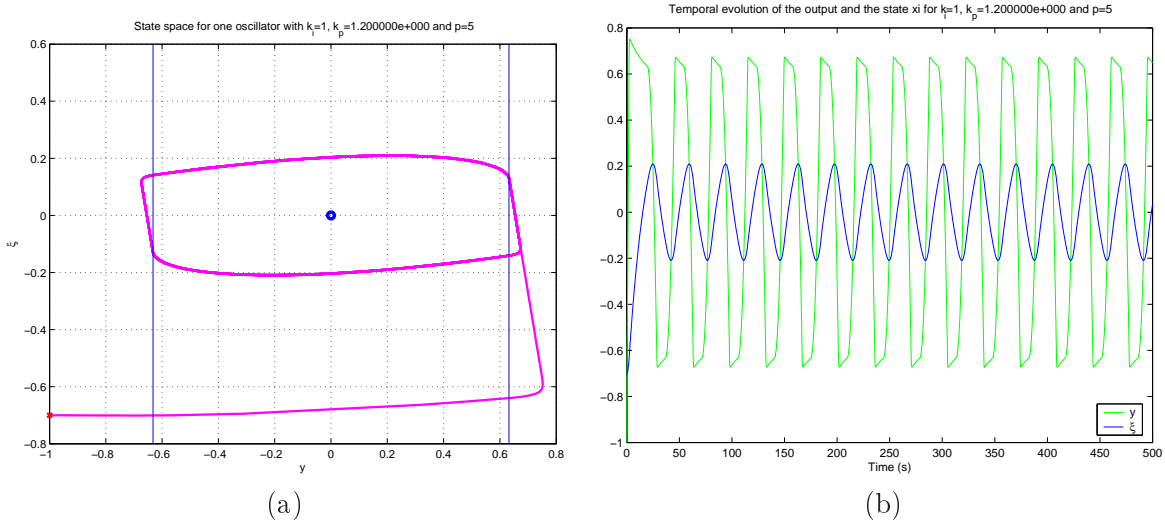


Figure 3.24: Simulation results for the PLS defined by the parameters values $\alpha = 1$, $k = 1.2$, $p = 5$ and $\tau = 20$. Column (a): state-space. Column (b): time evolution of the state variables.

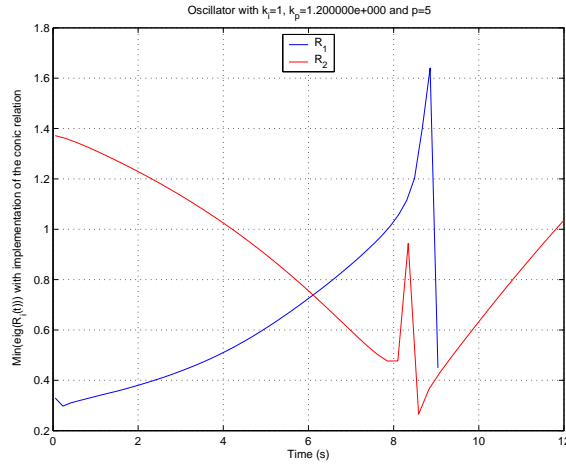


Figure 3.25: Time evolution of the minimum eigenvalues of $P_1(t_1)$ and $P_{2b}(t_{2b})$ for the PLS defined by the parameters values $\alpha = 1$, $k = 1.2$, $p = 5$ and $\tau = 20$.

interconnection of $H_k(s) = \frac{H(s)}{1-kH(s)} = \frac{\tau s+1}{\tau s^2+(1+(\alpha-k)\tau)s+(1+\alpha-k)}$ with the static nonlinear function $\phi(y) = y^3$. The critical value at which $H_k(s)$ loses passivity is $k_{passive}^* = \alpha$. For $\tau > 1$, a HOPF bifurcation occurs at the critical value $k^* = \alpha + \frac{1}{\tau}$. The corresponding critical transfer function is $H_{k^*}(s) = \tau \frac{\tau s+1}{\tau^2 s^2+(\tau+1)}$. This critical transfer function is similar to the one obtained in Section 3.5.3. In that section we saw that, with such a transfer function, no multiplier could be found to prove absolute stability of the feedback system at $k = k^*$. In this case, the analytical results of our theorems do not apply. The application of the numerical method to the PLS resulting from the feedback interconnection of $H(s)$ with $f_{pls}(y)$ can then be useful to numerically prove existence and global asymptotic stability of a limit cycle. To illustrate this, we performed a simulation with the same parameters values

except for $\tau = 2$ and $k = 1.8$. With these values, we obtain $k_{passive}^* = 1$, $k^* = 1.5$, $m = 0.775$, and $d = 5.267$. The simulation results are shown in Figure 3.26.

The results of the application of the same numerical algorithm to this PLS are shown in Figure

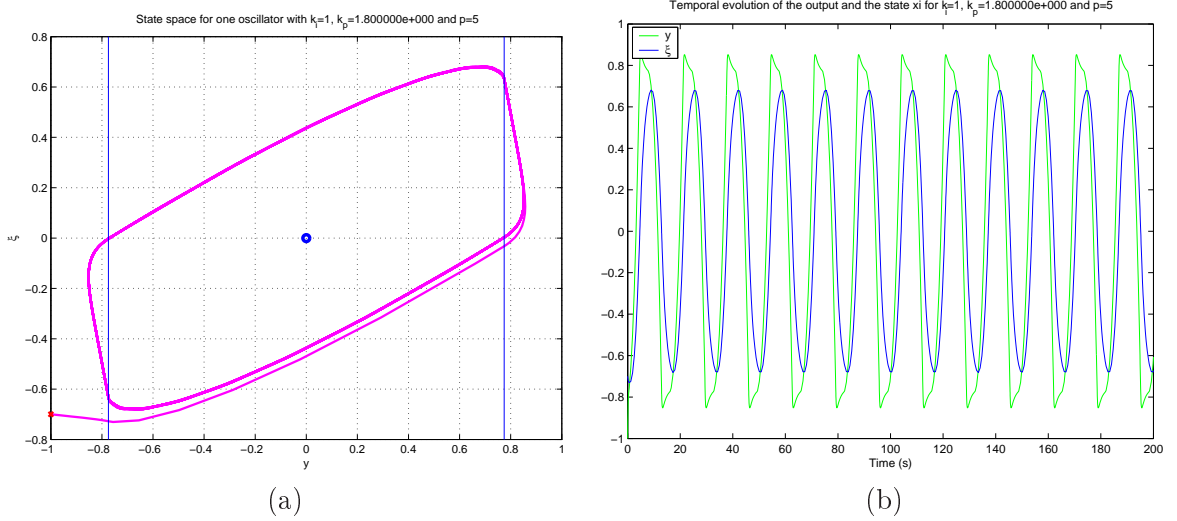


Figure 3.26: Simulation results for the PLS defined by the parameters values $\alpha = 1$, $k = 1.8$, $p = 5$ and $\tau = 2$. Column (a): state-space. Column (b): time evolution of the state variables.

3.27. The number of (t_1^*, t_2^*) solutions found by the algorithm for (3.54) and (3.55) is equal to one, i.e. $t_1^* = 3.1227$ and $t_2^* = 5.1617$. These values agree with those found by simulation of the dynamical system. The set of expected switching times in this example are approximately $\mathcal{T}_1 = (0, 12)$ and $\mathcal{T}_{2b} = (0, 5.3291)$. Once again, the PLS was numerically proved to be characterized by a GAS limit cycle in $\mathbb{R}^2 \setminus \{0\}$ since the minimum eigenvalues of $P_1(t_1)$ and $P_{2b}(t_{2b})$ are positive on their respective set of expected switching times.

3.7 Summary

The point of view developed in this chapter is that of oscillators as *open* systems. To this end, we considered an external characterization of oscillators which fits their description by physical state space models and, at the same time, has implications for their *global* stability analysis. This external characterization of oscillators is expressed by a dissipation inequality that was shown to enable global limit cycle oscillations in the isolated system. The presented theory covers two global oscillation mechanisms which are present in the celebrated low dimensional models of VAN DER POL and FITZHUGH-NAGUMO. These two global oscillation mechanisms were extended to higher dimensional systems composed of a strongly passive system in feedback with a slope parametrized static nonlinearity. We showed that this feedback interconnection undergoes either a supercritical HOPF, or a supercritical pitchfork bifurcation (Theorem 3.8). The global oscillation results either from the supercritical HOPF bifurcation or from the addition of a slow adaptation dynamic to the globally bistable system created by the supercritical pitchfork bifurcation (Theorem 3.9). The main assumption that allows the global asymptotic stability of the unique equilibrium point to be retained by

3.7. SUMMARY

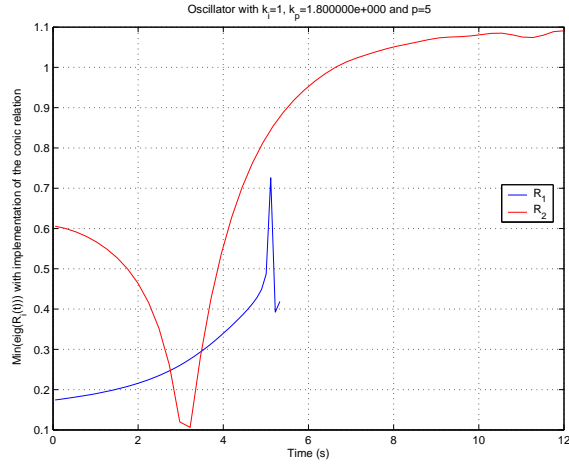


Figure 3.27: Time evolution of the minimum eigenvalues of $P_1(t_1)$ and $P_{2b}(t_{2b})$ for the PLS defined by the parameters values $\alpha = 1$, $k = 1.8$, $p = 5$ and $\tau = 2$.

the bifurcated solution is the absolute stability of the system at criticality. A sufficient condition for this assumption to be satisfied is the simultaneous loss of stability and passivity of the bifurcation parameter at a certain critical value. This condition has been relaxed with the help of multipliers (Theorem 3.12), thereby broadening the class of passive oscillators. These results were illustrated on a simple mechanical example. Finally, we considered an equivalent piecewise linear characterization of the passive oscillator and adapted a numerical method recently proposed in the literature to prove global stability of the limit cycle for fixed values of the parameter. This method was successfully applied to numerically study global asymptotic stability of the limit cycle solution of a second order piecewise linear, passive oscillator.

Chapter 4

Global results for interconnected oscillators

The aim of the previous chapter was to show that dissipativity theory can be usefully applied to study existence and global asymptotic stability of limit cycles and to give simple explanations for the feedback mechanisms responsible for these nonlinear oscillations. As we have pointed out previously, an important benefit is that a dissipativity approach is not restricted to low-dimensional systems. In this chapter, we focus on the second important benefit of a dissipativity approach: the analysis of interconnections. In Section 4.1, we show that the characterization of a globally asymptotically stable limit cycle for one oscillator extends in a straightforward manner when several passive oscillators are arranged in a network configuration through input-output coupling. Section 4.2 contains the first main results of the chapter: extension of the results presented in Chapter 3 to networks of passive oscillators. In Section 4.3, we consider some illustrative examples of these results, i.e. we consider networks of increasing sizes for which the existence of a globally asymptotically stable limit cycle can be directly deduced from the results of Section 4.2. In Section 4.4 we present the second main result of this chapter: sufficient network topology conditions leading to existence and global asymptotic stability of synchronic oscillations in networks of identical passive oscillators. The emphasis is on synchronization as a design principle, that is on the use of synchronization to achieve globally stable oscillations in interconnected systems. We propose an explanation for the global synchronization of identical oscillators based on an input-output characterization that we name *incremental passivity*. Finally, in Section 4.5 we present simulation results to illustrate our theory.

4.1 Networks of passive oscillators

Consider a network of N passive oscillators, coupled through their input and output. The oscillators are constructed according to the LURE feedback structure shown in Figure 3.8. The static feedback nonlinearities used in each passive oscillator are identical, i.e. $\phi_k(y_i) = -ky_i + \phi(y_i)$, $\forall i = 1, \dots, N$, where y_i represents the output of passive oscillator i . Only the feedforward blocks Σ_i may differ. The network may be seen as a MIMO system whose inputs and outputs are respectively $U = (u_1, \dots, u_N)^T$ and $Y = (y_1, \dots, y_N)^T$ where u_i and y_i are the scalar input and output of passive oscillator i respectively. The network admits the representation in Figure 4.1 which is a MIMO extension of the block diagram of Figure 3.8. In the case of a network of identical passive oscillators, all

the forward Σ_i blocks of the passive oscillators are identical. This is then emphasized by the notation $\Upsilon = \text{diag}\{\Sigma\}$. In Figure 4.1, $F(Y)$ represents the coupling between the oscillators while the static nonlinearity $\Phi_k(Y)$ is described as $\Phi_k(Y) = (\phi_k(y_1), \dots, \phi_k(y_N))^T$. The repeated nonlinear element is the static nonlinear function $\phi_k(y)$ given in (3.17) and satisfying the associated assumptions given in Section 3.3.1. Repeated nonlinearities are generally denoted by $\text{diag}\{\phi(\cdot)\}$.

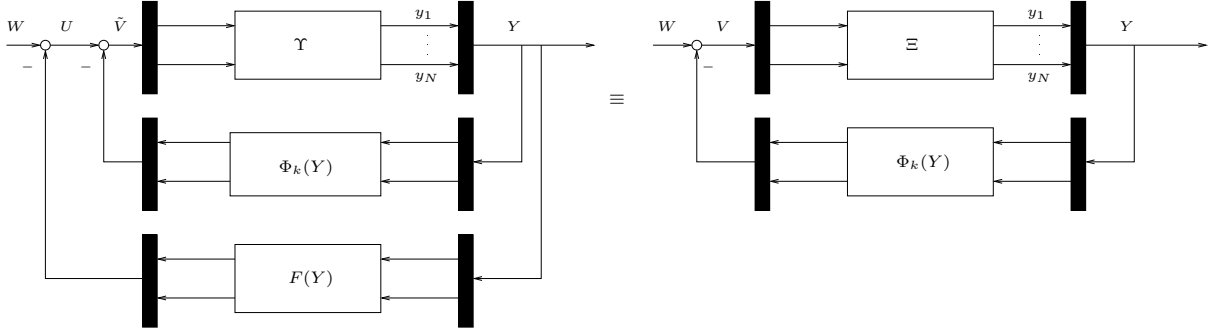


Figure 4.1: MIMO representation of a network of passive oscillators. $\Phi_k(Y) = (\phi_k(y_1), \dots, \phi_k(y_N))^T$ is a multivariable repeated nonlinearity. The repeated nonlinear element is $\phi_k(y) = -ky + \phi(y)$ where $\phi(\cdot)$ is a static nonlinear function that satisfies the assumptions of Section 3.3.1. $F(Y)$ characterizes the coupling. Ξ denotes the feedback interconnection of Υ and $F(Y)$.

As parallel interconnection of the input-affine Σ_i blocks defined in (3.16), Υ admits the input-affine state model

$$(\Upsilon) \begin{cases} \dot{X} &= f_{\Upsilon}(X) + g_{\Upsilon}(X)\tilde{V} \\ Y &= h_{\Upsilon}(X) \end{cases} \quad (4.1)$$

where $X = (x_1^T, \dots, x_N^T)^T$ with x_i denoting the state of passive oscillator i . f_{Υ} , g_{Υ} and h_{Υ} inherit the properties of the functions f_i , g_i and h_i defining the Σ_i blocks, i.e. f_{Υ} , g_{Υ} and h_{Υ} are smooth, and satisfy $f_{\Upsilon}(0) = 0$, $h_{\Upsilon}(0) = 0$, and $g_{\Upsilon}(0) \neq 0$.

We denote by Ξ the feedback interconnection of Υ with $F(Y)$ and by Ξ_k the (positive) feedback interconnection of Ξ with the MIMO feedback static gain $\text{diag}\{k\}$. The MIMO feedback system in Figure 4.1 is thus equivalently represented as the feedback interconnection of Ξ and $\Phi_k(\cdot)$, or as the feedback interconnection of Ξ_k and $\Phi(\cdot)$ (see Figure 4.2).

Remark 4.1 *The MIMO system Ξ obviously admits an input-affine state model of the form (4.1) with $f_{\Xi}(X) = f_{\Upsilon}(X) - g_{\Upsilon}(X)F(h_{\Upsilon}(X))$, $g_{\Xi}(X) = g_{\Upsilon}(X)$ and $h_{\Xi}(X) = h_{\Upsilon}(X)$.*

As parallel interconnection of strongly passive systems, the forward block Υ has the same passivity properties as the forward systems Σ_i of each passive oscillator. Not taking into account the coupling, the dissipativity inequality satisfied by the MIMO system in Figure 4.1 is thus (see Lemma 2.15)

$$\dot{S} \leq (k - k_{passive}^*) Y^T Y - Y^T \Phi(Y) + Y^T U, \quad (4.2)$$

where $S(X)$ is the sum of the storage functions of the passive oscillators of the network.

The coupling between the oscillators is described by the relation

$$U = -F(Y) + W, \quad (4.3)$$

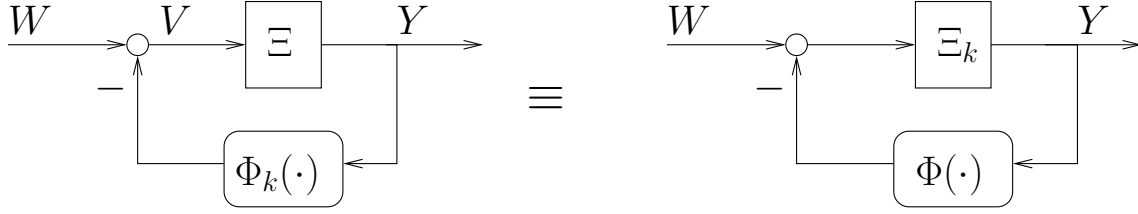


Figure 4.2: Two equivalent representations of the LURE MIMO nonlinear system studied in this chapter. $\Phi_k(Y) = (\phi_k(y_1), \dots, \phi_k(y_N))^T$ is a multivariable repeated nonlinearity. The repeated nonlinear element is $\phi_k(y) = -ky + \phi(y)$ where $\phi(\cdot)$ is a static nonlinear function that satisfies the assumptions of Section 3.3.1.

where $F(\cdot)$ is a \mathcal{C}^1 function in \mathbb{R}^N defining the topology of the network and W is the external input of the network. We assume that $F(0) = 0$ and that the coupling function $F(\cdot)$ satisfies the passivity condition

$$Y^T F(Y) \geq 0, \forall Y \in \mathbb{R}^N. \quad (4.4)$$

This directly implies that the passivity properties of Υ transmit to Ξ , i.e. that Ξ is strongly passive. As a result, the dissipativity characterization of the MIMO system in Figure 4.1 is similar to the dissipativity characterization of the SISO system in Figure 3.8, i.e.

$$\dot{S} \leq (k - k_{passive}^*) Y^T Y - Y^T \Phi(Y) + Y^T W. \quad (4.5)$$

This means that, under the assumption of passive coupling, the network dissipativity characterization is similar to that of one of its constituting passive oscillator.

If we assume linear coupling, $F(Y) = \Gamma Y$, and (4.3) becomes

$$U = -\Gamma Y + W, \quad (4.6)$$

where $\Gamma \in \mathbb{R}^{N \times N}$ represents the interconnection matrix. The passivity condition (4.4) implies that Γ is a real positive semidefinite matrix¹. Note that even the positive semidefiniteness condition on Γ may be relaxed through a parameter shift. Let k_0 be a scalar such that $\Gamma' = \Gamma + k_0 I_N$ is a real positive semidefinite matrix of rank $q < N$ and define $k' = k + k_0$. This simply amounts to define the coupling as $U = -(\Gamma + k_0 I_N) Y + k_0 Y + W$. The network admits the representation of Figure 4.1 where $F(Y) = \Gamma' Y$ and k is replaced by k' . The dissipation inequality (4.5) becomes

$$\begin{aligned} \dot{S} &\leq -\underbrace{Y^T \Gamma' Y}_{\geq 0} + (k - k_{passive}^* + k_0) Y^T Y - Y^T \Phi(Y) + Y^T W \\ &\leq (k' - k_{passive}^*) Y^T Y - Y^T \Phi(Y) + Y^T W \end{aligned}$$

which is similar to (4.5) with k' replacing k .

To pursue the analogy with the SISO situation, we will assume that the network is unforced, i.e. $W \equiv 0$. This external network input is important for the analysis of interconnected networks. The

¹We recall that a real matrix A is positive semidefinite iff $x^T A x \geq 0$ for all $x \in \mathbb{R}^n$. As a consequence of this definition, a real matrix A is positive semidefinite iff its symmetric part $\frac{1}{2}(A + A^T)$ is positive semidefinite. This allows to consider matrices which are not symmetric (see also Appendix A for some properties of real positive definite matrices).

argument developed in this chapter directly extends to this situation. This allows the analysis of networks of increasing complexity through the same methodology. This emphasizes the far reaching implications of an input-output point of view for the characterization of limit cycle oscillations.

4.2 Second result of this thesis - Networks of passive oscillators

In this section we present an extension of the bifurcation results presented in Chapter 3. The statement of the results in Chapter 3 were global in the state-space. To this end, we introduced the additional assumption that the feedback interconnection of Σ and $\phi_k(\cdot)$ is ultimately bounded. Following a result of ARCAK [AT02], we remarked in Section 3.3.2 that this assumption was always satisfied for Σ linear, passive and detectable. In the following section, we extend this result to the corresponding MIMO situation when Υ is linear, passive and detectable, $F(Y) = \Gamma Y$, with $\Gamma \in \mathbb{R}^{N \times N}$ and $\Gamma \geq 0$, and $\Phi_k(\cdot) = \text{diag}\{\phi_k(\cdot)\}$ is a multivariable repeated nonlinearity where $\phi(\cdot)$ is assumed to satisfy the assumptions of Section 3.3.1 and to be additionally monotone increasing. For the general case when Υ is nonlinear, we will explicitly assume that the unforced ($W \equiv 0$) MIMO feedback system in Figure 4.2 is ultimately bounded.

4.2.1 Global boundedness result for Υ linear and linear coupling

In the case of Υ linear and linear coupling, we extend the global boundedness results of ARCAK [AT02] to networks of passive oscillators.

We have seen in Section 3.3.2 that (3.23) does not imply (3.24) for general multivariable nonlinearities. However, in the case of multivariable repeated nonlinearities, denoted by

$$\Phi(Y) = (\phi(y_1), \dots, \phi(y_N))^T, \quad (4.7)$$

conditions (3.23) and (3.24) are satisfied if the repeated nonlinearity $\phi(\cdot)$ satisfies (3.25), (3.26) and is monotone increasing. We summarize this result in Theorem 4.2.

Theorem 4.2 *If $\phi(\cdot) : \mathbb{R} \rightarrow \mathbb{R}$ satisfies (3.25), (3.26) and is monotone increasing then the multivariable repeated nonlinearity (4.7) satisfies (3.23) and (3.24).*

Proof

First, we prove property (3.23).

$$\begin{aligned} Y^T \Phi(Y) &= \sum_{i \neq k} y_i \phi(y_i) + y_k \phi(y_k), \text{ where } k \text{ is s.t. } \|Y\|_\infty = |y_k| \\ &\geq y_k \phi(y_k) \\ &\geq |y_k| \phi_l(|y_k|) \\ &\geq \|Y\|_\infty \phi_l(\|Y\|_\infty). \end{aligned}$$

The second inequality is a consequence of the sector condition (3.25) and the growth condition (3.26): for scalar nonlinearities, the sector condition (3.25) combined with the growth condition (3.26) is equivalent to property (3.23) (see Remark 3.4).

Second, we prove property (3.24)

$$\begin{aligned}
 Y^T \Phi(Y) &= \sum_{i \neq k} y_i \phi(y_i) + y_k \phi(y_k), \text{ where } k \text{ is s.t. } \|Y\|_\infty = |y_k| \\
 &\geq |y_k| |\phi(y_k)| \\
 &\geq |\phi(y_k)|, \text{ when } |y_k| \geq 1 \\
 &= \|\Phi(Y)\|_\infty, \text{ when } \|Y\|_\infty \geq 1 \text{ since } \phi(\cdot) \text{ is monotone increasing.}
 \end{aligned}$$

■

From Theorem 4.2, we may conclude to global boundedness of the solutions of the network if Ξ is a linear system. This result is summarized in Theorem 4.3.

Theorem 4.3 *Consider the system represented in Figure 4.2, where Ξ is a linear, passive and detectable system and $\Phi_k(\cdot) = \text{diag}\{\phi_k(\cdot)\} : \mathbb{R}^N \rightarrow \mathbb{R}^N$ is a multivariable repeated nonlinearity. If the repeated nonlinearity $\phi_k(\cdot)$ satisfies*

$$\phi_k(y) \rightarrow \infty \text{ as } y \rightarrow \infty \text{ and } \phi_k(y) \rightarrow -\infty \text{ as } y \rightarrow -\infty, \quad (4.8)$$

and is such that $\phi_k(y)$ is monotone increasing for $|y| > b$ for some $b \geq 0$, then the trajectories are bounded.

Proof

We first note that from (4.8) we can find a constant $a > 0$ such that

$$|y| > a \Rightarrow y\phi_k(y) > 0.$$

Then, we let $\tilde{\phi}(y)$ be a continuous, monotone increasing function such that

$$\tilde{\phi}(y) = \phi_k(y) \text{ when } |y| > c = \max(a, b)$$

and $y\tilde{\phi}(y) > 0$ for all $y \neq 0$. It follows that (3.25) and (3.26) hold for $\tilde{\phi}$. From Theorem 4.2, this implies that the repeated multivariable nonlinearity $\tilde{\Phi}(Y) = \left(\tilde{\phi}(y_1), \dots, \tilde{\phi}(y_N)\right)^T$ satisfies conditions (3.23) and (3.24).

The dynamics of the isolated ($W \equiv 0$) feedback system represented in Figure 4.2 may be written as

$$\dot{X} = AX + B[-\tilde{\Phi}(Y) + \tilde{D}(Y)], \quad (4.9)$$

where $\tilde{D}(Y) = \tilde{\Phi}(Y) - \Phi_k(Y)$ is bounded because $\left(\tilde{D}(Y)\right)_i = 0$ when $|y_i| > c$. Since, by assumption, the linear system Ξ is passive and detectable, and $\tilde{\Phi}(\cdot)$ satisfies (3.23) and (3.24), we conclude from Theorem 3.2 that the trajectories of (4.9) are bounded. ■

Remark 4.4 *The assumptions on Ξ are obviously satisfied for Υ linear, passive and detectable and $F(Y)$ linear and passive. The assumptions on $\Phi_k(\cdot) = \text{diag}\{\phi_k(\cdot)\}$ are obviously satisfied for $\phi_k(y) = -ky + y\phi(y)$ with $\phi(\cdot)$ satisfying the assumptions of Section 3.3.1 and monotone increasing.*

4.2.2 Bifurcations in networks of passive oscillators

In this section, we focus on the bifurcations that may arise in a network of passive oscillators satisfying the representation in Figure 4.2. We first present a MIMO generalization of Theorem 3.8, then we show its usefulness for the bifurcation analysis in networks of passive oscillators.

Similarly to the SISO situation of Section 3.3.3, the MIMO system in Figure 4.2 may be seen as the (positive) feedback interconnection of an absolutely stable MIMO system with the MIMO static gain $\text{diag}\{k\}$. Generically, a bifurcation occurs when k is increased². We note $R(s)$ the MIMO transfer function of the linearization of Ξ at $X = 0$. Similarly, we note $R_k(s)$ the MIMO transfer function of the linearization of Ξ_k at $X = 0$.

Theorem 4.5 *Consider the unforced ($W \equiv 0$) system shown in Figure 4.2. Assume that Ξ is strongly passive, that both Ξ and its linearization are zero-state detectable and that the feedback interconnection of Ξ and $\Phi_k(\cdot)$ is ultimately bounded. Let $k_{\text{network}}^* \geq 0$ be the minimum value for which the MIMO transfer function $R_k(s)$ has a pole on the imaginary axis.*

If $R_{k_{\text{network}}^}(s)$ has a unique pole on the imaginary axis and if $\Xi_{k_{\text{network}}^*}$ is strongly passive, then the bifurcation is a supercritical pitchfork bifurcation; for $k \gtrsim k_{\text{network}}^*$ the system is globally bistable, that is, the equilibrium $X = 0$ is a saddle and its stable manifold $E_s(0)$ separates the state space in two open sets, each of which is the basin of attraction of a stable equilibrium.*

If $R_{k_{\text{network}}^}(s)$ has a unique pair of conjugated poles on the imaginary axis and if $\Xi_{k_{\text{network}}^*}$ is strongly passive, then the bifurcation is a supercritical HOPF bifurcation; for $k \gtrsim k_{\text{network}}^*$ the system has a stable limit cycle which is globally asymptotically stable in $\mathbb{R}^{nN} \setminus E_s(0)$.*

Proof

The proof is a straightforward extension of the SISO case presented in the proof of Theorem 3.8. It relies on the dissipation inequality at the bifurcation point,

$$\dot{S} \leq -Y^T \Phi(Y), \quad (4.10)$$

where S denotes the storage function of $\Xi_{k_{\text{network}}^*}$. The global part of the proof is identical: it relies on absolute stability of the MIMO system at criticality. The local part is similar. For a one dimensional manifold, the output of the system is $Y = C\xi + \mathcal{O}(|\xi|^2)$ with $C \in \mathbb{R}^N$ and $\xi \in \mathbb{R}$. Since the linearization of the center manifold dynamics is observable, C is full rank which means that at least one component of C is nonzero. The corresponding component of Y qualifies for a local coordinate

²This is easily seen from the ISIDORI normal form of the linearization of Ξ_k at $X = 0$, i.e.

$$\begin{aligned} \dot{Z} &= QZ + DY \\ \dot{Y} &= EZ + (K + kCB)Y, \end{aligned}$$

where $CB = (CB)^T > 0$ from the strong passivity assumption of Ξ_k (see [SJK97, Section 2.4.2]). The system necessarily becomes unstable for large positive values of k . To see this, we note that for k sufficiently large, the symmetric matrix $K_s + kCB$ (where K_s denotes the symmetric part of K) is symmetric positive definite (e.g. from WEYL theorem [HJ85, Theorem 4.3.1, p. 181] which allows to compare the eigenvalues of $K_s + kCB$ with those of K_s and kCB : $\lambda_{\min}(K_s) + \lambda_{\min}(kCB) \leq \lambda_{\min}(K_s + kCB)$). This in turn implies that $K + kCB$ is positive definite and thus that all its eigenvalues have positive real parts (see Appendix A). Using the SCHUR complement of the Jacobian matrix $\begin{pmatrix} Q & D \\ E & K + kCB \end{pmatrix}$, it is then easy to show that the system is unstable for k sufficiently large.

in the center manifold, i.e. $\exists i \in \{1, \dots, N\}$ such that $y_i = c_i \xi + \mathcal{O}(|\xi|^2)$ with $c_i \neq 0$ and the proof follows as in the SISO case. For a two dimensional manifold, the proof directly follows as in the SISO case (see [SS05b] for an explicit proof in the MIMO framework). ■

Remark 4.6 *As the feedback interconnection of Υ and $F(Y)$, Ξ and its linearization are zero-state detectable if Υ and its linearization are zero-state detectable. Similarly, $\Xi_{k^*_{network}}$ is strongly passive if $\Upsilon_{k^*_{network}}$ is strongly passive since the coupling $F(Y)$ is assumed to be passive. For networks of identical passive oscillators, i.e. $\Upsilon = \text{diag}\{\Sigma\}$, these conditions are satisfied if they hold for Σ .*

4.2.2.1 Dimension of the center manifold for a network of identical passive oscillators with linear symmetric coupling

The results of Theorem 4.5 restrict the dimension of the center manifold at the bifurcation. The dimension is generically one or two in a general interconnection. However, it can be higher in symmetric interconnections of identical oscillators: when the network possesses symmetry, multiple eigenvalues may cross the imaginary axis simultaneously even in the generic case (see [GS02]), and the dimension of the center manifold can be greater than 2. The situation is much more complicated and a deeper analysis has to be done – this is the case, for example, of the equivariant bifurcations described in [GSS88]. In this thesis, we do not consider such degenerate situations.

Knowing the dimension of the center manifold of one isolated passive oscillator, what can be said about the dimension of the center manifold of a network of identical passive oscillators? This question is easily answered in the case of a network of identical passive oscillators with linear and symmetric positive semi-definite coupling. If we assume linear symmetric, positive semi-definite coupling, i.e. $U = -\Gamma Y$ with $\Gamma = \Gamma^T \geq 0$ and $\text{rank}(\Gamma) = q < N$, the poles of the MIMO transfer function $R_k(s)$ are easily obtained from the poles of the SISO transfer function $G_k(s)$. The poles of the MIMO transfer function $R_k(s)$ are the complex values of s such that

$$\text{rank} \left(\frac{1 - kG(s)}{G(s)} I_N + \Gamma \right) < N.$$

Because Γ is a symmetric positive semidefinite matrix of rank q , there exists an orthogonal matrix L such that $\Gamma = L^T \Lambda L$ where $\Lambda = \text{diag}(0, \dots, 0, \lambda_{N-q+1}, \dots, \lambda_N)$ with $0 < \lambda_{N-q+1} \leq \dots \leq \lambda_N$. We thus have to search for the complex values of s that render the diagonal matrix $\left(\frac{1 - kG(s)}{G(s)} I_N + \Lambda \right)$ singular. This matrix is singular for each complex value of s solution of one of the equations $\frac{1 - (k - \lambda_i)G(s)}{G(s)} = 0$, $i = 1, \dots, N$. Thus the poles of the MIMO closed-loop transfer function are found by replacing k by $k - \lambda_i$, $i = 1, \dots, N$ in the expression of the poles of $G_k(s)$. As a consequence, at $k = k^*$, the MIMO system possesses a center manifold of dimension $m(N - q)$ where m is the dimension of the center manifold of one isolated passive oscillator at criticality. In Theorem 3.8 we have shown that, generically, $m \in \{1, 2\}$. As a result, if $q = N - 1$ we are in the situation described by Theorem 4.5.

Remark 4.7 *As we have noted in Section 4.1, if the matrix Γ is only symmetric, a shift by $k_0 I_N$ transforms Γ into a positive semidefinite matrix $\Gamma' = \Gamma + k_0 I_N$ of rank $q < N$. The critical bifurcation value for network, $k^*_{network}$, is then linked to the critical value for an isolated passive oscillator k^* by the relation $k^*_{network} = k^* - k_0$.*

These considerations lead to the following proposition.

Proposition 4.8 *Consider a network of N identical passive oscillators with linear symmetric coupling $U = -\Gamma Y$, where $\Gamma = \Gamma^T$. Let k_0 be the minimal shift such that $\Gamma' = \Gamma'^T = \Gamma + k_0 I_N \geq 0$ and $\text{rank}(\Gamma') = N - 1^3$. If one isolated oscillator has a center manifold of dimension one or two at $k = k^*$, then the network possesses a center manifold of the same dimension at the bifurcation value $k_{network}^* = k^* - k_0$.*

4.2.2.2 Relaxation oscillations in networks of passive oscillators

In this section we give an extension of Theorem 3.9 which transforms the global bistability result of Theorem 4.5 into a relaxation oscillation result. For this, we consider the addition of a feedback adaptation loop to the globally bistable system in Figure 4.2. The adaptation loop is represented on Figure 4.3. As we have seen in the proof of Theorem 4.5, there always exists (at least) one output component that qualifies for a local coordinate in the center manifold. Let y_i be this component. The adaptation we consider is diagonal and acts only on y_i , i.e. only the corresponding component w_i of the external input W is nonzero. This component is such that $w_i = -R_i$ where R_i is the state variable of the additional adaptation dynamic.

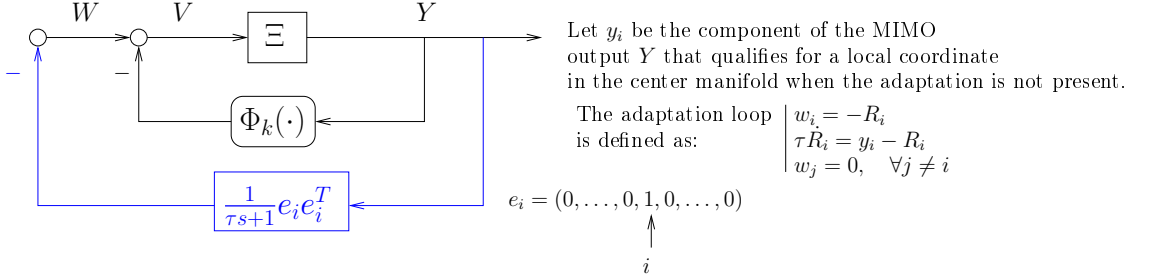


Figure 4.3: Converting the global bistability scenario into a relaxation oscillator with a slow adaptation mechanism ($\tau \gg (k - k_{network}^*)^{-1}$).

With this additional feedback adaptation loop, the global bistability result of Theorem 4.5 can be transformed into a global relaxation oscillation for the network. This result is summarized in Theorem 4.9.

Theorem 4.9 *Under the assumptions of Theorem 4.5, suppose that the feedback interconnection of Ξ and $\Phi_k(\cdot)$ undergoes a supercritical pitchfork bifurcation at $k = k_{network}^*$ and that the feedback system shown in Figure 4.3 is ultimately bounded. Then there exists constants $\bar{\epsilon} > 0$, and $\tau > 0$ such that $\forall k \in (k_{network}^*, k_{network}^* + \bar{\epsilon})$ and $\tau \gg (k - k_{network}^*)^{-1}$, the feedback system shown in Figure 4.3 has a globally asymptotically stable limit cycle in $\mathbb{R}^{nN+1} \setminus E_s(0)$.*

Proof

The proof is similar to the proof of Theorem 3.9. Let $\epsilon = (k - k_{network}^*)$ and consider the system represented on Figure 4.3. By assumption, the feedback interconnection of Ξ and $\Phi_k(\cdot)$ possesses a one dimensional center manifold at $\epsilon = 0$. For $W \neq 0$, strong passivity of Ξ implies that the

³This condition can be satisfied iff the minimal eigenvalue of Γ has an algebraic multiplicity equal to one.

center-unstable manifold equation writes⁴

$$\dot{y}_i = \epsilon y_i - \kappa' y_i^3 + \sum_{j=1}^N \alpha_j w_j + \mathcal{O}(y_i^4),$$

where $\kappa' > 0$ and w_j represents the j^{th} component of the network external input vector W . Thus, if we augment the one-dimensional center-unstable manifold of the original system (without adaptation) with the adaptation equation, we obtain

$$\begin{aligned} \dot{y}_i &= \epsilon y_i - \kappa' y_i^3 - b R_i + \mathcal{O}(|(y_i, R_i)|^4), & \kappa' > 0, \quad b > 0 \\ \dot{R}_i &= \delta (-R_i + y_i), \\ (\dot{\epsilon} &= 0, \\ \dot{\delta} &= 0), \end{aligned} \tag{4.11}$$

where $\delta = \tau^{-1}$. The dynamics (4.11) are identical to those obtained in the SISO case (see (3.38)). The local part of the proof is thus similar to the SISO case.

The global part of the proof follows as in Theorem 4.5: for $\delta > 0$ and $\epsilon = 0$, the equilibrium $(x, R_i) = (0, 0)$ is globally asymptotically stable because the augmented storage $V = \delta S + \frac{1}{2} R_i^2$ satisfies the dissipation inequality $\dot{V} = \delta \dot{S} + \dot{R}_i R_i = -\delta Y^T \Phi(Y) - \delta y_i R_i + \delta R_i (-R_i + y_i) \leq -\delta Y^T \Phi(Y)$ which is analogous to (4.10). ■

Remark 4.10 *If the forward system Ξ is linear, strongly passive and detectable and the repeated nonlinearity $\phi(\cdot)$ satisfies the assumptions of Section 3.3.1 and is monotone increasing, then ultimate boundedness results from Theorem 4.3 since the adaptation dynamics are passive.*

4.2.3 Relaxation of the assumptions of Theorem 4.5 - Use of multipliers

The key to our results is the absolute stability of the feedback system at criticality. The strong passivity of $\Xi_{k^*_{network}}$ is a sufficient condition for such a property. Nevertheless, it is rather restrictive since it requires that Ξ_k loses stability and passivity for the same value of the parameter k . Multipliers can be used to extend the results of Theorem 4.5 to more general situations. In Theorem 4.11, we present an extension of Theorem 3.11 that provides sufficient conditions for absolute stability of the feedback system of Figure 4.2.

Theorem 4.11 *Consider the system shown in Figure 4.2 with $W \equiv 0$. Assume that Ξ and its linearization are zero-state detectable and that the feedback interconnection of Ξ and $\Phi_k(\cdot)$ is ultimately bounded. Then each of the following conditions is sufficient for global asymptotic stability of the equilibrium $X = 0$ of the feedback system.*

- $\Phi(\cdot) = \text{diag}\{\phi(\cdot)\}$ with $\phi(\cdot)$ in the sector $(0, \infty)$ and there exists $\gamma > 0$ such that $(1 + \gamma s)I_N \Xi_k$ is strongly passive;

⁴The strong passivity of Ξ (and g_Ξ full rank) implies that Ξ has relative degree one at $X = 0$. This, in turn, implies that for X in a neighborhood of the origin, the input V of Ξ directly enters the \dot{Y} dynamics, i.e. $\dot{Y} = \frac{\partial h_\Xi}{\partial X} \dot{X} = L_{f_\Xi} h_\Xi(X) + L_{g_\Xi} h_\Xi(X) V$ with $L_{g_\Xi} h_\Xi(0) = \frac{\partial h_\Xi}{\partial X} \Big|_{X=0} g_\Xi(0)$ being a symmetric positive definite matrix.

- $\Phi(\cdot) = \text{diag}\{\phi(\cdot)\}$ with $\phi(\cdot)$ monotone in the sector $(0, \infty)$ and there exists $M(s)I_N = H_1(s)H_2(-s)I_N$ with $M(s)$ in the form (3.39), $z(t) \geq 0$, such that $\tilde{\Xi}_k = H_1I_N\Xi_kH_2^{-1}I_N$ is strongly passive;
- $\Phi(\cdot) = \text{diag}\{\phi(\cdot)\}$ with $\phi(\cdot)$ odd, monotone in the sector $(0, \infty)$ and there exists $M(s)I_N = H_1(s)H_2(-s)I_N$ with $M(s)$ in the form (3.39) such that $\tilde{\Xi}_k = H_1I_N\Xi_kH_2^{-1}I_N$ is strongly passive.

Proof

For POPOV MIMO multipliers, the assumption that $(1 + \gamma s)I_N\Xi_k$ is strongly passive implies that $\dot{S} \leq -(\Phi(Y))^T (Y + \gamma \dot{Y})$. A LYAPUNOV function for the interconnection is $V = S + \gamma \sum_{i=1}^N \int_0^{y_i} \phi(s) ds$, which satisfies $\dot{V} \leq -(\Phi(Y))^T Y$.

For ZAMES-FALB MIMO multipliers $M(s)I_N$, with $M(s)$ in the form (3.39), sufficient conditions for the *strict positivity (strict passivity)* of the MIMO nonlinearity $\tilde{\Phi}(\cdot) = H_2I_N\Phi(\cdot)H_1^{-1}I_N$ are given in [SK00, Theorem 1] :

$$\begin{aligned} \Phi(0) &= 0, \\ \int_{-\infty}^{+\infty} (r(t) - s(t))^T (\Phi(r(t)) - \Phi(s(t))) dt &\geq 0, \\ \left(\frac{d\Phi}{ds}(s) \right) - \left(\frac{d\Phi}{ds}(s) \right)^T &= 0. \end{aligned}$$

These conditions are satisfied for a repeated monotone nonlinearity $\Phi(\cdot) = \text{diag}\{\phi(\cdot)\}$ with $\phi(\cdot)$ monotone increasing and satisfying $\phi(0) = 0$. The rest of the proof directly follows as the one of Theorem 3.11. \blacksquare

We now present Theorem 4.12. It is an extension of Theorem 3.12 that generalizes the results of Theorem 4.5 through the use of multipliers.

Theorem 4.12 *The statements of Theorem 4.5 hold if the strong passivity assumption on $\Xi_{k^*}^*$ is replaced by one of the following conditions:*

- $\Phi(\cdot) = \text{diag}\{\phi(\cdot)\}$ with $\phi(\cdot)$ in the sector $(0, \infty)$ and there exists $\gamma > 0$ such that $(1 + \gamma s)I_N\Xi_{k^*}^*$ is strongly passive;
- $\Phi(\cdot) = \text{diag}\{\phi(\cdot)\}$ with $\phi(\cdot)$ monotone in the sector $(0, \infty)$ and there exists $M(s)I_N = H_1(s)H_2(-s)I_N$ with $M(s)$ in the form (3.39), $z(t) \geq 0$, such that $\tilde{\Xi}_{k^*}^* = H_1I_N\Xi_{k^*}^*H_2^{-1}I_N$ is strongly passive;
- $\Phi(\cdot) = \text{diag}\{\phi(\cdot)\}$ with $\phi(\cdot)$ odd, monotone in the sector $(0, \infty)$ and there exists $M(s)I_N = H_1(s)H_2(-s)I_N$ with $M(s)$ in the form (3.39) such that $\tilde{\Xi}_{k^*}^* = H_1I_N\Xi_{k^*}^*H_2^{-1}I_N$ is strongly passive.

Proof

The proof is similar to that of Theorem 3.12. An explicit proof in the MIMO framework can be found in [SS05b]. \blacksquare

Remark 4.13 Suppose that a passive oscillator is constructed through the use of a multiplier $M(s)$ as described in Theorem 3.12. Consider a network of such identical passive oscillators represented according to Figure 4.1. We would like to use the MIMO repeated version of this multiplier $M(s)I_N$ to conclude about bifurcation with the help of Theorem 4.12. A sufficient condition is that the repeated multiplier also preserves the positivity of the coupling (since the MIMO repeated multiplier $M(s)I_N$ already ensures that $\text{diag}\{\Sigma_k\}$ is strongly passive for $k \leq k_{network}^*$). For this condition to be satisfied, the coupling $F(Y)$ has to be the gradient of a convex function (see [SK00]). In the case of linear coupling $F(Y) = \Gamma Y$, a sufficient condition is $\Gamma = \Gamma^T \geq 0$.

4.3 Illustrative examples

In this section, we illustrate the results of Theorems 3.8 or 4.12 by examples of networks of identical passive oscillators of order 3. These passive oscillators were presented in Section 3.5.1. In these oscillators, the forward block appearing in Figure 3.8 is filled with a passive linear system whose corresponding transfer function is

$$G(s) = \frac{s(\tau s + \omega_n^2)}{s^3 + 2\zeta\omega_n s^2 + (\tau + \omega_n^2)s + \omega_n^2}, \quad (4.12)$$

with

$$2\zeta \geq \frac{\omega_n}{\tau} > 0, \quad (4.13)$$

and the static nonlinearity is

$$\phi_k(y) = y^3 - ky. \quad (4.14)$$

As mentioned in Section 3.5.1, the presence of a single zero at $s = 0$ forces the HOPF bifurcation scenario described in Theorem 3.8. The critical values k^* and $k_{passive}^*$ of $G_k(s)$ are given in (3.48) and (3.49) respectively.

Using Theorem 3.8 or 3.12, we have shown in Section 3.5.1 that, for particular values of the parameters, this system satisfies the definition of a passive oscillator given in Section 3.3.4 for $k \gtrsim k^*$, i.e.

1. the feedback system satisfies the dissipation inequality $\dot{S} \leq (k - k_{passive}^*)y^2 - y^4 + uy$;
2. when isolated, this system possesses a global limit cycle for $k \gtrsim k^*$.

We now illustrate some network topologies which allow for a direct application of Theorem 4.5 (or 4.12, depending on the parameters values). We successively consider networks composed of an increasing number of oscillators: $N = 2$, $N = 3$, and $N > 3$.

4.3.1 Case 1: $N = 2$

Consider the positive (resp. negative) feedback coupling of 2 identical passive oscillators of type (4.12)-(4.14) as illustrated in Figure 4.4. The interconnection matrices corresponding to these cases are respectively $\Gamma_1 = \begin{pmatrix} 0 & -1 \\ -1 & 0 \end{pmatrix}$ for column (a) and $\Gamma_2 = \begin{pmatrix} 0 & 1 \\ 1 & 0 \end{pmatrix}$ for column (b). The network is unchanged by the shifts $\Gamma' = \Gamma + k_0 I_N$ and $k' = k + k_0$. In both cases, choosing $k_0 = 1$, the

shifted matrices $\Gamma'_1 = \begin{pmatrix} 1 & -1 \\ -1 & 1 \end{pmatrix}$ and $\Gamma'_2 = \begin{pmatrix} 1 & 1 \\ 1 & 1 \end{pmatrix}$ are positive semidefinite with rank 1. By Proposition 4.8, the dimension of the center manifold of the network is 2. The critical bifurcation value for the network is $k_{network}^* = k^* - 1$. From Theorem 4.5 (or Theorem 4.12, depending on the parameters values), we conclude that the network possesses a limit cycle for $k \gtrsim k_{network}^*$. This is illustrated by the simulation results presented in Figure 4.4. In this simulation, the chosen parameter values are the same as in Section 3.5.1.1, i.e. $\omega_n = 1$, $\zeta = 1.25$, $\tau = 2$. For these parameter values, we obtain $k^* = k_{passive}^* = 1$ (see Section 3.5.1.1) and $k_{network}^* = 0$. As can be seen on these simulation results, the interconnection defined by Γ_1 leads to synchrone oscillations while the interconnection defined by Γ_2 leads to anti-synchrone oscillations.

4.3.2 Case 2: $N = 3$

We consider now a network of 3 oscillators of type (4.12)-(4.14) connected according to the chain structure of Figure 4.5.

The corresponding interconnection matrix is

$$\Gamma = \begin{pmatrix} 3 & 1 & 1 \\ 1 & 2 & 0 \\ 1 & 0 & 2 \end{pmatrix} > 0 \quad (4.15)$$

The eigenvalues of Γ being 1, 2 and 4, the shift k_0 required to transform Γ into a positive semidefinite matrix of rank 2 is $k_0 = -1$. The shifted matrix Γ' is then $\begin{pmatrix} 2 & 1 & 1 \\ 1 & 1 & 0 \\ 1 & 0 & 1 \end{pmatrix} \geq 0$. By Proposition 4.8, the dimension of the center manifold is 2. The critical bifurcation value for the network is $k_{network}^* = k^* + 1$. From Theorem 4.5 (or Theorem 4.12 according to the parameter values), we conclude that the network possesses a limit cycle for $k \gtrsim k_{network}^*$. This is illustrated by the simulation results presented in Figure 4.6. For this simulation we considered a network of 3 identical passive oscillators of type (4.12)-(4.14) coupled according to (4.15). Once again, we chosed the parameters values $\omega_n = 1$, $\zeta = 1.25$, $\tau = 2$. These parameter values lead to a critical bifurcation value $k_{network}^* = 2$.

4.3.3 Case 3: $N > 3$

As an illustration for a large number of oscillators, we first consider a S_N symmetry (all-to-all) network of passive oscillators of type (4.12)-(4.14). The S_N symmetry coupling corresponds to the interconnection matrix

$$\Gamma = \begin{pmatrix} (N-1)K & -K & \cdots & -K \\ -K & (N-1)K & \cdots & -K \\ \vdots & \vdots & \ddots & \vdots \\ -K & -K & \cdots & (N-1)K \end{pmatrix} \quad (4.16)$$

where K is the coupling strength characterizing the S_N symmetry network. The eigenvalues of Γ are NK with a multiplicity $N - 1$ and 0. As a consequence, the rank of Γ is $N - 1$. By Proposition 4.8, the dimension of the center manifold is 2. The critical bifurcation value for the network is $k_{network}^* = k^*$. From Theorem 4.5 (or Theorem 4.12 according to the parameter values), we conclude

4.3. ILLUSTRATIVE EXAMPLES

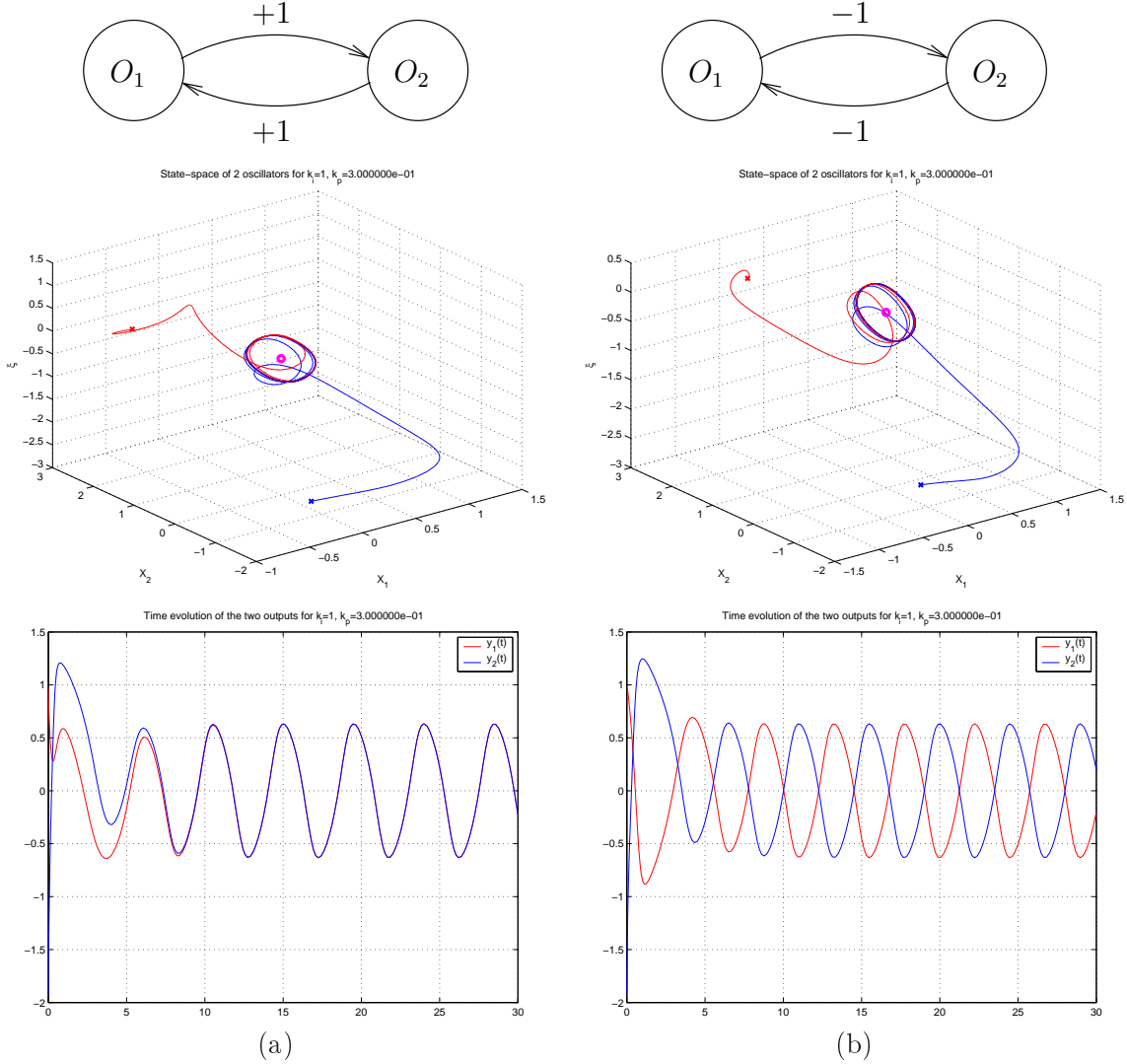


Figure 4.4: Simulation results for a network of 2 identical oscillators of type (4.12)-(4.14). The circles represent the oscillators. Column (a) corresponds to Γ_1 and column (b) corresponds to Γ_2 . The parameters values are $\omega_n = 1$, $\zeta = 1.25$, $\tau = 2$, $k = 0.3$. The critical bifurcation value for an isolated oscillator is $k^* = 1$ and the corresponding bifurcation value for the network is $k_{network}^* = 0$. The trajectories generated in the state space of each oscillator are represented on the second row. A different color is used for each oscillator (red for the trajectory of oscillator 1 and blue for the trajectory of oscillator 2). The third row represents the time evolution of the outputs of the oscillators.

that the network possesses a limit cycle for $k \gtrsim k_{network}^*$. This is illustrated by the simulation results presented in Figure 4.7. For this simulation we considered a network of 5 identical passive oscillators of type (4.12)-(4.14) coupled according to S_5 symmetry. The parameters values are $\omega_n = 1$, $\zeta = 1.25$, $\tau = 2$. This leads to a critical bifurcation value $k_{network}^* = 1$.

The results of Theorems 4.5, or 4.12 hold only for $k \gtrsim k_{network}^*$. Nevertheless, we expect these results to hold valid for a (large) range of the bifurcation parameter k . To illustrate this we selected $k =$

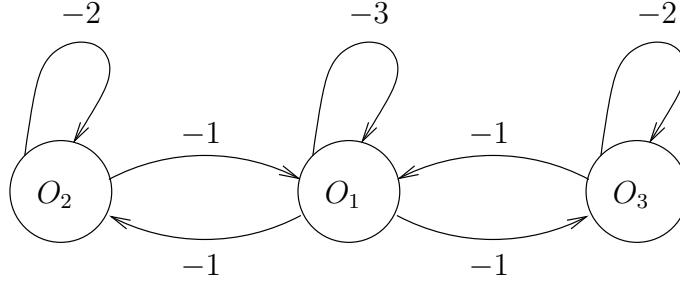


Figure 4.5: Network of 3 oscillators in chain structure.

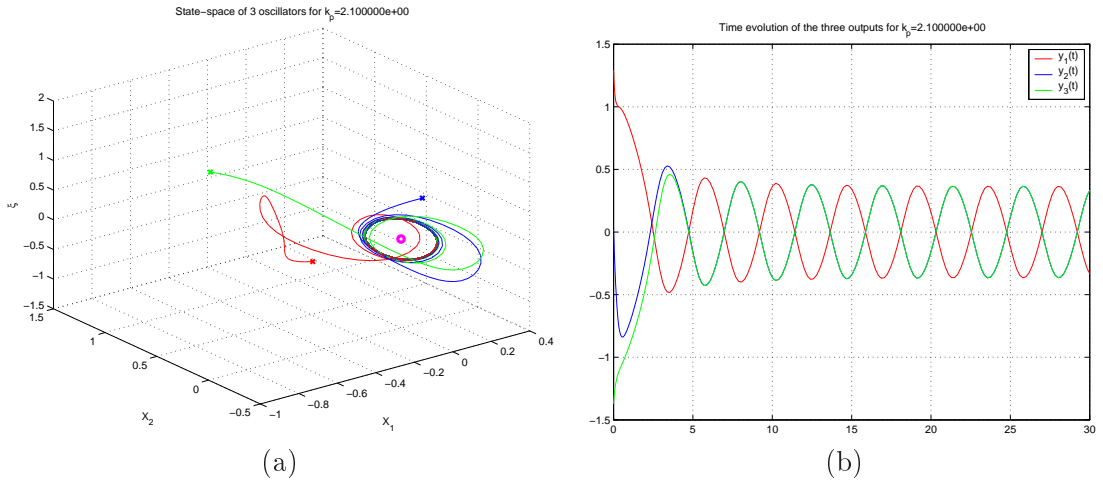


Figure 4.6: Simulation results for a network of 3 identical oscillators of type (4.12)-(4.14) coupled according to Figure 4.5. The parameters values are $\omega_n = 1$, $\zeta = 1.25$, $\tau = 2$, $k = 2.1$. The critical bifurcation value for an isolated oscillator is $k^* = 1$ and the corresponding bifurcation value for the network is $k_{network}^* = 2$.

2. In this simulation, we see that all the oscillators synchronize. We will return to the synchronization behavior in Section 4.4.2.

The same results hold for D_N symmetry networks, i.e. bidirectional rings of oscillators. In the case of D_N symmetry networks, the matrix Γ has the form

$$\Gamma = \begin{pmatrix} 2K & -K & 0 & \cdots & 0 & -K \\ -K & 2K & -K & 0 & \cdots & 0 \\ 0 & -K & \ddots & \ddots & \ddots & \vdots \\ \vdots & 0 & \ddots & 2K & -K & 0 \\ 0 & \vdots & \ddots & -K & 2K & -K \\ -K & 0 & \cdots & 0 & -K & 2K \end{pmatrix}. \quad (4.17)$$

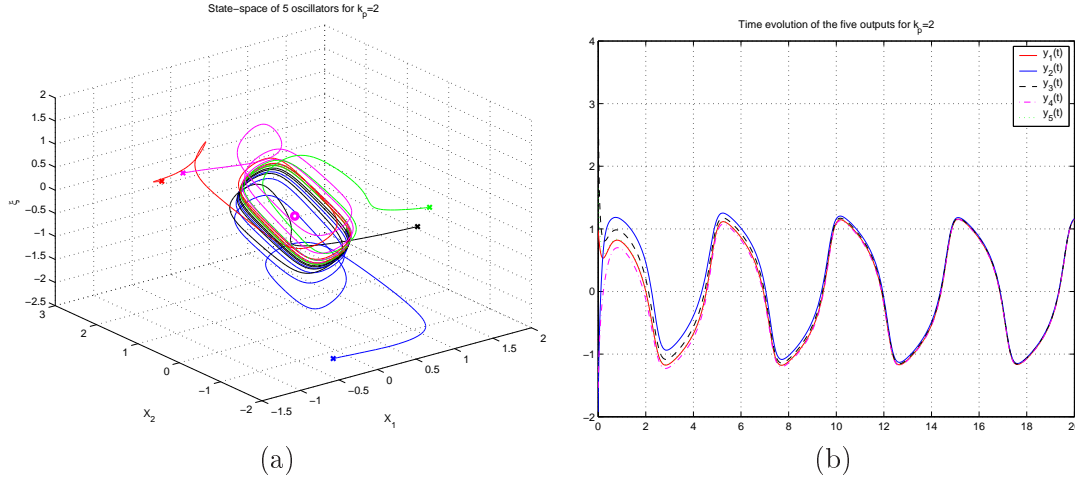


Figure 4.7: Simulation results for a network of 5 identical oscillators of type (4.12)-(4.14) coupled through S_5 symmetry. The parameters values are $\omega_n = 1$, $\zeta = 1.25$, $\tau = 2$, $k = 2$, and $K = 1$. The critical bifurcation value for an isolated oscillator is $k^* = 1$ and the corresponding bifurcation value for the network is $k_{network}^* = 1$.

This matrix is cyclic and its eigenvalues can be calculated analytically (see e.g. [Hop86]): $\lambda_j(\Gamma) = 2K \left(1 - \cos\left(\frac{2\pi j}{N}\right)\right) \geq 0$, $j = 1, \dots, N$. The rank of Γ is once again equal to $N - 1$ and the results of Theorems 4.5 (or 4.12 according to the parameter values) may be directly applied.

4.4 Third result of this thesis - Incremental passivity and synchronization

After having determined the existence and stability of sustained oscillations in a network of interconnected passive oscillators, the next step is to characterize their relative oscillating behavior, i.e. one with respect to the other ones. The question of global synchronization among the oscillators is particularly relevant. Synchronization refers to the tendency of interconnected oscillators to produce ensemble phenomena, that is, to phase lock as if an invisible conductor was orchestrating them. Synchronization is a convergence property for the *difference* between the solutions of different systems. Convergence properties for the difference between solutions of a closed system are characterized by notions of *incremental* stability [Ang02, LS98, PPvdWN04]. For open systems, the corresponding notion is *incremental passivity*.

In the next section, we define the notion of incremental passivity and give sufficient conditions under which passive oscillators are incrementally passive. In Section 4.4.2, we show the implications of incremental passivity for synchronization and derive sufficient network topology conditions for the existence of globally asymptotically stable synchronic oscillations in networks of oscillators. The results concern the interconnection of N identical passive oscillators with network topologies that include S_N symmetry (all-to-all topology), D_N symmetry (bidirectional ring topology), Z_N symmetry (unidirectional ring topology) and open chain symmetry. Exploiting the properties of passive oscillators, we additionally show that the network solutions are bounded and that the global limit cycle stability analysis carried out for an isolated oscillator extends to the network. These results are

related to other recent synchronization results in the literature [SW03, Pog98, Ang02] that are all based on incremental stability notions.

4.4.1 Incremental passivity

Consider two different solutions $x_a(t)$ and $x_b(t)$ of the input-affine system Σ given in (3.16) with corresponding inputs and outputs $(u_a(t), y_a(t))$ and $(u_b(t), y_b(t))$. Denote the incremental variables by $\Delta x = x_a - x_b$, $\Delta u = u_a - u_b$, and $\Delta y = y_a - y_b$. The system is *incrementally dissipative* if it satisfies a dissipation inequality of the form

$$\dot{\Delta S} \leq w(\Delta u, \Delta y) \quad (4.18)$$

for the scalar *incremental storage function* $\Delta S(\Delta x) \geq 0$ with the *incremental supply rate* $w(\Delta u, \Delta y)$. Incremental dissipativity (4.18) with the incremental supply rate $w(\Delta u, \Delta y) = (\Delta u)^T \Delta y$ is called *incremental passivity*.

Passivity implies incremental passivity for linear systems, that is, if the quadratic storage $S(x) = x^T P x$ satisfies the dissipation inequality $\dot{S} \leq u^T y$ then the incremental storage $\Delta S(\Delta x) = (\Delta x)^T P \Delta x$ satisfies the incremental dissipation inequality $\dot{\Delta S} \leq (\Delta u)^T \Delta y$. Passivity also implies incremental passivity for monotone increasing, static nonlinearity: if $\phi(\cdot)$ is monotone increasing, then $(s_1 - s_2)(\phi(s_1) - \phi(s_2)) = \Delta s \Delta \phi(s) \geq \Delta s \psi(\Delta s) \geq 0$, $\forall \Delta s = s_1 - s_2$ for some static nonlinearity $\psi(\cdot)$.

Passive oscillators made of the feedback interconnection of a linear system Σ_k with a monotone increasing nonlinearity $\phi(\cdot)$ are thus also incrementally passive. In the following sections we restrict ourselves to linear passive systems Σ and to nonlinearities $\phi(\cdot)$ that are monotone increasing.

4.4.2 Synchronization

Consider a network of N identical passive oscillators of type (3.16),(3.17),(3.18). We assume that the only nonlinearity in each passive oscillator is due to the nonlinear monotone increasing function $\phi(\cdot)$ appearing in the definition of $\phi_k(\cdot)$. The dynamics for oscillator $i = 1, \dots, N$ write

$$\begin{cases} \dot{x}_i &= Ax_i - B\phi_k(y_i) + Bu_i \\ y_i &= Cx_i \end{cases}$$

where u_i represents the external input of oscillator i . The dynamics of the network are easily represented with the help of the KRONECKER product (see Section 2.7 for a reminder of the main properties of the KRONECKER product).

$$\begin{cases} \dot{X} &= (I_N \otimes A) X - (I_N \otimes B) \Phi_k(Y) + (I_N \otimes B) U \\ Y &= (I_N \otimes C) X \end{cases} \quad (4.19)$$

where $X = (x_1^T, \dots, x_N^T)^T \in \mathbb{R}^{nN}$, $Y = (y_1, \dots, y_N)^T \in \mathbb{R}^N$,

$\Phi_k(Y) = (\phi_k(y_1), \dots, \phi_k(y_N))^T \in \mathbb{R}^N$, and I_N represents the N by N identity matrix.

We assume linear coupling, i.e. the topology of the network is defined by the input-output relation

$$U = -\Gamma Y. \quad (4.20)$$

Furthermore, we make the following network topology assumptions:

4.4. THIRD RESULT OF THIS THESIS - INCREMENTAL PASSIVITY AND SYNCHRONIZATION

- We assume that Γ is real and positive semidefinite, and that $\mathbf{1}$ (the vector $(1, \dots, 1)^T \in \mathbb{R}^N$) belongs to the kernel of Γ . This is equivalent to the assumption that all rows of Γ sum to zero which implies that the coupling between the oscillators disappears when synchronization is reached.
- We assume that the rank of Γ is equal to $N - 1$, i.e. Γ has only one zero eigenvalue. This is equivalent to the assumption that the network is connected.
- We do not require the interconnection matrix Γ to be symmetric but we assume that $\ker(\Gamma) = \ker(\Gamma^T) = \text{range}(\mathbf{1})$.

Theorem 4.15 gives sufficient conditions for the existence of a globally asymptotically stable oscillation in a network of identical passive oscillators satisfying the above made assumptions.

Definition 4.14 We denote by $\lambda_{\min \neq 0}(\Gamma_s)$ the smallest nonzero eigenvalue of the symmetric part of Γ .

Theorem 4.15 Consider the MIMO system (4.19)-(4.20) representing a network of N identical incrementally passive oscillators. Assume that (A, C) is observable, $\phi(\cdot)$ is monotone increasing and each isolated oscillator ($u_i \equiv 0$) possesses a globally asymptotically stable limit cycle in $\mathbb{R}^n \setminus E_s(0)$ where $E_s(0)$ denotes the stable manifold of the origin. If the interconnection matrix Γ is a real, positive semidefinite matrix such that $\ker(\Gamma) = \ker(\Gamma^T) = \text{range}(\mathbf{1})$ then for $\lambda_{\min \neq 0}(\Gamma_s) > k - k_{passive}^*$ (strong coupling), the network has a limit cycle which attracts all solutions except those belonging to the stable manifold of the origin, and all the oscillators of the network exponentially synchronize.

Proof

We compare the solution of each oscillator in the network to that of an isolated reference oscillator. The isolated reference oscillator dynamics are

$$\begin{cases} \dot{x}_0 &= Ax_0 - B\phi_k(y_0) \\ y_0 &= Cx_0 \end{cases}$$

where $x_0 \in \mathbb{R}^n$ and $y_0 \in \mathbb{R}$. Consider the incremental dynamics

$$\begin{cases} \Delta \dot{X} &= (I_N \otimes A) \Delta X - (I_N \otimes B) \Delta \Phi_k(Y) + (I_N \otimes B) U \\ \Delta Y &= (I_N \otimes C) \Delta X \end{cases} \quad (4.21)$$

where $\Delta X = X - \mathbf{1} \otimes x_0$ with X satisfying the dynamics (4.19), $\mathbf{1} \in \mathbb{R}^N$ and $\Delta \Phi_k(Y) = \Phi_k(Y) - \mathbf{1} \otimes \phi_k(y_0)$. Since each passive oscillator is incrementally passive, the incremental system (4.21) satisfies the incremental dissipation inequality

$$\begin{aligned} \dot{S}_\Delta &\leq (k - k_{passive}^*) \Delta Y^T \Delta Y - \Delta Y^T \Delta \Phi(Y) + \Delta Y^T U \\ &\leq \bar{k} \Delta Y^T \Delta Y + \Delta Y^T U \\ &\leq \bar{k} \Delta Y^T \Delta Y - \Delta Y^T \Gamma \Delta Y, \end{aligned} \quad (4.22)$$

where $\bar{k} = k - k_{passive}^*$ and $S_\Delta = \frac{1}{2} \Delta X^T (I_N \otimes P) \Delta X$ with $P = P^T > 0$ defining the storage function associated to each incrementally passive oscillator (i.e. $S_i = x_i^T P x_i$). S_Δ is the sum of the incremental storage functions of the incrementally passive oscillators. The second inequality comes

from the monotone increasing property of $\phi(\cdot)$. The third inequality comes from the properties of Γ , i.e. $U = -\Gamma Y = -\Gamma(\Delta Y + \mathbf{1} \otimes y_0) = -\Gamma \Delta Y$ since $\mathbf{1} \in \ker(\Gamma)$.

Decompose (uniquely) the vector X into two components belonging respectively to the kernel of $\Gamma \otimes I_n$ and to its orthogonal complement, i.e. $X = X_{\ker} + X_{\ker^\perp}$ where $X_{\ker} \in \ker(\Gamma \otimes I_n)$ and $X_{\ker^\perp} \in \ker(\Gamma \otimes I_n)^\perp = \{V \in \mathbb{R}^{nN} : V^T W = 0, \forall W \in \ker(\Gamma \otimes I_n)\}$. The corresponding output decomposition is $Y = Y_{\ker} + Y_{\ker^\perp}$ with $Y_{\ker} = (I_N \otimes C) X_{\ker} \in \ker(\Gamma)$ and $Y_{\ker^\perp} = (I_N \otimes C) X_{\ker^\perp} \in (\ker(\Gamma))^\perp$ (this is obvious from the KRONECKER product properties, see Propositions A.6 and A.7 in Appendix A). From the assumption $\ker(\Gamma) = \text{range}(\mathbf{1})$, we have $X_{\ker} = \mathbf{1} \otimes x_{\ker}$ and $Y_{\ker} = \mathbf{1} \otimes y_{\ker}$, with $\mathbf{1} \in \mathbb{R}^N$. We thus write $\Delta X = \mathbf{1} \otimes (x_{\ker} - x_0) + X_{\ker^\perp}$ and $\Delta Y = \mathbf{1} \otimes (y_{\ker} - y_0) + Y_{\ker^\perp}$. Under the assumption that $\ker(\Gamma) = \ker(\Gamma^T)$, it can be shown that $-\Delta Y^T \Gamma \Delta Y \leq -\lambda_{\min \neq 0}(\Gamma_s) |Y_{\ker^\perp}|^2$ where $\lambda_{\min \neq 0}(\Gamma_s)$ represents the smallest nonzero eigenvalue of the symmetric part of Γ (see Proposition A.5 in Appendix A). The incremental passivity inequality (4.22) then writes

$$\dot{S}_\Delta \leq \bar{k} |\mathbf{1} \otimes (y_{\ker} - y_0)|^2 + (\bar{k} - \lambda_{\min \neq 0}(\Gamma_s)) |Y_{\ker^\perp}|^2 \quad (4.23)$$

Assume that the initial condition of the reference oscillator $x_0(0)$ is chosen to be equal to the initial condition of the kernel component of X , i.e. $x_0(0) = x_{\ker}(0)$. The invariance of the kernel dynamics (see Appendix A) implies that $x_0(t) = x_{\ker}(t)$, $\forall t \geq 0$ and thus that $y_{\ker}(t) - y_0(t) = 0$, $\forall t \geq 0$. The incremental passivity inequality now writes

$$\dot{S}_\Delta \leq (\bar{k} - \lambda_{\min \neq 0}(\Gamma_s)) |Y_{\ker^\perp}|^2. \quad (4.24)$$

From the strong coupling assumption, we have

$$\gamma = \lambda_{\min \neq 0}(\Gamma_s) - \bar{k} > 0. \quad (4.25)$$

Integrating (4.24) over $[t_0, t_0 + \delta]$ where $\delta > 0$ is arbitrarily chosen, we obtain

$$\begin{aligned} \int_{t_0}^{t_0+\delta} \dot{S}_\Delta d\tau &\leq -\gamma \int_{t_0}^{t_0+\delta} |Y_{\ker^\perp}(\tau)|^2 d\tau \\ &\leq -\alpha \gamma |X_{\ker^\perp}(t_0)|^2, \quad \alpha > 0, \end{aligned} \quad (4.26)$$

for all $X_{\ker^\perp}(t_0)$, $t_0 \geq 0$. The last inequality comes from the observability of the pair (A, C) (see Appendix A). Global exponential stability (GES) of $X_{\ker^\perp}(t)$ is then deduced from classical exponential stability theorems (see, for example, [SB89, Theorem 1.5.2]). This means that with a particular choice of initial condition for the reference oscillator, we were able to show that $\Delta X(t) = 0$ is GES. GES of the solution $\Delta X = 0$ for the difference system (4.21) implies that all solutions of the network (4.19) exponentially converge to the invariant subspace

$$\{X \in \mathbb{R}^{nN} : x_1 = \dots = x_N = x_0\} \quad (4.27)$$

where the dynamics are decoupled. Because the dynamics of the network decouple in the invariant

4.4. THIRD RESULT OF THIS THESIS - INCREMENTAL PASSIVITY AND SYNCHRONIZATION

subspace (4.27), GES of the solution $\Delta X = 0$ for the difference system (4.21) implies that all bounded solutions converge to the ω -limit sets of the decoupled system and that all oscillators synchronize asymptotically.

Combining GES of the difference system (4.21) and global boundedness of the solutions (see Section 4.2.1), we conclude that, for strong coupling, all solutions of the network (4.19) converge to the ω -limit sets of the uncoupled dynamics, i.e. all solutions except those belonging to the stable manifold of the origin of the network converge towards a unique limit cycle. ■

Remark 4.16 *The result still holds if the observability assumption on the pair (A, C) is relaxed to a detectability assumption.*

Remark 4.17 *The GES result of $\Delta X = 0$ may be viewed as an incremental input-to-state stability (δ -ISS) property of the network with $S(X)$ being the corresponding δ -ISS LYAPUNOV function [Ang02].*

Remark 4.18 *Theorem 4.15 is closely linked to recent synchronization results by SLOTINE [SW03] and POGROMSKY [Pog98]. This may easily be noticed from the normal form of passive systems. The normal form for oscillator i of the network is [SJK97]*

$$\begin{aligned} \begin{pmatrix} \dot{z}_i \\ \dot{y}_i \end{pmatrix} &= \begin{pmatrix} Q & e \\ f^T & g \end{pmatrix} \begin{pmatrix} z_i \\ y_i \end{pmatrix} + \begin{pmatrix} \mathbf{0} \\ CB \end{pmatrix} (ky_i - \phi(y_i)) \\ &\quad - \sum_{j=1}^N \gamma_{ij} \begin{pmatrix} 0 & \mathbf{0}^T \\ \mathbf{0} & CB \end{pmatrix} \left(\begin{pmatrix} z_j \\ y_j \end{pmatrix} - \begin{pmatrix} z_i \\ y_i \end{pmatrix} \right), \end{aligned}$$

where CB is positive definite from the strong passivity assumption. Assume, as it is done by SLOTINE and POGROMSKY, that $\gamma_{ij} \leq 0$ for $i \neq j$, and that $\gamma_{ii} = \sum_{j=1}^N |\gamma_{ij}|$, then the couplings $-\gamma_{ij} \begin{pmatrix} 0 & \mathbf{0}^T \\ \mathbf{0} & CB \end{pmatrix}$ are positive semidefinite. The symmetric part of the Jacobian of the uncoupled dynamics, divided according to the coupling structure, is given by

$$J_{is} = \begin{pmatrix} Q_s & \frac{1}{2}(e+f) \\ \frac{1}{2}(e+f)^T & g + CBk - CB \frac{d\phi(y_i)}{dy_i} \end{pmatrix}.$$

It is then easily seen that the sufficient conditions given by SLOTINE [SW03, Remark 3 of Theorem 2] are satisfied, i.e.

1. Q_s is contracting since it is HURWITZ from the passivity and detectability assumptions;
2. $\lambda_{\max}(g + CBk - CB \frac{d\phi(y_i)}{dy_i}) < g + CBk < \infty$ from the monotone increasing assumption;
3. $\sigma_{\max}(\frac{1}{2}(e+f)) = \left| \frac{e+f}{2} \right|^2 < \infty$.

Exploiting the special structure of passive oscillators, Theorem 4.15 additionally proves that the network solutions are bounded and that the limit cycle stability analysis carried out for an isolated oscillator extends to the network.

4.5 Examples and simulation results

As an illustration of Theorem 4.15 for a non symmetric interconnection matrix, we consider a Z_N symmetry network of passive oscillators of type (4.12)-(4.14). In the case of Z_N symmetry networks, the matrix Γ has the form

$$\Gamma = \begin{pmatrix} K & -K & \cdots & \cdots & 0 \\ 0 & K & -K & \cdots & 0 \\ \vdots & 0 & K & \ddots & \vdots \\ \vdots & \vdots & \ddots & \ddots & -K \\ -K & 0 & \cdots & 0 & K \end{pmatrix} \quad (4.28)$$

and it can be easily shown that $\text{rank}(\Gamma) = N - 1^5$ and that all its eigenvalues have nonnegative real parts (this results from a simple application of the GERSHGORIN Theorem [GvL89]). Indeed, it can be shown that $\lambda_{\min_{\neq 0}}(\Gamma_s) = K(1 - \cos(\frac{2\pi}{N}))$. From the strong coupling condition (4.25), this implies that synchronization is guaranteed if $K > K_{Z_N}$ with $K_{Z_N} = \frac{k - k_{passive}^*}{(1 - \cos(\frac{2\pi}{N}))}$. Moreover, from Theorem 4.15, we conclude that for $K > K_{Z_N}$, all solutions, except those belonging to the stable manifold, converge towards the ω -limit set of the uncoupled system which is a globally attractive limit cycle for $k \gtrsim k^*$.

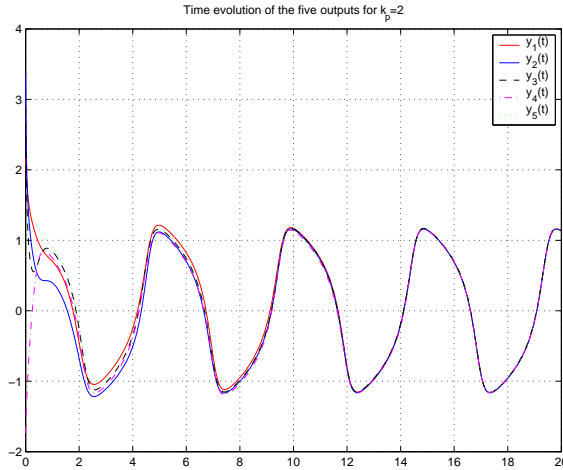


Figure 4.8: Time evolution of the outputs in a network of 5 oscillators coupled through Z_5 symmetry.

Simulation results for a Z_5 symmetry network of passive oscillators of type (4.12)-(4.14) are presented in Figure 4.8. For this simulation, we have chosen the following values of the parameters: $\tau = 2$, $\zeta = 1.25$ and $\omega_n = 1$. This leads to a critical bifurcation value $k^* = 1$ while the loss of passivity occurs at $k_{passive}^* = 1$. The value of the bifurcation parameter k has been chosen equal to 2. The initial conditions for this simulation have been chosen at random. For global synchronization, the common coupling strength K has to be strong enough (i.e., $K > \frac{2-1}{1 - \cos(\frac{2\pi}{5})} = 1.4472$). For this simulation, the value of K was equal to 2.

⁵The characteristic polynomial is $(K - x)^N - K^N$ which has only one root equal to zero for any N .

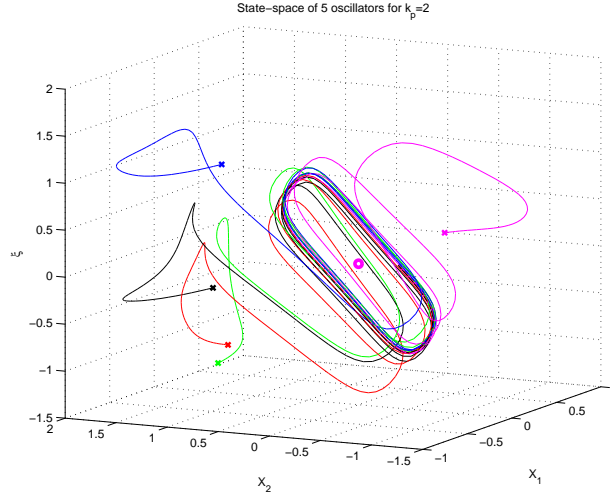


Figure 4.9: Superposition of the state spaces of the 5 passive oscillators coupled through Z_5 symmetry.

In Figure 4.9, we clearly see that the oscillators synchronize around a common limit cycle. This limit cycle is identical to the one obtained for an isolated oscillator.

The same global synchronization results hold for D_N and S_N symmetry networks. For D_N symmetry networks, the coupling strength synchronization threshold is $K_{D_N} = \frac{k - k_{passive}^*}{2(1 - \cos(\frac{2\pi}{N}))}$. For S_N symmetry networks, the coupling strength synchronization threshold is $K_{S_N} = \frac{k - k_{passive}^*}{N}$.

Finally, the case of bidirectional open chain structures is also included in Theorem 4.15. Consider the network represented on Figure 4.10. The corresponding interconnection matrix Γ is symmetric tridiagonal and writes

$$\Gamma = \begin{pmatrix} K & -K & 0 & \cdots & 0 & 0 \\ -K & 2K & -K & 0 & \cdots & 0 \\ 0 & -K & \ddots & \ddots & \ddots & \vdots \\ \vdots & 0 & \ddots & 2K & -K & 0 \\ 0 & \vdots & \ddots & -K & 2K & -K \\ 0 & 0 & \cdots & 0 & -K & K \end{pmatrix}$$

and it is easy to show that its eigenvalues are $\lambda_j = 2K \left(1 - \cos\left(\frac{j\pi}{N}\right)\right)$, $j \in \{0, \dots, N-1\}$. The coupling strength threshold is $K_{Open\ chain} = \frac{k - k_{passive}^*}{2(1 - \cos(\frac{\pi}{N}))}$.

We see that the 'larger' the symmetry of the synchronizing interconnection structure, the smaller the coupling strength threshold, i.e. $K_{S_N} < K_{D_N} < K_{Z_N} < K_{Open\ chain}$. This is in accordance with the results of SLOTINE [WS] which predict that the synchronization rate is proportional to the number of oscillators in the network and to the symmetry of the network. The higher the number of oscillators or the symmetry, the higher the synchronization rate. This is confirmed by the simulations results in Figure 4.11 where we consider four different topologies with the same number of oscillators, the same initial conditions and the same coupling strength. We see from Figure 4.11 that the synchronization rate increases with the symmetry of the network.



Figure 4.10: Synchronizing bidirectional open chain structure.

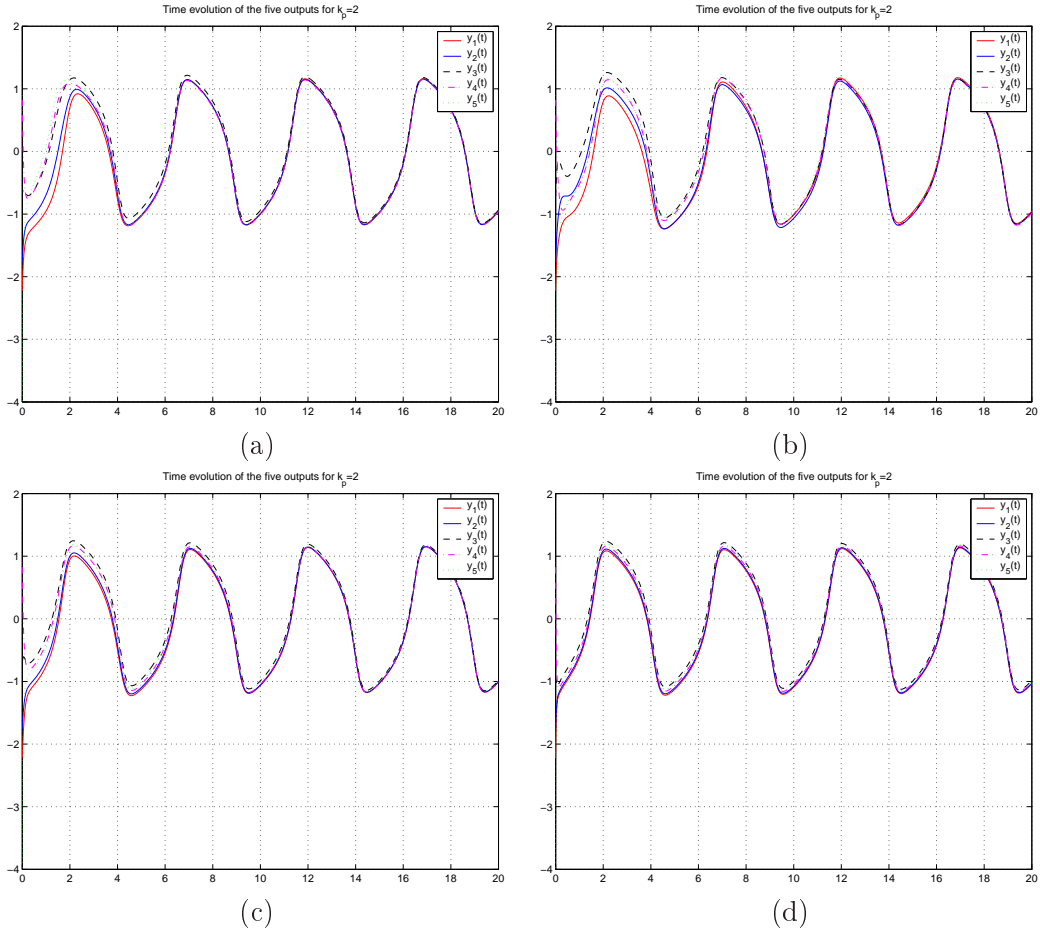


Figure 4.11: Simulation results for networks of five identical passive oscillators. (a) Open chain, (b) Z_5 symmetry, (c) D_5 symmetry, (d) S_5 symmetry. The parameters values are $\omega_n = 1$, $\zeta = 1.25$, $\tau = 2$, $k = 2$. The critical bifurcation value for an isolated oscillator is $k^* = 1$ and the corresponding bifurcation value for the network is $k_{network}^* = 1$. The coupling strength value is $K = 3$. The same initial conditions have been used for the different network topologies.

4.6 Summary

In the previous chapter, we showed that dissipativity theory has implication for the global stability analysis of the limit cycle solution of passive oscillators. In this chapter, we extended the dissipative

characterization of passive oscillators to networks. This was done by considering a MIMO feedback representation of the network that is similar to the feedback structure of each isolated passive oscillator. The main assumption was the passivity (positivity) of the coupling. Under this assumption, we obtained a dissipation inequality for the network that is similar to that satisfied by each isolated passive oscillator. Based on this dissipativity inequality, we showed that the results of Chapter 3 extend in a straightforward manner to networks of passive oscillators (Theorems 4.5, 4.9, and 4.12). As a second result, we showed that global synchronization is implied by an incremental dissipativity characterization of the network that we named *incremental passivity*. We provided sufficient conditions under which passive oscillators are incrementally passive and derived sufficient network topology conditions for the existence of globally asymptotically stable synchronic oscillations in networks of identical oscillators (Theorem 4.15). This synchronization result concerns network topologies that include S_N symmetry (all-to-all topology), D_N symmetry (bidirectional ring topology), Z_N symmetry (unidirectional ring topology) and open chain symmetry. We compared our result with recent literature results on global synchronization and showed that generically passive oscillators satisfy the required conditions.

Chapter 5

Synthesis of stable oscillations

In this chapter, we adopt a synthesis point of view for the generation of stable limit cycle oscillations. We examine how to design a simple controller that yields stable limit cycle oscillations in a stabilizable system. The problem of synthesis of stable oscillations finds many applications. For example, in the field of robotics, it plays an important role for (underactuated) rhythmic task robots such as walking robots ([CAA⁺03, WGC02, TYS91]), juggling robots ([SA93, SA94, BKK94, ZRB99, LB01, GS04, RLS04]) or general dexterous robots (see e.g. [Wil99a]). In Section 5.1, we propose a proportional-integral controller to generate oscillations in stabilizable systems. The proposed controller is directly inspired from the theory introduced in the previous chapters. In Section 5.2 we show that this controller is a natural choice for the generation of limit cycle oscillations in mechanical systems. We also show that for conservative stabilizable (mechanical) systems in feedback with our controller, the only assumption of our theorems that is not satisfied is the low dimension of the center manifold: these systems are generically characterized by a degenerate bifurcation. In Section 5.3 we propose a method to regularize the degenerate bifurcation. We also show that this regularization method is only possible for fully actuated, two degrees of freedom mechanical systems. In Section 5.4, we provide simulation results for the cart-pendulum system as a typical example of an underactuated mechanical system for which direct application of the proposed controller results in generation of stable limit cycle oscillations. Finally, as a second illustration, we describe the research project that we have initiated with the Laboratoire d'Automatique de Grenoble. This project concerns the balancing control of the bipedal robot RABBIT.

5.1 A proportional-integral mechanism to generate oscillations in a stabilizable system

In this section, we consider the problem of generation of limit cycle oscillations in stabilizable systems. To this end, we introduce the definition of a stabilizable system.

Consider an input-affine nonlinear system Σ represented by the state space model

$$\dot{x} = f(x) + g(x)u, \tag{5.1}$$

where $x \in \mathbb{R}^n$ is the state and $u \in \mathbb{R}^m$ is the input.

Definition 5.1 *The input affine system (5.1) is called stabilizable if there exists a control law $u(x)$ and a LYAPUNOV function $V(x)$ whose time derivative is rendered negative definite by $u(x)$.*

We also introduce the concept of a “control LYAPUNOV function” (CLF) [SJK97, Section 3.5.3], which is strongly linked with definition 5.1.

Definition 5.2 [SJK97, Section 3.5.3] *A smooth, positive definite, and radially unbounded function $V(x)$ is called a control LYAPUNOV function (CLF) for the input affine system (5.1) if, for all $x \neq 0$,*

$$L_g V(x) = 0 \Rightarrow L_f V(x) < 0. \quad (5.2)$$

By definition, any LYAPUNOV function whose time derivative can be rendered negative definite (by control) is a CLF.

Proposition 5.3 *If system (5.1) with LYAPUNOV function $V(x)$ is stabilizable by the control $r(x)$, then it is passive and ZSD with respect to the input $v = u - r(x)$ and the output $y = (L_g V(x))^T$.*

Proof

The time derivative of the LYAPUNOV function $V(x)$ along the trajectories of system (5.1) is given by

$$\dot{V} = L_f V(x) + L_g V(x)u.$$

Using feedback control $u = r(x) + v$, we obtain

$$\dot{V} < y^T v,$$

which implies passivity of the system w.r.t. input v and output y . Furthermore, by definition, $V(x)$ is a CLF and thus satisfies (5.2). This directly implies zero-state detectability of system (5.1) w.r.t. y . ■

Assume that the system (5.1) is stabilizable by the control $r(x)$. To generate stable limit cycle oscillations, we consider the output $y = (L_g V(x))^T \in \mathbb{R}^m$ and close the loop with the nonlinear proportional (P) and integral (I) controller

$$u(t) = r(x(t)) - \Phi_k(y(t)) - K_I \int_0^t y(\tau) d\tau, \quad (5.3)$$

where $r(x)$ is referred to as the stabilization part, $\Phi_k(y(t))$ as the “proportional part”, and $K_I \int_0^t y(\tau) d\tau$ (with $K_I = K_I^T > 0$) as the “integral part” (see Figure 5.1). The nonlinear function $\Phi_k(\cdot) = \text{diag}\{\phi_k(\cdot)\}$ defining the proportional part is a multivariable repeated nonlinearity. The repeated nonlinearity $\phi_k(y) = -ky + \phi(y)$ is assumed to satisfy the assumptions given in Section 3.3.1, and $\phi(\cdot)$ is furthermore assumed to be monotone increasing.

To intuitively understand the effect of this controller, consider the SISO case when $u \in \mathbb{R}$ and $y \in \mathbb{R}$. The proportional part is then denoted by $\phi_k(y)$. Its sign varies according to the magnitude of the output. For small values of the output, the proportional part is sign opposed to y whereas for large values of the output, the proportional part has the same sign as y . This means that the sign of the dissipation injected into the system through the proportional part depends on the magnitude of

the output y . Since the feedback system dissipates energy for large values of the output and restores it for small values, a limit cycle is expected to appear. As we have seen in Chapter 3, the integral part generically forces a HOPF bifurcation because of the presence of a zero at the origin for the linearized system. If the system already includes an integral action, the integral part of the controller is unnecessary and may be omitted.

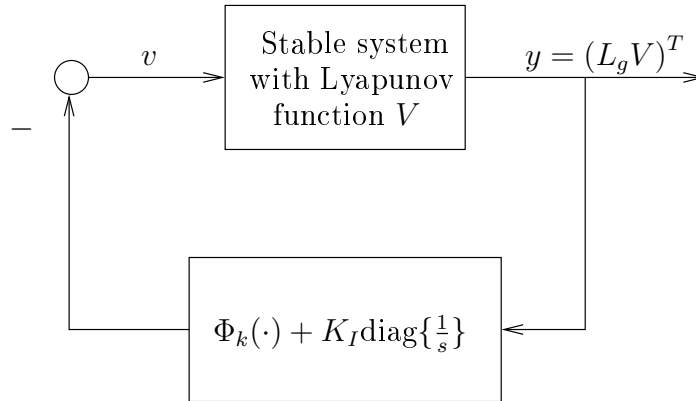


Figure 5.1: Synthesis of oscillations by nonlinear PI control of a stable system.

Controller (5.3) is inspired by classical PI controllers $u = r(x(t)) - K_P y - K_I \int_0^t y(\tau) d\tau$ used in equilibrium point stabilization and regulation theory (see e.g. [CSB96, Chapter 2]). These controllers are well-known for their robustness to constant perturbations: for any $K_P = K_P^T > 0$, $K_I = K_I^T > 0$, the feedback system is (globally) asymptotically stable. This is an immediate consequence of Theorem 2.15, Lemma 2.14 and Proposition 5.3: the feedback interconnection of system (5.1) with the integral part of the PI controller yields a passive and ZSD system characterized by the storage function $S = V + \frac{1}{2} x_I^T K_I x_I$ where x_I denotes the state of the integrator part of the controller. The whole feedback system is then characterized by the dissipation inequality $\dot{S} < -y^T K_P y$. This last inequality together with ZSD implies global asymptotic stability of the system composed of a forward passive block in feedback with the classical PI controller $u = K_P y + K_I \int_0^t y(\tau) d\tau$.

Other solutions for the generation of oscillation in stable systems have been proposed in the literature. We classify them mainly in two categories:

- Output regulation where the idea is to force the stable system with an external oscillating input (see e.g. [Isi95, Chapter 8], [Pav04]).
- Inversion and zero dynamics shaping where the idea is to design a particular output such that, when forced to zero, the remaining dynamics yield a stable limit cycle oscillation (see e.g. [GAGE03, BAGGE04, GEBAG05], [BM94, BM95a, BM95b, BMS96], [CEU02, SC04]).

Output regulation methods deal with asymptotic tracking of prescribed reference signals. The class of reference signals consists of solutions of some external autonomous system called the *exosystem*. Reference signals generated by the exosystem are called *exosignals*. The output to regulate is called the *regulated output* (e.g. the tracking error in the tracking problem). The output available for measurement is called the *measured output*. The idea is to find a measured output feedback controller such that the closed loop system is internally stable and the regulated output tends to zero along

solutions of the closed loop system. The internal stability requirement roughly means that all solutions of the closed loop system “forget” their initial conditions and converge to some limit solution which is determined only by the exosignal. To generate oscillation the exosystem is designed to produce a specific oscillating exosignal. The use of output regulation methods to produce stable limit cycle oscillations is generally not easy because of the need to design specific output and controller that render the closed loop system internally stable and at the same time allow to solve the regulation problem. Their advantage is that they allow to track a specific orbit in the state space.

Inversion methods generally require precise models of the system. They use the control to destroy unwanted (generally nonlinear) parts of the dynamics in order to feedback transform the system into a specific, easier to control, system (e.g. partially linear system). To generate oscillations, the control is used to force the output of the transformed system to zero and simultaneously to induce a zero dynamics that yields stable limit cycle oscillations. The main drawback of these methods are their lack of robustness to unmodeled dynamics, and/or the difficulty to perform the required zero dynamics shaping for complex nonlinear systems.

The main advantage of the PI controller (5.3) is that it relies on stabilization theory for equilibrium points. It is thus easy to implement: once a stabilizing, passive output has been designed for the system, it is used to close the loop with the controller in order to generate limit cycle oscillations. The design of a stabilizing, passive output is a central topic in nonlinear control theory and many methods already exist to solve this problem (feedback passivation designs [vdS00, SJK97], controlled Hamiltonian and Lagrangian theory [BLM01, BCLM01, BOvdS02], energy shaping methods [OvdSMM01, OvdSME02], etc.). Furthermore, this passivity based controller is expected to have good robustness properties to model uncertainties and perturbations because it does not rely on the exact cancellation of parts of the dynamics. The counterpart is that it does not allow to track a specific orbit and, as we have seen in Theorem 4.5¹, that specific assumptions have to be satisfied:

- ultimate boundedness of the closed-loop system;
- absolute stability at criticality, that is, when $k = k^*$.

The ultimate boundedness assumption is a technical assumption. As we have seen in Chapter 3, it is always satisfied when the forward block is linear. For a general nonlinear forward block, this assumption is difficult to verify. Nevertheless, for a passive, zero-state detectable, forward system, unbounded solutions are unlikely to happen. This is intuitively clear if one considers the sign of the dissipation added by the nonlinear proportional part of the controller. For large values of the output, the sign of the dissipation is positive leading intuitively to bounded solutions.

The absolute stability assumption is thus the most critical one. Numerous criteria have been developed in order to verify absolute stability of a feedback system: e.g. circle criterion, POPOV criterion, ZAMES-FALB multipliers, and numerical methods (e.g. Integral-Quadratic-Constraints – see [MR97] for a general and recent treatment). In the next section, we introduce and justify the use of a passivity based controller for the generation of limit cycle oscillations in mechanical systems.

¹In this chapter, Theorem 4.5 is used to characterize oscillations in MIMO feedback systems. For this, we consider Theorem 4.5 where Ξ is not supposed to result from the interconnection of several SISO systems as in Chapter 4, but from the interconnection of the stabilizable MIMO system (5.1) with the integral part of controller (5.3). As such, Theorem 4.5 is the direct and immediate extension of Theorem 3.8 to the feedback interconnection of a MIMO strongly passive system Ξ with the multivariable repeated nonlinearity $\Phi_k(\cdot)$. Since the notion of network has no sense here, we denote the critical value of bifurcation by k^* instead of $k_{network}^*$. With these considerations in mind, the formulation of the Theorem is identical.

5.2 Synthesis of stable oscillations in mechanical systems

For the generation of stable oscillations in mechanical systems, the nonlinear PI controller (5.3) is natural for several reasons:

- The total energy of the mechanical system is generally a good LYAPUNOV function candidate.
- Passivity is a natural physical property between conjugated variables of the system.
- Even for unstable mechanical systems (e.g. the cart-pendulum with pendulum in inverted position), various energy shaping methods exist to feedback transform the initial system into a stable and conservative system.

Using the PI controller (5.3), global limit cycle oscillations are obtained for $k \gtrsim k^*$ if the assumptions of Theorem 4.5 are satisfied. As we have seen, the critical assumption is the absolute stability of the feedback system at $k = k^*$. In order to satisfy this assumption, we may consider systems for which it is trivially satisfied. This is the case for general conservative systems which typically loose stability and passivity simultaneously at $k^* = 0$ when put in feedback with controller (5.3). Unfortunately, the resulting feedback system is generically characterized by a degenerate bifurcation, i.e. the number of eigenvalues crossing the imaginary axis at $k = 0$ is typically greater than 2 (see Appendix B). Three solutions may be considered at this stage:

- Solution 1: Take into account RAYLEIGH dissipation in the model and check if all the assumptions of Theorem 4.5 are satisfied (that is, mainly the absolute stability at criticality).
- Solution 2: Regularize the bifurcation by feedback in order to return to the standard bifurcation scenario.
- Solution 3: Generalize Theorem 4.5 to the case of degenerate bifurcations.

Solution 3 is beyond the scope of this chapter and will be the subject of future work. Solution 2 is considered in Section 5.3. The idea is to inject dissipation into the conservative system in order to return to a non-degenerate bifurcation situation. In Section 5.3, we show that generically, this regularization is possible only for fully actuated, two degrees of freedom mechanical systems.

5.3 Fully actuated, two degrees of freedom mechanical systems

In this section we present a method to regularize the degenerate bifurcation that generically appears when considering the feedback interconnection of a linear, conservative system with controller (5.3). This method consists in injecting specific dissipation into the system in order to 'push' all eigenvalues but two in the open left-half complex plane, thus keeping the critical value $k^* = 0$ unchanged but regularizing the bifurcation. Sufficient conditions that allow for the feedback implementation of this specific dissipation are presented in Section 5.3.1. We show that the proposed sufficient conditions can be satisfied only for fully actuated, two degrees of freedom mechanical system.

5.3.1 Transforming a linear PCH system into a passive system that satisfies the assumptions of Theorem 4.5

Consider the feedback interconnection of Figure 5.1 where the forward block, denoted by Σ , is linear, strongly conservative and detectable. We denote by Ξ , the feedback interconnection of Σ with the integral part of the controller. As feedback interconnection of two conservative systems, Ξ is conservative w.r.t. its input w and its output y . It is also easy to show that Ξ is detectable.

Let z denote the state variable of Ξ . The dynamics of the linear system Ξ are given by

$$\begin{aligned}\dot{z} &= Az + Bw \\ y &= Cz\end{aligned}\tag{5.4}$$

Since Ξ is conservative, there exists a matrix $P = P^T > 0$ such that the HILL-MOYLAN conditions

$$A^T P + PA = 0\tag{5.5}$$

$$C = B^T P\tag{5.6}$$

are satisfied. Taking $J = AP^{-1}$, the first HILL-MOYLAN condition (5.5) leads to $J = -J^T$ which shows that J is a skew symmetric matrix and that the system (5.4) may be written as a port controlled Hamiltonian (PCH) system (see [vds00, section 4.2.2]).

$$\dot{z} = JPz + Bw = J \frac{\partial H}{\partial z}(z) + Bw\tag{5.7}$$

$$y = B^T Pz = B^T \frac{\partial H}{\partial z}(z)\tag{5.8}$$

where the Hamiltonian function $H(z)$ is the storage function $S(z)$ associated to the (strongly) conservative system (5.4), i.e. $H(z) = S(z) = \frac{1}{2}z^T Pz$ with $P = P^T > 0$.

We now present a method that transforms the linear PCH system (5.7),(5.8) into a system that satisfies the assumptions of Theorem 4.5. The intuitive idea is to inject dissipation into the system in order to push all the eigenvalues but two into the open left-half complex plane.

Consider system (5.7),(5.8). There always exists a real orthogonal matrix Q that transforms it into a block triangular system, i.e. a system with a block triangular Jacobian matrix (see [HJ85, p. 82, theorem 2.3.4]). Under this coordinate transformation, equations (5.7),(5.8) write

$$\dot{\tilde{z}} = \tilde{J}\tilde{P}\tilde{z} + \tilde{B}w\tag{5.9}$$

$$y = \tilde{B}^T \tilde{P}\tilde{z}\tag{5.10}$$

where $\tilde{z} = Qz$, $\tilde{B} = QB$, $\tilde{J} = QJQ^T = -\tilde{J}^T$, and $\tilde{P} = QPQ^T = \tilde{P}^T > 0$. Since passivity (conservativeness) is a coordinate independent property, system (5.9),(5.10) is also conservative w.r.t. input w and output y . In these coordinates, the matrix $\tilde{J}\tilde{P}$ writes

$$\tilde{J}\tilde{P} = \begin{pmatrix} \delta & \star \\ 0 & \Delta \end{pmatrix},\tag{5.11}$$

where δ is a 2×2 matrix, and both δ and Δ have all their eigenvalues on the imaginary axis (see Appendix B). The idea of the method is to design a dissipation matrix $R = R^T \geq 0$ such that the resulting port controlled Hamiltonian system with dissipation (PCHD):

$$\dot{\tilde{z}} = (\tilde{J} - R) \tilde{P} \tilde{z} + \tilde{B} w \quad (5.12)$$

$$y = \tilde{B}^T \tilde{P} \tilde{z} \quad (5.13)$$

has only two eigenvalues on the imaginary axis, the other eigenvalues having strictly negative real parts.

Thus, given P , we want to find $R = R^T \geq 0$ such that $(\tilde{J} - R) \tilde{P}$ has the form

$$\begin{pmatrix} \delta & \star \\ 0 & \Delta - \epsilon I \end{pmatrix}.$$

This amounts to find a symmetric positive semidefinite matrix R such that

$$R = \begin{pmatrix} 0 & \star \\ 0 & \epsilon I \end{pmatrix} \tilde{P}^{-1}.$$

If we choose $\star = \epsilon P_{12} P_{22}^{-1}$, where P_{12} and P_{22} appear in the block decomposition of \tilde{P}^{-1} corresponding to the block decomposition of $\tilde{J} \tilde{P}$, i.e. $\tilde{P}^{-1} = \begin{pmatrix} P_{11} & P_{12} \\ P_{12}^T & P_{22} \end{pmatrix} = (\tilde{P}^{-1})^T > 0$, then R is a symmetric positive semidefinite matrix. This is proved hereafter.

Proof

With $\star = \epsilon P_{12} P_{22}^{-1}$, we have $R = \begin{pmatrix} 0 & \epsilon P_{12} P_{22}^{-1} \\ 0 & \epsilon I \end{pmatrix} \begin{pmatrix} P_{11} & P_{12} \\ P_{12}^T & P_{22} \end{pmatrix} = \epsilon \begin{pmatrix} P_{12} P_{22}^{-1} P_{12}^T & P_{12} \\ P_{12}^T & P_{22} \end{pmatrix}$, which is obviously symmetric. Moreover, it is positive semidefinite for $\epsilon > 0$ since ϵP_{22} is symmetric positive definite and its SCHUR complement is positive semidefinite² (see [HJ85, Theorem 7.7.6]). ■

Generically, the PCHD system (5.12)-(5.13) with the dissipation matrix

$$R = \epsilon \begin{pmatrix} P_{12} P_{22}^{-1} P_{12}^T & P_{12} \\ P_{12}^T & P_{22} \end{pmatrix}$$

will satisfy all the assumptions of Theorem 4.5. In order to have a constructive way that allows to regularize the bifurcation, we now present a method to implement this dissipation matrix by feedback.

5.3.2 Implementing specific dissipation by feedback

The following algorithm leads to the computation of the feedback law implementing the desired dissipation matrix R . This algorithm is derived from the more general *matching theorem* of port-controlled Hamiltonian systems given in [OvdSMM01, OvdSME02, BOvds02]:

1. Compute the image of \tilde{B} , i.e. $W = \text{Im}(\tilde{B}) = \{p \in \mathbb{R}^n : \tilde{B}v = p, \forall v \in \mathbb{R}^m\}$
2. Compute the left annihilator of W , i.e. $W^\circ = \text{Ann}(W) = \{l \in \mathbb{R}^n : lp = 0, \forall p \in W\}$

²The SCHUR complement is 0.

3. If $\exists l \in W^\circ$ such that $lR\tilde{P}\tilde{z} = 0, \forall \tilde{z} \in \mathbb{R}^n$, then $-R\tilde{P}\tilde{z} \in W$ for all $\tilde{z} \in \mathbb{R}^n$, which in turn implies that there exists a control $w \in \mathbb{R}^m$ such that $\tilde{B}w = -R\tilde{P}\tilde{z}$ for all $\tilde{z} \in \mathbb{R}^n$
4. The control law that implements the dissipation matrix R is $w = -\left(\tilde{B}^T\tilde{B}\right)^{-1}\tilde{B}^TR\tilde{P}\tilde{z} + \tilde{w}$ where \tilde{w} denotes the new control input of the system.

For the particular matrix R that we have chosen, the condition $\exists l \in W^\circ$ s.t. $lR\tilde{P}\tilde{z} = 0, \forall \tilde{z} \in \mathbb{R}^n$ amounts to verify that $Im\left(\begin{smallmatrix} P_{12} \\ P_{22} \end{smallmatrix}\right) \subseteq Im(\tilde{B})$. This is easily seen by partitioning the vector l according to the partition of $R\tilde{P}$. The condition then writes $\exists l \in W^\circ$ s.t. $\epsilon\left(\begin{smallmatrix} l_1 & l_2 \end{smallmatrix}\right)\begin{pmatrix} 0 & P_{12}P_{22}^{-1} \\ 0 & I \end{pmatrix}\begin{pmatrix} z_1 \\ z_2 \end{pmatrix} = 0, \forall z \in \mathbb{R}^n$, which amounts to verify that $\exists l \in W^\circ$ s.t. $\left(\begin{smallmatrix} l_1 & l_2 \end{smallmatrix}\right)\begin{pmatrix} P_{12} \\ P_{22} \end{pmatrix} = 0$. This condition is satisfied if and only if $Im\left(\begin{smallmatrix} P_{12} \\ P_{22} \end{smallmatrix}\right) \subseteq Im(\tilde{B})$.

The matrix $\begin{pmatrix} P_{12} \\ P_{22} \end{pmatrix}$ is a $n \times (n-2)$ matrix. The matrix \tilde{B} is a $n \times m$ matrix where n denotes the dimension of the system and m the number of control inputs. For fully actuated mechanical systems, we have $m = \frac{n}{2}$, where $\frac{n}{2}$ is an integer that denotes the number of degrees of freedom of the mechanical system. It results that the condition $Im\left(\begin{smallmatrix} P_{12} \\ P_{22} \end{smallmatrix}\right) \subseteq Im(\tilde{B})$ can generically be satisfied only for $n = 4$ and $m = 2$, i.e. for a fully actuated mechanical systems with two degrees of freedom.

This dissipation implementation method has been given here for the sake of completeness. Indeed, because of its limited application field, and since our final goal is to generalize Theorem 4.5 to degenerate bifurcations, we chosed not to investigate further in this way but rather to have a first insight into the qualitative behavior in the degenerate case. In this case, we cannot conclude to the existence, uniqueness and global asymptotic stability of limit cycle oscillations generated by controller (5.3). Nevertheless, we intuitively expect this controller to yield limit cycle oscillations when used in feedback with a stabilizable, conservative system. To show this, we provide, in the next section, simulation results for the cart pendulum system as a typical example of underactuated, conservative mechanical systems for which direct application of our controller leads to limit cycle oscillations. These simulation results show that, even in the presence of a degenerate bifurcation, a limit cycle oscillation with a large basin of attraction is generated. This tends to confirm that our results should hold even if the bifurcation is degenerate, which would allow to apply controller (5.3) directly to any stabilizable, conservative system.

5.4 Direct application to underactuated, mechanical systems

As an illustration of the application of our theory to underactuated, mechanical systems we consider the cart-pendulum example and provide simulation results when the loop is closed with our controller. We have chosen this simple example because it constitutes a benchmark, underactuated, mechanical system for which stabilization by energy shaping has already been solved. The limit cycle generation method is explained in the next sections. The general idea is the following: first, we use energy shaping to feedback transform the system into a conservative, stabilizable system, and second, we use the corresponding conservative output to close the loop with our controller. This idea is used

to generate limit cycle oscillations both around the stable and the unstable position of the pendulum. As we have remarked in Section 5.2, generically the bifurcation is degenerate and Theorem 4.5 does not allow to draw conclusions about limit cycle oscillations. Nevertheless, simulation results show that, even in the degenerate bifurcation case, limit cycle oscillations with large basin of attraction are generated. The proof of this claim (Solution 3 in Section 5.2) is beyond the scope of this chapter and will be the subject of future work. As a second illustration, we present, in Section 5.4.4, our current research project in collaboration with the Laboratoire d'Automatique de Grenoble (France) involving the problem of balancing control of the bipedal robot RABBIT.

5.4.1 Typical example of underactuated mechanical system: the inverted pendulum on a cart

We consider the cart-pendulum system without friction. We derive a non-linear control law aimed at producing limit cycle oscillations around the origin of the cart axis. For the pendulum, two situations are considered: oscillations around the stable position of the pendulum and oscillations around its unstable position.

We denote by x the cart position, by $v = \dot{x}$ the cart velocity, by θ the angle between the vertical axis and the pendulum, by $\omega = \dot{\theta}$ the angular velocity of the pendulum, and by F the lateral force applied to the cart (see Figure 5.2). With these notations, the cart-pendulum equations of motion are

$$\begin{cases} J\dot{\omega} - mgl \sin \theta + ml\dot{v} \cos \theta & = 0 \\ M\dot{v} + ml\dot{\omega} \cos \theta - ml\omega^2 \sin \theta & = F \end{cases} \quad (5.14)$$

where $J = ml^2$ is the moment of inertia with respect to the pivot point, m the mass of the pendulum, m_c the mass of the cart and $M = m + m_c$. Equivalently we have

$$\begin{cases} J\dot{\omega} - mgl \sin \theta + ml\dot{v} \cos \theta & = 0 \\ \left(M - m(\cos \theta)^2 \right) \dot{v} - ml\omega^2 \sin \theta + mg \sin \theta \cos \theta & = F \end{cases}$$

The (nonsingular) feedback transformation

$$\left(M - m(\cos \theta)^2 \right) a - ml\omega^2 \sin \theta + mg \sin \theta \cos \theta = F$$

yields the simplified dynamics

$$\begin{cases} J\dot{\omega} - mgl \sin \theta + mla \cos \theta & = 0 \\ \dot{v} & = a \end{cases} \quad (5.15)$$

where the new input a directly controls the cart acceleration.

The open-loop structure of this system is

$$\begin{cases} \ddot{x} & = a \\ \dot{E}_{pendulum} & = ay_2 = a(-ml\omega \cos \theta) \end{cases}$$

where $E_{pendulum} = \frac{1}{2}J\omega^2 + mgl \cos \theta$ and $y_2 = -ml \sin \theta$.

5.4.2 Around the stable position of the pendulum

In order to generate limit cycle oscillations around the stable position of the pendulum, we first design a conservative output y that allows stabilization of the system by damping injection. We then use this output to generate oscillations in the whole system by closing the loop with $\phi_k(y) = -ky + y^3$.

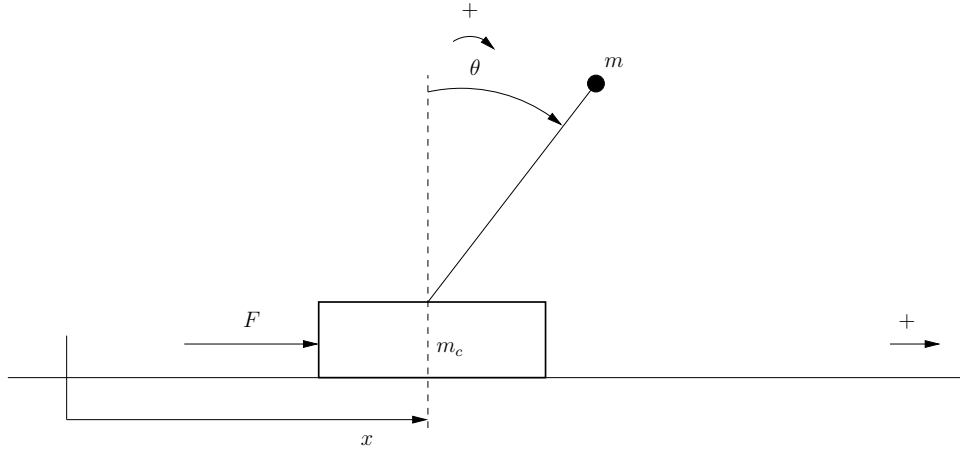


Figure 5.2: The cart-pendulum system

5.4.2.1 Design of a stabilizing output

The total energy of the system is given by

$$\tilde{E} = E_{pendulum} + \frac{1}{2}v^2,$$

whose derivative is

$$\dot{\tilde{E}} = a\dot{z}$$

where $z = x + y_2 = x - ml \sin \theta$.

In order to create a minimum at $(x, \dot{x}, \theta, \dot{\theta}) = (0, 0, \pi, 0)$, we perform (potential) energy shaping by considering the energy function

$$V = \tilde{E} + \frac{1}{2}K_p z^2, \quad K_p > 0$$

whose derivative is

$$\dot{V} = (a + K_p z)\dot{z}.$$

Taking the control input a to be $a = -K_p z + u$, we get

$$\dot{V} = uy$$

where $y = \dot{z}$ is the output with respect to which the system is conservative.

5.4.2.2 Stabilization of the system

The damping control $u = -K_d y$, asymptotically stabilizes the pendulum at its stable position and the cart at the origin. The corresponding acceleration control is given by

$$a = -K_p z - K_d y.$$

5.4.2.3 Creation of a limit cycle oscillation

After feedback transformation into a stabilizable, conservative system, we consider the poles/zeros configuration of the linearization around $(\theta, \dot{\theta}, x, \dot{x}) = (\pi, 0, 0, 0)$. This poles/zeros map is sketched on Figure 5.3. As can be seen the system already possesses a zero at the origin. The integral part of the controller is thus not necessary.

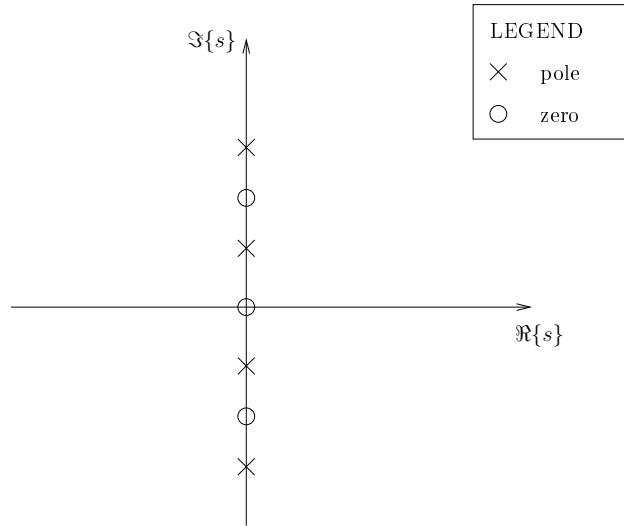


Figure 5.3: Poles/zeros configuration for the cart pendulum system after feedback transformation into a stabilizable and conservative system.

For $k \gtrsim 0$, the control law $u = ky - y^3$ is expected to produce a limit cycle oscillation around the stabilized position of Section 5.4.2.2. The corresponding acceleration control is given by

$$a = -K_p z + ky - y^3. \quad (5.16)$$

5.4.2.4 Simulation results

In this section, we present the simulation results obtained with the control law (5.16) for different values of the control parameter k . The physical parameters of the system have been chosen in order to correspond to reality: $m = 0.14$ kg, $m_c = 0.44$ kg, $g = 9.81$ m/s², $l = 0.215$ m. The control parameter K_p was chosen equal to 10. The initial condition was (arbitrarily) chosen as $x(0) = 1$, $\dot{x}(0) = 0.3$, $\theta(0) = \pi + 0.2$, and $\dot{\theta}(0) = 0.1$. We then have considered three values of the parameter k , respectively $k = -1$, $k = 1$, and $k = 2$.

In Figure 5.4, we clearly see that the origin of the system is asymptotically stable for $k = -1$, and unstable for $k = 1$ and $k = 2$. Moreover, as expected, a limit cycle whose radius depends on k appears for $k > 0$. The same steady state responses were obtained when other initial conditions were used.

5.4.3 Around the unstable position of the pendulum

Similarly to the idea presented in Section 5.4.2, we first design a conservative output y that allows stabilization of the system with pendulum in inverted position and cart at the origin. As we did

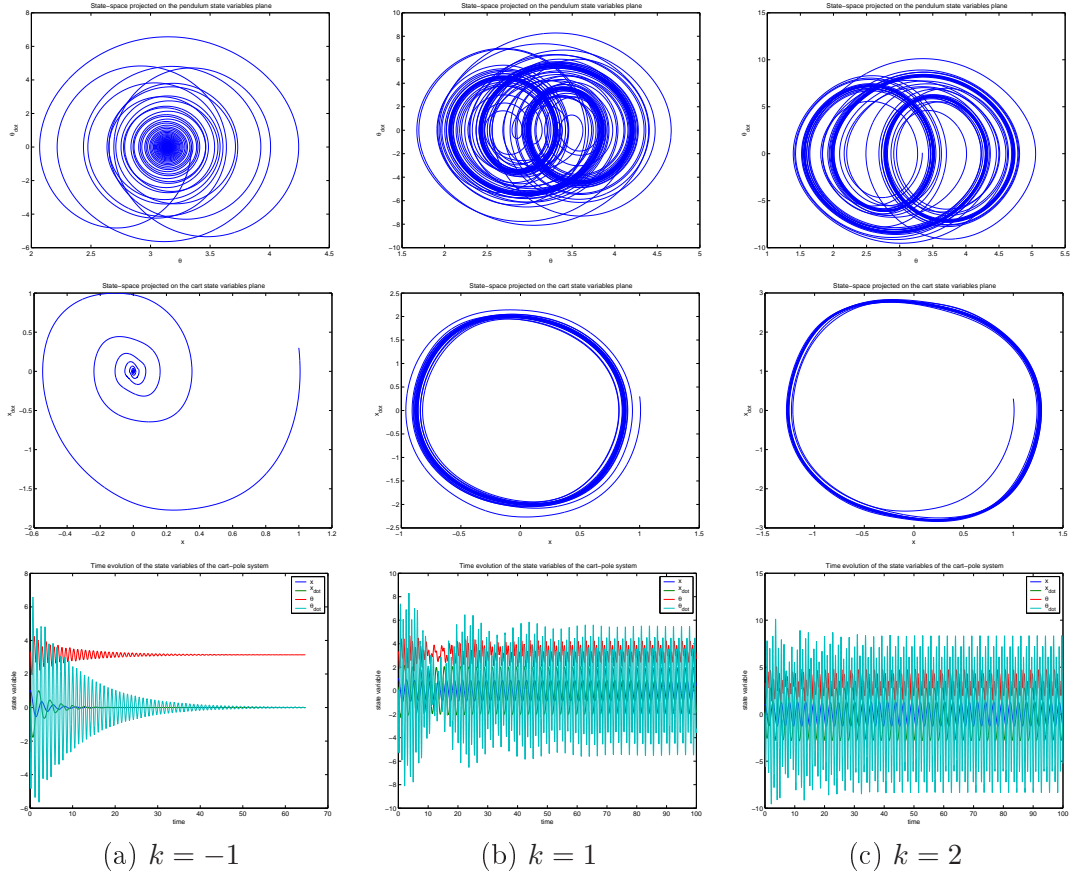


Figure 5.4: Cart-pendulum system: creation of oscillations around the stable position of the pendulum. Column (a) $k = -1$, Column (b) $k = 1$, Column (c) $k = 2$. The first line represents the projection of the state space on the pendulum state variables plane. The second line represents the projection on the cart state variables plane. The third line represents the temporal evolution of the state variables.

in section 5.4.2, we then use this output to generate oscillations in the whole system by closing the loop with $\phi_k(y) = -ky + y^3$. The stabilization part is directly inspired by literature results (see [BLM01, BCLM01, BOvdS02]).

5.4.3.1 Design of a stabilizing output

In the first step, the kinetic energy of the pendulum is shaped by $\frac{1}{2}k_p\dot{y}_2^2$ ($k_p < 0$). In the second step, overall energy shaping is achieved.

- Step 1

We use the feedback $a = -k_p\dot{y}_2 + w$ to obtain

$$\begin{cases} \ddot{z} & = w \\ \dot{\tilde{E}}_{pendulum} & = w\dot{y}_2 \end{cases}$$

with $z = x + k_p y_2$, and $\tilde{E}_{pendulum} = E_{pendulum} + \frac{1}{2}k_p \dot{y}_2^2$. This leads to $\tilde{E}_{pendulum} = \frac{1}{2}J\dot{\theta}^2 + m \cos \theta \left(gl + \frac{1}{2}Jk_p \dot{\theta}^2 \cos \theta \right)$.

- Step 2

We perform overall energy shaping by considering the energy function

$$V = \tilde{E}_{pendulum} + \frac{1}{2}\dot{z}^2 + \frac{1}{2}K_p (z + y_2)^2,$$

whose derivative is

$$\dot{V} = (\dot{z} + \dot{y}_2) (w + K_p (z + y_2)).$$

Taking the control input w to be $w = u - K_p (z + y_2)$, we get

$$\dot{V} = uy,$$

where $y = \dot{z} + \dot{y}_2$ is the output with respect to which the system is conservative.

5.4.3.2 Stabilization of the system

The damping control $u = -K_d y$ stabilizes the pendulum in the inverted position and the cart at the origin (see [BLM01]). The corresponding acceleration control is given by

$$a = -k_p \ddot{y}_2 - K_p (z + y_2) - K_d y.$$

Taking into account the definitions of y_2 and z , and the dynamics (5.15) for the elimination of \ddot{y}_2 from the equation, we obtain

$$a = \frac{k_p mg \sin \theta \cos \theta - k_p ml \dot{\theta}^2 \sin \theta - K_p (x - (k_p + 1) ml \sin \theta) - K_d (\dot{x} - (k_p + 1) ml \dot{\theta} \cos \theta)}{1 + k_p m (\cos \theta)^2}.$$

5.4.3.3 Creation of a limit cycle oscillation

After feedback transformation into a stabilizable, conservative system, the poles/zeros configuration of the linearization around $(\theta, \dot{\theta}, x, \dot{x}) = (0, 0, 0, 0)$ is similar to that sketched in Figure 5.3. The system being conservative w.r.t. the output y , the control law $u = ky - y^3$ is expected to produce a limit cycle oscillation around the stabilized position of Section 5.4.3.2 for $k \gtrsim 0$. The corresponding acceleration control is given by

$$a = -k_p \ddot{y}_2 - K_p (z + y_2) + ky - y^3.$$

Taking into account the definitions of y_2 and z , and the dynamics (5.15) for the elimination of \ddot{y}_2 from the equation, we obtain

$$a = \frac{k_p mg \sin \theta \cos \theta - k_p ml \dot{\theta}^2 \sin \theta - K_p (x - (k_p + 1) ml \sin \theta) + k (\dot{x} - (k_p + 1) ml \dot{\theta} \cos \theta) - (\dot{x} - (k_p + 1) ml \dot{\theta} \cos \theta)^3}{1 + k_p m (\cos \theta)^2}. \quad (5.17)$$

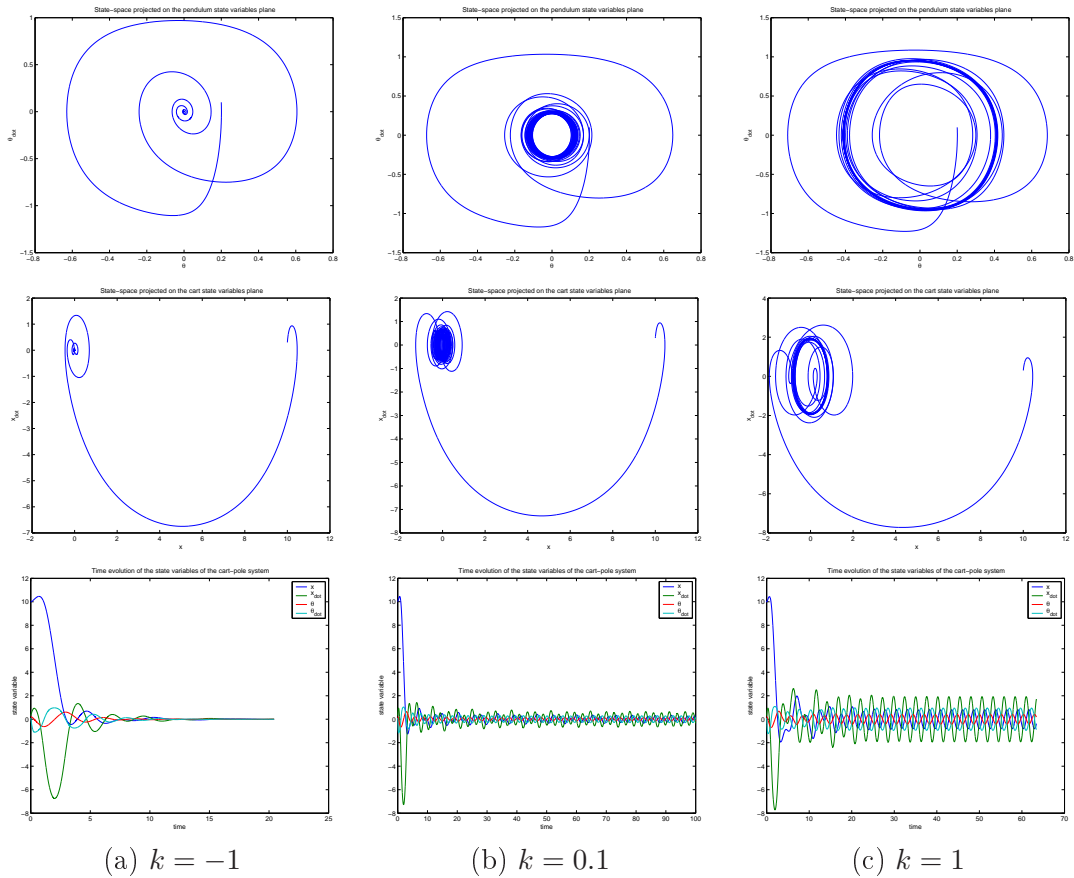


Figure 5.5: Cart-pendulum system: creation of oscillations around the unstable position of the pendulum. Column (a) $k = -1$, Column (b) $k = 0.1$, Column (c) $k = 1$. The first line represents the projection of the state space on the pendulum state variables plane. The second line represents the projection on the cart state variables plane. The third line represents the temporal evolution of the state variables.

5.4.3.4 Simulation results

In this section, we present the simulations results obtained with the control law (5.17) for different values of the control parameter k . The values of physical parameters are the same as in Section 5.4.2.4. The value of the control parameters k_p and K_p are chosen equal to -80 and 2 respectively (see [BLM01]). The initial conditions are $x(0) = 10$, $\dot{x}(0) = 0.3$, $\theta(0) = 0.2$, and $\dot{\theta}(0) = 0.1$. Note the large initial deviation of position of the cart with respect to the origin. Once again we have considered three values of the parameter k , respectively $k = -1$, $k = 0.1$, and $k = 1$.

In Figure 5.4, we clearly see that the origin of the system is asymptotically stable for $k = -1$, and unstable for $k = 0.1$ and $k = 1$. Moreover, as expected, a limit cycle whose radius depends on k appears for $k > 0$. Using different initial conditions, we have obtained the same steady state responses, which tends to confirm that the created limit cycle has a large basin of attraction.

As a second illustration of the application of our controller to the generation of stable limit cycle oscillations in mechanical systems, we present, in the next section, our current research project in

collaboration with the Laboratoire d'Automatique de Grenoble (France).

5.4.4 Balancing control of RABBIT

RABBIT is a bipedal robot specifically designed to advance the fundamental understanding of controlled legged locomotion (see [CAA⁺03] for an excellent introduction to the RABBIT project). A picture of RABBIT is displayed in Figure 5.6. A canonical problem in bipedal robots is the design of a controller that generates closed-loop motions such as walking, running, or balancing, that are periodic and stable (i.e. limit cycles).



Figure 5.6: The bipedal robot RABBIT

During a balancing motion, RABBIT is modeled as a three link inverted pendulum (see Figure 5.7): the stance leg is supposed to be rigidified in such a way that the tibia, femur and torso are aligned while the balancing leg is actuated at the hip and knee. The goal is to find a feedback control law that induces a non-trivial, limit cycle in the three-link inverted pendulum. As emphasized in [CAA⁺03]: “what makes this control problem quite different from walking is that ground impacts are not considered in balancing. At first glance, this may seem to simplify the problem, but, upon further reflection, this is not the case. The difficulty lies in the fact that the class of stable, periodic motions that can be achieved by balancing seems to be much smaller than what can be achieved through allowing impacts.” A solution to the balancing problem has been recently proposed in [CEU02, SC04]. This solution is based on the concepts of zero dynamics shaping and virtual constraints. It allows to generate locally stable periodic orbits for the balancing motions of the three-link pendulum model of RABBIT.

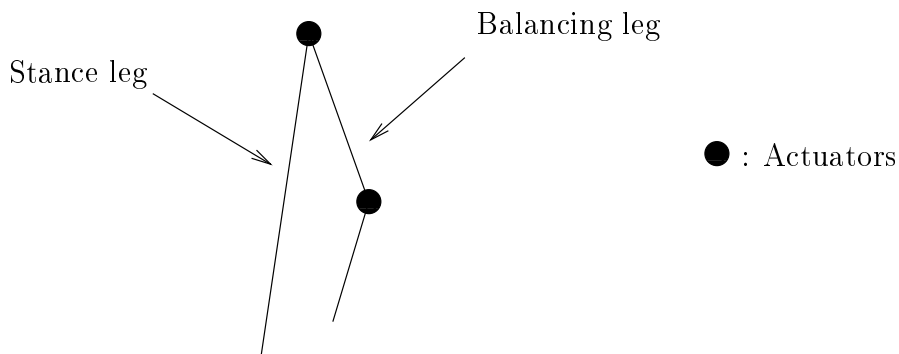


Figure 5.7: Modelization of RABBIT as a three-link inverted pendulum.

In ongoing research, we envision to apply our nonlinear PI controller to generate stable balancing motions for RABBIT. The aim is to illustrate our theory and to show that our PI controller provides a

simple and robust method to generate limit cycle oscillations in such a complex system as RABBIT. To support this idea, we consider some analogies with the problem of generating limit cycle oscillations in the cart-pendulum system. The modelization of RABBIT as a three-link inverted pendulum indicates several similarities with this system. First, it constitutes an underactuated system with one degree of underactuation. Second, if we consider small deviation of the stance leg (corresponding to the free link of the three-link pendulum) w.r.t. the vertical axis, the movement of the hip is almost horizontal and may be assimilated to the translational degree of freedom of the cart. Preliminary works show that the dynamics of the three link inverted pendulum for small deviation around the inverted vertical position (free link in inverted position and actuated links hanging in stable position) is very similar to that of the cart-pendulum except for some additional centrifugal terms in the (free) pendulum dynamics. Based on these analogies, application of our controller to the three-link pendulum is expected to allow for the development of a simple and robust control law for the balancing control of RABBIT.

5.5 Summary

In this chapter we adopted a synthesis point of view for the generation of stable limit cycle oscillations in stabilizable systems. Based on the theory developed in the previous chapters, we presented a proportional-integral feedback controller to answer the synthesis question and briefly compared it with other solutions proposed in the literature. Under some technical assumptions presented in the previous chapters, we showed that this controller is useful to generate oscillations in stabilizable systems. The main advantage of this controller is that it relies on existing stabilization theory for equilibrium points: once a stabilizing, passive output has been designed for the system, it is used to close the loop with the controller in order to generate limit cycle oscillations with large basins of attraction. The design of a stabilizing, passive output is a central topic in nonlinear control theory and many methods already exist to solve this problem (feedback passivation designs, controlled Hamiltonian and Lagrangian theory, energy shaping methods, etc.). However, the use of the proposed controller does not allow to directly draw conclusions from the theorems presented in the previous chapter. The main reason is the difficulty of verifying the absolute stability assumption at criticality. To guarantee that this assumption is satisfied, we have considered the class of stabilizable, conservative systems for which it generically holds. Unfortunately, we have shown that the corresponding bifurcation is generically degenerate. To regularize the degenerate bifurcation we have proposed a method based on the feedback injection of specific damping into the system. This solution has been shown to be applicable only to fully actuated two degrees of freedom mechanical systems. Even in the case when the degenerate bifurcation is not regularized, the proposed controller is expected to yield stable limit cycle oscillations thus providing a simple method to force oscillations by feedback. As an illustration of the proposed synthesis method to underactuated mechanical systems, we have shown simulation results for the cart-pendulum. In future work, we plan to extend our theorems to include degenerate bifurcations and apply this controller to the balancing control of the bipedal robot RABBIT.

Chapter 6

Conclusion and future work

6.1 Summary

The central theme of this thesis is the *global analysis and synthesis* of oscillators. Our aim has been to develop a global analysis method for oscillators which is independent of their dimension and provides an interconnection theory. The proposed approach was to consider a dissipativity characterization of oscillators which fits their description by physical state space models and, at the same time, has implications for their *global* stability analysis. This theory includes two global oscillation mechanisms which are illustrated in their simplest way in the celebrated low dimensional models of VAN DER POL and FITZHUGH-NAGUMO. A first main contribution has been the extension of these global oscillation mechanisms to high-dimensional systems composed of a strongly passive system in feedback with a slope parametrized, static nonlinearity. Under some technical assumptions, we showed that, generically, this feedback interconnection undergoes either a supercritical HOPF, or a supercritical pitchfork bifurcation. The global oscillation results either directly from the supercritical HOPF bifurcation or from the addition of a slow adaptation dynamic to the globally bistable system created by the supercritical pitchfork bifurcation.

As a second contribution, we have shown that the results obtained for an isolated passive oscillator extend to passive interconnections of passive oscillators. Moreover, we showed that global synchronization is implied by an incremental dissipativity characterization of the network that we named *incremental passivity*. We also provided sufficient conditions under which passive oscillators are incrementally passive and derived sufficient network topology conditions for the existence of globally asymptotically stable synchronic oscillations in networks of identical passive oscillators. This global synchronization result concerns network topologies that include S_N symmetry (all-to-all topology), D_N symmetry (bidirectional ring topology), Z_N symmetry (unidirectional ring topology) and open chain symmetry. We compared our synchronization result with other recent results on global synchronization and showed that generically passive oscillators satisfy the required conditions.

Finally, based on these analysis results, we presented a proportional-integral feedback controller to answer the limit cycle synthesis question and briefly compared it with other solutions proposed in the literature. The main advantage of the proposed controller is that it relies on existing stabilization theory for equilibrium points: once a stabilizing, passive output has been designed for the system, it can be used to close the loop with the controller in order to generate limit cycle oscillations with large basins of attraction. The design of a stabilizing, passive output is a central topic in nonlinear control theory and many methods already exist to solve this problem (feedback passivation designs,

controlled Hamiltonian and Lagrangian theory, energy shaping methods, etc.). As an illustration of the application of this controller to underactuated mechanical systems, we showed simulation results for the cart-pendulum for which limit cycle oscillations with large basins of attraction were successfully generated.

6.2 Future work

In future work, we plan to investigate the following open questions:

- Extension of the numerical method proposed in Section 3.6 to piecewise linear passive oscillators of order greater than two.
This extension would lead to a global numerical analysis method for piecewise linear approximations of passive oscillators. Such a method would be very interesting for testing numerically the existence and global stability of the limit cycle for a particular value of the bifurcation parameter.
- Generalization of our theorems to the degenerate bifurcation situation when more than two eigenvalues cross the imaginary axis simultaneously at criticality.
This generalization would yield analytical results proving that, even if the bifurcation is degenerate, a globally asymptotically stable limit cycle is created. This result is particularly important for the synthesis of global oscillations in conservative systems.
- Application and experimental validation of our limit cycle oscillations synthesis method to underactuated mechanical systems including the pendubot, the acrobot, and the balancing control of the bipedal robot RABBIT.
- Extension of the synchronization results to networks of non identical passive oscillators.
- Analysis of other feedback oscillation mechanisms through an input-output approach.
The feedback mechanisms presented in this thesis were based on bifurcations caused by an inversion of the feedback static gain. Other feedback mechanisms based on bifurcations caused by inversion of the phase are common in biochemistry. This phase inversion is generally due to the presence of a delay in the feedback loop. The use of an input-output approach to perform analysis of delay feedback systems yielding globally stable limit cycle oscillations constitutes an important open question that is currently investigated.

Appendix A

Complement to Chapter 4

A.1 Real positive definite matrices

In this section we give the definition of real positive definite matrices. This definition does not implicitly assume, as is often the case in the literature, that the matrix is symmetric. This distinction is important in the context of interconnection of passive oscillators since it allows for non symmetric network topologies to be considered.

Definition A.1 *A real matrix A is positive definite iff $x^T A x > 0, \forall x \in \mathbb{R}^n \setminus \{0\}$.*

For positive semi-definite matrices, the same definition holds except that the inequality is non-strict. Note that these definitions of positive (semi) definite matrices hold for non-symmetric matrices. In fact, since any matrix A may be written under the form $A_s + A_a$ where $A_s = \frac{1}{2}(A + A^T)$ is the symmetric part of A and $A_a = \frac{1}{2}(A - A^T)$ is the anti-symmetric part of A , we immediately see that $x^T A x = x^T A_s x$, for all $x \in \mathbb{R}$ if A is real. Thus a real matrix is positive (semi) definite if and only if its symmetric part is positive (semi) definite.

For a symmetric positive definite matrix the eigenvalues are positive. The corresponding property for non symmetric positive definite matrix is given in Theorem A.2.

Theorem A.2 *The eigenvalues of a real positive definite matrix have positive real parts.*

Proof

If $\lambda = (\lambda_R + i\lambda_I) \in \mathbb{C}$ is an eigenvalue of A , then, by definition,

$$\lambda v = Av, v \in \mathbb{C}^n, \tag{A.1}$$

where $v = v_R + iv_I$ denotes the corresponding eigenvector.

From equation (A.1), we get the system of equations

$$\begin{cases} \lambda_R v_R - \lambda_I v_I &= Av_R \\ \lambda_I v_R + \lambda_R v_I &= Av_I \end{cases} \tag{A.2}$$

Since A is positive definite, we have

$$\begin{cases} v_R^T A v_R > 0 \\ v_I^T A v_I > 0 \end{cases} \quad (\text{A.3})$$

Injecting the equations appearing in (A.2) into (A.3), we obtain

$$\begin{cases} |v_R|^2 \lambda_R - \lambda_I v_R^T v_I > 0 \\ |v_I|^2 \lambda_R + \lambda_I v_I^T v_R > 0 \end{cases} \quad (\text{A.4})$$

Summing these two inequalities, we get the following condition which has to be respected for any eigenvalue λ

$$\lambda_R |v|^2 > 0.$$

This condition implies $\lambda_R > 0$. ■

A.2 Synchronization topologies

The synchronic oscillation result of Theorem 4.15 requires some particular assumptions on the interconnection matrix Γ . These assumptions are

- $\Gamma \in \mathbb{R}^{N \times N}$ is positive semidefinite, i.e. $Y^T \Gamma Y \geq 0$, $\forall y \in \mathbb{R}^N$;
- $\ker(\Gamma) = \ker(\Gamma^T) = \text{range}(\mathbf{1})$.

Note that these assumptions do not require the interconnection matrix Γ to be symmetric.

We will concentrate on the $\ker(\Gamma) = \ker(\Gamma^T)$ assumption. This assumption is essential for proving that $Y_{\ker^\perp}^T \Gamma Y_{\ker^\perp} > \lambda_{\min \neq 0}(\Gamma_s) |Y_{\ker^\perp}|^2$ for any Y_{\ker^\perp} belonging to the orthogonal complement of $\ker(\Gamma)$, i.e. for any $Y_{\ker^\perp} \in (\ker(\Gamma))^\perp = \{Y \in \mathbb{R}^N : Y^T Z = 0, \forall Z \in \ker(\Gamma)\}$. First of all, we note some propositions concerning the implications of this assumption.

Proposition A.3 *If $\ker(\Gamma) = \ker(\Gamma^T)$, then $Y \in \ker(\Gamma) \Rightarrow Y \in \ker(\Gamma_s)$.*

Proof

Obvious. ■

This property is important for the Z_N symmetry case.

Proposition A.4 *If $\ker(\Gamma) = \ker(\Gamma^T)$ and $Y = Y_{\ker} + Y_{\ker^\perp}$ where $Y_{\ker} \in \ker(\Gamma)$ and $Y_{\ker^\perp} \in (\ker(\Gamma))^\perp$, then $Y^T \Gamma Y = Y_{\ker^\perp}^T \Gamma_s Y_{\ker^\perp}$.*

Proof

Obvious from proposition A.3. ■

We are now ready to prove the main result. This result is summarized in Proposition A.5.

Proposition A.5 *If Γ is a real, positive semidefinite matrix such that $\ker(\Gamma) = \ker(\Gamma^T) = \text{range}(\mathbf{1})$ and $Y = Y_{\ker} + Y_{\ker^\perp}$ where $Y_{\ker} \in \ker(\Gamma)$ and $Y_{\ker^\perp} \in (\ker(\Gamma))^\perp$, then $Y_{\ker^\perp}^T \Gamma Y_{\ker^\perp} \geq \lambda_{\min \neq 0}(\Gamma_s) |Y_{\ker^\perp}|^2$ where $\lambda_{\min \neq 0}(\Gamma_s)$ denotes the smallest nonzero eigenvalue of (Γ_s) .*

Proof

$Y_{\ker^\perp}^T \Gamma Y_{\ker^\perp} = Y_{\ker^\perp}^T \Gamma_s Y_{\ker^\perp}$ where $\Gamma_s = \frac{1}{2}(\Gamma + \Gamma^T)$. Since Γ_s is symmetric, there always exists an orthogonal matrix L that diagonalizes Γ_s , i.e. $L\Gamma_s L^T = \Lambda$ where $\Lambda = \text{diag}(0, \lambda_2, \dots, \lambda_N)$ with $0 < \lambda_2 \leq \dots \leq \lambda_N$. We thus have

$$\begin{aligned} Y_{\ker^\perp}^T \Gamma_s Y_{\ker^\perp} &= Y_{\ker^\perp}^T L^T \Lambda L Y_{\ker^\perp} \\ &= \lambda_2 z_2^2 + \dots + \lambda_N z_N^2 \\ &\geq \lambda_2 (z_2^2 + \dots + z_N^2) \\ &= \lambda_2 |LY_{\ker^\perp}|^2 \\ &= \lambda_2 |Y_{\ker^\perp}|^2, \end{aligned}$$

where $z_i, i = 1, \dots, N$ denotes the i^{th} component of LY_{\ker^\perp} . The third equality comes from $z_1 = 0$ which results from the definition of Y_{\ker^\perp} . \blacksquare

Finally, we give two propositions allowing to compare $\ker(\Gamma)$ and $\ker(\Gamma \otimes I_n)$.

Proposition A.6 *If $w \in \ker(\Gamma)$, then $(I_N \otimes B)w \in \ker(\Gamma \otimes I_n), \forall B \in \mathbb{R}^{n \times 1}$.*

Proof

$$(\Gamma \otimes I_n)(I_N \otimes B)w = (I_N \otimes B)\Gamma w = 0, \forall w \in \ker(\Gamma). \quad \blacksquare$$

This proposition directly implies that $Y_{\ker^\perp} = (I_N \otimes C)X_{\ker^\perp} \in (\ker(\Gamma))^\perp, \forall X_{\ker^\perp} \in (\ker(\Gamma \otimes I_n))^\perp$ since $\forall w \in \ker(\Gamma)$ we have $(Y_{\ker^\perp})^T w = (X_{\ker^\perp})^T (I_N \otimes C^T)w = 0$.

Proposition A.7 *If $X \in \ker(\Gamma \otimes I_n)$, then $(I_N \otimes C)X \in \ker(\Gamma), \forall C \in \mathbb{R}^{1 \times n}$.*

Proof

$$\Gamma(I_N \otimes C)X = (I_N \otimes C)(\Gamma \otimes I_n)X = 0, \forall X \in \ker(\Gamma \otimes I_n). \quad \blacksquare$$

This proposition directly implies that $Y_{\ker} = (I_N \otimes C)X_{\ker} \in (\ker(\Gamma)), \forall X \in (\ker(\Gamma \otimes I_n))$.

A.3 Invariance of the kernel dynamics

In this section, we prove invariance of the kernel dynamics corresponding to equation (4.19).

Let X_{\ker} belong to the kernel of $\Gamma \otimes I_n$. According to (4.19), X_{\ker} satisfies the dynamics

$$\begin{cases} \dot{X}_{\ker} &= (I_N \otimes A)X_{\ker} - (I_N \otimes B)\Phi_k(Y_{\ker}) + (I_N \otimes B)U \\ Y_{\ker} &= (I_N \otimes C)X_{\ker} \end{cases} \quad (\text{A.5})$$

Assume linear coupling, i.e. $U = -\Gamma Y_{\ker}$. Since, by definition, $(\Gamma \otimes I_n)X_{\ker} = 0$, we obtain $U = -\Gamma(I_N \otimes C)X_{\ker} = -(I_N \otimes C)(\Gamma \otimes I_n)X_{\ker} = 0$. It is now easy to see that the kernel dynamics (A.5) are invariant since

$$(\Gamma \otimes I_n)\dot{X}_{\ker} = (I_N \otimes A)(\Gamma \otimes I_n)X_{\ker} - (I_N \otimes B)\Gamma\Phi_k(Y_{\ker}) = 0,$$

for any $X_{\ker} \in \ker(\Gamma \otimes I_n)$.

A.4 Implication of observability for linear systems

Proposition A.8 *For linear systems satisfying the state-space model*

$$\begin{cases} \dot{x} &= Ax + Bu \\ y &= Cx \end{cases} \quad (\text{A.6})$$

observability of the pair (A, C) implies $\exists \beta_1 > 0, \beta_2 > 0$ such that $\forall \bar{t} > 0$

$$\beta_1 |x_0|^2 \leq \int_0^{\bar{t}} |\tilde{y}(\tau)|^2 d\tau \leq \beta_2 |x_0|^2.$$

Proof

Observability of the pair (A, C) implies

$$\forall \bar{t}, \quad W_o(0, \bar{t}) = \int_0^{\bar{t}} (e^{A\tau})^T C^T C e^{A\tau} d\tau > 0,$$

where $W_o(0, \bar{t})$ denotes the observability Grammian (see [AM97, p. 253]). Thus, for an observable linear time-invariant system, $W_o(0, \bar{t})$ is a symmetric positive definite matrix, for any $\bar{t} > 0$. This means that for any $\bar{t} > 0$, there exists $\beta_1 > 0$ and $\beta_2 > 0$ such that

$$\beta_1 I \leq W_o(0, \bar{t}) \leq \beta_2 I \quad (\text{A.7})$$

The output of the linear system is given by

$$y(t) = C e^{At} x_0 + \int_0^t C e^{A(t-\tau)} B u(\tau) d\tau$$

where $x_0 = x(0)$. Consider the “input-free” output $\tilde{y}(t) = y(t) - \int_0^t C e^{A(t-\tau)} B u(\tau) d\tau = C e^{At} x_0$. This yields $x_0^T W_o(0, \bar{t}) x_0 = \int_0^{\bar{t}} x_0^T e^{A^T \tau} C^T C e^{A\tau} x_0 d\tau = \int_0^{\bar{t}} |\tilde{y}(\tau)|^2 d\tau$. Now, the condition (A.7) equivalently writes

$$\beta_1 |x_0|^2 \leq \int_0^{\bar{t}} |\tilde{y}(\tau)|^2 d\tau \leq \beta_2 |x_0|^2 \quad (\text{A.8})$$

for any $\bar{t} > 0$. In particular, for an unforced linear time-invariant system ($u \equiv 0$), we have $\tilde{y}(t) = y(t)$ and inequalities (A.8) express bounds on the output energy as functions of the initial condition energy.

■

Appendix B

Degenerate bifurcation in linear, conservative and detectable systems

In this appendix, we characterize the complex plane position of poles and zeros for a linear conservative system. Furthermore, we show that, the feedback interconnection of a conservative system with a proportional gain is such that generically, all the poles cross the imaginary axis simultaneously. This shows that the bifurcation is generically degenerate for conservative systems.

B.1 Poles/zeros map of linear conservative systems

In this section we consider the feedback interconnection of Figure 5.1 where the forward block, denoted by Σ , is linear, strongly conservative, and detectable. We denote by Ξ , the feedback interconnection of Σ with the integral part of the controller. Being the feedback interconnection of two conservative systems, Ξ is conservative w.r.t. its input w and its output y . It is also easy to prove that Ξ is detectable.

We now show that the critical bifurcation value of the feedback system is $k^* = 0$ and that generically a degenerate bifurcation appears at $k^* = 0$.

The dynamics of the linear system Ξ are given by

$$\begin{aligned}\dot{z} &= Az + Bw \\ y &= Cz\end{aligned}\tag{B.1}$$

From the assumption that Ξ is a conservative system, there exists a matrix $P = P^T > 0$ such that the HILL-MOYLAN conditions

$$A^T P + PA = 0\tag{B.2}$$

$$C = B^T P\tag{B.3}$$

are satisfied. From the first HILL-MOYLAN condition (B.2), we may deduce that all the eigenvalues of A lie on the imaginary axis.

Proposition B.1 *The poles of a linear, conservative system are all located on the imaginary axis.*

Proof

Let e be an eigenvector of A and λ the corresponding eigenvalue i.e. $Ae = \lambda e$ with $\lambda = \sigma + j\omega$. We have thus $e^*(A^*P + PA)e = \bar{\lambda}e^*Pe + \lambda e^*Pe = 2\sigma e^*Pe$ where $*$ denotes the conjugate transpose operator and $\bar{\lambda}$ the conjugate of λ . Since A is a real matrix we have $A^* = A^T$. This proves that $\sigma = 0$ since $P = P^T > 0$. Thus every eigenvalue of A has a zero real part. ■

Moreover, Ξ being a conservative system we know that it is weakly minimum phase (see Section 2.1.7). Thus the zeros of Ξ are located in the closed left-half complex plane. In fact all zeros of Ξ lie on the imaginary axis. We prove this statement hereafter.

Proposition B.2 *The zeros of a linear, conservative system are all located on the imaginary axis.*

Proof

From the second HILL-MOYLAN condition (B.3) it follows that the matrix $CB = B^T P B$ is positive definite; hence system (B.1) has relative degree one. A linear change of coordinates

$$\begin{pmatrix} \xi_0 \\ Y \end{pmatrix} = \begin{pmatrix} T \\ C \end{pmatrix} z$$

exists such that $TB = 0$. In these coordinates, system (B.1) is expressed in normal form:

$$\begin{aligned} \dot{\xi}_0 &= Q_{11}\xi_0 + Q_{12}y \\ \dot{y} &= Q_{21}\xi_0 + Q_{22}y + CBw \end{aligned}$$

The system Ξ expressed in the new coordinates (ξ_0, y) is still conservative since passivity is a coordinate independent property. The zero dynamics are $\dot{\xi}_0 = Q_{11}\xi_0$. Partitioning the corresponding passivity matrix $\tilde{P} = \tilde{P}^T > 0$ according to the state partition (ξ_0, y) the second HILL-MOYLAN condition $\begin{pmatrix} 0^T & (CB)^T \end{pmatrix} \tilde{P} = \begin{pmatrix} 0^T & 1 \end{pmatrix}$ yields

$$\begin{aligned} \tilde{P}_{12} = \tilde{P}_{21}^T &= 0 \\ \tilde{P}_{22} &= (CB)^{-T} \end{aligned}$$

whereas the first HILL-MOYLAN condition $\tilde{P} \begin{pmatrix} Q_{11} & Q_{12} \\ Q_{21} & Q_{22} \end{pmatrix} + \begin{pmatrix} Q_{11}^T & Q_{21}^T \\ Q_{12}^T & Q_{22}^T \end{pmatrix} \tilde{P} = 0$ reduces to

$$\tilde{P}_{11}Q_{11} + Q_{11}^T\tilde{P}_{11} = 0, \quad \tilde{P}_{11} = \tilde{P}_{11}^T > 0.$$

This equality shows that all eigenvalues of Q_{11} are located on the imaginary axis. ■

We thus have proved that the (MIMO) transfer function of a linear conservative system has all its zeros and poles on the imaginary axis.

Remark B.3 *The poles/zeros position of a linear, conservative, and detectable system may be further characterized: poles and zeros alternate on the imaginary axis. This is proved hereafter.*

B.2. DEGENERATE BIFURCATION

Denote by Ξ_k the (positive) feedback interconnection of Ξ with the static gain k . Being the feedback interconnection of a conservative, and detectable system (Ξ) with a static, strictly input passive system ($w = -ky$), Ξ_k must be asymptotically stable for $k < 0$ since it is output strictly passive and detectable (Lemma 2.14). Analyzing the poles/zeros configuration leading to an asymptotically stable system for negative values of k , a root locus argument shows, that the only possibility is to have a simple alternance of zeros and poles on the imaginary axis. To illustrate this, consider the three following systems

$$\begin{aligned}\Xi_a &= \frac{s(s^2 + 4)}{(s^2 + 1)(s^2 + 9)} \\ \Xi_b &= \frac{s(s^2 + 1)}{(s^2 + 4)(s^2 + 9)} \\ \Xi_c &= \frac{s(s^2 + 9)}{(s^2 + 1)(s^2 + 4)}\end{aligned}$$

The corresponding root loci of their (positive) feedback interconnection with the static gain k , i.e. Ξ_{i_k} , $i = a, b, c$, are represented on Figure B.1. On this Figure we clearly see, that only Ξ_{a_k} is asymptotically stable for any negative value of k .

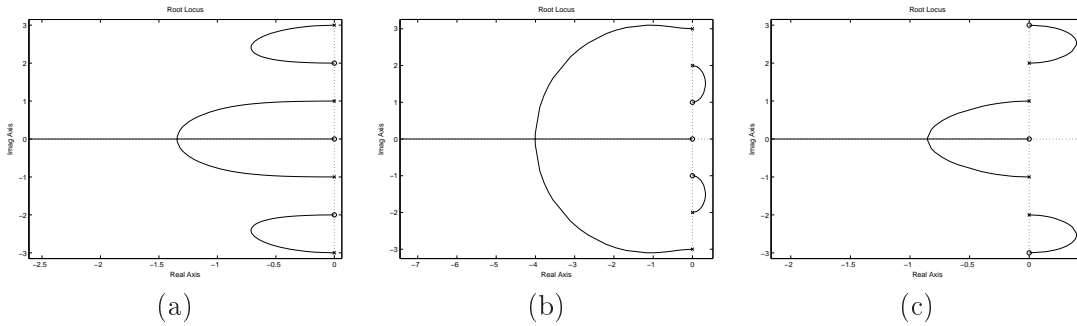


Figure B.1: Root locus. (a) Ξ_{a_k} , (b) Ξ_{b_k} , (c) Ξ_{c_k} . Legend: \times represent a pole, \circ represents a zero. The solid curves represents the root locus.

B.2 Degenerate bifurcation

Now that we know the normal position of the zeros and poles of a conservative system in the complex plane, we perform the bifurcation analysis for Ξ_k . We show that generically the bifurcation at $k = 0$ is degenerate, i.e. all eigenvalues cross the imaginary axis simultaneously at $k = 0$.

Proposition B.4 *The positive feedback interconnection of a linear, conservative, and detectable system Ξ with the proportional gain k is characterized by a degenerate bifurcation at $k = 0$.*

Proof

Consider two systems. The original system Ξ

$$\begin{aligned}\dot{z} &= Az + Bw \\ y &= Cz\end{aligned}$$

and its anti-stable counterpart $\tilde{\Xi}$ whose dynamics are given by

$$\begin{aligned}\dot{z} &= -Az + Bv \\ y &= Cz\end{aligned}$$

Both Ξ and $\tilde{\Xi}$ are conservative since they satisfy the HILL-MOYLAN conditions (B.2)-(B.3) for the same matrix $P = P^T > 0$. For $k < 0$, Ξ_k and $\tilde{\Xi}_k$ are output strictly passive and detectable. From Lemma 2.14, they are both asymptotically stable for $k < 0$. This means that the matrices $A+kBB^T P$ and $-A+kBB^T P$ are both HURWITZ for $k < 0$, or that $A-kBB^T P$ is anti-HURWITZ and $A+kBB^T P$ is HURWITZ for $k < 0$. Thus, we have proved that a *degenerate* bifurcation appears at $k^* = 0$ since all the eigenvalues cross the imaginary axis simultaneously at $k = 0$. ■

Appendix C

Application of MEES results to our class of systems

The approach we present in Chapter 3 is related to the work of MEES [MC79, Mee81]. In his work MEES presents a “frequency-domain” HOPF bifurcation theorem and graphical conditions corresponding to rigorous versions of the describing functions method to conclude about local stability of limit cycles in feedback loops. In this appendix, we recall the graphical interpretation of the HOPF bifurcation theorem given by MEES and use it to prove that if a HOPF bifurcation occurs in systems satisfying the assumptions of Theorem 3.8 then this bifurcation is supercritical and leads to a locally asymptotically stable limit cycle.

C.1 The frequency domain HOPF bifurcation theorem

The results of MEES are an extension of ALLWRIGHT’s proof of the HOPF bifurcation theorem [All77] which is based on an application of the method of harmonic balance. This approach provides a describing function-like graphical interpretation of the HOPF bifurcation theorem. This graphical interpretation is based on the characteristic locus idea¹. For a system parametrized by a real number μ , the graphical HOPF theorem shows how harmonic balance with harmonics zero to two is enough to determine whether the system undergoes a HOPF bifurcation, and to say whether the limit cycle is stable or unstable. It shows how to construct estimates of the frequency and amplitude of the limit cycle, the error in frequency being $\mathcal{O}\left(|\mu - \mu_0|^2\right)$ and that in amplitude being $\mathcal{O}\left(|\mu - \mu_0|^{\frac{3}{2}}\right)$. The estimates of frequency ω and first harmonic amplitude θ may be read directly from a graph. In this appendix, we apply Theorem C.1 to the feedback system represented in Figure 3.8 and conclude about the existence of a supercritical HOPF bifurcation for values of $k \gtrsim k^*$.

The main result of MEES is summarized in Theorem C.1.

Theorem C.1 (*Frequency domain HOPF bifurcation theorem*) [Mee81]

Let S be an autonomous feedback system described by

$$gf(e) + e = 0,$$

¹A characteristic locus corresponds to the (generalized) NYQUIST locus of a characteristic function. The definition and theory of characteristic functions is given in [Mee81, page 76]. In the SISO case, the characteristic locus simply corresponds to the NYQUIST locus.

where g is a linear operator with proper rational transfer function G such that $G(s) \in \mathbb{C}^{l \times m}$ and $f: \mathbb{R}^l \rightarrow \mathbb{R}^m$ is \mathcal{C}^4 in e . Suppose \hat{e} is a solution of $G(0)f(\hat{e}) + \hat{e} = 0$, and write D_1 for $(Df)_{\hat{e}}$.

Let $G(s)D_1$ have characteristic functions $\lambda_k(s)$ ($k = 1, \dots, p$) and suppose g and f depend on a real parameter μ in such a way that as μ passes through μ_0 , the locus of a single characteristic function $\hat{\lambda}(j\omega)$ passes through -1 at a unique frequency ω_0 , and the derivative $\frac{\partial \hat{\lambda}}{\partial \omega}$ and $\frac{\partial \hat{\lambda}}{\partial \mu}$ exist at (μ_0, ω_0) , where they are nonzero and are not parallel.

Define $L_1(\theta, \omega)$ as below (Table C.1) and suppose that when $\mu = \mu_0$, the locus of $L_1(\theta, \omega_0)$ as θ varies is transverse to the $\hat{\lambda}$ locus where they intersect at -1 .

Then for $\mu = \mu_0 + \chi\delta^2$, where $\chi = -1$ or $\chi = +1$ and $\delta > 0$ is small, the $L_1(\theta, \omega_0)$ locus intersects the $\hat{\lambda}(j\omega)$ locus transversely at, say $\hat{\lambda}(i\omega_1)$, when $\theta = \theta_1$. If δ is sufficiently small the nonlinear system can support oscillations of the form

$$e(t) = \hat{e} + \Re \sum_{k=0}^2 a_k e^{jkvt} + \mathcal{O}(\delta^3),$$

where

$$\begin{aligned} v &= \omega_1 + \mathcal{O}(\delta^3), \\ a_0 &= \theta_1^2 v_0 + \mathcal{O}(\delta^3), \\ a_1 &= \theta_1 v_1 + \mathcal{O}(\delta^2), \\ a_2 &= \theta_1 v_2 + \mathcal{O}(\delta^3), \end{aligned}$$

and each v_k , defined below (Table C.1), is $\mathcal{O}(1)$ in δ as $\delta \rightarrow 0$. Moreover, $e(t)$ is the unique periodic solution in a neighbourhood of \hat{e} .

Suppose the linearized feedback system (with D_1 replacing f) has two more poles in the right half-plane when $\mu = \mu_0 + \psi\delta^2$ ($\psi = \pm 1$) than when $\mu = \mu_0 - \psi\delta^2$. If $\psi\chi = +1$ the bifurcation is supercritical while if $\psi\chi = -1$ it is subcritical; in particular, the periodic solution is stable if there are no poles in $\Re\{s\} > 0$ for $\mu = \mu_0 - \psi\delta^2$ and $\psi\chi = +1$.

The statements about derivatives of $\hat{\lambda}$ just say that the $\hat{\lambda}$ locus moves through -1 “in a generic way”. In practice, one needs only draw the loci for a given value of μ as in figure C.1, and use the frequency ω_R at which $\hat{\lambda}(j\omega)$ intersects the negative real axis near -1 (i.e. $\Re\{\hat{\lambda}(j\omega)\}$ is closest to -1 and $\Im\{\hat{\lambda}(j\omega)\} = 0$) in place of ω_0 . MEES shows that $|\omega_R - \omega_0| = \mathcal{O}(\delta^2)$ and thus the approximation consisting in taking ω_R instead of ω_0 is valid.

The statements about stability are easiest to understand in the case where the linearized system is stable before bifurcation, in which case $\chi = +1$ implies a supercritical bifurcation to a stable limit cycle. This means that the closed-loop system has two poles in $\Re\{s\} > 0$ and the L_1 locus points *outwards*, towards the region of stable feedback gains (see Figure C.1). This is a rigorous version of a heuristic test often used with describing functions [Ath75], and there is an obvious generalization in terms of right half-plane poles and numbers of encirclements of the point $L_1(\theta, \omega_0)$ by all the loci. Essentially, MEES is saying that the behavior within the center manifold is described by the change in the number of poles with positive real part as μ increases through μ_0 , while the question of whether the manifold is itself attracting can be answered by looking at those poles which do not cross the imaginary axis as μ increases through μ_0 . However, the proof of MEES *does not* depend on center manifold theory.

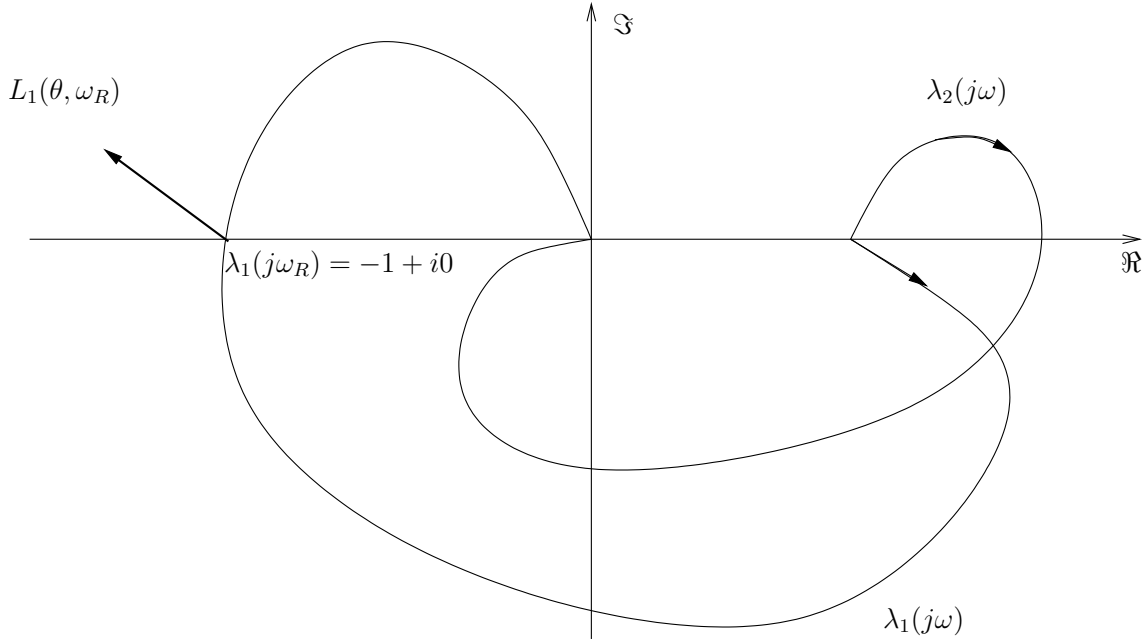


Figure C.1: Theorem C.1 in the case when $p = 2$. The characteristic loci are only shown for positive ω . The L_1 locus is the heavy straight line emanating from -1 : if the system was stable before bifurcation, and the λ_1 locus moves outwards to engulf -1 after bifurcation, the bifurcation is supercritical and the limit cycle is stable.

Summing up, then, the $L_1(\theta, \omega)$ locus behaves very like a describing function locus $-\frac{1}{N(\theta)}$: it allows us to read off the values of frequency and amplitude of oscillation and to see, very easily how changes in the system will affect the limit cycle. The general procedure to compute the locus of points $L_1(\theta, \omega)$ as θ varies is summarized in Table C.1.

Remark C.2 The symbol \otimes appearing in Table C.1 denotes the tensor product. The formulas given at point 2 can be understood in the following way:

1. $f : \mathbb{R}^l \rightarrow \mathbb{R}^m : X \rightarrow Y = f(X)$.
2. $D^1 f = \frac{\partial f(X)}{\partial X}$ is a $m \times l$ matrix and thus $G(s)D_1$ is a $l \times l$ matrix.
3. $D^2 f = \frac{\partial^2 f(X)}{\partial X^2}$ is a $m \times l \times l$ tensor and thus $Q = (D^2 f)|_{\hat{X}} E = D_2 E$ (where E is a $l \times 1$ vector) is a $m \times l$ matrix s.t. $Q_{jk} = \sum_{p=1}^l f_{pk}^j E_p$.
4. $D^3 f = \frac{\partial^3 f(X)}{\partial X^3}$ is a $m \times l \times l \times l$ tensor and thus $L = (D^3 f)|_{\hat{X}} E \otimes E = D_3 E \otimes E$ is a $m \times l$ matrix s.t. $L_{jk} = \sum_{p=1}^l \sum_{q=1}^l f_{pqk}^j E_p E_q$.
5. $D_2 E \otimes \bar{E} = Q \cdot \bar{E}$ and $D_3 E \otimes E \otimes \bar{E} = L \cdot \bar{E}$ where \cdot denotes the matrix product.

The locus of L_1 for fixed ω is just a straight line emanating from -1 and pointing in the direction $-z_1$. If $z_1 = 0$ then the locus is degenerate, but this is excluded by transversality.

Suppose $G(0)f(\hat{e}) + \hat{e} = 0$ and $D_k = (D^k f)_{\hat{e}}$ for $k = 1, 2, 3$. Identify $\hat{\lambda}$ as in Theorem C.1 and let u^T and v be the left and right eigenvectors of $G(j\omega)D_1$ belonging to $\hat{\lambda}(j\omega)$. Write $G_{D_1}(j\omega) = (I + G(j\omega)D_1)^{-1}G(j\omega)$.

1. Normalize v so that $|v| = 1$ and u so that $u^T v = 1$ (so $|u| \geq 1$).
2. Let

$$\begin{aligned} v_0 &= -\frac{1}{4}G_{D_1}(0)D_2v \otimes \bar{v}, \\ v_1 &= v, \\ v_2 &= -\frac{1}{4}G_{D_1}(2j\omega)D_2v \otimes v, \end{aligned}$$

where the k^{th} element of $D_2v \otimes \bar{v}$ is $(D_2v \otimes \bar{v})_k = \sum_{r,s=1}^m \frac{\partial^2 f_k(e)}{\partial e_r \partial e_s} \Big|_{e=\hat{e}} v_r \bar{v}_s$ where $k = 1, \dots, m$ and where \bar{v} denotes the complex conjugate of v .

3. Let $p(\omega) = D_2(v_0 \otimes v + \frac{1}{2}\bar{v} \otimes v_2) + \frac{1}{8}D_3v \otimes v \otimes \bar{v}$ where the k^{th} element of $D_3v \otimes v \otimes \bar{v}$ is $(v_0 \otimes v + \frac{1}{2}\bar{v} \otimes v_2)_k = \sum_{r,s,t=1}^m \frac{\partial^3 f_k(e)}{\partial e_r \partial e_s \partial e_t} \Big|_{e=\hat{e}} v_r v_s \bar{v}_t$.
4. Let $z_1(\omega) = u^T G(j\omega)p(\omega)$.
5. Then $L_1(\theta, \omega) = -1 - \theta^2 z_1(\omega)$.

Table C.1: Calculation of $L_1(\theta, \omega)$ [Mee81].

In the SISO case where $G(s) \in \mathbb{C}$ and $f : \mathbb{R} \rightarrow \mathbb{R}$ is \mathcal{C}^4 , the only characteristic function is $G(s)D_1$. Its locus corresponds to the NYQUIST diagram of $G(j\omega)D_1$. Since $G(j\omega)D_1$ is a scalar, the right and left eigenvectors for $\hat{\lambda}(j\omega_0)$ are given by $v = 1$ and $u = 1$.

C.2 Application of Theorem C.1 to our class of systems

Consider the feedback system represented in Figure 3.8 where Σ represents a linear system and $\phi_k(\cdot)$ satisfies the assumptions of Theorem 3.8. To force the HOPF bifurcation scenario, we consider that Σ is the feedback interconnection of a linear, passive system H with a simple integrator (see Chapter 3). Using the notations of MEES (see Theorem C.1) we have $f(\cdot) = \phi_k(\cdot)$ and $G = \Sigma$. Calculating the quantities appearing in Theorem C.1, we get $G(s) = \frac{sH(s)}{s+H(s)} \in \mathbb{C}$ where $H(s)$ is the transfer function of the passive system H and $D_1 = \phi'_k(0) = -k$, $D_2 = 0$ and $D_3 = \phi'''_k(0) = \kappa > 0$. Thus,

$$\begin{aligned}
 \lambda(s) &= G(s)D_1 = -kG(s), \\
 G_{D_1}(j\omega) &= \frac{G(j\omega)}{1 - kG(j\omega)}, \\
 v_0 &= 0, \\
 v_1 &= 1, \\
 v_2 &= 0, \\
 p(\omega) &= \frac{\kappa}{8}, \\
 z_1(\omega) &= \frac{\kappa}{8}G(j\omega), \\
 L_1(\theta, \omega) &= -1 - \frac{\kappa}{8}\theta^2 G(j\omega).
 \end{aligned}$$

The characteristic locus of $\lambda(j\omega)$ is the NYQUIST diagram of $-kG(j\omega)$. Since $G(s)$ is the transfer function of a passive system, the NYQUIST plot of $-kG(j\omega)$ lies entirely in the left half-plane for $k > 0$. When k increases the NYQUIST plot of $-kG(j\omega)$ corresponds to that of $G(j\omega)$ dilated by $-k$. Since the feedback system becomes unstable at $k = k^* \geq 0$ we know that the NYQUIST plot of $-kG(j\omega)$ engulfs the point -1 when $k = k^*$. Thus, $\psi = +1$.

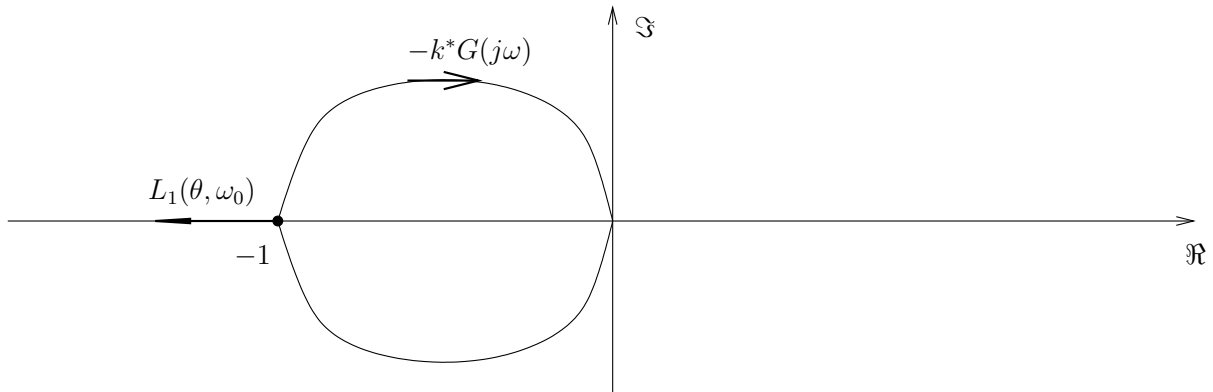


Figure C.2: Characteristic locus of $-kG(j\omega)$ for passive oscillators. The characteristic locus (i.e. the NYQUIST plot) is only shown for positive ω .

At $k = k^*$, the NYQUIST plot of $-kG(j\omega)$ crosses the real axis at -1 for $\omega = \omega_0$ and thus $G(j\omega_0) = \frac{1}{k^*}$. We conclude that $L_1(\theta, \omega_0) = -1 - \frac{3}{4k^*}\theta^2$. Thus, $L_1(\theta, \omega_0)$ is a vector starting at -1 and pointing towards $-\infty$ along the real axis (see Figure C.2). We thus have $\chi = +1$. We conclude from Theorem C.1 that the HOPF bifurcation is supercritical and leads to a locally stable limit cycle.

Bibliography

- [All77] D. J. ALLWRIGHT, *Harmonic balance and the Hopf bifurcation*, Math. Proc. Camb. Phil. Soc. **82** (1977), 453–467.
- [AM97] P. J. ANTSAKLIS and A. N. MICHEL, *Linear systems*, McGraw-Hill, 1997.
- [Ang02] D. ANGELI, *A Lyapunov approach to incremental stability properties*, IEEE Trans. on Automatic Control **47** (2002), 410–422.
- [AT02] M. ARCAK and A. TEEL, *Input-to-state stability and boundedness in Lurie systems*, Automatica **38** (2002), no. 11, 1945–1949.
- [Ath75] D. P. ATHERTON, *Nonlinear control engineering*, van Nostrand-Reinold, NY, 1975.
- [AVK65] A. A. ANDRONOV, A. A. VITT, and S. E. KHAIKIN, *Theorie der schwingungen*, Akademie-Verlag, Berlin, 1965, in German.
- [AVK66] ———, *The theory of oscillations*, Pergamon, Oxford, 1966.
- [BAGGE04] A. BARREIRO, J. ARACIL, F. GORDILLO, and F. GOMEZ-ESTERN, *Domain of attraction of autonomous oscillations in underactuated systems*, In Proceedings of 6th IFAC Symposium on Nonlinear Systems (NOLCOS), Stuttgart, Germany (2004).
- [BCLM01] A. M. BLOCH, D. E. CHANG, N. E. LEONARD, and J. E. MARSDEN, *Controlled Lagrangians and the stabilization of mechanical systems II: Potential shaping*, IEEE Trans. on Automatic Control **46** (2001), 1556–1571.
- [BIW91] C. I. BYRNES, A. ISIDORI, and J. C. WILLEMS, *Passivity, feedback equivalence, and global stabilization of minimum phase systems*, IEEE Trans. on Automatic Control **36** (1991), 1128–1240.
- [BKK94] M. BUEHLER, D. KODITSCHKE, and P. KINDLMANN, *Planning and control of robotic juggling and catching tasks*, International Journal of Robotics Research **13** (1994), no. 2, 101–118.
- [BLM01] A. M. BLOCH, N. E. LEONARD, and J. E. MARSDEN, *Controlled Lagrangians and the stabilization of mechanical systems I: The first matching theorem*, IEEE Trans. on Systems and Control **45** (2001), 2253–2270.
- [BM94] A. BACCIOTTI and L. MAZZI, *Floquet theory and stabilization of periodic solutions*, Rev. Roumaine Math. Pures Appl. **34** (1994), no. 4, 285–293.

BIBLIOGRAPHY

- [BM95a] ———, *The limit cycle stabilization problem*, Proceedings of the 3rd European Control Conference, vol. 4 (Part One), Roma, Italy, September 1995, pp. 3052–3055.
- [BM95b] ———, *Stabilization of periodic solutions*, Systems & Control Letters **24** (1995), 97–101.
- [BMH04] E. BROWN, J. MOEHLIS, and P. J. HOLMES, *On phase reduction and response dynamics of neural oscillator populations*, Neural Computation **16** (2004), no. 4, 673–715.
- [BMS96] A. BACCIOTTI, L. MAZZI, and M. SABATINI, *Generation of stable limit cycles in controllable linear systems*, Systems & Control Letters **28** (1996), 43–48.
- [BOvdS02] G. BLANKENSTEIN, R. ORTEGA, and A. J. VAN DER SCHAFT, *The matching conditions of controlled Lagrangians and IDA-passivity based control*, Int. J. Control **75** (2002), no. 9, 645–665.
- [CAA⁺03] C. CHEVALLEREAU, G. ABBA, Y. Aoustin, F. PLESTAN, E. R. WESTERVELT, C. CANUDAS-DE-WIT, and J. W. GRIZZLE, *Rabbit: A testbed for advanced control theory*, IEEE Control Systems Magazine **23** (2003), no. 5, 57–79.
- [Car81] J. CARR, *Applications of center manifold theory*, Springer-Verlag: New-York, Heidelberg, Berlin, 1981.
- [CEU02] C. CANUDAS-DE-WIT, B. ESPIAU, and C. URREA, *Orbital stabilization of underactuated mechanical systems*, IFAC, 15th Triennial World Congress, Barcelona, Spain, 2002.
- [CH95] C. C. CHUNG and J. HAUSER, *Nonlinear control of a swinging pendulum*, Automatica **31** (1995), no. 6, 851–862.
- [CH97] ———, *Nonlinear \mathcal{H}_∞ control around periodic orbits*, Systems & Control Letters **30** (1997), 127–137.
- [CH98] ———, *Relationships between input-output stability and exponentially stable periodic orbits*, Proceedings of the American Control Conference, Pennsylvania (1998), 2790–2794.
- [CL55] E. A. CODDINGTON and N. LEVINSON, *The theory of ordinary differential equations*, McGraw Hill, NY, 1955.
- [CSB96] C. CANUDAS-DE-WIT, B. SICILLIANO, and G. BASTIN, *Theory of robot control*, Communications and control engineering series, Springer-Verlag, London, 1996.
- [DM01] W. P. DAYAWANSA and C. F. MARTIN, *Van der Pol networks with symmetry*, Proceedings of the 40th IEEE Conference on Decision and Control, Orlando, Florida, USA, 2001.
- [Far94] M. FARKAS, *Periodic motions*, Applied Mathematical Sciences, 104, Springer Verlag, 1994.

BIBLIOGRAPHY

- [GAGE03] F. GORDILLO, J. ARACIL, and F. GOMEZ-ESTERN, *A family of oscillating generalized Hamiltonian systems*, Submitted to the 2nd IFAC Workshop on Lagrangian and Hamiltonian Methods in Nonlinear Control LHMNLC (2003).
- [GEBAG05] F. GOMEZ-ESTERN, A. BARREIRO, J. ARACIL, and F. GORDILLO, *Strict Lyapunov functions for inducing robust oscillations in nonlinear systems*, Submitted to the 16th IFAC World Congress, Prague, Czech Republic (2005).
- [GGEOA02] F. GORDILLO, F. GOMEZ-ESTERN, R. ORTEGA, and J. ARACIL, *On the ball and beam problem: regulation with guaranteed transient performance and tracking periodic functions*, 15th Mathematical Theory of Networks and Systems, Notre Dame, Indiana, USA (2002).
- [GMD01] J. GONCALVES, A. MEGRETSKI, and M. DAHLEH, *Global stability of relay feedback systems*, IEEE Trans. on Automatic Control **46** (2001), no. 4, 550–562.
- [GMD03] ———, *Global analysis of piecewise linear systems using impact maps and quadratic surface Lyapunov functions*, IEEE Trans. on Automatic Control **48** (2003), no. 12, 2089–2106.
- [Gol96] A. GOLDBETER, *Biochemical oscillations and cellular rhythms: The molecular bases of periodic and chaotic behaviour*, Cambridge University Press, Cambridge, 1996.
- [Gra81] A. GRAHAM, *Kronecker products and matrix calculus with applications*, Ellis Horwood Series, 1981.
- [Gri90] R. GRIMSHAW, *Nonlinear ordinary differential equations*, Blackwell, Oxford, England, 1990.
- [GS02] M. GOLUBITSKY and I. STEWART, *The symmetry perspective, from equilibrium to chaos in phase space and physical space*, Progress in mathematics, 200, Birkhäuser Verlag, 2002.
- [GS04] M. GÉRARD and R. SEPULCHRE, *Stabilization through weak and occasional interactions : a billiard benchmark*, Proceedings of the 6th IFAC Symposium on Nonlinear Control Systems (NOLCOS), Stuttgart, Germany, September 2004.
- [GSS85] M. GOLUBITSKY, I. STEWART, and D. G. SCHAEFFER, *Singularities and groups in bifurcation theory*, Applied Mathematical Sciences, 51, vol. I, Springer Verlag, 1985.
- [GSS88] ———, *Singularities and groups in bifurcation theory*, Applied Mathematical Sciences, 69, vol. II, Springer Verlag, 1988.
- [GvL89] G. H. GOLUB and C. F. VAN LOAN, *Matrix computations*, second ed., The Johns Hopkins University Press, 1989.
- [HC94] J. HAUSER and C. C. CHUNG, *Converse Lyapunov functions for exponentially stable periodic orbits*, Systems & Control Letters **23** (1994), 27–34.

BIBLIOGRAPHY

- [HH52] A. L. HODGKIN and A. F. HUXLEY, *A quantitative description of membrane current and its application to conduction and excitation in nerve*, *Physiol. (Lond.)* **117** (1952), 500–544.
- [HI97] F. C. HOPPENSTEADT and E. M. IZHIKEVICH, *Weakly connected neural networks*, Applied Mathematical Sciences, 126, Springer Verlag, 1997.
- [HJ85] R. HORN and C. JOHNSON, *Matrix analysis*, Cambridge University Press, 1985.
- [HKW81] B. HASSARD, N. KAZARINOFF, and Y.-H. WAN, *Theory and applications of Hopf bifurcation*, London Mathematical Society, Lecture Notes Series 41, Cambridge University Press, 1981.
- [HM76] D. J. HILL and P. J. MOYLAN, *The stability of nonlinear dissipative systems*, *IEEE Trans. on Automatic Control* **21** (1976), 708–711.
- [Hop42] E. HOPF, *Bifurcations of a periodic solution from a stationary solution of a system of differential equations*, *Berichten der Mathematische Physikalische Klassen der Sachisen Acad. Wissenschaften, Leipzig* **XCIV** (1942), 3–22, Technical note.
- [Hop82] J. J. HOPFIELD, *Neural networks and physical systems with emergent collective computational abilities*, *Proceedings of the National Academy of Sciences, USA* **79** (1982), 2554–2558.
- [Hop86] F. C. HOPPENSTEADT, *An introduction to the mathematics of neurons*, Cambridge, U.K.: Cambridge University Press, 1986.
- [Isi95] A. ISIDORI, *Nonlinear control systems*, third ed., Springer-Verlag, Berlin, 1995.
- [IT87] P. A. IOANNOU and G. TAO, *Frequency domain conditions for strictly positive real functions*, *IEEE Trans. on Automatic Control* **32** (1987), 53–54.
- [JS87] D. W. JORDAN and P. SMITH, *Nonlinear ordinary differential equations*, second ed., Oxford University Press, Oxford, England, 1987.
- [KE02] N. KOPELL and G. B. ERMENTROUT, *Mechanisms of phase-locking and frequency control in pairs of coupled neural oscillators*, *Handbook on Dynamical Systems*, vol. 2, B. Fiedler, Elsevier, 2002, pp. 3–5.
- [Kha02] H. K. KHALIL, *Nonlinear systems*, third ed., Prentice Hall, 2002.
- [Kri97] P. S. KRISHNAPRASAD, *Motion control and coupled oscillators*, Board of Mathematical Sciences, National Research Council, Motion Control and Geometry: Proceedings of a Symposium, National Academy, Press, Washington D. C., 1997, pp. 52–65.
- [Kur84] Y. KURAMOTO, *Chemical oscillations, waves, and turbulence*, Springer Verlag, 1984.
- [Lan79] W. F. LANGFORD, *Periodic and steady state interactions lead to tori*, *SIAM J. Appl. Math.* **37** (1979), 22–48.

BIBLIOGRAPHY

- [LB01] K. LYNCH and C. BLACK, *Recurrence, controllability, and stabilization of juggling*, IEEE Trans. on Robotics and Automation **17** (2001), no. 2, 113–124.
- [LBS96] G. LEONOV, I. BURKIN, and A. SHEPELJAVYI, *Frequency methods in oscillation theory*, Kluwer Academic Publishers, 1996.
- [Lev44] N. LEVINSON, *Transformation theory of nonlinear differential equations of the second order*, Ann. Math. **45** (1944), no. 4, 723–737.
- [LS98] W. LOHMILLER and J.-J. E. SLOITINE, *On contraction analysis for nonlinear systems*, Automatica **34** (1998), no. 6, 683–696.
- [MA00] L. MOREAU and D. AEYELS, *Practical stability and stabilization*, IEEE Trans. on Automatic Control **45** (2000), 1554–1558.
- [MC79] A. I. MEES and L. O. CHUA, *The Hopf bifurcation theorem and its applications to nonlinear oscillations in circuits and systems*, IEEE Trans. on Circuits and Systems **CAS-26** (1979), no. 4, 235–254.
- [Mee81] A. MEES, *Dynamics of feedback systems*, Wiley-Interscience, 1981.
- [MM76] J. MARSDEN and M. MCCracken, *The Hopf bifurcation and its applications*, Springer Verlag, NY, 1976.
- [Mos97] E. MOSEKILDE, *Topics in nonlinear dynamics. Applications to physics, biology and economic systems*, World Scientific Press, Singapore, 1997.
- [MR97] A. MEGRETSKI and A. RANTZER, *System analysis via Integral Quadratic Constraints*, IEEE Trans. on Automatic Control **42** (1997), no. 6, 819–830.
- [Mur02] J. D. MURRAY, *Mathematical biology, I: An introduction*, third ed., Springer Verlag, 2002.
- [NRA03] H. NIJMEIJER and A. RODRIGUEZ-ANGELES, *Synchronization of mechanical systems*, vol. 46, World Scientific Series on Nonlinear Science, Series A, 2003.
- [OvdSME02] R. ORTEGA, A. VAN DER SCHAFT, B. MASCHKE, and G. ESCOBAR, *Interconnection and damping assignment passivity-based control of port-controlled Hamiltonian systems*, Automatica **38** (2002), no. 4, 585–596.
- [OvdSMM01] R. ORTEGA, A. VAN DER SCHAFT, A. J. MAREELS, and B. MASCHKE, *Putting energy back in control*, IEEE Control Syst. Magazine **21** (2001), no. 2, 18–33.
- [Pav04] A. V. PAVLOV, *The output regulation problem: a convergent dynamics approach*, Ph.D. thesis, Technische Universiteit Eindhoven, December 2004.
- [Per91] L. PERKO, *Differential equations and dynamical systems*, Springer, New York, 1991.
- [PGN99] A. POGROMSKY, T. GLAD, and H. NIJMEIJER, *On diffusion driven oscillations in coupled dynamical systems*, International Journal of Bifurcation and Chaos **9** (1999), no. 4, 629–644.

BIBLIOGRAPHY

- [PN01] A. POGROMSKY and H. NIJMEIJER, *Cooperative oscillatory behavior of mutually coupled dynamical systems*, IEEE Trans. on circuits and systems **48** (2001), 152–162.
- [Pog98] A. POGROMSKY, *Passivity based desing of synchronizing systems*, Int. J. Bifurcation and Chaos **8** (1998), 295–319.
- [Pop62] V. M. POPOV, *Absolute stability of nonlinear control systems of automatic control*, Automation and Remote Control **22** (1962), 857–875.
- [Pop73] ———, *Hyperstability of control systems*, Springer-Verlag, 1973.
- [PPvdWN04] A. PAVLOV, A. POGROMSKY, N. VAN DE WOUW, and H. NIJMEIJER, *Convergent dynamics, a tribute to Boris Pavlovich Demidovich*, Systems & Control Letters **52** (2004), 257–261.
- [PSN02a] A. POGROMSKY, G. SANTOBONI, and H. NIJMEIJER, *Partial synchronization : from symmetry towards stability*, Physica D **172** (2002), 65–87.
- [PSN02b] ———, *Partial synchronization through permutation symmetry*, 15th Triennial World Congress of the International Federation of Automatic Control, no. 1266, Barcelona, Spain, 2002.
- [RA03] J. A. ROGGE and D. AEYELS, *Synchronization and total phase locking of mutually coupled oscillators*, SIAM Conference on Applications of Dynamical Systems, Snowbird, UT, USA, May 2003.
- [RAN04] A. RODRIGUEZ-ANGELES and H. NIJMEIJER, *Mutual synchronization of robots via estimated state feedback: A cooperative approach*, IEEE Trans. on Control and Systems Technology **12** (2004), no. 4, 542–554.
- [RLS04] R. RONSSE, P. LEFEVRE, and R. SEPULCHRE, *Open-loop stabilization of 2d impact juggling*, In proceedings of the 6th IFAC Symposium on Nonlinear Control Systems (NOLCOS), Stuttgart, Germany, 2004.
- [SA93] S. SCHAAL and C. G. ATKESON, *Open loop stable control strategies for robot juggling*, IEEE International Conference on Robotics and Automation, vol. 3, 1993, pp. 913–918.
- [SA94] ———, *Robot juggling - implementation of memory-based learning*, IEEE Control Systems Magazine **14** (1994), no. 1, 57–71.
- [San64a] I. W. SANDBERG, *A frequency domain condition for the stability of systems containing a single time-invariant nonlinear element*, The Bell System Technical Journal **43** (1964), 1601–1638.
- [San64b] ———, *On the \mathcal{L}_2 -boundedness of solutions of nonlinear functional equations*, The Bell System Technical Journal **43** (1964), 1581–1599.
- [SB89] S. SASTRY and M. BODSON, *Adaptive control: Stability, convergence, and robustness*, Prentice Hall, 1989.

BIBLIOGRAPHY

- [SC04] A. SHIRIAEV and C. CANUDAS-DE-WIT, *Virtual constraints: A constructive tool for orbital stabilization of underactuated nonlinear systems*, Submitted to IEEE Trans. on Automatic Control (2004).
- [Sep04] R. SEPULCHRE, *Oscillators as systems and synchrony as a design principle*, To appear in the proceedings of the ACTRA workshop held in Rome, at the occasion of the 70th birthday of P. Kokotovic and S. Nicosia, June 2004.
- [SJK97] R. SEPULCHRE, M. JANKOVIC, and P. KOKOTOVIC, *Constructive nonlinear control*, Springer Verlag, London, 1997.
- [SK00] M. G. SAFONOV and V. V. KULKARNI, *Zames-Falb multipliers for MIMO nonlinearities*, Int. J. Robust Nonlinear Control **10** (2000), 1025–1038.
- [Smi79] R. SMITH, *The Poincaré-Bendixon theorem for certain differential equations of higher order*, Proc. Royal Soc. Edinburgh, Sect. A **83** (1979), 63–79.
- [Smi86] ———, *Orbital stability for ordinary differential equations*, J. Differential Equations **69** (1986), 265–287.
- [Son89] E. D. SONTAG, *Smooth stabilization implies coprime factorization*, IEEE Trans. on Automatic Control **34** (1989), 435–443.
- [SS93] S. H. STROGATZ and I. STEWART, *Coupled oscillators and biological synchronization*, Scientific American **269** (1993), no. 6, 102–109.
- [SS03] G.-B. STAN and R. SEPULCHRE, *Dissipativity characterization of a class of oscillators and networks of oscillators*, 42nd IEEE Conf. on Decision and Control, Maui, Hawaii, USA, 2003, pp. 4169–4173.
- [SS04a] ———, *Dissipativity and global analysis of limit cycles in networks of oscillators*, In proceedings of the 16th International Symposium on Mathematical Theory of Networks and Systems (MTNS), Leuven, Belgium, 2004.
- [SS04b] ———, *Global analysis of limit cycles in networks of oscillators*, In proceedings of the 6th IFAC Symposium on Nonlinear Control Systems (NOLCOS), Stuttgart, Germany, 2004, pp. 1433–1438.
- [SS05a] R. SEPULCHRE and G.-B. STAN, *Feedback mechanisms for global oscillations in Lure systems*, Systems and Control Letters **54** (2005), no. 8, 809–818.
- [SS05b] G.-B. STAN and R. SEPULCHRE, *Dissipativity and global analysis of limit cycles*, Submitted for publication in IEEE Trans. on Automatic Control (2005).
- [Str00] S. H. STROGATZ, *Nonlinear dynamics and chaos*, Westview Press, 2000.
- [Str03] ———, *Sync: the emerging science of spontaneous order*, Hyperion, 2003.
- [SW03] J.-J. SLOTINE and W. WANG, *A study of synchronization and group cooperation using partial contraction theory*, Block Island Workshop on Cooperative Control (K. V., ed.), Springer-Verlag, 2003.

- [SWR04] J.-J. SLOTINE, W. WANG, and K. E. RIFAI, *Contraction analysis of synchronisation and desynchronisation in networks of nonlinearly coupled oscillators*, In proceedings of the 16th International Symposium on Mathematical Theory of Networks and Systems (MTNS), Leuven, Belgium, 2004.
- [TI88] G. TAO and P. A. IOANNOU, *Strictly positive real matrices and the Lefschetz-Kalman-Yakubovich lemma*, IEEE Trans. on Automatic Control **33** (1988), 1183–1185.
- [TY89] E. A. TOMBERG and V. A. YAKUBOVICH, *Conditions for auto-oscillations in nonlinear systems*, Siberian Math. J. **30** (1989), no. 4, 180–194.
- [TYS91] G. TAGA, Y. YAMAGUCHI, and H. SHIMIZU, *Self-organized control of bipedal locomotion by neural oscillators in unpredictable environment*, Biological Cybernetics **65** (1991), no. 3, 147–159.
- [vdS00] A. VAN DER SCHAFT, *\mathcal{L}_2 -gain and passivity techniques in nonlinear control*, Springer Verlag, London, 2000.
- [VG01] S. VARIGONDA and T. T. GEORGIU, *Dynamics of relay relaxation oscillators*, IEEE Trans. on Automatic Control **46** (2001), no. 1, 65–77.
- [WGC02] E. R. WESTERVELT, J. W. GRIZZLE, and C. CANUDAS-DE-WIT, *Switching and PI control of walking motions of planar biped walkers*, IEEE Trans. on Automatic Control **48** (2002), no. 2, 308–312, Technical note.
- [Wig90] S. WIGGINS, *Introduction to applied nonlinear dynamical systems and chaos*, Texts in Applied Mathematics, 2, Springer Verlag, 1990.
- [Wil72] J. C. WILLEMS, *Dissipative dynamical systems, parts I and II*, Arch. Rational Mechanics and Analysis **45** (1972), 321–393.
- [Wil99a] M. M. WILLIAMSON, *Robot arm control exploiting natural dynamics*, Ph.D. thesis, Massachusetts Institute of Technology, May 1999.
- [Wil99b] H. R. WILSON, *Spikes, decisions and actions - dynamical foundations of neuroscience*, Oxford University Press, 1999.
- [WS] W. WANG and J.-J. SLOTINE, *On partial contraction analysis for coupled nonlinear oscillators*, To be published in Biological Cybernetics.
- [Yak73] V. A. YAKUBOVICH, *Frequency-domain criteria for oscillation in nonlinear systems with one stationary nonlinear component*, Siberian Math. J. **15** (1973), no. 5, 1100–1129.
- [ZF68] G. ZAMES and P. L. FALB, *Stability conditions for systems with monotone and slope-restricted nonlinearities*, SIAM Journal of Control and Optimization **6** (1968), no. 1, 89–108.
- [ZRB99] A. ZAVALA-RIO and B. BROGLIATO, *On the control of a one degree-of-freedom juggling robot*, Dynamics and Control **9** (1999), 67–90.